Alginate based composite scaffold for biomedical engineering applications

Pichaya Srisuk

A thesis submitted to the University of Bristol in accordance with the requirements for award of the degree of Doctor of Philosophy in the Faculty of Engineering.

June 2021

Word count: 40155

Abstract

Alginate is a natural polysaccharide polymer which is extracted from seaweed or bacteria. It forms gel with unique ability which widely used for medical applications. Alginate is limited in mechanical properties and abilities. This has led the possibility of improving the performance of using them. This study aims to enhance and understand the properties and applications of alginate-based materials for both engineering and biomedical scheme.

Firstly, conductive fibres were prepared to determine mechanical properties and electrical conductivity. Fibres were spun by wet spinning process, organic solvent and heated treatment were applied to improve their properties. The result shows that fibre with both treatments presented the highest in conductivity but the lowest in mechanical properties. It can be assumed by the result in the stimulated circuit that potential composite benefits to the smart textile and engineering applications.

Secondly, neurons were seeded into alginate based conductive films and observed at 7 and 14 days. Neuronal growth attached to the composite substrates which developed greater in axon compared to neat alginate films but still less than control well. It can be assumed that conductive composite was biocompatible and could be improved for tissue engineering.

Thirdly, controlled drug release was studied by loading ibuprofen into alginate and organoclay hydrogel to determine the release rate and physical properties. The clays contain cationic organic functionalities which non-covalently interact with anionic functional groups associated with alginate to produce self-supported hybrid hydrogel. Drug delivery was studied in water and room temperature and found that it was quick released in the beginning and slow release subsequently over 30h.

The research demonstrates a variety of methods and experiments which could be further explored and developed for biomedical engineering applications.

Acknowledgements

For their guidance, support, patience, time, supervision and making this whole process possible I would like to sincerely thank my supervisors Ian Hamerton and Avinash Patil.

I would like to thank Kevin Potter, for giving me the opportunity in joining the ACCIS department by considering my application as a PhD student. My experience here has been wonderful which thanks to all staff and everyone within ACCIS and Engineering department team for their help and support. Julie Etches and Steve Rae for their time on training me on many different types of equipment. This also includes Chemistry support staff which very helpful throughout my time here.

Jacopo Ciambella and Sean Davis have been very kind and guidance within my annual review, with their comments I could keep my research and experiments right on track and right in time.

The Centre for Nanoscience and Quantum Information (NSQI) and Stuart Bellamy for the technical support, training and access to wet lap and the clean room for tissue engineering in my first two years, without his support this work could have not processed.

Peter Duckworth who is a lab partner, friend and consultant on what I need in my research also in the University as well. Also, a proof reader on my work which I am very appreciated that.

Lastly, I should acknowledge my family, who have always been there and support me for everything. And Pipe, my partner who always take care, understand and his encouragement with me during my study and comfort me on my thesis writing.

Declaration

I declare that the work in this dissertation was carried out in accordance with the requirements of the University's Regulations and Code of Practice for Research Degree Programmes and that it has not been submitted for any other academic award. Except where indicated by specific reference in the text, the work is the candidate's own. Work done in collaboration with, or with the assistance of, others, is indicated as such. Any views expressed in the dissertation are those of the author.

:……..…… Date: ……..

Pichaya Srisuk

Contents

List of figures

List of table

List of Abbreviations

I_0	(Beer-Lambert Law) intensity of transmitted light
˚C	*Degree Celsius*
ΔL	(Young's modulus equation) change in length
2D	Two Dimensional
3D	Three Dimensional
3T3-L1	Mouse fibroblasts
6-OHDA	6-Hydroxydopamine
A	(Beer-Lambert Law) Absorption
A	Cross-section area
AAD	Adipic acid dihydrazide
Ag	Silver
$AgNO_3$	Silver nitrate
ALG	Alginate
ASTM	American Society for Testing and Materials
BBB	*Blood brain barrier*
BV-2	Mouse microglia cell line
C	(Beer-Lambert Law) concentration of the compound
C6	Rat astrocytoma cell line
Ca	Calcium
Ca^{2+}	Calcium (II) ion
$CaCl_2$	Calcium chloride
$CaCO_3$	Calcium carbonate
$CaSO_4$	Calcium sulfate

cm	Centimetre
CMC	Carboxymethyl cellulose
CO_2	Carbon dioxide
CPs	Conductive polymers
d	day(s)
D_2	Deuterium
DBS	Deep brain stimulation
DI	Deionised
DMSO	Dimethyl sulfoxide
DNA	Deoxyribonucleic acid
DSC	Differential scanning calorimeter
E	Young's modulus
e.g.	Exempli gratia
ECM	Extracellular matrix
ECoG	Electrocorticography
EDOT	3-4-ethylenedioxythiophene
EG	Ethylene glycol
EIS	Electrochemical impedance spectroscopy
etc.	Et cetera
F	force
FDA	Food and Drug Administration of the United States of America
FTIR	Fourier transform infrared spectroscopy
G'	Storage modulus
G	(1,4) α-L-guluronate

g	Gram
G"	Loss modulus
g/mol	Gram per mole
GOPS	3-glycidoxypropyltrimethoxysilane
GPa	Gigapascal
h	Hours
H/S	Horse serum
H^+	Hydrogen ion
H_2SO_4	Sulfuric acid
HA	Hyaluronic acid
HAP	Hydroxyapatite
HCl	Hydrochloric acid
hESCs	Human embryonic stem cells
hiPSC	Human induced pluripotent stem cells
HOMO	Highest occupied molecular orbital
Hz	Hertz
I	(Beer-Lambert Law) intensity of incident light
I	(Ohm's law) current
i.e.	Id est
in situ	In the original place
in vitro	Within the glass
in vivo	Within the living organism
iPSC	Induced pluripotent stem cells
IR	Infrared

kDa	Kilodalton
KD_{elim}	Rate of elimination of free drug from the body
KDRC	Rate of release of free drug at the non-target site
KDS_{elim}	Rate of elimination of the drug-carrier conjugate
KR	Rate of elimination of drug-carrier conjugate
KT	Rate of delivery of drug-carrier conjugate to the target site
KTDC	Rate of removal of free drug from the target site
KTDR	Rate of release of free drug at the target site
kV	Kilovoltage
L	(Conductivity calculation) gauge length
l	(Young's modulus equation) original length
L	Litre
l	(Beer-Lambert Law) pathlength through sample (cm)
L929	Mouse fibroblast cell line
LCP	Liquid crystal polymer
LED	Light emitting diode
LUMO	Lowest unoccupied molecular orbital
M	Molarity
M	(1,4) β-D-mannuronate
m	Metre
MEA	Multi-electrode array
mg	Milligram
min	Minute(s)
mL	Millilitre

mM	Millimolarity
MPa	Mega pascal
mPas	Millipascal Second
MW	Molecular weight
N.B.	Nota bene
N_2	Nitrogen
Na^+	Sodium ion
Na_2CO_3	Sodium carbonate
NaClO	Sodium hypochlorite
$NaHCO_3$	Sodium Bicarbonate
NIH/3T3	Mouse embryonic fibroblast cell line
NIPAAm	N-isopropylacrylamide
nm	Nanometre
NSAID	Non-steroidal anti-inflammatory drug
NSC	Neural stem cell
NT2	Neuroprotective agent
o/n	Over night
OECT	Electrochemical transistor
P(TMC-CL)	Poly(trimethylene carbonate-co-caprolactone)
P/S	Penicillin-Streptomycin
PA	Polyacetylene
PAG	Poly(aldehyde gluronate)
PAH	Poly(acrylaminde-*co*-hydrazide)
PAN	polyacrylonitrile
PANI	Polyaniline

PC-12	Rat pheochromocytoma cell line
PCL	Polycaprolactone
PDMS	Polydimethylsiloxane
PEDOT	Poly-(3-4-ethylenedioxythiophene)
PEDOT:GAG	Poly(3,4-ethylenedioxythiophene): glycosaminoglycan
PEDOT:PSS – ALG – PEG	Poly-(3-4-ethylenedioxythiophene): poly(styrene sulfonic acid) ,alginate and poly(ethylene glycol)
PEDOT:PSS	Poly-(3-4-ethylenedioxythiophene): poly(styrene sulfonic acid)
PEDOT:PSS-ALG	Poly-(3-4-ethylenedioxythiophene): poly(styrene sulfonic acid) and alginate
PEG	Poly(ethylene glycol)
PEG-*co*-PCL	Poly(ethylene glycol)-*co*-poly(ε-caprolactone)
PEO	Poly(ethylene oxide)
PET	Poly(ethylene terephthalate)
PG	Polygulronate
PGLA	Poly(lactic-co-glycolic acid)
pH	Potential of hydrogen
PHA	Polyhydroxyalkanoate
PHB	Polyhydroxybutyrate
PHBV	Poly(3-hydroxybutyrate-co-3-hydroxyvalerate)
PLA	Polylactic acid
PLL	Poly-L-lysine
PNIPAAm	Poly(N-isopropylacrylamide)
PP	Polypropylene
PPX	Poly(*p*-xylylene)

PPy	Polyacetylene
PSS	Poly(styrene sulfonic acid)
Pt	Platinum
PT	Polythiophene
PU	Polyurethane
PVA	Polyvinyl alcohol
Q	Swelling ratio
Q	Glutamax I
R	Resistance
Ref	Reference
RGD	Arginine-Glycine-Aspartic acid
S	(Conductivity calculation) conductivity
S	Siemen
SEM	Scanning electron microscopy
semi-IPN	Semi-interpenetrating polymer network
SH-SY5Y	human neuroblastoma cell line
SNR	Signal-to-noise ratio
SWNT	Single walled carbon nanotubes
T_c	Temperature of the peak of crystallisation
Ti-Al-V	Titanium-Aluminum-Vanadium
T_M	Temperature of the peak of melting
T_{OC}	Onset temperature of the peak of crystallisation
T_{OM}	Onset temperature of the peak of melting
UK	United Kingdom
USA	United States of America

UV	Ultraviolet
UV/Vis	Ultraviolet/Visible spectroscopy
V	Voltage
via	Vertical interconnect access
Wd	Dried gel mass
We	Swollen gel mass
Y	Young's modulus
Zn	Zn
$ZnCl_2$	Zinc chloride
ρ	Conductive
%wt	Weight percentage
μ	Micro
α	Alpha
β	Beta
ε	(Beer-Lambert Law) molar absorptivity of the compound
σ	(Young's modulus equation) engineering stress
ε	(Young's modulus equation) engineering strain
Ω	Ohm (Unit of resistnce)

Chapter 1

Literature review

1.1 Introduction to natural polymers

The main focus of this chapter is to provide a brief introduction to natural polymers with particular emphasis on alginate. The review will also discuss the physico-chemical properties of alginate and provide a brief overview of applications of the biopolymer in the biomedical and engineering fields. Furthermore, more specific and relevant literature will be presented in each experimental chapter.

Polymers are large macromolecules comprising small chemical units (monomers) interconnected with covalent bonds to form a polymeric chain. The number of monomeric units governs the molecular weight of a polymer [1], whereas the chemical structure and functional groups associated with the monomer units dictate the physical and chemical properties of the polymer [2]. Polymers in general can be classified into three main groups: (a) natural polymers also known as biopolymers, (b) semi-synthetic polymers, and (c) synthetic polymers [1][2]. Among these, synthetic polymers have found a myriad of applications in many industrial sectors including, automobile, textile and household products. Further, the revolution in the chemical industry has enabled the cost-effective synthesis of

polymers and products [3]. However, their non-biodegradable nature is causing a huge impact on our environment. In contrast, natural polymers can be obtained from a range of biological sources
and therefore are more sustainable and environmentally benign [4]. As a result, scientists and engineers are working to develop new materials with improved properties using biopolymers. Natural polymers or biopolymers can be further classified based on their chemical structure into three main types *i.e.* polysaccharides, proteins, and polyesters. Biopolymer structures can be found in protein, deoxyribonucleic acid (DNA), silk, and wool, and can be formed by a range of routes including bacterial biosynthesis.[5]

Biopolymers can now be obtained by the fermentation of micro-organisms or enzymatic processes with an advance biotechnology. Amongst the biopolymers, the most common natural polymer is cellulose, which is an integral part of all plants on the planet. Plants have proved to be a useful source of biopolymers, they not only provided cellulose but also starch and alginate [6]. The chart of polymers classification is given in Figure. 1.1 which depicts types of biopolymers available based on their chemical structure. [7].

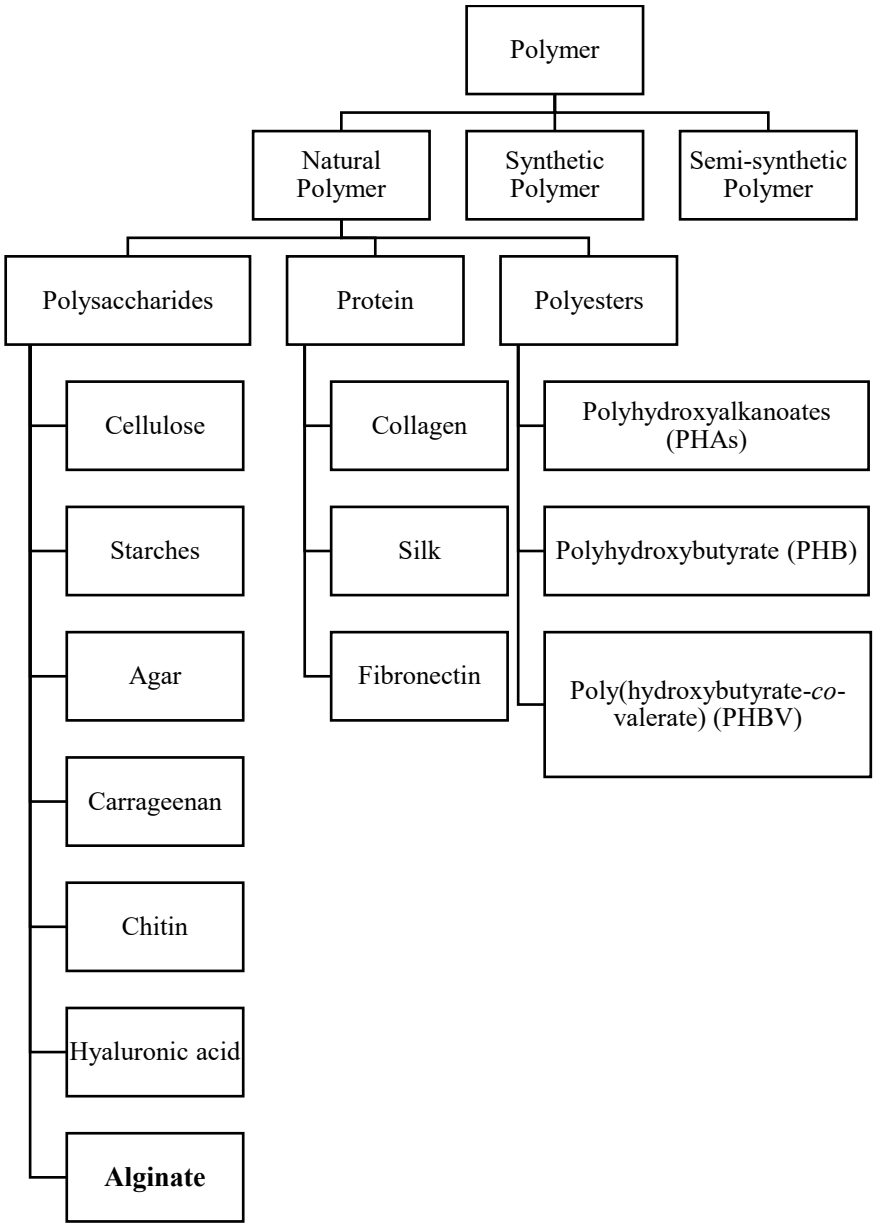

Figure. 1.1 Classification of biopolymers and their sources according to their chemical structure: polysaccharides, protein, and polyesters. (*N.B.* alginate is highlighted) [7].

Owing to their properties such as biodegradability, renewable sources and aqueous processability, biopolymer are being used in wide range of industries [8]. However, the physical and chemical properties are lower than synthetic polymers due to biodegradable ability, but recent developments in scientific research and technology have successfully employed range of biopolymers for the fabrication of products for packaging, agriculture, pharmaceutical, biomedical and engineering fields [9].

The most commonly used of biopolymers are polysaccharides (*e.g.* starch, chitosan, chitin, and cellulose) and proteins, which include collagen, gelatine, and alginate. Starch can be prepared and used for making biodegradable plastics using classical plastic manufacturing methods: extrusion, foaming, and blowing [5].

However, starch is a hydrophilic material which cannot withstand environments involving high humidity, so it can be mixed as a composite with other biopolymers such as chitosan, and poly(*L*-lactic acid) (PLA), *etc.*[10] to make it stronger and tougher. Chitosan is the most popular biopolymer, used in drug delivery systems because of its high degree of biocompatibility and low toxicity, properties it shares chitin [11].

Moreover, chitosan also has a strong antibacterial property which offers benefits in tissue engineering. Both are considered as weak mechanical properties materials but can be improved by combining with other polymers and cross-linked in the polymer matrix to form composites [12]. Cellulose is arguably the most important biopolymer, which can be found throughout the natural environment [9]. It can be used in the raw state or implemented in many fields because it has very strong mechanical properties compared to other biomaterials, retaining the characteristics of biocompatibility, biodegradability, hydrophilicity, and thermostability [3]. Collagen is perhaps the most important biomaterials for biomedical applications as it derives from animals with skins, of which the major structural component of bone [13]. It benefits for wound dressing, tissue engineering, plastic surgery, and the artificial dermis. The most important application from collagen is to use for the replacement of human tissue to reduce the healing time and improve the healing process [14]. The main

focus of this study will be based on alginate, as it is soluble with unique gelling ability, and can be modified by both chemical and physical systems.

1.2Introduction to alginate

As this research study examines alginate and its applications by improving properties and abilities in the engineering and biomedical settings, the characteristics, behaviour and relevant literature are addressed here separately.

1.2.1 Alginate background

Alginate comprises a natural polymer which can be found in brown seaweeds (the *Laminaria* and *Ascophyllum* species) and was first extracted by E.C.C. Standford in 1881 [15]. Several bacteria can also be used to produce alginate exocellularly, but the process is slow and cost of production significantly higher than seaweed sources [16]. In general, the extraction process involves converting the alginate salt into its sodium salts by heating cut seaweed with an alkali solution, commonly sodium carbonate (1.5 wt%) at 50-90 ˚C for 1-2 h. The dissolved solution gives layers of sodium alginate and the alkali-insoluble seaweed residue. Precipitation in a diluted filtered solution yields sodium alginate. Obtaining the sodium salt can be achieved through two methods: via alginic acid, or the corresponding calcium salt [17]. The schematic of the alginate extraction process is illustrated in Figure 1.2.

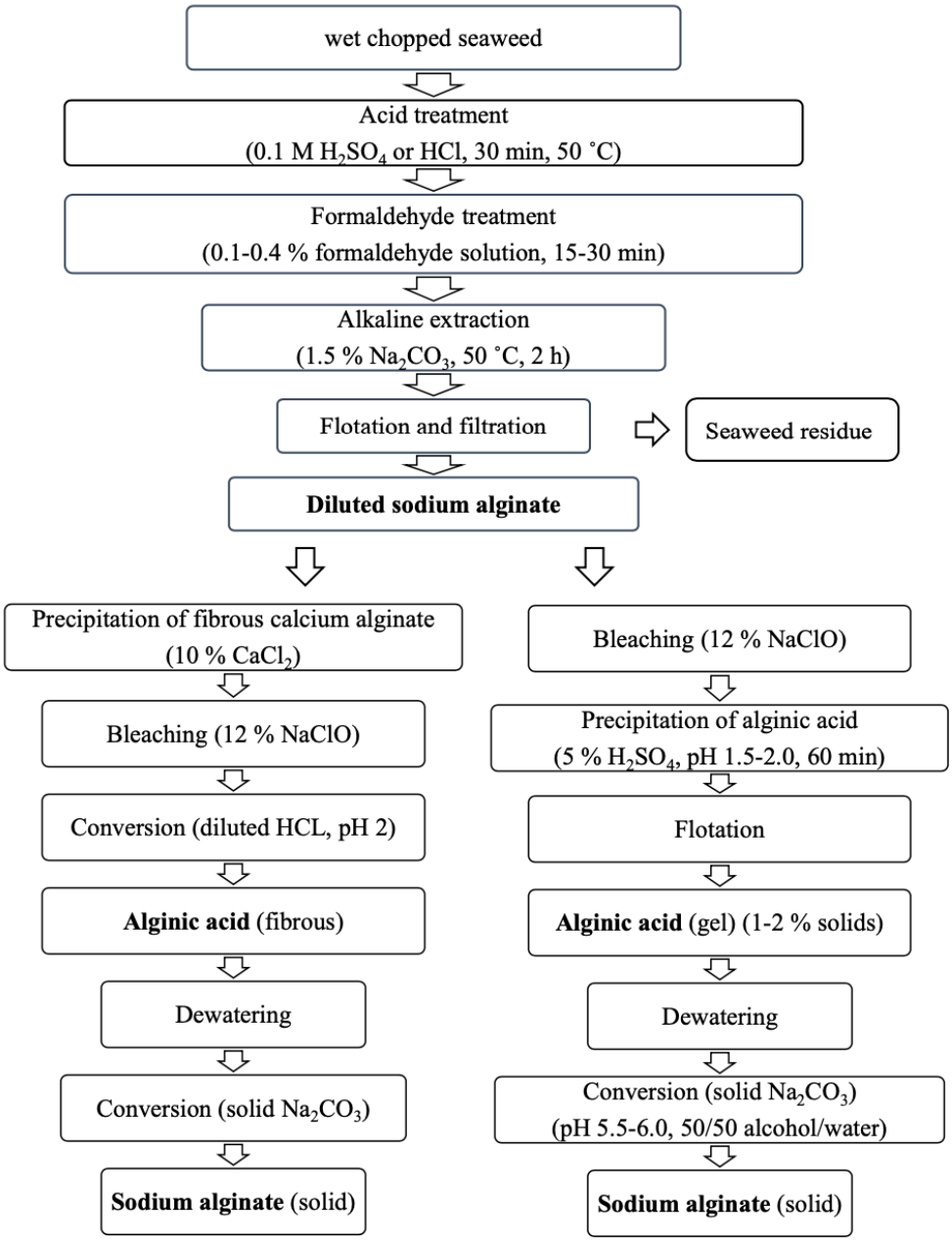

Figure1.2 A flowchart showing the preparation of sodium alginate from seaweed.

The first method is performed by adding calcium chloride solution (10 wt%) into the sodium alginate solution which causes fibres of calcium alginate to form. The fibres are then separated, washed, dewatered bleached with sodium hypochlorite (NaClO) solution (12 wt%) before the calcium alginate was converted into alginic acid by stirring in HCl (0.5 M, pH less

than 2). The alginic acid in fibrous form is then dehydrated and mixed with sodium carbonate to form a paste which is extruded into pellets, dried, and milled.

The second method involves bleaching diluted sodium alginate with NaClO (12 wt%) followed by the addition of H_2SO_4 (5 wt%, pH 1.5-2.0, 60 min) to precipitate alginic acid. The flotation step is applied after to obtain the alginic acid as a gel comprising 1-2 % solid content. Removing water from the gel can be done in three different ways: pressing or squeezing, centrifugation, or by mixing with alcohol. Pressing or squeezing can increase the solids content to 25-30% while centrifuging increases this by 7-8%, but no difference is observed by mixing with alcohol and thus large-scale production is uneconomical through this route. The conversion from alginic acid to sodium alginate is achieved by adding a mixture of alcohol and water (50:50) then adding Na_2CO_3 to form into a paste which is then extruded into pellets, dried, and milled.

Both methods have benefits and drawbacks including an extra step in the first process, but the fibrous forms of calcium alginate and alginic acid are easier to handle. For the second method, the gel form of alginic acid is difficult to separate and suffers a greater loss in alginic acid than the first process. Moreover, using alcohol to convert alginic acid to sodium alginate makes the process more expensive as well. The largest commercial production of alginate takes place in China while the total production all around the world is about 33,000 tonnes *per annum* of which 16,000 tonnes are in Europe, 14,000 tonnes in the Asian Pacific, and 3,000 tonnes in the Americas [18].

The type of alginate structure is influenced by the seaweed source as well as the growing conditions [19]. Moreover, it could be obtained from the bacterial sources as well. Alginate is a natural polysaccharide which is made up of two linear copolymers: β-(1-4)-D-mannuronic acid (M) and α-(1-4)-L-guluronic acid (G) (Figure.1.3).

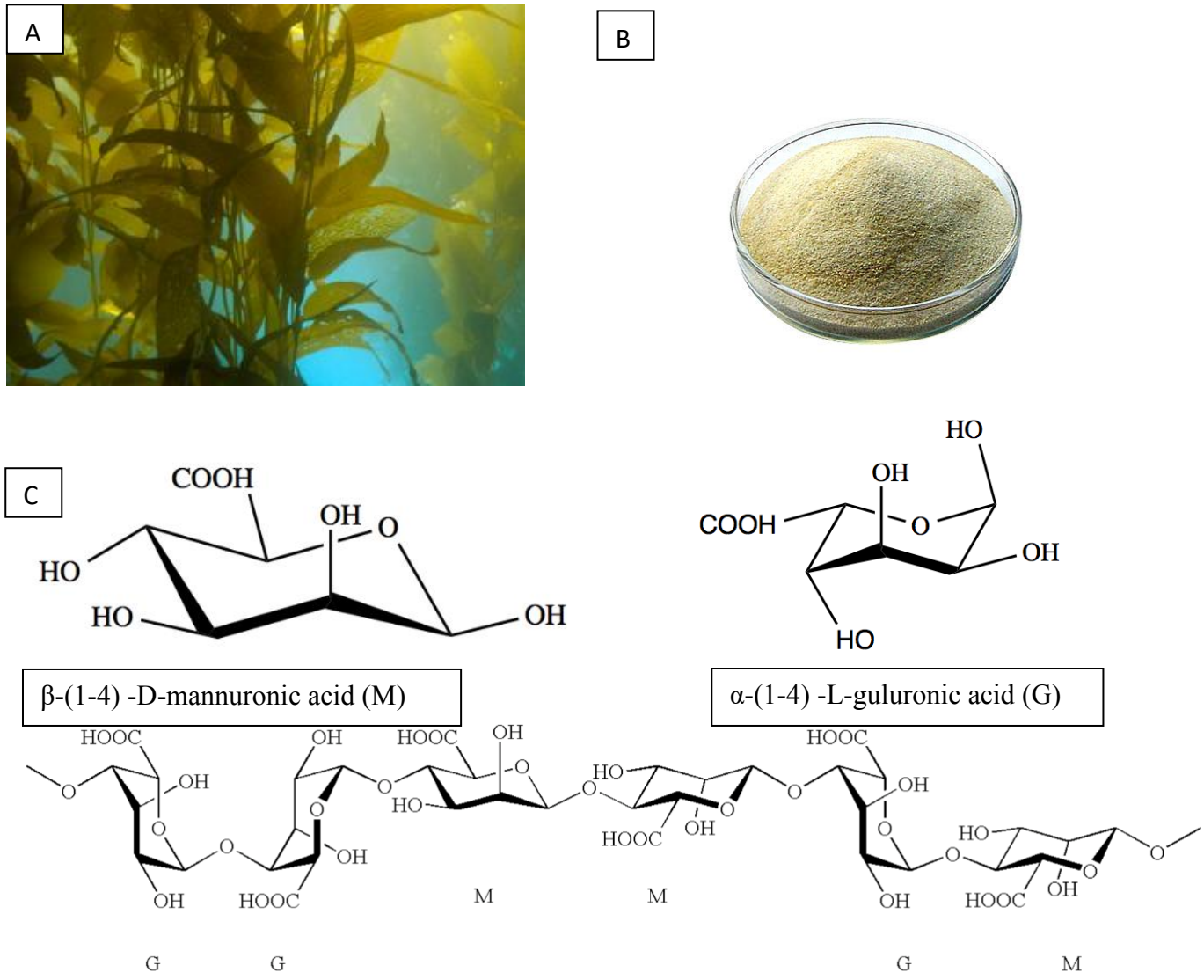

Figure 1.3 (A) A photograph of kelp, the most common type of seaweed used for extracting alginate (Britannica, E., *giant kelp*. Available at: https://www.britannica.com/science/seaweed.), (B) A photograph showing a typical appearance of sodium alginate powder (*Sodium Alginate*. Available at: https://www.meronbiopolymers.com/sodium-alginate), (C) Chemical structures of the two main linear monomers that combine to form alginate: β-(1-4) -D-mannuronic acid (M) and α-(1-4) -L-guluronic acid (G), and an alginate polymer chain with G-G, M-M, and G-M compositions.

The composition and sequential order of the alginate monomer units can be varied with blocks of: GGGG, MMMM, or GMGMGM. This is of great importance for its function [20]. For instance, alginate oligomers with a high composition of the G units form strong and

brittle materials with good thermal stability whereas, oligomers rich in M units form more stronger and elastic gels. So, the high or low concentration of the cross-linker with high M content will form the stronger gel [21]. From the structure of alginate, covalent bonding connects each block of copolymer together via the hydroxyl group. Alginate exhibits strong interactions with divalent cations which causes its unique gelling ability. This is attributed to specific ionic interactions with the G units of the biopolymer. The "Egg-box" shape (Figure.1.4) is found in the cross-linking area of the composition of G-G regions [22]. The gel forming structure can be described as part solid and part solution and other residues are trapped inside the alginate matrix with capillary forces. Moreover, alginate has been used in many applications especially in medical applications as their properties are water soluble, non-flammable, non-toxic and poor for microbial growth [23]. Owing to its properties and gelling ability, alginate has been used not only in therapeutic applications but also in the food, welding, textile, and paper industries as well.

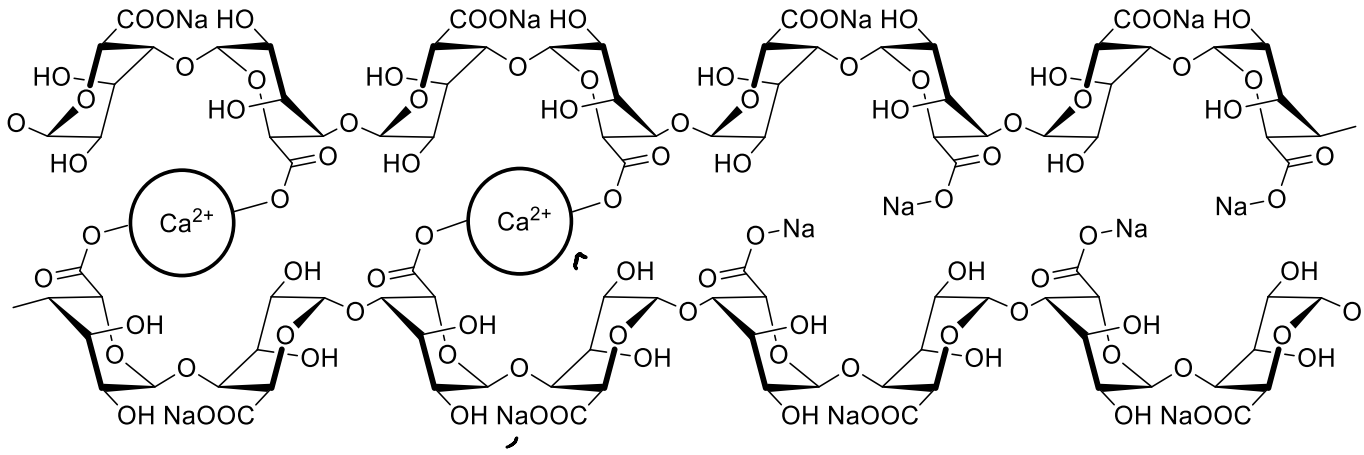

Figure 1.4 Alginate can be ionically crosslinked by a divalent cation (Ca^{2+}) displacing the monovalent (Na^{2+}) counterions of carboxyl groups on adjacent chains in G-blocks into "Egg box" shaped cross-linked network.

The molecular weight of alginate is in the range 32,000-400,000 g/mol and the viscosity of alginate solution depends on the pH as the solution is thicker when pH decreases, at pH 3.0-

3.5 the carboxylic group is protonated and forms hydrogen bonds [23]. The higher molecular weight of alginate results in the improvement of the gel's physical properties, but the viscosity of the solution is also more higher and thus harder to process [24]. Therefore, the molecular weight affect the solution viscosity and the stiffness of the alginate product by the modulus can increase when the viscosity undergoes minimal increase [25].

1.2.2 Biocompatibility

Although, alginate has been used both *in vitro* and *in vivo*, there is still some disagreement within scientific community about the composition of alginate which confers biocompatibility [26]. Mostly, it has been reported that alginate forms with high M content are immunogenic and more potent in inducing cytokine compared to high G content forms [27], but some reports have found no immunoresponse associated with alginate implants [28]. However, given that alginate the immunoresponse may be assigned to impurities within alginate as it is derived from natural sources and contains various impurities such as heavy metals, endotoxins, proteins, or polyphenolic compounds [29]. Moreover, the high purity form of alginate did not display an effect on an animal's body reaction in the same manner as the inflammatory response when in the form of an injection or implant [30].

1.2.3 Derivatives

Amphiphilic alginate has been prepared by adding hydrophobic moieties to alginate backbones which yield and results in self-assembled structures, which can prepare by introducing alkyl chains to the alginate [31]. The solution of such these derivatives offer benefits to the rheological properties which are cross-linked, gel networks that useful for cells repair or regeneration [32]. Microparticles with diameters of around 136 nm can be prepared by dispersing these derivatives in a sodium chloride solution. Such biopolymer based nanoparticles can be used for encapsulation and release of biomolecules [33], such as proteins and enzymes [26]. Hydrogels from this alginate demonstrate long-term stability in media compared to other alginate derivatives [34]. To prolong the drug release, sodium alginate has been hydrophobically modified with poly(butyl methacrylate) [35].

Cell-interactive alginate has been prepared by introducing peptides as side chains. As alginate has less mammalian cell adhesive, peptides can promote and use as adhesion ligands for various cell types [36][37]. For example, RGD (sequence arginine-glycine-aspartic acid) has been used adhesion and growth in 2-D and 3-D cultures of different cells with various concentrations [31].

1.2.4 Hydrogel formation and properties

Alginate is mostly used in a hydrogel form for biomedical applications. The properties of these hydrogel are dependent on the cross-linking processes, *e.g.* ionic cross-linking, covalent cross-linking, thermal gelation, and cell cross-linking used for the gel formation [38].

Ionic cross-linking is the most popular process of preparing alginate hydrogels. The divalent cations is bound with the gluronate (G) blocks. The structure of gluronate blocks are only interacted with a high degree of the divalent ions coordinated. The gluronate blocks of one chain form a conjugate with another gluronate blocks from another chain in the shape of egg-box model (Figure 1.4) [22], resulting in a gel structure. The most common cross-linker is calcium chloride ($CaCl_2$) salt which can rapidly form alginate solution into gel but controlling the rate of gelation is difficult, due to the high solubility in the solutions. The gelation rate can be controlled by using a buffer containing phosphate *e.g.* sodium hexametaphosphate [39]. The phosphate groups compete with the carboxyl groups in the reaction with the calcium ions. In addition, calcium sulfate ($CaSO_4$) and calcium carbonate ($CaCO_3$) reduce the gelation rate as well because of their solubilities. The gelation rate is important to hydrogel as it affects hydrogel uniformity and strength so, the lower the gelation time the more uniform the resultant structures and the better the mechanical properties obtained [40]. Temperature is also a key factor as the gelation rate is reduced at lower temperatures, thus the formation of ionic cross-linking is reduced, leading to a slower gelation and reduced mechanical properties [41]. The disadvantage of using ionic cross-linking is the stability of the gel in long term used in physiological conditions [42]. The gel can be dissolved and exchange the divalent ions in the medium. The calcium ions released from the gel leads to haemostasis in the first stage of

the healing process, but it may be useful or negative depending on the situation [43]. Nevertheless, minimising the degree of biological reaction that occurs reduces the risk to the biological system.

Covalent cross-linking has been used to improve the physical properties of gels mostly for biomedical applications. The application of stress to ionic cross-linked alginate gels resulted in dissociation and subsequent reformation elsewhere in the network, water was lost and plastic deformation was seen to have occurred [44]. Moreover, elastic deformation has been found to occur when water is transferred within the covalent cross-linked gels as the stress is reduced so that the substance cannot reform bonds and dissociate. However, toxicity and the unreacted chemicals from covalent cross-linking gels might not suitable for *in vivo* use and might need to be removed. The first cross-linker, which has been introduced into alginate, is various molecular weights of poly(ethylene glycol)-diamines to obtain hydrogels with different range of mechanical properties. The cross-linking density or weight of poly(ethylene glycol) (PEG) [45] impacts directly on the elastic modulus. The molecular weight of the crosslinker significantly influences the densities and swelling ratio of the resulting alginate hydrogels [46]. Moreover, consideration of more varieties of multi-functional cross linkers may be introduced to make gels with better properties. For instance, to enhance mechanical properties and prolong the degradation rate of poly(aldehyde gluronate) (PAG) by cross linking with multifunction or bifurcating cross-linkers: poly(acrylaminde-*co*-hydrazide) (PAH), or adipic acid dihydrazide (AAD) have been used. The use of PAG/PAH cross-linked gels gave better mechanical properties and longer degradation times than PAG/AAD gels, which could be because of the greater number of attachment points in PAH as well as the higher concentration of the functional groups [47]. Moreover, alginate can be cross-linked by photo cross-linking process which contact directly with cells or drugs by excited with chemical initiators to gelation stage. Alginate gel was prepared by using modified methacrylate that can be cross-linked by photo crosslinker with laser (argon ion laser, 514 nm) for 30 s. This method is very useful to the surgery as it is mostly presences *in vivo* production. However, toxic species may be released from the high resolution of lights thus, an alternative photo crosslinking were presented by using partially

modified polyallylamine with α-phenoxycinnamyldiene acetylchloride then cross-linked by the light exposure at 330 nm [48]. This led to an improvement in mechanical properties for the gels produced from photosensitive polyallylamine and alginate and pervaded to cytochrome c and myoglobin [49].

Thermal gelation has been widely studied to work with drug delivery system because their swelling properties in different temperature can be modified to the allow suitable drug releases from the gels. The most relevant gel which adapts to the thermal gelation process is poly(N-isopropylacrylamide) (PNIPAAm), in which the phase can be reversed near the temperature of the body in suitable media [50]. Alginate has no inherent thermosensitivity, so it has only been used as part of a semi-interpenetrating polymer network (semi-IPN) prepared *via* copolymerisation *in situ* with N-isopropylacrylamide (NIPAAm) and poly(ethylene glycol)-*co*-poly(ε-caprolactone) (PEG-*co*-PCL) under UV irradiation [51]. The concentration of sodium alginate and constant temperature can increase the swelling ratio of the gel and it will decrease when the temperature is higher.

Cell cross-linking had been carried after the potential of using alginate gel with cells by modifying with both chemical and physical methods. Once the cell was added into RGD (arginine-glycine-aspartic acid conjugated to sodium alginate) modified alginate solution, the cross-linked network structure appears without adding any cross-linking agent [52]. It is considered as shear reversible and the action can be repeated several times because when shear force is applied to the gel the structure is broken down and it will recover cross-linking within minutes. This could benefit cell delivery because it can be injected in the liquid state and turned into a semi-solid when injected. However, as cells are added into non-modified alginate solution, the gel cannot be uniform because of the cell-cell interactions. To date, most published studies have explored the use of alginate for drug and cell delivery, which prompts the need to understand more about the biomedical applications of alginate [53].

1.2.5 Biomedical applications

Medical applications that employ alginate can be divided into three main classifications, which are diffusion/setting, vehicle agents, and wound dressing.

Cell culture. In reports of tissue engineering, it has been stated that alginate could be used as a biopolymeric scaffold for cell growth in the forms of both films (2D) and fibres (3D). has been considered as a means of using alginate gels both in 2D and 3D structures. Although, alginate has no mammalian cell receptors, it is biocompatible and easy to combine with proteins and peptides, and the lack of cell adhesion has proved that alginate can be used in cell culture both *in vitro* and *in vivo*. RGD-modified alginate has been studied widely including its use to control the phenotype of interacting myoblasts [54], chondrocytes [55][56], osteoblasts [57], ovarian follicle and bone stromal cells. Many studies have shown that the density of the RGD-modified alginate influences the grow rate of the cell; a more detailed review of cell culture of alginate is provided in Chapter 4.

Diffusion setting. The most common use in which alginate has been used is for the delivery of drugs, cells, or proteins. Whether as immobilised biocatalysts or controlled release of chemical agents, both use the properties of alginate in the form of gel beads formed from diffusion and setting; the basic method involves preparing a solution containing alginate then dropping this into an aqueous calcium salt. The alginate will carry the drug [58] or load cell [59] in the gel form and substance will be protected within the gel until release. In addition, alginate gels have also been used as a glue for repairing the nerve systems and for restoring the cartilage in animal models as well [60][39]. More information about the formation of delivery systems from alginate for pharmaceutical applications is provided in Chapter 5.

Wound dressing. Alginate-based wound dressings have been studied for many years and they offer superior results for wound healing by providing constant moist environment while the pharmaceutical drugs and calcium ions are delivered into the wound to aid faster

recovery. Alginate wound dressings can be produced by using calcium ions to cross-link the alginate into a gel and then freeze-drying into sheets; fibres are also obtained by injecting an alginate solution into a coagulation bath for cross-linking or the electrospinning method . Alginate wound dressings absorb the fluid from the wound and turn this into a gel, which can maintain a physiologically moist environment and minimise the bacterial infection in the wound [61]. Moreover, adding dibutyryl cyclic adenosine monophosphate into the alginate wound dressing helps the wound to heal and the re-epithelialisation thickness to occur within 10 days in rat models [62]. To reduce scar formation, alginate wound dressings have been prepared which release stromal cell-derived factor-1 in surgical pigs [63]. Addition of silver ions in alginate wound dressings can increase the antimicrobial and antioxidant capacity and improve the rate of elastase binding. The zinc ion has also been used to cross link alginate and spin wound dressing fabric which can be help to generate immunomodulatory, antimicrobial, increase keratinocyte migration, and the levels of endogenous growth factors [64].

Figure 1.5 A photograph of a commercially available alginate wound dressing marketed by Medline Industries (Industries, M., (2014) *Maxorb II Alginate Dressings*. Available at: http://punchout.medline.com/product/Maxorb-II-Alginate-Dressings/Alginate-Dressings.)

Alginate has been used widely for medical applications therefore a consideration of its degradation pathway is important when discussing biocompatibility.

1.2.6 Biodegradation of alginate

The ability and applications of alginate have been studied widely, and they have been found to be non-degradable in mammals because the latter lack the appropriate digestive enzyme. However, the ionic cross-linked alginate can be dissolved after releasing the cross-linking ion into the appropriate environment. Once the alginate gel has been dissolved, the high molecular weight of alginate is still higher than the renal clearance threshold of the kidneys so, some of alginate will remain in the body [65]. There are still some potential ways to reduce the alginate or make it degradable in physiological conditions by oxidising the alginate chains which leads to the degradation of alginate in aqueous media [66]. Sodium periodate is used to oxidised alginate by breaking the C-C bond of the *cis*-diol group, leading to a slight reduction in the molecular weight of alginate. However, the temperature and the pH of the medium are also important to the rate of degradation as well. As the gel can only form within the G-blocks of the alginate, thus the oxidation of the G-block facilitates the degradation. For example, at pH 2.85 the oxidation of polygulronate (PG) occurs to form poly(aldehyde guluronate) (PAG) which can cross link with adipic acid dihydrazide (AAD). As this is a covalent cross-linking reaction, the gels form very quickly and degrade in aqueous media; in the same manner as the salt, increasing the AAD concentration influences the degradation rate [67]. This clearly indicates that alginate oxidation can be degraded over time with the appropriate pH, temperature, and suitable cross-linker. In addition, the molecular weight of alginate not only controls the mechanical properties of the gels, but is also an important key factor in the rate of degradation as well [68][69].

1.2.7 Others applications

The other applications in which alginate can be used can be divided into four main groups: the food and beverages (*e.g.* as a thickening agent, gelling agent, emulsifier, stabiliser or texture improver') [70]; arts and crafts (*e.g.* as skin-safe moulds for body and wildlife casting

in art pieces and special effects) [71]; industrial and technical (*e.g.* as thickening agents, texturants and binding agents); the leisure industry (*e.g.* facials and spa treatments) [71].

1.3 Summary and focus of research

Alginates have unique properties that give them the potential to combine and blend with other substances to improve the physical, chemical and/or mechanical properties of the resulting composite materials. Notably, the water solubility and swelling properties of the biopolymer, offer benefits to medical applications, the formation of alginate-based films and fibres should offer the possibility for new smart materials for industrial and tissue culturing. In addition, this research will look at two main applications, medical dressings and neural planting, and this leads to the following questions:

1. Can alginate, in the forms of both films and fibres, display extrinsic electrical conductivity?
2. If alginate can display extrinsic conductivity, will this form also display desirable mechanical properties?
3. Is it possible for neuron loading to occur on the conductive alginate-based surface?
4. Can layered materials such as organically modified synthetic clays (organoclays) cross-link alginates and the resulting nanocomposite networks encapsulate and release drug molecules such ibuprofen?

The motivation of this research is to examine the methods and develop biomedical materials with function properties based on alginate nanocomposite. Through this thesis, selected chemical and mechanical properties, *e.g.* strength, electrical conductivity *etc.* of alginate have been explored to determine the suitability of the biopolymer as implants and devices.

1.4 Thesis outline

Following this initial chapter, in which the reader is introduced to the general field of alginate chemistry, the thesis is broken down into six chapters, of which three (Chapters 3-5) deal with experimental themes.

1.4.1 Chapter 2, Materials and Experiment

The materials used in this research and the fundamental operation of the characterisation methods employed are explained in this chapter.

1.4.2 Chapter 3, Alginate based conductive fibres

Chapter 3 presents the experiments carried out on alginate based fibres, which have been prepared by a wet-spinning process. The alginate is doped with the commercial conducting polymer PEDOT:PSS and combined with a commercial PEG and subjected to heat treatment. The resulting materials are characterised (using FTIR and SEM) and stimulated electrical circuits are formed, to determine their conductivity and mechanical properties. The effect of the thermal treatment on the mechanical and conductivity properties are examined.

1.4.3 Chapter 4, Conductive films for neurons implant

Chapter 4 investigates the biocompatibility of alginate based conductive composite films, produced in Chapter 3, with neurite implants to explore the possibility of using the functional films for tissue engineering. Samples of alginate are combined with different compositions of PEDOT:PSS and crosslinked and calcium chloride, in order to determine the optimum combination to support cell growth.

1.4.4 Chapter 5, Biopolymer-organoclay composite Hydrogels for controlled drug delivery

The results of Chapter 4 demonstrated the biocompatibility of the alginate in connection with supporting cell growth, and Chapter 5 explores the potential of these materials for *in vivo* drug delivery. This chapter investigates different application of alginate based soft composite materials. In this study, alginate –organoclay hydrogels are prepared for drug delivery

applications. Range of physic-chemical characterisation techniques including rheology, electron microscopy and spectroscopy is used to characterise the nanocomposite hydrogels. Moreover, the rheology, FTIR and swelling ratio were carried out and compared to alginate cross-linked with calcium chloride.

1.4.5 Chapter 6, Conclusions and future work

The final chapter contains a summary of the work obtained within this thesis and implications of the results obtained from each chapter. Recommendations for future experiments and the development of the research are also given in this chapter.

Chapter 2

Experimental Materials and Methods

This chapter describes the materials and methods which are used in the experiments detailed in Chapters 3, 4, and 5. A brief description of the principles of the analytical techniques and the methodology for evaluation of the results is included. More detailed procedures are given in each of the experimental chapters.

2.1 Materials

2.1.1 Conductive fibres experiment

Two types of sodium alginate (ALG, obtained from FMC biopolymer, Cork, Ireland) were used: (a) medium viscosity, with high mannuronic acid (M) content (Protanal DH), molecular weight is 10 – 160 kDa, guluronic acid:mannuronic acid (G:M) ratio is 30 – 40 % : 60 – 70 %, viscosity is 40 – 90 mPas, 1 % sol., particle size is 250 microns and (b) high guluronic acid (G) content (product code LF 10/60), molecular weight is 90 – 130 kDa, G:M ratio is 60 – 70 % : 30 – 40 %, viscosity is 30 – 60 mPas, 1 % sol., particle size is 250 μm (as received from the supplier). Poly(ethylene glycol) (molecular weight 200 g/mol.) (PEG) and calcium chloride ($CaCl_2$) were purchased from Sigma Aldrich (Gillingham, UK). PEDOT: PSS (Clevis PH100), 1.1 wt% in water was obtained from Heraeus (Leverkusen, Germany).

2.1.2 Neurons experiment

Poly(vinyl alcohol) (PVA) (molecular weight 130 kDa) was purchased from Sigma Aldrich (Gillingham, UK). 24 well-plates (Falcon™ Polystyrene Microplates) and glass coverslips were obtained from Fisher Scientific. The plating medium was consisted with poly-L-lysine (PLL), Neurobasal-A medium, 2 wt% of B-27 supplements, 1 wt% of Glutamax I (Q), Horse serum (H/S) with 5 wt%, Penicillin-Streptomycin (P/S) 1 wt%. The feeding medium was composed of Neurobasal-A medium, 2 wt% B-27 supplements and 0.4 wt% of both Glutamax and Penicillin-Streptomycin. Water for tissue engineering (Gibco™ distilled water) was prepared by distillation and filtration (0.1 μm) with no additive and PBS were also from Thermo fisher Scientific (Paisley, UK). Rat cortical neurons were dissected from E15-17 rat embryos and supported by the Centre for Synaptic Plasticity group, Dr Jonathan Hanley's lab (University of Bristol, Neuroscience, UK). A viability/cytotoxicity assay kit for animal was obtained from Biotium (California, USA) and used to observe living and dead cells.

2.1.3 Biopolymer-Organoclay Hydrogel

Organoclays were synthesised using magnesium chloride hexahydrate and 3-aminopropyltriethoxysilane, both were purchased from Sigma Aldrich (Gillingham, UK). Alginate with high G content (W201502) and Ibuprofen were also obtained from Sigma Aldrich (Gillingham, UK).

2.2. Characterisation

2.2.1 Ultra Violet – Visible Spectroscopy

UV-vis absorption spectroscopy technique is used to relate the specific wavelength with the wavelength of concentration of the sample solutions in the cuvette. This technique also can determine the nature of the chemical compound, production or consumption during reaction in the solution. The light absorption and concentration of the solution can be related and explained by the Beer-Lambert law as follows:

$$A = \log_{10}\left(\frac{I_0}{I}\right) = \varepsilon C l \tag{2.1}$$

where A is absorption, I_0 is the intensity of transmitted light, I is the intensity of incident light, ε is the molar absorptivity of the compound, C is the concentration of the compound and l is the path length of the sample.

The compound in samples will absorb the wavelength of light when the energy is equivalent to the highest occupied molecular orbital (HOMO) and lowest unoccupied molecular orbital (LUMO).

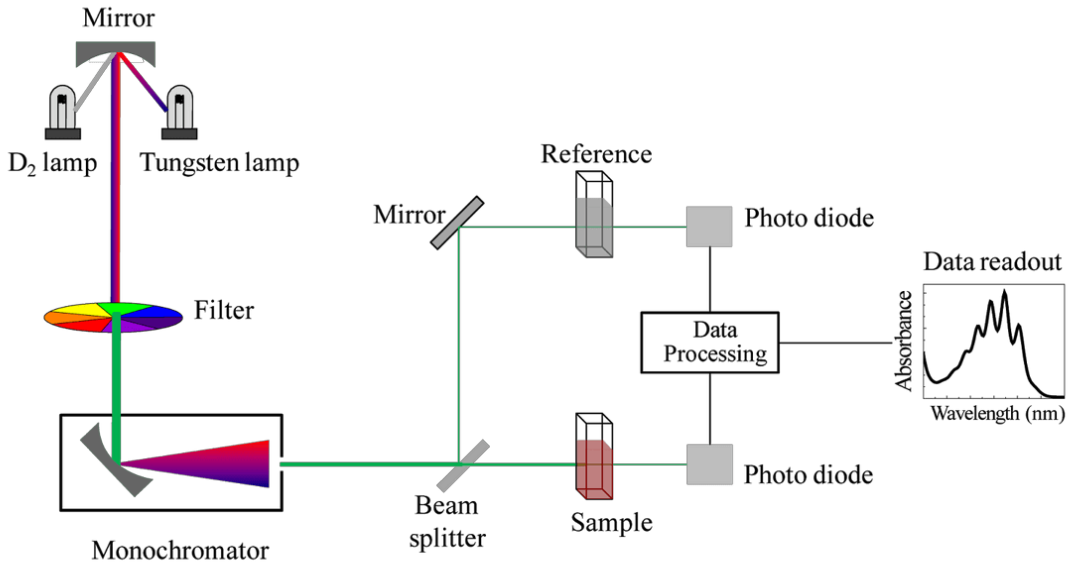

Figure 2.1 Schematic showing the operation of the UV—visible spectrophotometer to produce a spectrum as a function of absorbance against wavelength [73].

This technique is generally used to determine the concentration, or chemical conversion, of a component in solution. A widely used use of this is to measure drug delivery system by monitoring the absorbance peak of the compound within a liquid sample. The system is highly sensitive and can be used to give the concentration of the drug dispersed in the solution by comparing with the absorbance peaks of a set of standard solutions. Therefore, UV-vis absorption spectroscopy was used to observe the concentration of drug loaded into hydrogel various of time. Hydrogels containing Ibuprofen were placed into a 1 L dI water

flask bottle with the sealed cap. The solution was taken at regular time intervals. The release rate of Ibuprofen was monitored by the measuring the changes of absorption intensity peaks at 264 nm (Figure 2.2), using UV-Vis spectroscopy. An average of 10 samples were collected and calculated.

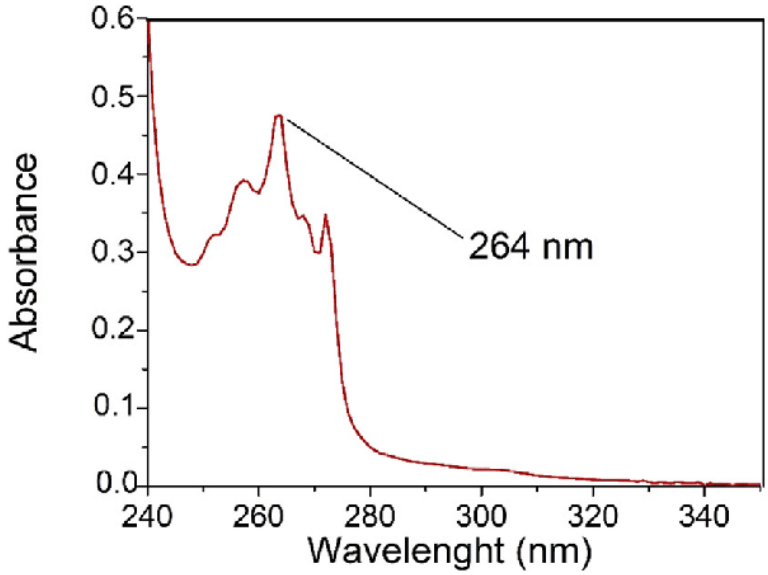

Figure 2.2 Typical UV-Vis absorption spectrum of ibuprofen in distilled water (500 μg/mL) showing the characteristic peak at 264 nm, which was used as the reference to monitor the release rate of the drug molecules from the hybrid hydrogel samples.

2.2.2 Fourier Transform Infrared spectroscopy

Fourier Transform Infrared spectroscopy (FTIR) is used to determine common chemical bonding present within samples by the absorption of infrared radiation, causing the vibration of the chemical bonds to increase in amplitude. The characteristic absorption wavelengths may be related to specific functional groups and chemical moieties (Table 2.1). FTIR spectra were obtained using a Spectrum 100 Optical (PerkinElmer, UK). This technique was used to analyse samples in each experimental chapter to identify chemical changes and interactions between the materials within the samples.

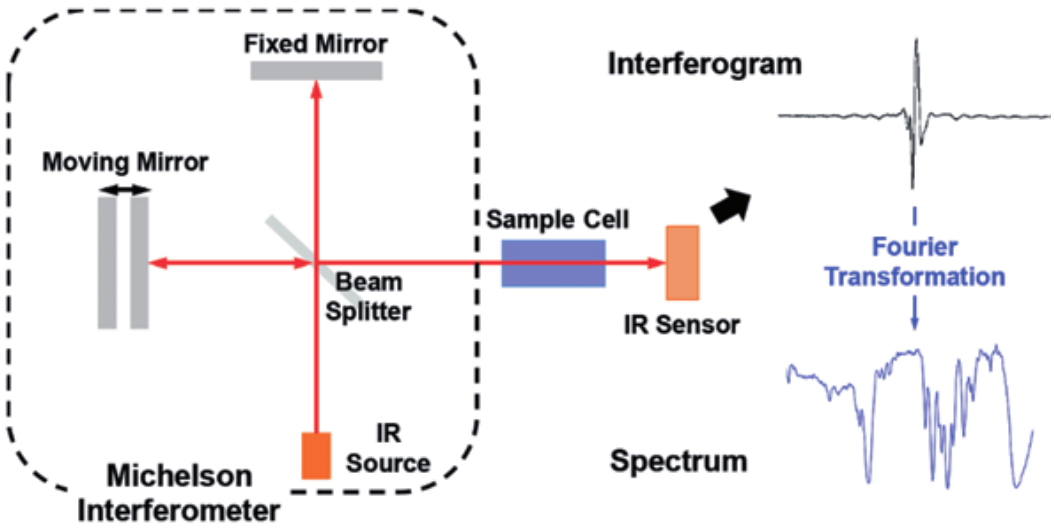

Figure 2.3 Schematic showing the operation of the FTIR spectrometer to produce an interferogram and an infrared spectrum through Fourier transform [74].

Table 2.1 Common infrared structural assignments [73]

Wavenumber (cm^{-1})	Functional groups	Wavenumber (cm^{-1})	Functional groups
3400 - 3650	Alcohol O-H	1730	Aldehyde C=O
3300 - 3500	Amine N-H	1715	Ketone C=O
3300	Alkyne ≡C-H	1710	Carboxylic acid C=O
3200, 3400	Amide N-H	1690	Amide C=O
3020 - 3100	Alkene =C-H	1660 - 2000 1450 - 1600	Arene C=C
3030	Arene C-H	1640 - 1680	Alkene C=C
2500 - 3100	Carboxylic acid O-H	1540	Nitro
2720	Aldehyde C-H	1030 - 1230	Amine C-H
2100 - 2260	Alkyne C≡C	1050 - 1150	Alcohol C-O
2210 - 2260	Nitrile C≡N	900 - 600	Finger print
1735	Ester C=O		

2.2.3 Differential Scanning Calorimetry

The Differential Scanning Calorimetry (DSC) technique is used to measure the heat flux (heat evolved as exothermic transitions or absorbed as endothermic transitions) for different thermal events (Figure 2.4).

(a)

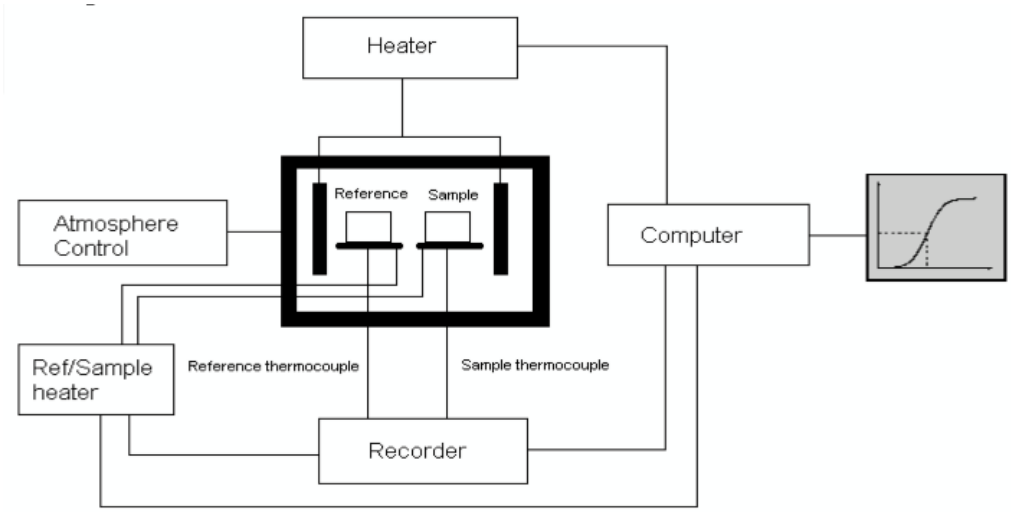

(b)

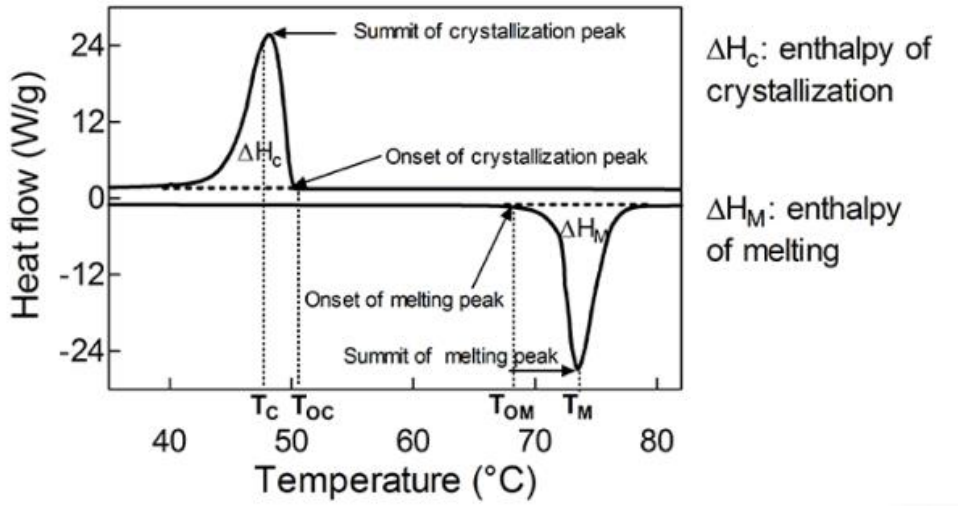

Figure 2.4 (a) Schematic showing the operation of the DSC technique [75], (b) a typical DSC thermogram obtained from a controlled heating tamp experiment showing some of the parameters that may be obtained (the temperature of the peak of crystallisation T_c, melting peak T_M, onset of crystallisation, T_{OC}, and onset of melting peak, T_{OM}).

This technique is frequently used in chemistry, biochemistry, cell biology, pharmacology, and nanoscience to measure the characteristic properties of a sample which may undergo

fusion, crystallisation, glass transition, oxidation as well as other chemical reactions. In this research DSC was used to examine the glass transition temperature of the hydrogels in Chapter 5. For this, TA Q200 differential scanning calorimeter using hermetically-sealed aluminium pans was employed. The freeze-dried hydrogel samples were heated at a rate of 10 °C/min from 20 to 300 °C in a flowing N_2 atmosphere (40 ml/minute). Samples were cycled for six times and the thermal response was recorded.

2.2.4 Rheology

Rheology is a method for describing the flow behaviour of materials in the fluid state by measuring flow by subjecting the sample to controlled strains (torsional or oscillatory) at different speeds and amplitudes. The rheometer measures stress through a rotating spindle that applies a constant torque or rotation speed and reports data as shear stress or shear rate. There are three different geometries to test depending on the appearance of samples: concentric cylinders are for very low to medium viscosity, cone and plate for very low to high viscosity and parallel plates for low viscosity to soft solids. The materials examined in this study contain a mixture of both liquid and solids and exhibit both viscous and elastic behaviour when sheared which is called viscoelasticity. Rheometry yields data for the storage modulus G' and the loss modulus G". The storage modulus represents the elastic behaviour in the materials or solid-stage behaviour, while the loss modulus represents the viscous portion or liquid-stage behaviour in the materials.

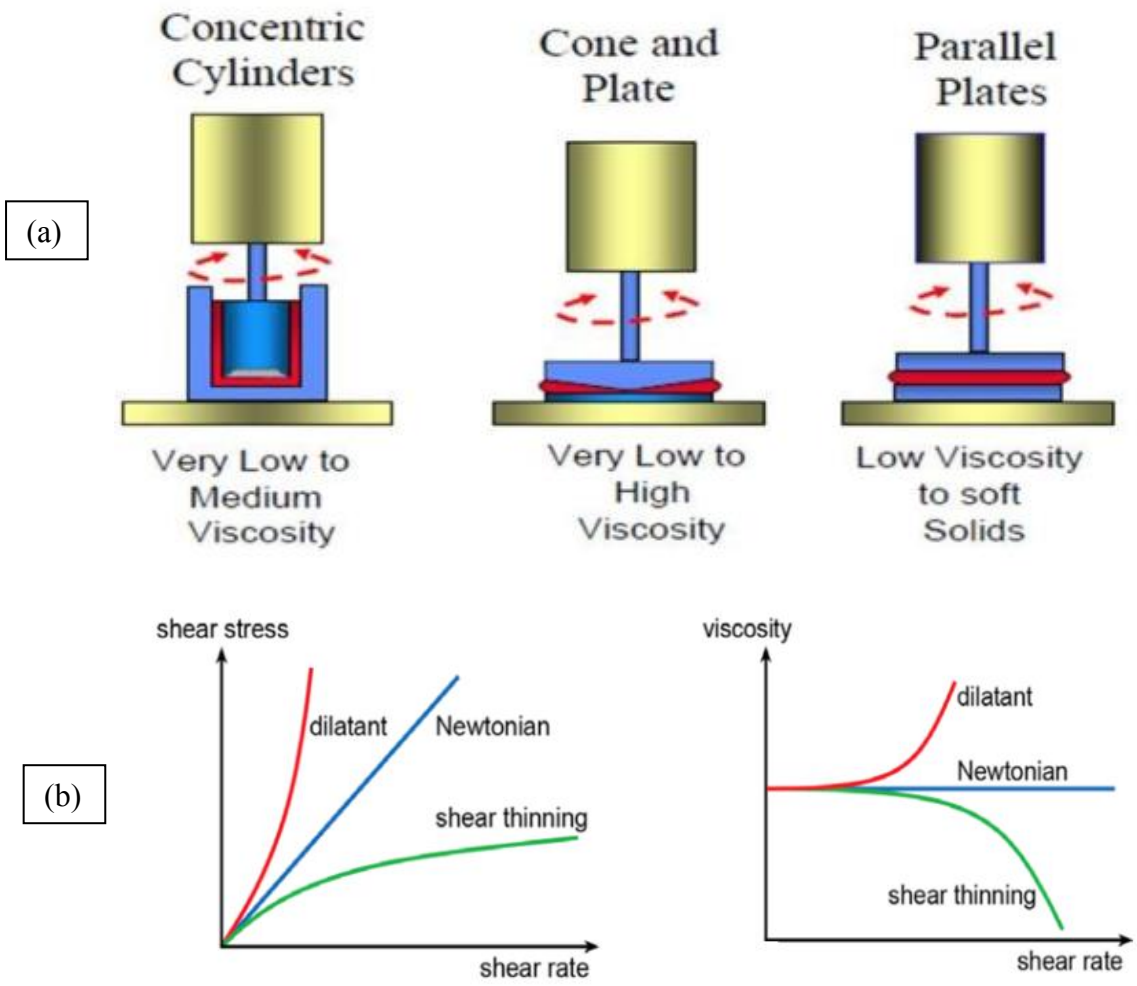

Figure 2.5 a) Schematic showing operation of different rheometer modes [76], b) Typical flow curves for shear stress and viscosity as function of shear rate.

The viscosity measurements were carried out using a Haake Mars II Rheometer; typical testing sample size was 5 ml. The plates were set at 20 °C with a 1 mm separation, and the shear rate was modified between 0.1 to 100 (1/s) in logarithmic steps. As with the FTIR, hydrogel with the calcium chloride cross linker was used as a comparison with the organo composite hydrogel.

2.2.5 Optical and Fluorescence microscopy

The optical microscopy technique is operated by using magnification lenses to enlarge the sample image using illumination. The objective lenses change the reflection angle of the light through glass and air then reflect this into optical lenses or a camera. Optical microscopy can also be combined with a UV lamp which allows the excited samples to be imaged by the emitted light. Fluorescent microscopy was used to detect the distribution of the fluorescent compounds in the samples. The resolution of images and visual view from the microscope are dependent on wavelength which is set between 180 and 400 nm that control the numerical aperture of objective lenses. The operation of the microscope is shown in Figure 2.6.

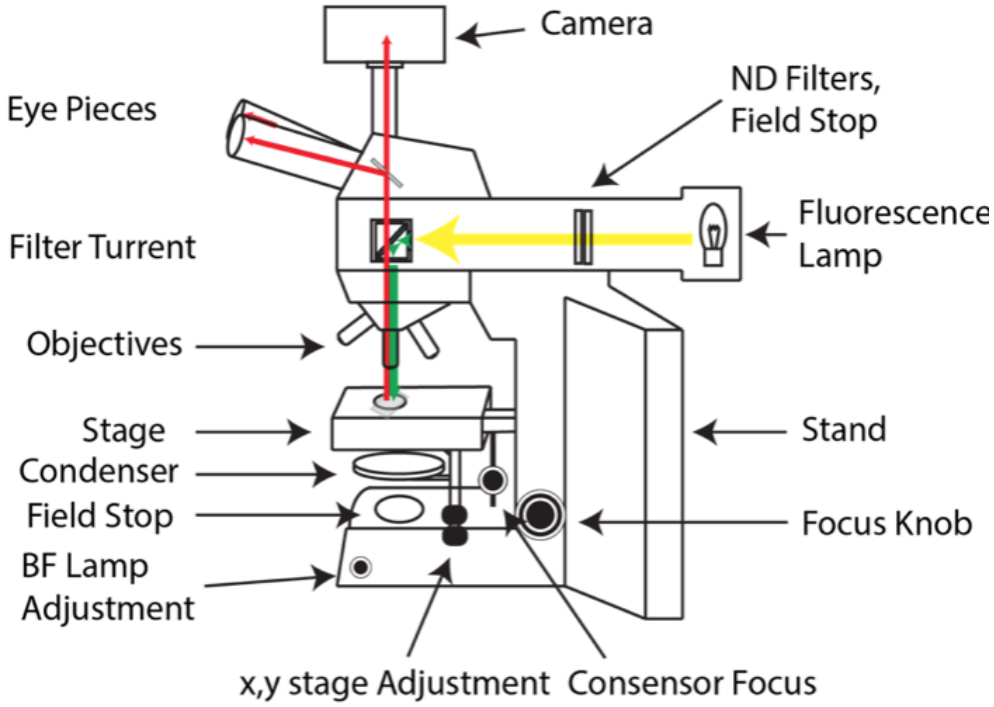

Figure 2.6 The wide field-fluorescence microscopy principle which is included the fluorescence lamp to excite the sample and show the UV detected area only. The colour blue green and red wavelength are used to illuminate the stained sample [77].

The optical microscope (DMI 300B Microscopy, Leica, Watzlar, Germany) was used to observe samples within Chapter 3.

For the study of the neurons, the 7-day old plate was rinsed with PBS and observed by viability/cytotoxicity assay kit for animal, living and dead cells which purchased from Biotium. The assay was diluted in PBS by using the transparent solution (substrate calcein) 2 % wt and the red solution (Ethidium homodier III) 0.5 %wt then each well was filled with the prepared stain solution (200 µl). Each Film was taken and placed on the glass slide then investigated with fluorescent microscopy (wide-field imaging, Leica DM IRBE inverted microscope), images were recorded in different regions of the film using Volocity software. These steps also were applied to the 14 days old plate. Data were transferred to imageJ software to count the number of dead and live cells. An average of 10 films were prepared and compared with samples obtained following treatment conditions, the absence of treatment, and from the control samples.

2.2.6 Scanning Electron Microscopy

Scanning Electron Microscopy (SEM) is technique in which a beam of electrons is produced by heating a filament or applying an electric field then pass this through an anode which forces the negatively charged electron beam to undergo an acceleration. Magnetic lenses are used to narrow and focus the beam on to the surface of the sample. The atoms on the surface of the sample interact with the electron beam and transform the beam into a scattered electron pattern, which is then detected. Sophisticated computer software translates the signal into highly resolved images of the surface.

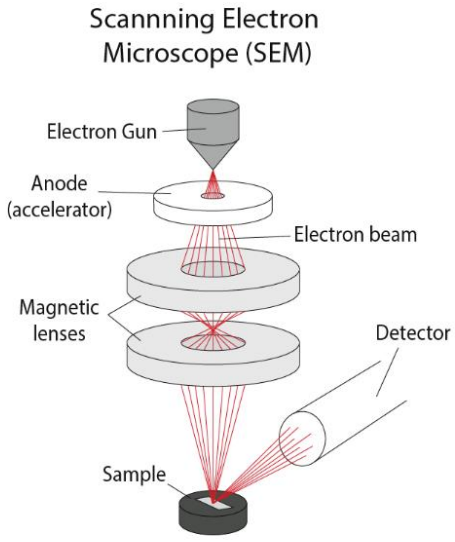

Figure 2.7 Schematic showing the operation of Scanning Electron Microscopy [78].

Each experimental chapter in this research used different SEM methods, *e.g.* in Chapter 3 a Zeiss EVO 40 SEM (Carl Zeiss, Germany) was used and samples were sputtered with silver; in Chapter 5 a JEOL IT 300 SEM was used and samples were sputtered with gold.

2.2.7 Conductivity testing

Electrical properties are testing under the standard of American Society for Testing and Materials (ASTM); ASTM B 193-87. Conductivity testing involves a measurement of the resistance (R) of the specimen, carried out using an Ohmmeter, then calculated using Ohm's law for typical material with the following equation:

$$V = IR \tag{2.2}$$

where V is voltage, I is current and R is resistance.

However, thin, small or fibrous materials cannot be tested directly by an Ohmmeter so, a bridge circuit or potentiometer is introduced to measure the resistance instead. The four-point probe method (Figure 2.8) is the most accurate when testing conductive fibres as a constant potential is applied all along the sample. Four copper wires are stretched on a non-conductive materials block, with a precise gauge length fixed between two inner wires. Four copper wires are then connected to individual copper terminal blocks. The outer leads are then connected to the current source while the inner leads are used to check the drop in voltage across the sample. A fibre sample which may be pasted and painted with conductive silver is laid along the lead wires then the resistance measured and the conductivity calculated using the equation follow:

$$S = \frac{RA}{L} \tag{2.3}$$

where S is conductivity, R is resistance, A is cross-sectional area and L is gauge length.

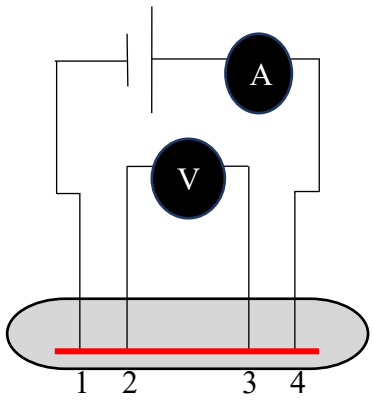

Figure 2.8 Four probe conductivity testing system while a single fibre is placed along current probe (1 and 4) and voltage probe (2 and 3) [79]. The gauge length is the distance between the voltage probe (2 and 3). The ammeter and voltmeter provide some readable value which the resistance can be calculate from the equation $V = IR$

The conductivity testing was set with the gauge length at 2 mm. This testing was carried with 10 samples for each condition.

2.2.8 Tensile testing

Tensile testing technique is used to understand the samples behaviour and properties when giving tension until failure. The measurement from this technique gives values of stress, strain, maximum elongation, and breaking point, which then can be used to calculate the Young's modulus, yield strength, and strain hardening characteristics of the samples as follows:

$$\text{Young's modulus equation; } Y = \frac{\sigma}{\varepsilon} \tag{2.4}$$

$$\text{Engineering stress equation; } \sigma = \frac{F}{A} \tag{2.5}$$

$$\text{Engineering strain equation; } \varepsilon = \frac{\Delta L}{l} \tag{2.6}$$

where Y is Young's modulus, σ is engineering stress, ε is engineering strain, F is force, A is cross section area, ΔL is the change in length, and l is the original length. The analysis of a typical tensile graph is shown in Figure 2.9.

(a)

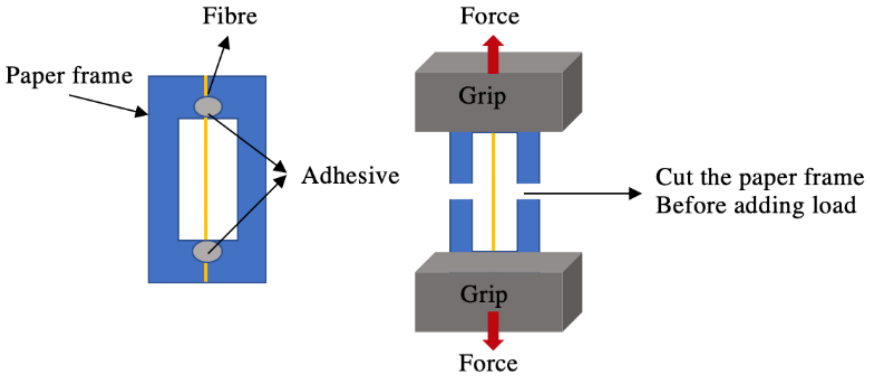

(b)

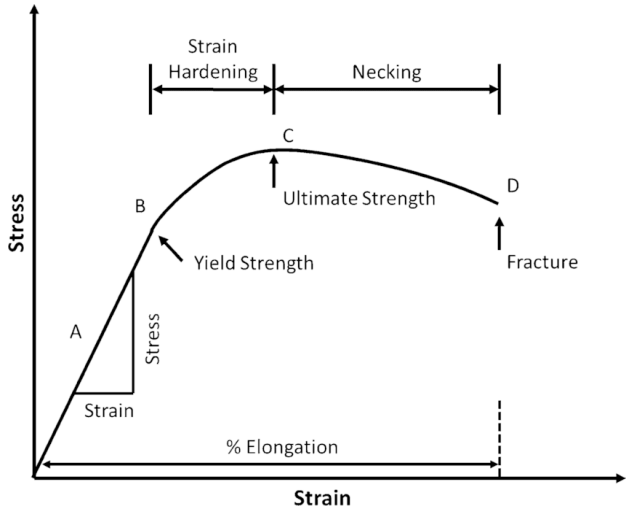

Figure 2.9 a) Tensile testing of single fibre by using paper frame which the fibre was fixed on the paper frame with super glue before place between the grips and cut the paper frame in half for both sides before adding load for tensile testing. b) The graph of standard stress and strain from materials tensile testing where the area A is the Young's modulus of the materials, B is the elastic stage of the materials, C is the plastic stage of the materials and D is the breaking point [80].

The specimen for tensile testing is different for each material which follows the standard of American Society for Testing and Materials (ASTM). For single fibre testing in Chapter 3 is followed the ASTM C1157 using paper frame as Figure 2.8 and tested by an Instron 3343. The gauge length was fixed at 15 mm for every sample. The diameter of each fibre was observed in three different areas for ten samples each condition while they were placed on the paper frame.

2.2.9 Swelling ratio

The swelling is the unique property of polymers and hydrogels which can absorb liquid or water without dissolving. The swelling ability of the hydrogel depends on the crosslinking reaction within polymer which can be either reversible or irreversible. Typically, the swelling ratio can be calculated from the difference in weight before and after exposure as follows:

$$Q = \frac{We - Wd}{Wd} \tag{2.7}$$

where Q is the swelling ratio, We is swollen gel mass, and Wd is dried gel mass.

The swelling property was determined by mass measurements. As prepared organoclay-alginate and Ca-alginate hydrogels were completely dried at room temperature until a constant weight was achieved, cut into pieces 1 x 1 cm, and soaked in water at different time intervals (15 mins, 30 mins, 1 h, and 2 h) as depicted in Figure 2.10.

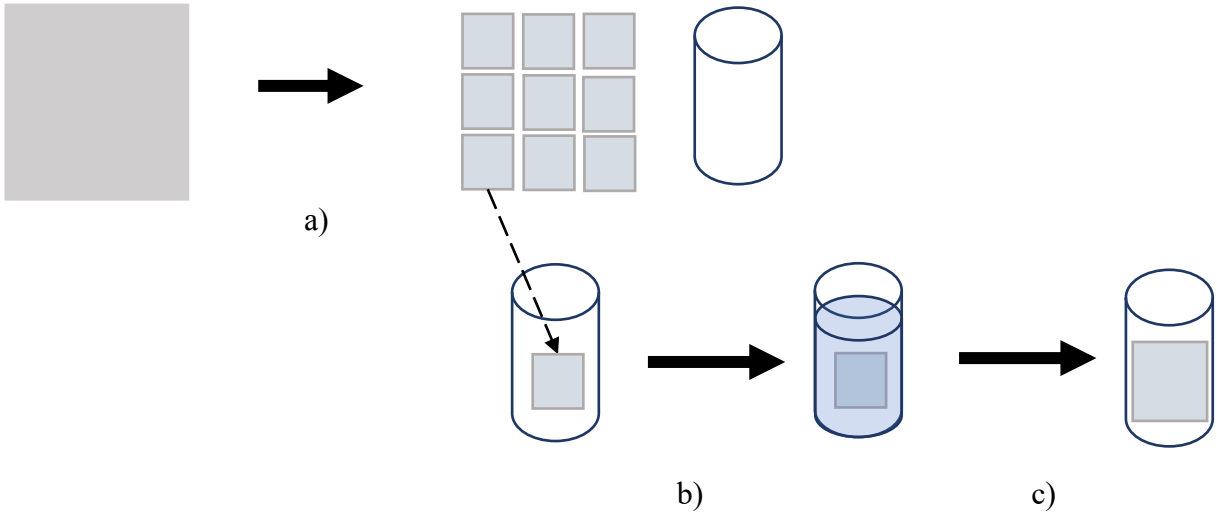

Figure 2.10 Schematic representation of the experiments performed to calculate swelling ratio (a) dried hydrogel at room temperature was cut into small pieces (1 x 1 cm), weighing each piece and vial before being filled up with water (5 ml) (b), and (c) water was removed at different time intervals and the re-hydrated swollen hydrogel samples were weighed.

2.3. Conclusion

Experimental materials and a brief introduction to physicochemical characterisation techniques employed in this study are provided in this chapter. Each experimental chapter utilises alginate as a base material which is integrated with various biological, organic, inorganic materials either *via* non-covalent interactions or through physical blending processes to produce functional composite materials with desired properties for medical applications. Further, specific details of experimental conditions, data analysis and properties of the samples produced in various projects are described in each experimental chapter.

Chapter 3

Alginate based conductive fibres

Nowadays, not only metal constituents and nanoparticles but also synthesis polymer which is more flexible to use and lightweight, are conductive for generally used as well. Owing to their electrochemical properties, low costs and well-established synthesis protocols, conductive polymers are being investigated for range of applications, for example, flexible electronics and textile. Conductive textiles are emerging materials that could find applications in the development of healthcare devices, electronics as well as in advanced aerospace engineering technologies such as waste water treatment, censer and energy *etc.*[81][82]

Fibres were considered as flexible structure of materials in term of using, they can form into many shape and size depending on the applications in used. Also, they can easily add into others materials to improve the properties and ability to meet the requirements, such as composite materials *etc.*[82] Therefore, both natural fibres or synthetic fibres are widely found as important component in advance materials.

The aim of this study was to expand the possible applications of alginate-based conductive fibres by wet spinning process which mainly focus in biomedical applications, while the electrical conductivity achieved through conductive polymer to reach the minimum requirement in mechanical and electrical properties.

3.1 Alginate fibres

According to alginate properties and applications discussed in Chapter 1, wet spinning of alginate converts alginate powder into fibre forms by dissolving sodium alginate in water and spinning through a coagulation bath; calcium chloride is the most common cross-linker for alginate. Fibres obtained can be stretched during the process then washed in water and dried at room temperature. The properties of calcium alginate fibres depend on type, molecular weight of alginate, concentration of spinning solution, temperature, concentration of calcium chloride, and stretching rate. To obtain the best properties, the time required for coagulation is about 5 s and the typical diameter is around 100 μm with a circular cross section.

Alginate can also be spun as fibres containing additives such as silver, pectin, carboxymethyl cellulose, drug, enzyme, cells, or nano materials which depend on the properties and ability required which summarised in Table 3.1.

Table 3.1 The summaries of example of alginate fibres and methodology

Alginate fibres	Methodology	Ref
Sodium alginate fibres	Treated Ca-alginate fibres with HCl, the Ca^{2+} was replaced by H^+ then, treated with Na_2CO_3 or NaOH result that H^+ was replaced by Na^+. The fibres obtained was contained with both Ca^{2+} and Na^+, but the fibres become more absorbent.	[83]
Alginic acid fibres	Alginic acid fibres is simply made by extrusion Na-alginate into H_2SO_4 bath. Another method is to convert Ca-alginate fibres by washing with hydrochloric acid, the alginate fibres will remain solid without Ca^{2+} residue.	[84]
Zinc alginate fibres	Na-alginate solution can be injected into $ZnCl_2$ coagulation bath to obtain Zn-alginate fibres. Or treated Ca-alginate fibres with $ZnCl_2$ solution, ion exchange will be occurred and result in Zn-alginate fibres.	[85]
Silver-containing alginate fibres	$AgNO_3$ was mixed with Na-alginate and low concentrate of $CaCl_2$ solution, then extrude to $CaCl_2$ mixed with $AgNO_3$ result in formation of Ca-alginate fibres containing Ag^+.	[86]
Alginate fibres containing pectin and carboxymethyl cellulose	Fibres from alginate mixed with pectin and CMC was spun and stretched at 80 °C and wash with acetone then dried with heat air.	[87]

3.2 Introduction to alginate fibre spinning process

Polymer processing in the form of fibres provides an excellent opportunity to fabricate functional composite materials.

3.2.1 Electrospinning

Electrospinning is the method for fabrication of uniform nanofibers from variety of materials. The process involves with electric field between the syringe and collector platform. The basic electrospinning set up consists of high voltage generator, syringe pump, syringe and the collector platform as shown in Figure 3.1. The surface tension holds the polymer droplet at the tip of syringe while the electric field generates a jet ejection which result of stretching and elongating polymer into dry fibres at the collector. The ejection starts with a straight line of fibres and continue by whipping instability. The fibres obtained properties can be controlled by the process parameters which are polymer solutions (viscosity, conductivity, surface tension, concentration), equipment set up (voltage, distance between tip and collector, shape of collector, ejection rate, needle diameter), and environment factors (temperature and humidity) [88].

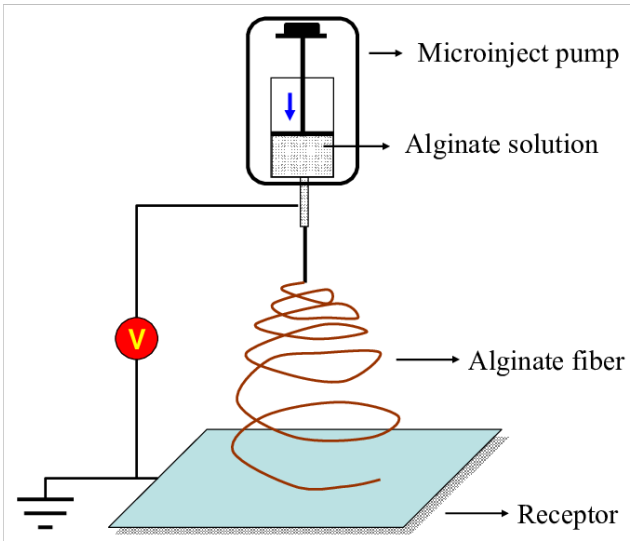

Figure 3.1 The electrospinning setup for alginate nanofibres spinning [89].

According to the structure of alginate which is polyelectrolytes, alginate alone cannot spin via electrospinning method. Therefore, there are numerous studies on alginate electrospinning which the methods contribute with hydro soluble polymers blending, co-solvent system, and structure modified alginate as summarised in Table 3.2.

Table 3.2 An example of alginate fibres obtained from electrospinning.

Method	Description	Ref
Pure alginate	Electrospinning of alginate solution without carrier polymer employed, only droplet was observed at the collector due to lack of entanglement between molecular chains.	[90] [91]
Co-Solvent systems	One or two solvents (*e.g.* glycerol and water, ethanol and $CaCl_2$) was introduced to fabrication of electrospun alginate.	[92]
Hydro soluble polymers	To facilitate alginate spinnability, hydro soluble polymer (*e.g.* PVA, PEO, *etc.*) was added in alginate solution to enhance the spinnability.	[93] [94] [95]
Co-solvent/Surfactant and carrier polymers	To increase the content of alginate solution, surfactant and co-solvent were added to decrease the surface tension.	[96] [97]
Structural modification	The –OH groups was replaced by esterification, oxidation or sulfation to the rigidity in chain conformation.	[98] [99]
Advanced electrospinning	Combining alginate with other natural polymer (*e.g.* chitosan, PCL, *etc.*) has been reported by employing a co-axial electrospinning technique. This was included the collector modification to fabricate the desired shape.	[100] [101]
Other polymers	To facilitate the spinning ability of alginate, polymers (*e.g.* PLA, PGLA, *etc.*) to obtain bead-free nanofibers and have alginate dispersion along the fibres.	[102]

3.2.2 Wet spinning

Polymers can be changed their form into another form by converting themselves into the liquid state, spinning is one of the processes that converts polymer into fibre forms[103]. The polymer solution is extruded through small holes and emerges as fine fibres. Man-made fibres can be classified as wet and dry spinning processes which were developed in the 1800s. Wet spinning is the oldest and simplest and process to produce continuous fibres for several metres from polymer solutions by extruding through a small hole into a coagulation bath which compacts the polymer macular into chains and firm structure [104]. During this stage the polymer solution will convert into a single gel fibre. The properties and diameter of fibres were controlled by the initial injection speed and drawing speed which stretching the fibre. Dried fibres will be collected at the final stage which the solvent or water will be evaporated to leave the neat polymer fibres at the drum rolls (Figure 3.2). This method requires a homogenous and bubble-free solution to pass through the small needle so, it is widely applicable to different polymer solutions to be spun into fibre filaments, including composite fibres [105].

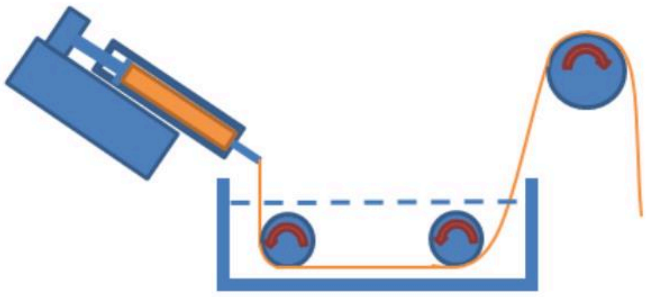

Figure 3.2 Wet spinning process by syringe pump system

The applications of alginate fibres both prepared by electrospinning and wet spinning can be used in biomedical which are wound dressing (explained in Chapter 1), tissue engineering (explained in Chapter 4), cancer therapy and delivery system (explained in Chapter 5).

3.3 Introduction to conductive polymers

Many research had brought conductive films and fibres into biomedical such as drug delivery, bioactuators or tissue engineering [106]. For cell growing and attaching abilities PEDOT was impressive in term of high conductivity and chemical stability to let cells settle down especially neurons [107]. Knowledge of conductive polymers and alginate lead the objective of producing the conductive films for biomedical and smart textile by wet spinning process with and without conductive enhancer then characterised the conductivity, mechanical properties and chemical bonding.

Conductive polymers (CPs) are a generation of organic materials with both conductive and optical properties, which were first invented in 1970s by Alan MacDiarmid, Hideki Shirakawa and Alan Heeger [81], polyacetylene (PA) which is semi-conductive itself doped with oxidised of iodine was reported a 10 million-fold increased in conductivity [108]. Since then, the oxyacetylene is one of the most studied in CPs field, but the handling and processing of these polymers is often hampered due to their non-cyclic chemical backbone and reactivity towards air. To overcome this challenge, there has been constant quest in the synthesis and development of stable, processable conductive polymers with tuneable electronic properties. As a result, this area of research has led to produce over 25 types of conductive polymers [82]. The key examples include polyprrole (PPy), polyaniline (PANI), polythiophenes (PT), and poly(3,4-ethylenedioxythiophene), *etc.* whose structures are shown in Figure 3.3.

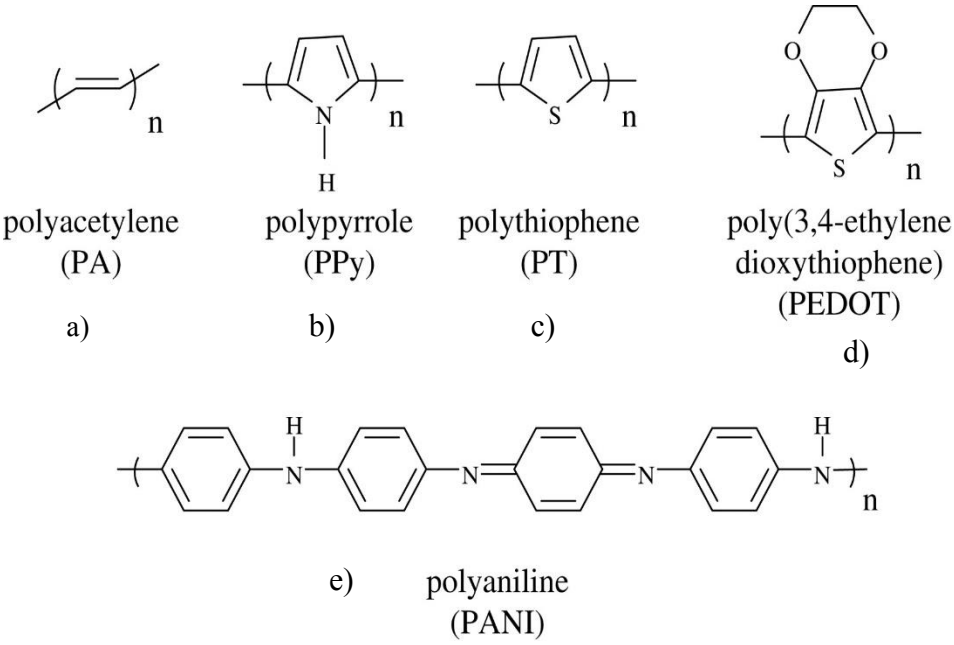

Figure 3.3 Chemical structures of common conductive polymers [109], a) polyacetylene (PA), b) polypyrrole (PPy), c) polythiophenes (PT), d) poly(3,4-ethylenedioxythiophene) (PEDOT) and e) polyaniline (PANI),

CPs are produced by chemical polymerisation or electrochemical polymerisation processes [110]. The monomer solution is mixed with the oxidising agent for chemical polymerisation, which creates a thick layer or powder of CPs. This process which included condensation polymerisation gives more options of CPs' backbone modification during or the end of the synthesis process and can produce in a large scale but the process is complicated [111]. On the other hand, electrochemical polymerisation is achieved by supplying electric current into a mixture of monomer solution, solvent and dopants through electrodes, the electric current is applied into a monomer solution, solvent and dopants trough electrodes for electrochemical polymerisation [112]. It is easy to prepare, can provide the thin film products also organic molecules can be trapped inside the polymer but modification of post-covalent are difficult [113]. CPs can be classified into three main categories; polypyrroles (PPy), polyanilines (PANI), and polythiophenes (PT) which can be doped with different organic compounds to improve their electrical conductivities [81]. Typical conductivities listed in the literature are descripted in Table 3.3 and these values can be enhanced by adding dopants, which are

mostly biocompatible molecules during synthesis process. The positive charge will occur in the molecule of CPs chemical structure and match with the positive charge from the molecules of additives. However, the size of molecules will also affect the mechanical properties of the CPs as well [114].

Table 3.3 Families of conductive polymers and their electrical conductivities (S cm^{-1}) [114]

Conductive polymers	Conductivity (S cm^{-1})
Polyacetylene (PA)	10^3 – 1.7 x 10^5
Polypyrrole (PPy)	10 ^{2} – 7.5 x 10^3
Polyaniline (PANI)	30- 200
Polythiophenes (PT)	10-10^3

3.3.1 Polypyrrole

Polypyrrole (PPy) has been widely studied in both covalently modified and unmodified forms, which enable to tune its electrochemical properties and processability. PPy has been reported to support cell interaction and also entrapped bioactive molecules, so can be identified as smart materials and bio-compatible with great chemical stability [115]. PPy can be prepared by electrochemical polymerisation in large quantities even in room temperature and can be easily modified with additives or adjusted the suitable properties for its applications. Once synthesised, PPy is difficult to modify chemically as the structure is no longer thermoplastic so, it is poor in mechanical properties also insoluble [116]. To date, PPy has been used in wide range of applications such as fuel cells, biosensors, tissue engineering, neurons, and nerve probes, *etc.*[117]

3.3.2 Polyaniline

Polyaniline (PANI) as known as aniline black conductive polymer has found in various forms depends on the oxidation level achieved during the preparation (emeraldine, nigraniline, and leucoemeraldine). Although, PANI is easy to synthesise, and has many advantages but it is

still being a conflict for its biocompatibility in many reports [118]. PANI is used for biosensors, tissue engineering and drug delivery system, *etc*. [119]

3.3.3 Polythiophenes (PT) and its conjugated forms

Along with PPy and PANI, Polythiophenes (PT) have emerged important class of conducting polymers. PT offer enhanced electrical conductivity which stems from cyclic monomer with dioxyalkylene and electrochemical polymerisation of 3,4-ethylenedioxythiophene as known as Poly(3,4-ethylenedioxythiophene) (PEDOT) [120]. PEDOT gives better conductivity, better stability in both chemical and environmental and spectroscopic property compare to PT and PPy. PEDOT is playing the important role in bioengineering as it compatible with many kinds of cells, including neurons [82]. It also can be formed in different shape for suitable applications. Therefore, the research in PEDOT is exploded in many fields, not only for bioengineering.

Moreover, poly(styrene sulfonic acid) (PSS), water soluble polyelectrolyte was introduced to PEDOT to balance the cations charge during synthesis process resulted in good film stability, higher conductivity, highly visible light transitivity and great stability in high temperature. PEDOT:PSS (Figure 3.4) can carry the higher conductivity up to 4600 S cm^{-1} by a post-treatment with an organic compound such as ethylene glycol (EG), poly(ethylene glycol) (PEG), dimethyl sulfoxide (DMSO) acids, alcohols, and amphiphilic fluorocompounds. It has been reported that PEG (Mw 200 g/mol.) gives the highest improvement of conductivity in the thickness-controlled films when compare with other enhancers. In addition, heat treatment at 120 °C longer than 20 mins can cause breaking of ionic bonds between PEDOT and PSS [121].

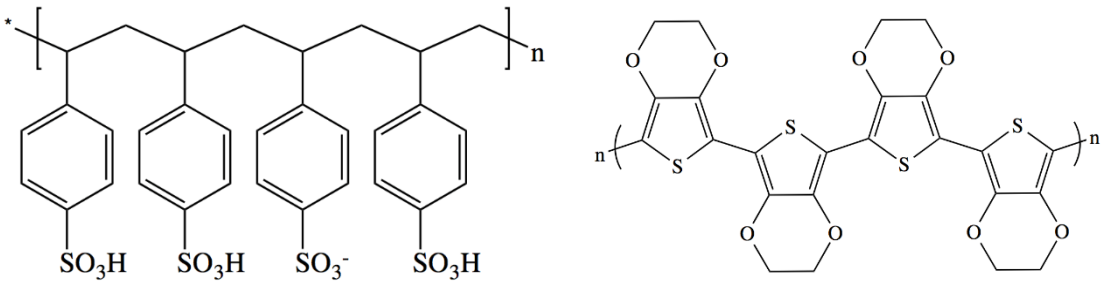

a) b)

Figure 3.4 Chemical structures [122] of a) poly(styrene sulfonic acid) (PSS) and b) poly(3,4-ethylenedioxythiophene) (PEDOT).

3.4 PEDOT:PSS fibres

Wet spinning of PEDOT:PSS based fibres were studied in many areas. PEDOT: PSS was spun into acetone coagulation bath and examined mechanical properties. The neat PEDOT:PSS fibres were spun into acetone coagulation bath and result of Young's modulus, tensile strength, and elongation at break for the resulting microfibre were 1.1±0.3 GPa, 17.2±5.1 MPa, and 4.3±2.3 % [123], respectively. Dip-treatment of fibres into ethylene glycol slightly increased their conductivity and Young's modulus after being dipped (3 mins) and dried at 160 ℃ for 1 h [124]. PEDOT:PSS was added PEG-SWNT into fibres and shown continuous and uniform composite fibres addition, nanotubes were enhancing the mechanical properties while PEG increased the conductivity [125]. Moreover, wet spun PEDOT:PSS fibres doped with PEG (Mw 200 g/mol.) in solutions gave slightly higher conductivity than the post treatment with EG but treated neat PEDOT:PSS with EG [126][127], the conductivity was higher than treated with PEG. The result of X-ray photoelectron spectroscopy, X-ray diffractometry, and atomic force microscopy had shown the

PEDOT:PSS enhanced the electrical and mechanical properties because of the removal of insulating PSS from grains surfaces and crystallisation [124].

Moreover, PEDOT:PSS also used for coating other textile to deposit electrical conductivity to the initial substance. Trends of increasing the conductivity were following the dipping cycles and even more increasing when dipped with 50 % evaporated water in PEDOT:PSS solution. However, annealing after dipping and stretching had no effect on the conductivity [126][125].

PEDOT:PSS composite fibres were prepared and well-studied due to their high conductivity and various applications that researchers and engineer have considered for development. Firstly, the dip-coating has been applied for preparing fibres, conductive field were deposited along the fibres surface and led the improving of yield strength and expanding the applications for the host fibres. Dip-coating has been found using on silk fibres, titania membranes or chitosan. Secondly, the wet-spinning process was used to prepare the composite fibres which claimed as potential strain-responsive sensors [83]. A summary of PEDOT:PSS fibres and composite processing methods is presented in Table 3.4.

Table 3.4 Summary of PEDOT:PSS and composite fibres [83]

Materials	Research	Method
PEDOT:PSS	Micro-fibres prepared characterised	Wet spinning
PEDOT:PSS	Micro-fibres prepared and treatment with ethylene glycol	Wet spinning
PEDOT:PSS	Simple chemical polymerisation synthesis fibres	*In situ* polymerisation
PEDOT:PSS and silk	Silk was casted with PEDOT:PSS and characterised	Dip-coating
PEDOT:PSS, EDOT and silk	Composite fibres were prepared for signal recording	Electrochemically deposition
PEDOT:PSS, chitosan and EG	Conducting fibres were loaded with antibiotic drug for smart release applications	Dip-coating
PEDOT:PSS and PAN	Blended fibres were prepared and their properties characterised	Wet spinning
Titania, PEDOT:PSS	Nanofibres were electrospun and coated with PEDOT:PSS	Electrospinning and Dip coating
PEDOT:PSS and PET	PET textile were coated with PEDOT:PSS in different compositions	Coating
PEDOT:PSS and PU	PU was mixed with different compositions of PEDOT:PSS for fibres spinning benefits in sensor applications	Wet spinning
PEDOT:PSS and PVA	Composite fibres were prepared to examine their mechanical properties	Wet spinning

3.5 Experimental: Materials and processing techniques

The composite fibres were spun at room temperature using a wet spinning process using the syringe pump (Nexus 6000, Chemyx Inc., USA). The solutions were extruded through an 18-gauge blunt needle (Terumo, UK) into an aqueous coagulation bath containing 15 wt% $CaCl_2$. The initial injection speed was controlled by pump at 2 ml min^{-1}. Fibres were collected at the winding machine (Rondol Technology LTD, UK), which controlled the linear speed at 3 m min^{-1}. The air gap between needle and coagulation bath were set at 2 cm. After spinning, fibres were washed with distilled water before being dried in room temperature for 24 h. Each fibre was cut into 20 pieces (2 cm lengths) for conductivity testing; half of them were heat treated at 150^{o} C about 10 minutes in the oven. The polymer solution for spinning PEDOT:PSS – ALG was prepared by evaporating water from 30 g of PEDOT:PSS to leaving 15 g remaining, at room temperature. The percentage of PEDOT:PSS in this experiment was set at 33% according to the product specification to ensure that there was 1.1% of PEDOT:PSS in the product.

4 wt% of ALG was added to the polymer solutions with magnetic stirring at 200 rpm (model UC151, Stuart, UK) for 3 h. For comparison, PEDOT:PSS – ALG – PEG was prepared by adding 0 wt% and 10 wt% of PEG into the solution with stirring for 1 hour. Next, the polymer solutions were transferred to a 20 mL luer lock syringe (Terumo, UK). Air-bubbles were removed by leaving at room temperature overnight. The solution preparation is shown in Figure 3.5 and a complete list of the fibres prepared for this study are summarised in Table 3.5.

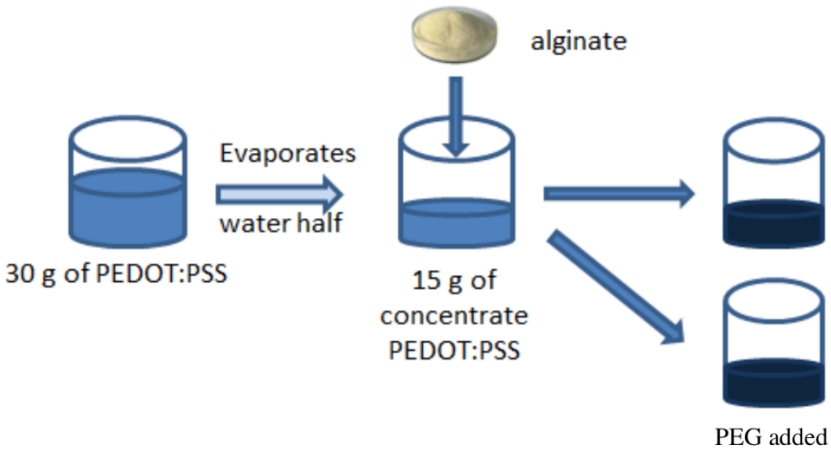

Figure 3.5 The polymer solutions used in spinning. Alginate and PEDOT:PSS consisted of 4 wt% alginate, 15g of concentrated PEPOT:PSS with or without 10 wt% PEG additive. These solutions were, separately, transferred into lock syringes and sat at room temperature overnight prior to spinning to remove air bubbles.

Table 3.5 A summary of fibres produced by a wet spinning process

Fibres sample	Compositions
ALG	4 wt% alginate
PEDOT:PSS - ALG	4 wt% alginate + 15 g PEDOT:PSS
PEDOT:PSS – ALG - PEG	4 wt% alginate + 15 g PEDOT:PSS + 10 wt% PEG
PEDOT:PSS – ALG(150°C)	4 wt% alginate + 15 g PEDOT:PSS and the fibres were heat treated
PEDOT:PSS – ALG – PEG(150°C)	4 wt% alginate + 15 g PEDOT:PSS + 10 wt% PEG and the fibres were heat treated

3.6 Characterisation and measurement techniques

3.6.1 Microscopy

Fibre diameters were examined using scanning electron microscopy and optical microscopy. Typically, ten samples were collected from each spinning condition and at examined in three different regions of the fibre. ImageJ software package was used for determining the diameter of each fibre to obtain an average value. The cross section of the fibres was also observed by using epoxy moulding each fibre in vertical position, each mould was polished before images were obtained using the microscope. Surface observation by electron microscopy

3.6.2 Fourier Transform Infrared Spectroscopy

Fourier Transform Infrared Spectroscopy (FTIR) (Spectrum 100, PerkinElmer, UK) was used to record transmittance spectra in the range 4000 and 650 cm^{-1} to examine the chemical structures and compositional aspects within the fibres.

3.6.3 Electrical conductivity

The electrical conductivity of each fibre was measured with a TTI400 LCR meter. Fibre samples (20 mm) long with alligator clips attached at both ends with fixed gap (2 mm) between them. The conductivity was calculated by using equation 2.1

$$\rho = \frac{R.A}{l} \tag{3.1}$$

where σ is the conductive (s/m), R is the resistance (Ω) between clips distance (m) L, and A is the cross-section area of the measurement location.

3.6.4 Single fibre tensile testing

Tensile strength measurements were carried out on single fibres using ASTM C1157 standard and paper frame method. An Instron 3343 with 10 Newton load cell was employed for the

mechanical testing. A single fibre was fixed on the card board paper frame by adhesive. The fibre gauge length was set at 15 mm and ten samples of each condition of fibre were tested. Data were analysed using the Bluehill software pack. Average of three areas of each fibre diameter were observed by optical microscope prior to the mechanical testing.

3.7 Result and discussion

3.7.1 Evaluation of spinning factors

Initial work involved determining suitable conditions for fibre spinning, including: concentration of alginate, spinning ratios, concentration of the coagulation bath, and winding speed.

4 and 5 wt% alginate solutions were spun into 10, 15, and 20 wt% of $CaCl_2$. The initial spinning speeds to set at 1 and 2 mm/min with reeling speed rates of 10 (2 x 10^{-2} m/s), 15 (2.5 x 10^{-2} m/s), 20 (3 x 10^{-2} m/s), and 25 (3.5 x 10^{-2} m/s). The mechanical testing results shown in Table 3.6 (Figure 3.6 and Figure 3.7) were used to examine the suitability of the fibres obtained.

Table 3.6 Tensile testing results of fibres spun from 4 and 5 wt% alginate solutions and crosslinked with 10, 15 and 20 wt% $CaCl_2$

Conditions	Max load (N)	Diameter (mm)	Modulus (GPa)	Extension (mm)
4% Alginate				
10% $CaCl_2$	1.59 ± 0.39	0.21 ± 0.012	1.81 ± 0.08	2.17 ± 1.10
15% $CaCl_2$	1.36 ± 0.69	0.22 ± 0.02	1.75 ± 0.16	1.94 ± 1.73
20% $CaCl_2$	1.20 ± 0.17	0.16 ± 0.02	1.96 ± 0.05	3.26 ± 0.89
5% Alginate				
10% $CaCl_2$	0.95 ± 0.50	0.18 ± 0.02	2.32 ± 0.14	1.08 ± 1.68
15% $CaCl_2$	1.31 ± 0.51	0.18 ± 0.01	2.64 ± 0.18	1.20 ± 1.23
20% $CaCl_2$	1.76 ± 0.24	0.18 ± 0.01	2.78 ± 0.08	1.99 ± 1.00

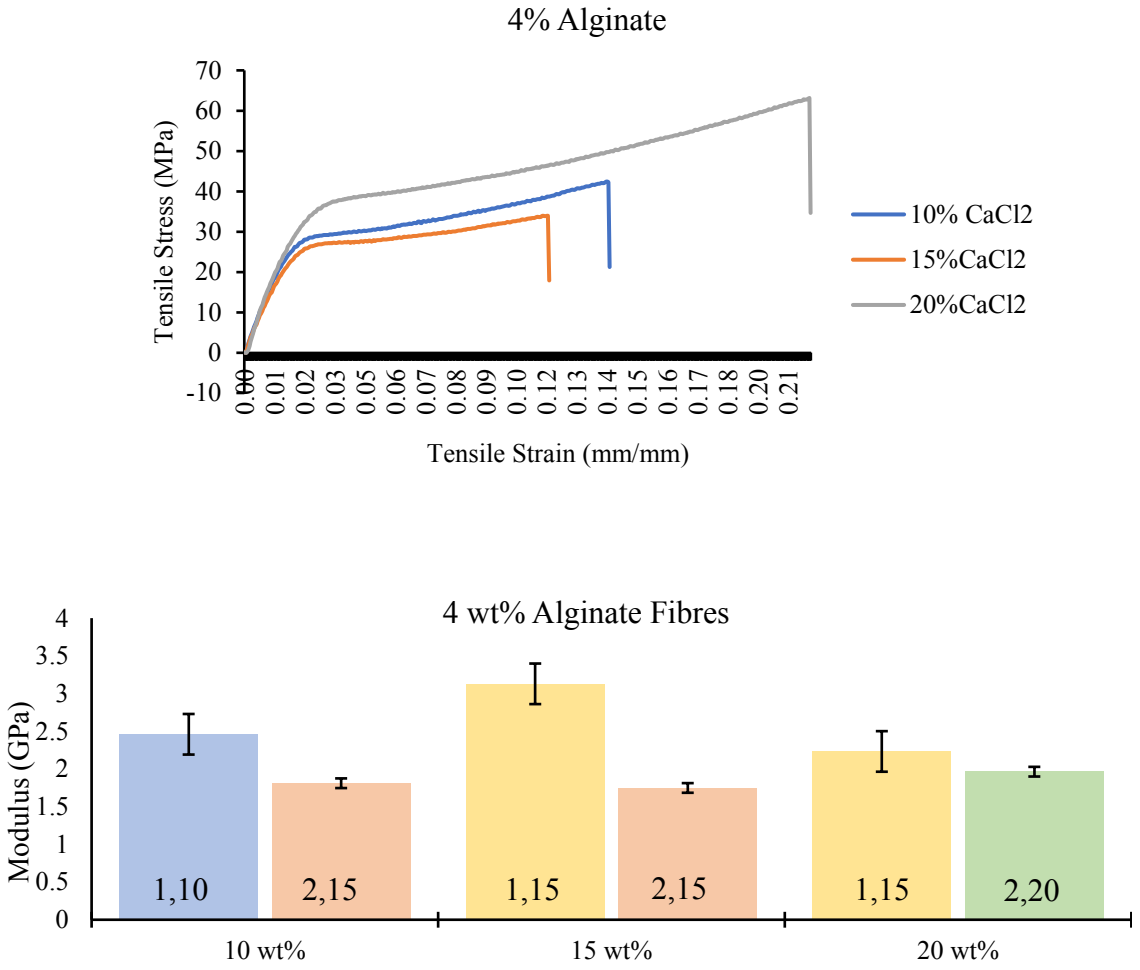

Figure 3.6 Tensile graph trend of 4 wt% alginate fibres crosslinked with 10, 15, and 20 wt% $CaCl_2$ and a chart showing the average modulus of these fibres. The numbers on the bars are the initial injection speed (at 1 or 2 mm/min) and the collection speed at reel (10 (2 x 10^{-2} m/s), 15 (2.5 x 10^{-2} m/s), or 20 (3 x 10^{-2} m/s)).

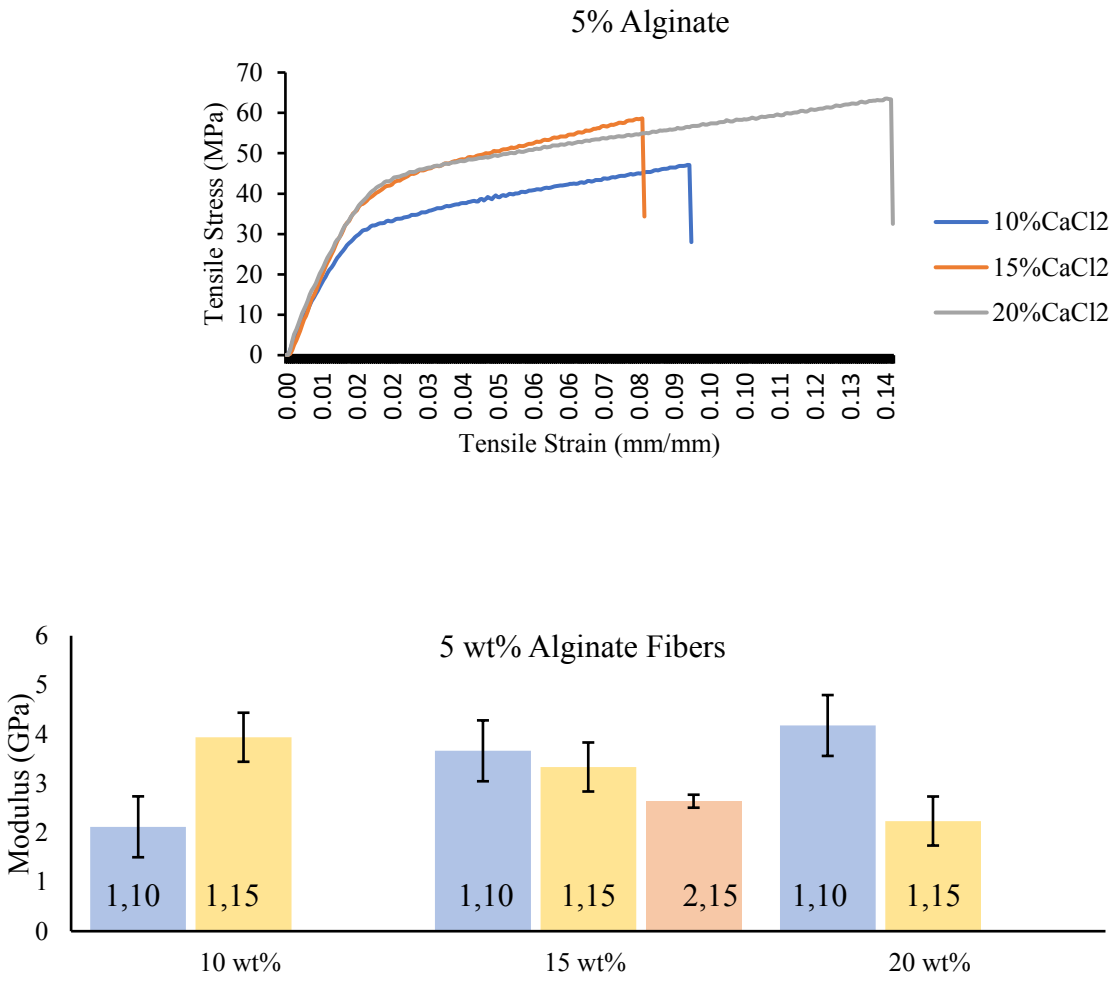

Figure 3.7 Tensile graph trend of 5 wt% alginate fibres crosslinked with 10, 15, and 20 wt% $CaCl_2$ and a chart showing the average modulus of these fibres. The numbers on the bars are the initial injection speed (at 1 or 2 mm/min) and the collection speed at the reel (10 (2 x 10^{-2} m/s), 15 (2.5 x 10^{-2} m/s), or 20 (3 x 10^{-2} m/s)).

The fibres obtained from 4 and 5 %wt of alginate through 10, 15, and 20 %wt $CaCl_2$ coagulation baths were selected by examining the mechanical properties of the fibres from which 4 wt% of alginate and 15 wt% of $CaCl_2$ were chosen for further experiment. Although, the fibres with 5 wt% of alginate gave better results on their mechanical properties, when composite solutions were prepared (by mixed with conductive polymers), the solution was

too viscous to spin into fibres so the conditions of spinning were chosen as descripted. Moreover, the spinning conditions were selected from the initial speed and rolling speed from solutions chosen previously. So, the fibres from 4 wt% alginate with the initial speed of 2 ml min^{-1} and the rolling speed 15 (2.5 x 10^{-2} m/s) displayed the best mechanical properties of the fibres tested, the results of tensile testing of the chosen conditions are shown in Figure 3.8.

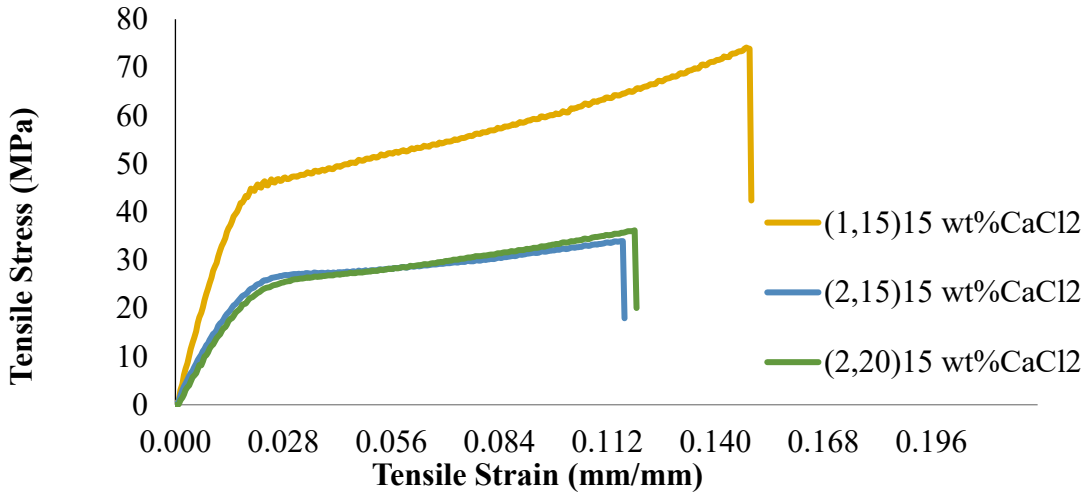

Figure 3.8 The tensile testing result of 4 wt% of alginate fibres, cross-linked with 10, 15, and 20 wt% of $CaCl_2$ spun at various spinning and reeling speeds.

It should be noted that, the fibres with 3 wt% alginate were also examined, however these fibres were too fragile to be collected in sufficient quantity to undertake further testing with.

3.7.2 FTIR analysis of alginate, PEDOT-PSS and Alginate-PEDOT-PSS composite fibres

The FTIR spectral bands (as percentage transmittance) reveal evidence of the chemical bonding present between ALG, PEDOT:PSS, PEDOT:PSS – ALG and PEDOT:PSS – ALG - PEG, and the heat-treated fibres. The individual spectra were analysed to understand the materials and their modifications *e.g.* the hydroxyl (O-H) band at 3241, 3308, 3184, 3214, 3266, and 3197 cm^{-1} respectively is shown in Figure 3.9 for all samples; the breadth and

intensity indicates the level of hydrogen bonding present. The stretching of C-O moiety is found in all samples which can be seen at 1590, 1587, 1590, 1579 and 1585 cm^{-1}. Evidence of PEG doping is found at 2871 cm^{-1} which stretched in C-H bond. However, the presence of PEDOT:PSS, which influences the composite fibres both with and without annealing, is represented by sulfonates and thiophene (S-O) bonding at 1416, 1414, 1439, 1350 and 1410 cm^{-1}. The FTIR spectrum are summarised in Table 3.7. On the other hand, when considering the FTIR spectra of the samples with and without heat treatment, there were no strong differences between them so it is assumed that there was no evidence of new chemical bonding or breaking during the annealing process.

Table 3.7 The FTIR spectrum analysis

Sample	IR spectrum analysis
Alginate	3241 cm^{-1} (hydroxyl O-H stretching), 1591 cm^{-1} (carboxylic acid C=O stretching),
PEDOT:PSS	3308 cm^{-1} (hydroxyl O-H stretching), 2921 cm^{-1} (C-H stretching), 1416 cm^{-1} (sulfonate S-O stretching)
PEDOT:PSS – ALG	3184 cm^{-1} (hydroxyl O-H stretching), 2871 cm^{-1} (C-H stretching), 1591 cm^{-1} (carboxylic acid C=O stretching), 1414 cm^{-1} (sulfonate S-O stretching)
PEDOT:PSS – ALG – PEG	3214 cm^{-1} (hydroxyl O-H stretching), 2871 cm^{-1} (C-H stretching), 1591 cm^{-1} (carboxylic acid C=O stretching), 1439 cm^{-1} (sulfonate S-O stretching)
PEDOT:PSS – ALG (150 °C)	3266 cm^{-1} (hydroxyl O-H stretching), 2871 cm^{-1} (C-H stretching), 1591 cm^{-1} (carboxylic acid C=O stretching), 1350 cm^{-1} (sulfonate S-O stretching)
PEDOT:PSS – ALG – PEG (150 °C)	3197 cm^{-1} (hydroxyl O-H stretching), 2871 cm^{-1} (C-H stretching), 1591 cm^{-1} (carboxylic acid C=O stretching), 1410 cm^{-1} (sulfonate S-O stretching)

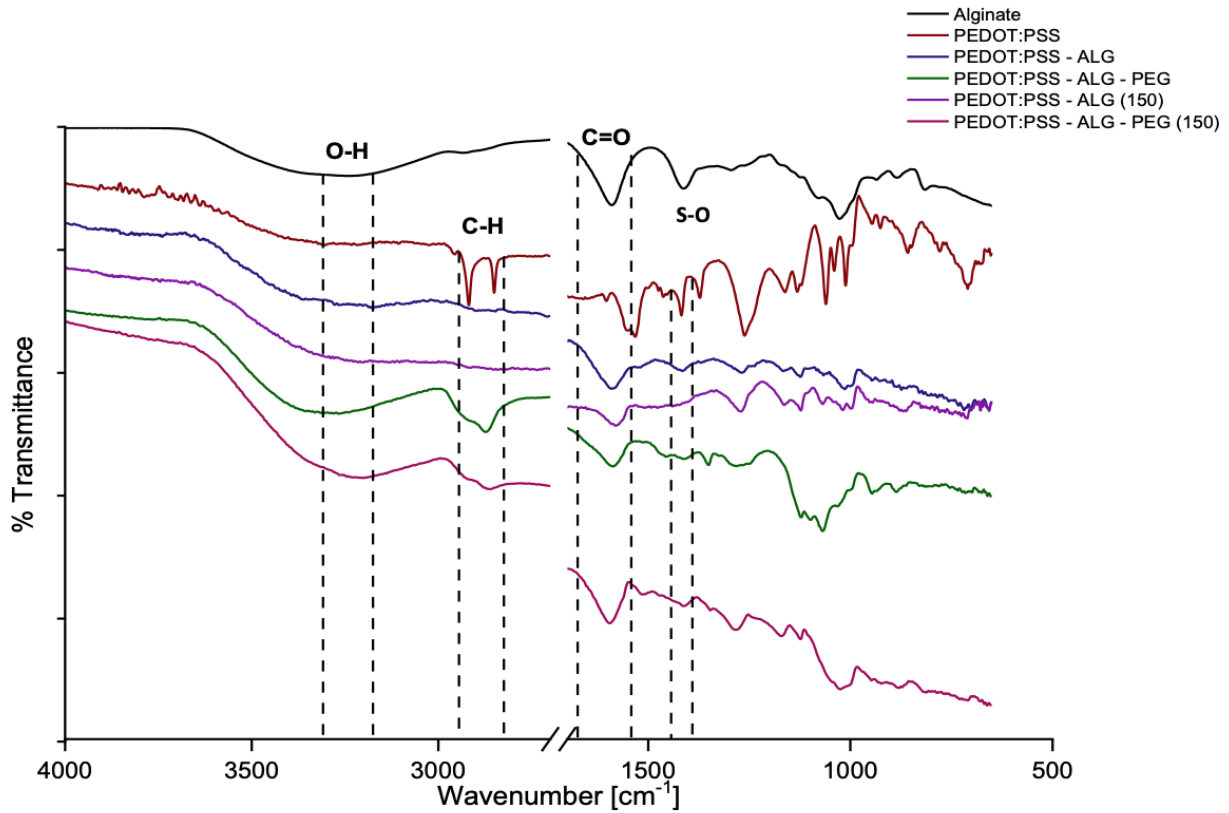

Figure 3.9 FTIR spectra (transmittance mode) for each of the fibres

3.7.3 Diameter and pre-analysis

Traditionally, PEDOT:PSS is processed as a water based solution and can be spun into fibres in an acetone bath including coated along fibres. However, these fibres were again dissolved in water and alginate was introduced as a carrier of PEDOT:PSS into this experiment to produce insoluble conductive fibres.

Composite fibres were smooth and spun continuously for several metres. The cross-sections of the conductive fibres were exposed by razor/scalpel and observed under optical microscope with 20x, bright field function. The cross-sectional images of the fibres showed average values of diameter ≈ 170 µm . SEM analysis revealed that the fibres had crumpled surface morphology of the fibres, almost circular uniformly along the fibres as seen in Figure 3.10. Moreover, diameter of fibres kept constant and slightly different around 10-20 µm shown Table 3.7. The surfaces of conductive fibres in Figure 3.7 were also taken by Zeiss EVO 40 SEM.

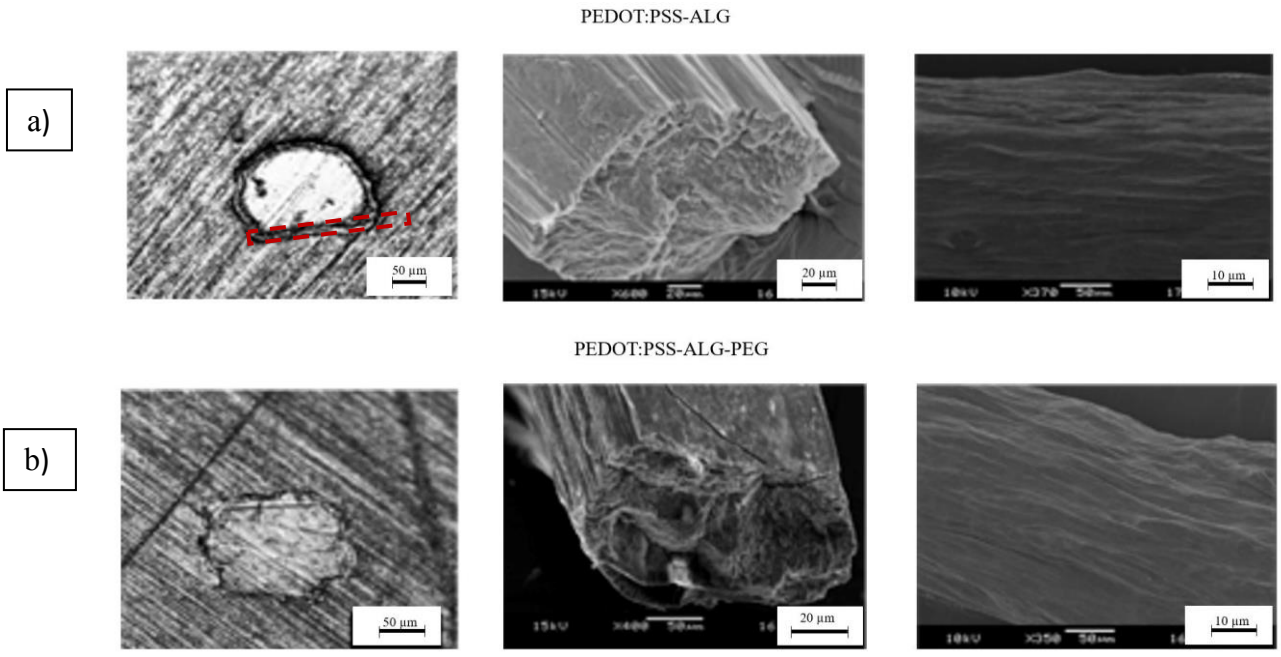

Figure 3.10 **Left:** Optical microscopy of cross-section, scale bar 50 µm (left); **Middle:** SEM cross-section, scale bar 20 µm; **Right:** SEM surfaces of composite fibres: scale bar 10 µm, of: **(a)** PEDOT:PSS-ALG and **(b)** PEDOT:PSS-ALG-PEG

Table 3.8 Average diameter of each fibre observed by optical microscope

Fibres sample	Average Diameter (μm)
ALG	188.2±10.3
PEDOT:PSS – ALG	169. 5±8.7
PEDOT:PSS – ALG – PEG	176.3±6.6
PEDOT:PSS – ALG(150°C)	159.5±7.7
PEDOT:PSS – ALG – PEG(150°C)	176.5±10.4

The fibres prepared without PEG clearly show that PEDOT:PSS was trapped inside the alginate shell (Figure 3.10 a)) but when combined with PEG, the fibres revealed a homogenous structure (Figure 3.10 b)).

3.7.4 Electrical conductivity of composite fibres

The average electrical conductivity of the fibres increased when PEG was added and further significantly improved after annealing at 150 °C for 10 mins. Significantly, conductivity of PEDOT:PSS – ALG – PEG fibres treated at 150 °C was 42.5 S m^{-1} which is 80 times higher than PEDOT:PSS – ALG (0.5 S m^{-1}). The conductivity of each fibres is shown in Table 3.9.

Table 3.9 Electrical conductivity of composite fibres

Fibres sample	Average Diameter (μm)	Conductivity (S m^{-1})
ALG	188.2±10.3	-
PEDOT:PSS - ALG	169.5±8.7	0.53±0.06
PEDOT:PSS – ALG - PEG	176.3±6.6	2.02±0.65
PEDOT:PSS – ALG(150°C)	159.5±7.7	0.86±0.20
PEDOT:PSS – ALG – PEG(150°C)	176.5±10.4	34.93±13.14

The result show that PEG dramatically increased the conductive of the fibres which was further enhanced when combined with heat treatment. However, heat treatment of PEDOT:PSS fibres in the absence of PEG at various time intervals led to a decrease in the conductivity. On the other hand, spun PEDOT:PSS fibres with additives needed the heat treatment to dope the conductivity in the specific range of time and temperature. Thus, PEDOT:PSS itself does not show the best conductivity and even decreases its ability when the heat treatment was applied, while the additive and post treatment dramatically improved conductivity. However, there is no evidence showing that alginate becoming an additive as spun alginate with PEDOT:PSS in the heat treated condition also displays a slight increase in conductivity. There is another way to increase the conductivity of PEDOT:PSS which is by soaking in EG solution followed by heat treatment to dry the fibres. However, there also was no improvement when mixing the additive and PEDOT:PSS fibres then treating again with EG solution.

In addition, the LED brightness from a simulated circuit (including an LED light) made up with the fibres is shown in Figure 3.11 with a 9V potential difference applied. The electrical conductivity was also calculated from the current (I) and resistance (R) in each circuit. The electrical data (Table 3.10) show that the fibre with PEG and heat treatment produced the highest LED intensity.

Table 3.10 Electrical conductivity of composite fibres observed by stimulate circuits

Fibres sample	Current (I) (μA)	Voltage (V)	Resistance (R)(kΩ)	Conductivity (S m^{-1})
ALG	-	-	-	-
PEDOT:PSS-ALG	44.87±1.50	6.90±0.03	153.91±5.63	0.62±0.02
PEDOT:PSS–ALG-PEG	193.03±18.72	6.87±0.04	35.80±3.25	1.21±0.03
PEDOT:PSS–ALG(150°)	66.27±2.20	6.88±0.05	104.01±3.98	1.04±0.04
PEDOT:PSS–ALG–PEG(150°)	178±8.48	6.50±0.10	3.63±4.01	22.52±0.28

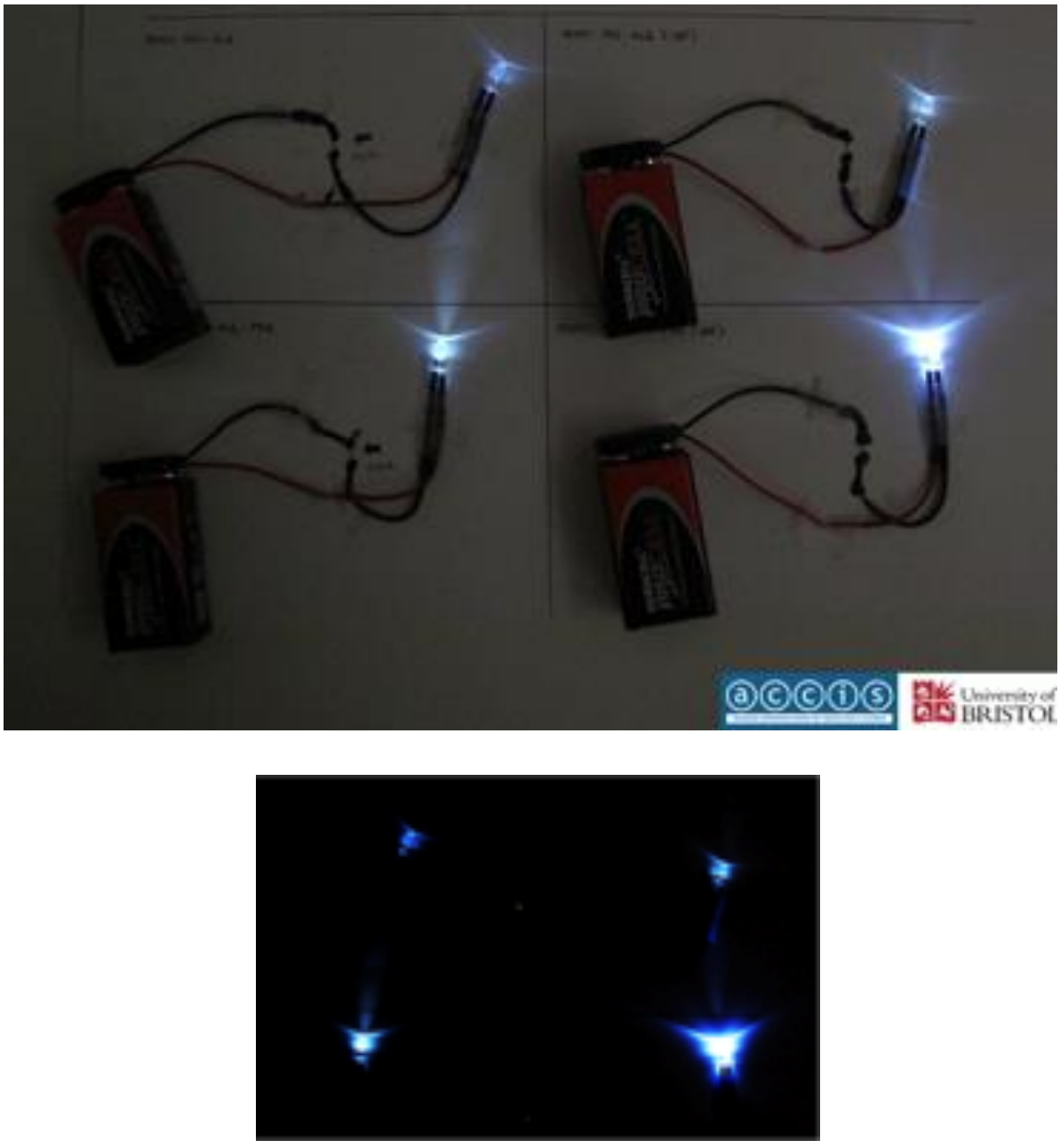

Figure 3.11 The simulated circuits for each of the fibres (top) and the brightness of LED (bottom). Clockwise from top left the fibres are: PEDOT:PSS-ALG, PEDOT:PSS-ALG (150 ºC), PEDOT:PSS-ALG-PEG (150 ºC) and PEDOT:PSS-ALG-PEG in the bottom left.

3.7.5 Mechanical properties

Mechanical properties were examined and compared between neat ALG and conductive fibres prepared which summarised in Table 3.11.

Table 3.11 Tensile result compare between neat alginate and composite fibres

Fibres sample	Young's modulus (GPa)	Ultimate stress (MPa)	Strain at break (%)
ALG	1.69±0.19	34.86±7.26	11.54±3.01
PEDOT:PSS-ALG	3.30±0.26	82.68±13.87	6.72±2.35
PEDOT:PSS–ALG-PEG	1.26±0.14	28.61±3.75	5.53±0.61
PEDOT:PSS–ALG(150°C)	4.19±0.34	126.99±12.14	8.56±0.87
PEDOT:PSS–ALG–PEG(150°C)	1.87±0.26	48.19±4.30	7.43±1.02

For the neat ALG, the addition of PEDOT:PSS enhances the mechanical properties and this is particularly evident from the increase in the ultimate tensile strength (UTS) and the Young's modulus, albeit at the expense of the strain at break, which falls in all cases. The addition of both PEDOT:PSS and PEG to ALG leads to a reduction in its mechanical properties. The presence of residual PEG within the fibres result in softer, plasticised fibres with lower in mechanical properties both Young's modulus and tensile stress. Heat treatment significantly improves both these properties in the case of PEDOT:PSS-ALG in which it is particularly marked in the case of the UTS, and to a lesser extent in the PEDOT:PSS-ALG-PEG (where the heat treatment may lead to some loss in the PEG through evaporation).

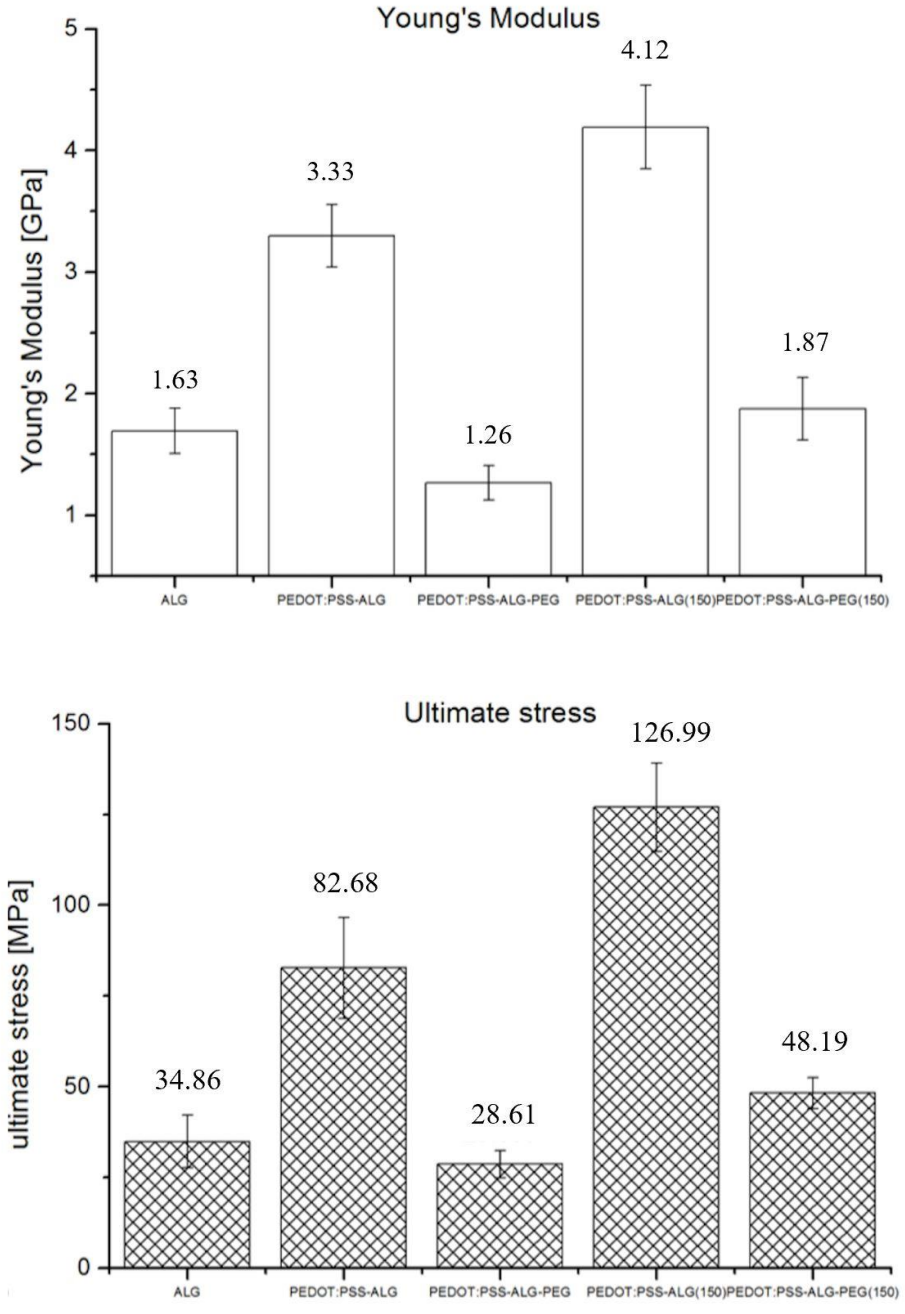

Figure 3.12 Young's modulus and ultimate stress of neat alginate and conductive fibres.

The composite alginate fibres showed enhanced conductivity over those of neat alginate, these materials could have benefits in medical applications and as cell culture scaffolds where the mechanical, chemical, and electrical conductivity properties are all important.

However, apart from the high conductivity that PEDOT:PSS imparted to the fibres, adding a high PEDOT:PSS content made the fibres more brittle compared to the neat alginate fibres. Moreover, similar research involving fibres manufactured with acetone, IPA, LiCl, and $CaCl_2$ [72] showed better mechanical properties, but with conductivity values over 100 times lower than the conductive fibres with added PEG obtained in this research. In addition, the alginate and PEDOT:PSS blended fibres alone showed a higher conductivity than those of the acetone and IPA research which was 0.04 ± 0.3 S m^{-1} while the fibres prepared here showed the values up to 0.53 ± 0.1 S m^{-1}. This is still lower than that of neat PEDOT:PSS fibres (520 ± 0.5 S m^{-1}) [123]. The decrease in conductivity of composite fibres following the introduction of alginate seen in this work is also seen across other research that involves alginate blending with conductive materials *e.g.* graphene, metals, conductive polymers, or carbon nanotubes *etc*. [128].

3.8 Conclusion

The blends of alginate and PEDOT:PSS fibres were examined and investigated in this chapter. A wet-spinning method was employed which gave uniform conductive fibres and this offers a great opportunity for further development for a wide range of applications. This results of this study can be summarised as follows:

1. The parameter finding experiment was set to focus on the best proportion of alginate concentration and $CaCl_2$ concentration, of which the 4 wt% of alginate with 15 wt% $CaCl_2$ was chosen for further experiment.
2. A wet spinning method was employed to fabricate alginate-based composite conducting fibres. The fibres were spun continuously with uniform diameter.

3. The FTIR of conductive fibres showed the presence of alginate and PEDOT:PSS within the fibres without any new bonding.
4. The results clearly showed that the electrical conductivity properties of PEDOT:PSS – ALG fibres and films were increased when PEG was added but this also decreased the mechanical properties.
5. A short annealing step also improved the conductivity of PEDOT:PSS composite without creating a new bonding.
6. The conductivity of the fibres was sufficient to light up an LED when used in a 9V circuit.
7. It was clearly shown that PEDOT:PSS and alginate can be spun into fibres without changing on their chemical structure or bonding.

These fibres will later be used as materials to examine neuronal outgrowth in Chapter 4 to investigate the biocompatibility of these materials.

Chapter 4

Conductive composite films for neural implants

4.1 Introduction to Biomaterials

The term biomaterial has a variety of definitions, but for this thesis it will be used to describe the class of materials which are used principally in contact with biological systems. A major application of these materials is to manufacture devices for use in or function as replacements for organs in the body [129]; produced from wholly synthetic or naturally occurring materials [130]. It combines the fields of medicine, biology, chemistry, and engineering to develop and improve their application [131]. Although most biomaterials are generally employed in biomedical applications, they are also used to assist cell growth in culture, as assays for blood proteins, and diagnostic gene arrays, *etc*. The current applications of biomaterials include functional materials for organs replacement or systems such as artificial joints, bone screws, cardiac pacemakers, and kidney dialysis machines, *etc.* [132]. and examples of these can be found in Table 4.1. Biomaterials are normally used by integrated into medical device or implants. The most important property for biomaterials is biocompatibility with the various environments of the body. Williams (1987) gave a definition for biocompatibility as

> *"Biocompatibility is the ability of a materials to perform with an appropriate host response in a specific application."*

The *appropriate host response* includes bacterial resistance, resistance to blood clotting, also the specific time that materials will be in contact with the system.

The *appropriate host response* includes bacterial resistance, resistance to blood clotting, also the specific time that materials will be in contact with the system.

Table 4.1 The example of biomaterials and their applications [133]

Applications	Biomaterials
Skeletal system	
Joint replacements (hip, knee)	Titanium, Ti-Al-V alloy, stainless steel, polyethylene
Bone plate for fracture fixation	Stainless steel, cobalt-chromium alloy
Bone cement	Poly(methyl methacrylate)
Bony defect repair	Hydroxylapatite
Artificial tendon and ligament	Teflon, Dacron
Dental implant for tooth fixation	Titanium, Ti-Al-V alloy, stainless steel, polyethylene
	Titanium, alumina, calcium phosphate
Cardiovascular system	
Blood vessel prosthesis	Dacron, Teflon, polyurethane
Heart valve	Reprocessed tissue, stainless steel, carbon
Catheter	Silicone rubber, Teflon, polyurethane
Organs	
Artificial heart	Polyurethane
Skin repair template	Silicone-collagen composite
Artificial kidney (haemodialyser)	Cellulose, polycrylonitrile
Heart-lung machine	Silicone rubber
Senses	
Cochlear replacement	Platinum electrodes
Intraocular lens	Poly(methyl methacrylate), silicone rubber, hydrogel
Contact lens	Silicone-acrylate, hydrogel
Corneal bandage	Collagen, hydrogel

The factors that impact the development of biomaterials are toxicity, mechanical properties, healing, functional tissue and pathobiology, industrial involvement, regulation, and ethics.

There are many concerns on ethics factor as biomaterials are playing their role on human being or living creature which are summarised by following list [134]:

1. *"Is the use of animals justified?"*
2. *"How should research using humans be conducted to minimise risk to the patient and offer a reasonable risk-to-benefit ratio?"*
3. *"How can the needs of the patient be best balanced with the financial goals of a company?"*
4. *"How can investigator bias be minimised in biomaterials research?"*
5. *"What is the trade-off between sustaining life and the quality of life with the device for the patient?"*
6. *"Do government regulatory agencies have sufficient information to define adequate tests for materials and devices and to properly regulate biomaterials?"*
7. *"Should the government or other "third-party payers" of medical costs pay for the health care of patients receiving devices that have not yet been formally approved for general use by the FDA and other regulatory bodies?"*
8. *"Should the manufacture consider the rate of successful biomaterials rather than their revenue?"*
9. *"Should the manufacture consider the two models (lifetime and short time) for the goal of saving resources and appropriated care for individuals?"*

However, there are some issues that still debating between ethics and uses of biomaterials.

The motivation of this research was to examine the biocompatibility of the conductive fibres obtained from previous chapter in neuronal tissue engineering to cultivate the suitable and less harmful to human which could benefit *in vivo* in the future.

4.2 Introduction to Tissue Engineering

Many biomaterials are invented for their use for cells culture involving cell outgrowth, stimulating the evolution of cell and molecular biology.

Chapter 4. Conductive composite films for neural implants

Disease can lead to tissue or organ damage in the human body, which may result in death, so treatments need to apply to reduce and cure this damage. Previously, transplants have involved taking some tissue from a donor and transferring this to a patient. This method has limitations, including rejection of the tissue by the patient's immune system, blood type matching, pain to both donor and patient, or some cross-infection from the donor to patient [135]. The shortage of donors is also concern so, the need of new method which construct tissue outside the body has developed [136]. Tissue engineering is the concept of combining biomedical technology and methodology for the purposes of repairing, maintaining, or replacing damaged or diseased tissues by engineered function [137]. Langer and Vacanti first presented the definition of tissue engineering in 1993 and this is still applied. Their statement was to develop, maintain, improve or restore the biological substitutes in damaged tissue. The focus of these works on both the small scale such as neurons, liver cells, muscle cells or bone cells, or on a large of scale: organ transplants in the human body [138]. Therefore, tissue engineering has achieved its goal of improving *in vitro* and repair *in vivo* of the damaged tissue in both 3D and 2D scaffold materials [139]. Therefore, the concept treatment of tissue engineering is the same patient can reduce some risk on this various occasion mentioned and this leads to the development of tissue engineering which aims to regenerate the damaged tissues instead of replacing them [135], as shown in Figure 4.1.

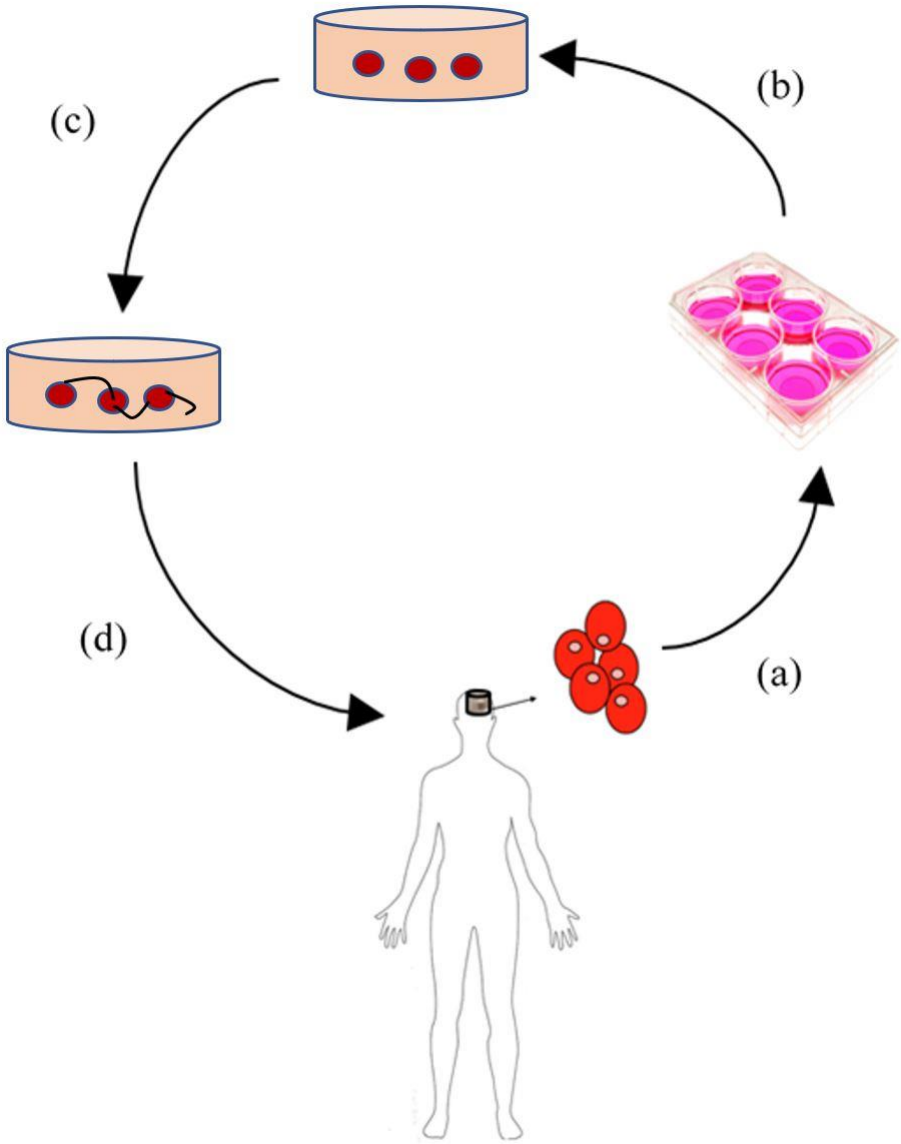

Figure 4.1 Schematic representation of tissue engineering process, (a) sample cells which could deliver from heart, liver, bone, muscle or neurons *etc.* are collected from patient which are (b) cultured in presence of biocompatible environment and (c) materials/scaffold (d), the healthy cells on biomaterial scaffolds are used to replace the damaged tissue/organ.

Tissue engineering is a means of combining three components: cells, scaffold (materials), and signalling for the purposes of repairing, maintaining, or replacing damaged or diseased tissues [137]. Consequently, the concept of tissue engineering is to produce and deliver a functional tissue from cells on substrate biomaterials to the site that regenerate, or repair required [140]. However, each biomaterial and cell have their own unique properties and only compatible with suitable conditions such as neurons that need special treatment to support them to regenerate and connected among them. As mentioned, tissue engineering consists with cells, scaffold and signalling biomolecule so, descripting about each individual part is presented.

4.2.1 Cells

There are several types of cells in the human body which can be damaged by disease. The problem of generating cells is that each cell needs different conditions to grow and survive for different periods of time. Cells for tissue engineering include stem cells, embryonic cells, or adult cells [141]. The embryonic cells can generate into any lineage, but their use is very strictly due to the ethical controlled and legal issues meaning that they still cannot be examined in the human body [142]. Therefore, animal models are generally have used for research. The adult cells have already developed themselves into shapes and have functionality so, they are quite limited for use in tissue engineering [143]. However, some specific cells including bone marrow, muscle, adipose tissue, and umbilical cord have been shown in isolated research and work very well with adult cells [144]. There are three different types of stem cells in human and animals which are Totipotent stem cells, Pluripotent stem cells, and Multipotent stem cells [145]. Totipotent stem cells can become any type of cells while Pluripotent stem cells can become only some types of cells and Multipotent stem cells can only be the specific or restrict type of cells [146]. The applications, cells type and uses of tissue engineering are summarised in Table 4.2.

Table 4.2 Selected applications of tissue engineering [147]

Applications	Cell types and material uses
Bone tissue engineering	Bones are different from other cells as they can repair, regenerate, and remodel themselves when they are injured. Large-scale damage requires supplementary of bone grafts as it exceeds the self-healing capability. 3D porous scaffolds for *in vivo* use were invented with hydroxyapatite (HA) which has similar composition to bone. These scaffolds consisted of natural hydrogels such as collagen, chitosan, alginate, and gelatin, *etc.*
Cartilage tissue engineering	The elastic tissue, cartilage has little capability for self-healing, so natural scaffolds have played an important role for cartilage repair. Collagen, fibrin, hyaluronan, agarose, alginate, or gelatin have been employed to help the regeneration for *in vivo* properties.
Cardiac tissue engineering	Heart transplant is the only solution currently; scaffolds were invented to help the lack of donors and immuno response. Heart tissue is divided into three layers: the epicardium, myocardium, and endocardium. Chitosan is the most commonly-selected material for both 2D and 3D scaffolds, but these materials are still in the developmental stages as many conditions are required to be optimized for therapy.
Pancreas tissue engineering	There are two units for pancreas: the exocrine and the endocrine but mostly are β-cells which are responsible for insulin. Production the most common 3D scaffold structure for culture is Matrigel^{TM} matrix which is a protein-based mixture to help control the glucose level in blood.

Vascular tissue engineering	The blood vessels consist of three tissue layers: Tunica Intima, Tunica Media, and Tunica Adventitia. Scaffolds derived from proteins were invented for both *in vivo* and *in vitro* use to deliver oxygen, nutrient, and effector molecules to address the damage within blood vessels.

The examples of cells and applications in Table 4.2 are mostly successful and being used within medical processes. However, there are some more cell that is still unavailable to use and hard to re-generate due to their speciality requirement. Although, there are some studies showing that those cells can facilitate out-growth *in vitro* not *in vivo*, such as neurons or nerve cells.

4.2.2 Neurons

The function of neurons or nerve cells is to send and receive messages within the body and brain by electrical and ionic signals and the human brain contains about 100 billion neurons. A neuron is composed of a nucleus, axons, and dendrites, shown in Figure 4.2. Neurons are among the most important cells in the body as they send messages from brain to control body, movement, sensation, sound, taste, pressure, and release of hormones [148][149][150]. Neural implants have been stimulated in experiments to understand the way in which the brain functions and the brain's diseases may be caused by neural damage. Once neurons are damaged, they cannot repair themselves and they will eliminate from the network. However, most of the research about neurons is still current and being determined using animal models.

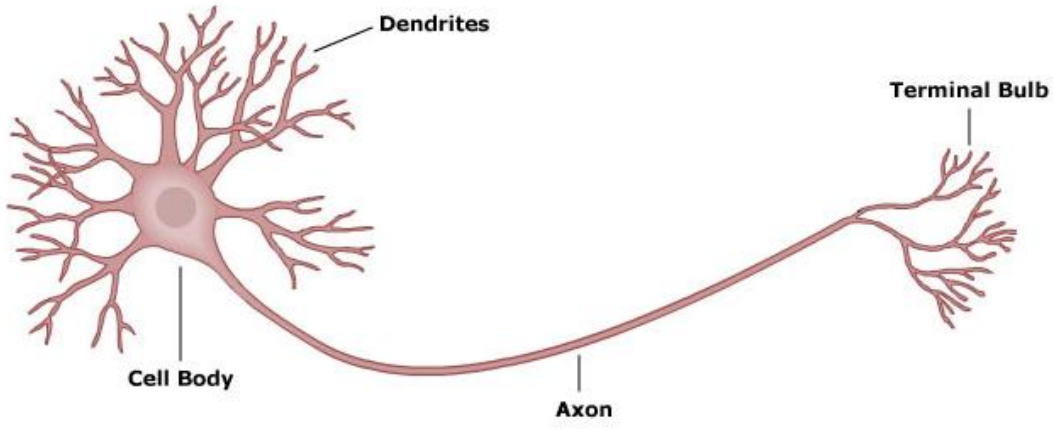

Figure 4.2 The structure of a neural cell [151].

Chapter 4. Conductive composite films for neural implants

Neural implants are systems to stimulate parts and structures of nerve system for regenerating nerve cells which could benefit many neurological diseases. Consequently, research has been conducted to develop implantable materials as shown in Table 4.3.

Table 4.3 Example of models and research established for neurons implantable materials.

Model	Cells specifics	Research	Reference
Immortalised cell cultures	BV-2 mouse microglia cell line	Cellular responses to nanotextured silicon surfaces	[152]
	C6 rat astrocytoma cell line	Effect to nanopatterned poly(methyl methacrylate) surfaces on astrocyte reactivity	[153]
	PC-12 rat pheochromocytoma cell line	Biocompatibility of polyurethane/poly(vinyl alcohol) hydrogel coatings	[154]
	SH-SY5Y human neuroblastoma cell line	Cytotoxicity of nanostructured Pt-coatings	[155]
	NIH/3T3 mouse embryonic fibroblast cell line	Cytocompatibility of polyaniline structures	[156]
	L929 mouse fibroblast cell line	Cytotoxicity of poly(3,4-ethylenedioxythiophene): glycosaminoglycan (PEDOT:GAG)	[157]
	NIH/3T3 mouse embryonic fibroblast cell line	Biocompatibility of hydrophilic copolymers	[158]
Primary cell cultures	Primary microglia	Responses to nanostructured titanium oxide surfaces	[159]
	Primary rat microglia	Response of microglia to P(TMC-CL)	[160]
	Primary mouse hippocampal neurons	Effects of nanotopography on neuronal cell signalling	[161]
	Primary rat hippocampal neurons	Biocompatibility of poly(3,4-ethylenedioxythiophene) doped with poly(styrene sulfonate) MEAs	[162] [163]
	Primary human dermal fibroblasts	Study of surface nano-topography and chemistry on collagen I and III production	[164]
	Primary rat cortical neurons	Development of a MEA-based *in vitro* model for drug screening	[165]
	Primary rat cortical and spinal cord astorcytes	Response of astrocytes to fibre surface nanopography	

2D mixed cell cultures	Primary rat mixed microglia, astrocytes and oligodendrocytes	2D *in vitro* glial scar assay to test biocompatibility of insulating silicone polymer coatings	[166]
	Primary rat astrocytes derived from neurospheres and rat embryonic spinal cord cells	2D *in vitro* model of spinal cord injury for drug screening	[167]
	Primary rat mixed neurons, microglia, astrocytes and oligodendrocytes	2D *in vitro* glial scar assay to test cellular response of dip-coated PEG films	[168]
	Rat primary astrocytes and dorsal root ganglia neurons	2D *in vitro* model of spinal cord injury to study isotropic-to-anisotropic cellular transitions	[169]
	Primary cortical and astrocytes	Cellular responses to nanoporous gold surfaces	[170]
3D *in vitro* cultures	Primary rat microglia and astrocytes	Hyaluronic-based hydrogel as a 3D model to test electrode biocompatibility	[171]
	Primary mouse mixed neurons, microglia, astrocytes and oligodendrocytes	Alvetex membrane scaffold as a 3D culture for high-throughput screening	[172]
	Primary rat cortical neurons and astrocytes	Alginate-based hydrogel as a 3D model of glial scar	[173]
	Primary rat mixed neurons, microglia, astrocytes and oligodendrocytes	Type I collagen-based hydrogel as a 3D model of glial scar	[174]
	Primary rat mixed microglia, astrocytes and oligodendrocytes	Hyaluronic acid-based hydrogel as a 3D model of glial scar	[175]
	PC-12, C6, human iPSC and rat primary dorsal root ganglia neurons	Type I collagen-based 3D hydrogel for high-throughput study of neurondegeration	[176]
Organotypic	Rat organotypic hippocampal slices	Biocompatibility of silicon-based electrode arrays	[177]

cultures	Rat organotypic brain slices	Biocompatibility of nano patterned polydimethylsioxane	[178]
	Mouse organotypic spinal cord slices	Characterisation of 3D meshed-carbon nanotubes to support neurite regrowth	[179]
	Chicken embryo organotypic brain and liver slices	Cyto-biocompartibility of thin-film transistors	[180]
Brain organoids	Human induced pluripotent stem cells (hiPSC) derived organoids	Model of autosomal recessive primary microcephaly	[181]
	Human embryonic stem cells (hESCs) derived organoids	Testing functionalised borosilicate glass capillaries for glutamate detection	[182]
	Human primary microvascular endothelial cells, perycites, and astrocytes, mixed iPSC derived oligodendrocytes, microglia and neural stem cells	3D spheroid model of BBB for high-throughput neurotoxicity screening and disease modelling	[183]
Microfludics	hiPSC-derived neurons and astrocytes	High-throughput screening of neurotoxic compounds	[184]
	Ventral spinal cord motoneurons, rat primary meningeal fibroblasts and astrocytes	*In vitro* model of glial scar	[185]
	Pre-differential hiPSC lines derived from skin fibroblasts	Brain organoids on chip for the study of impaired neurogenesis induced by cadmium	[186]
In vivo models	Unilateral 6-OHDA injection in adult rats to model nigrostriatal degeneration of Parkinson's disease	Analysis of c-fos expressing after DBS of the pedunculopontine tegmental nucleus	[187]
	Unilateral 6-OHDA injection adult rats to model nigrostriatal degeneration of Parkinson's disease	Analysis of subthalamic nucleus-DBS on behavioural performance	[188]

	Rat model of retinitis pigmentosa Induction of status epilepticus through injection of pilocarpine in adult rats	Analysis of a fully organic retinal prosthesis to treat degenerative blindness Study of long-term DBS of the anterior thalamic nucleus	[189] [190]

Neuronal cells are very delicate and easily damaged, so there are many factors to consider during implantation: long-term stability in environment, low material stiffness and sufficient electrical conductivity. The important factors of tissue engineering, not only cell type is considered but the second important factor is the platform for cell to regenerate on; biomaterials which is called scaffold.

4.2.3 Scaffolds

The scaffold or extracellular matrix (ECM) is produced from both natural and synthetic materials using different techniques to obtain both 3D and 2D shapes to adapt cells to them [191]. There are five categories of scaffold which based on the function of them. Firstly, the ECM provides structural support and physical environment for cells to grow, migrate and differentiate *in vivo* and *in vitro.* A porous structure material is considered for use with this type of ECM. Secondly, the ECM contributes the mechanical properties such as elasticity, stiffness, or rigidity of tissues. Materials that are compatible with cells, with sufficient mechanical properties are used for this function. Thirdly, the ECM interacts with cells activity and provides the bioactive cues to respond to microenvironment so, biomaterials with cell-adhesive is examined. Fourthly, the ECM provides the growth factor that potential to cell actions such as delivery vehicle. Finally, the ECM provides the flexible environment for cell and allows them to remodel to tissue such as wound healing [192]. A porous structure, and the ability to diffuse biomaterials controllably, is accepted for tissue compatibility. As a biomaterial, a scaffold must satisfy a number of key constraints to be considered for use in tissue engineering and these are discussed below [193].

- Biocompatibility

The most important factor for a scaffold is to allow cells to undergo adhesion and to be non-toxic to the immune system. The scaffold not only provides a surface to which the cells will adhere but must support and regenerate them to repair or replace the damaged tissue as well. It should not be rejected by the patient's body and not cause the serious inflammation after implantation [194].

- Biodegradability

The second factor to be considered for a biomaterial scaffold after implantation is to degrade with a reasonable time scale. Most scaffolds allow cell ingrowth on them and they need to release those cells to produce their own extracellular matrix. Consequently, scaffolds are not a permanent fixture in the human body and degrade without any interaction. The degradation products must also be non-toxic or harmful to the immune system or the organs [14][195].

- Mechanical properties

The scaffold must be strong enough to hold cells and allow handling during the surgery, so mechanical properties are also considered to be necessary for a successful implantation. However, the patient's age impacts the repair rate: elderly patients take longer to cure and repair their fracture, but younger patients may take only a few weeks [196]. Thus, mechanical properties are considered when designing scaffolds. At the same time, many materials can produce highly porous scaffolds, with benefits for *in vitro* use, but with low mechanical properties, and so the potential to use them *in vivo* is small [197]. Therefore, the balance struck between porosity and mechanical properties is also a key consideration when producing a scaffold.

- Structure

Not only are the mechanical properties important but, the structure of a scaffold should have space for the cell to form and regenerate the extra cellular matrix which can support the cell with food and nutrients [198]. On the other hand, the porosity also gives the space for the cell to remove waste by diffusion, which can be excreted from the body. The pore size of scaffolds determines the chemical signal between cells and stiffness of materials [199]. Natural polymers are considered as the most successful scaffolds without the implementation binding, but synthetic materials may need other substance to influence the cell adhesion.

- Manufacturing technology

The manufacturing process involves the larger scale production of biomaterials as scaffolds even when starting from the small batch. Practical considerations include the cost effectiveness, the production environment, and storage [200].

Thus, there are many polymers are considered to use for neural implants which are both synthetic polymers and natural polymers. The most well-established synthetic polymers are polyimides, polydimethylsiloxane (PDMS), poly(*p*-xylylene) (PPX) or Parylene, liquid crystal polymer (LCPs) and SU-8 a multicomponent photoresist based on epoxy SU-8 resin [201]. Natural polymers are used as scaffold for neurons outgrowth as well which are: collagen, chitosan, keratin, silk, elastin, hyaluronic acid, and alginate [202].

4.3 Alginate for tissue engineering

Alginate is widely used in medical applications including tissue engineering, and is often used for drug delivery, growth factors delivery, or cell delivery in 2D or 3D hydrogel form because of their properties (previously explained in Chapter 1). There are many forms of alginate have been used for different purposes in medical applications include scaffolds, cell or drug delivery, and bio-inks. Alginate scaffolds can be prepared in different various ways to support and regenerate cells as follow fabrication [203];

- Microfluidic fibre-shaped coaxial

The main principle for this method is to load cells into alginate fibre by spinning alginate into fibres as a core-shell hydrogel then, culturing cells to the core and finally degrading the alginate from the culture to leave only cultured cells in the environment. It has been used for cardiomyocyte-fibres, endothelial-fibres, and cortical-fibres [204].

- Freeform reversible embedding of hydrogels

This form of alginate can create complex structure which mostly use as fresh hydrogels to stimulate the environment and support the cell within their structure. Hydrogel is made before inject suitable media and transfer cells into them [205][206]. Moreover, it has also been used for drug delivery which will be explained in Chapter 5.

- Casting tubes and vascular

Alginate can create hollow structure by casting alginate over the object and remove the object after cross-linking, it will leave the hollow structure with same shape and size replace the object such as blood vessels or vascular organs [207].

- Spheroid formation

Alginate beads benefits both cells and drug delivery by simply add cell or drug into alginate solution and dropwise into cross linking agent. The spheroid obtains cell and drug inside them and will deliver when it transfers into the right environment and temperature [208]. Alginate beads have been transported and stable diffused many cell types including chondrocytes, bone marrow stromal cells, islets, myoblasts, fibroblasts, Schwann cells, kidney cells, epithelial cells, and hepatocytes [209][210].

- Modified alginate

Combining alginate with others compounds to enhance the ability and biocompatibility gives better support cell growth and more varieties of usage. Possible compounds that can be mixed with alginate include synthetic polymers, biopolymers, ceramics, or proteins, *etc.* [211].
Furthermore, it is possible to use 3D alginate scaffolds for cell culture for a wide range of applications and cell cultures in the form of a gel can be controlled with alginate concentration, type of alginate, the cross-linking agent, and its concentration. Selected examples of applications and cell cultures with alginate scaffolds which have been studied are summarised in Table 4.4.

Table 4.4 An example of alginate-based scaffold for tissue engineering

Cell type	Scaffolds and applications	Reference
Cartilage	Chondrocytes are suspended in alginate solution then mixed with calcium sulphate before injected into facial implants mould to pre-shaped cartilage. These cartilages were placed into mice and sheep, and it was found that the cartilage constructs and forms in a 3D shape after being implanted for 30 weeks.	[212] [213]
	Dried alginate hydrogels were formed into a macroporous shape which benefits the desired geometry shape of cartilage formation after being introduced into mice by using a small catheter. These dry porous scaffolds were returned to their actual shape and size within 1h by rehydrating with primary bovine articular chondrocytes. This study showed that alginate can form the shape-memorising scaffold, *etc.*	[214]
Bone	RGD-containing peptide was used to modified alginate to promote osteoblast adhesion and spreading which resulted of osteoblast increasing. Transplanting in mice with modified alginate also enhanced *in vivo* bone formation.	[215] [216]
	Alginate modified with PAG and AAD and mixed with rat calvarial osteoblasts were prepared to use for injection into a mouse's back. The bone tissue was observed and alginate was degraded after 9 weeks.	[217]
	Alginate and hydroxyapatite (HAP) mixed scaffold show significant bone cell adhesion, *etc.*	[218]
Nerve	Alginate first used in nerve cell as a glue for repairing the damage tissue that cannot be sutured.	[219]
	Hydrogel contains alginate and anisotropic has been introduced	[220]

	and intergraded into cervical spinal cord of rat and resulted as induced the nerve cell to regrow without any inflammation.	
	Ethylenediamine was used to cross-link alginate scaffold and used for improving the regeneration of peripheral nerves and spinal cords. Moreover, the scaffold also promoted the axons and astrocyte in rat spinal cords, *etc.*	[221]
Liver	Alginate hydrogel both dried and fresh can support hepatocytes which is possible to use for liver implantation.	[222] [223]
	Hepatocytes were seeded into fresh alginate hydrogel scaffold and it was found that the cells maintain viability and appear to synthesise fibronectin.	[224]
	The porous structure alginate was seeded with rat hepatocytes and the cells formed lines and aggregates in the pores, *etc*.	[225]
Ovarian follicle	To develop fertility, alginate hydrogel was used to maintain oocytes and cell-cell interactions, this confirmed by encapsulated mouse follicles *in vitro.*	[226]
	Modified alginate with the ECM component or RGD peptide were used to promote follicle maturation and produce oocytes meiotically.	[227]
	Encapsulated ovarian follicles in alginate hydrogel were cultured *in vitro* to support the follicle structure, *etc*.	[228]

Alginate scaffold for neurons implants

Alginate has been developed with serums and different treatments to facilitate the outgrowth of neurons, but only a small number of research studies were successful [229]; others displayed binding and cross-linking reactions which might be harmful to cells [42]. A summary of interesting experiments that have been performed on alginate and neurons

outgrowth are shown in Table 4.5. To date, the majority of studies have employed alginate-based microcapsules for encapsulation and growth of cells. In contrast, the current study utilises alginate and alginate-PEDOT:PSS based composite films as 2D support for immobilisation and regeneration of neural cells.

Table 4.5 A summary of alginate-based materials for neural stem cells

Research	Result	Reference
The effects of alginate composition on the viability of neural stem cells	Encapsulation of PC-12 with high L-guluronic acid (G) without serum coated may be useful for repairing the nerve tissue.	[230]
Development of a neuroprotective agent (NT2 neurons) from alginate against oxidative stress	Alginate reduced the amyloid β formation which is the cell line model for Alzheimer's disease.	[231]
3D neural cell culture by entrapped variety of neuron cells in alginate beads	Cell were suspended in alginate beads which functionalised with proteins and serums, neurons displayed the outgrowth over time.	[232]
Alginate hydrogel for neurite growth and protection against oxidative stress	Novel soft alginate hydrogels were prepared without any modification for regeneration of neurons cells.	[233]
Neural stem cells (NSCs) were cultured in alginate beads crosslinked with calcium chloride	NSCs was almost doubled and average cell retrieve is over 88.5 %. This also shown the capacity of multilineage differentiation into neurons and glial cells.	[234]

The research data for alginate scaffolds and their applications confirms that alginate is a suitable biopolymer to use in tissue engineering and this approach also been used in neurons implants. However, alginate still need conducting ability to promote neurons network effectively which conductive polymer are considered to use with them.

4.4 Conductive polymers for tissue engineering

Conductive polymers (CPs) (previously explained in Chapter 3) are synthetic polymer with electronic and/or ionic conductivity. Their properties with conductivity, reversible oxidation, redox stability, biocompatibility, hydrophobicity, 3D geometry and surface topography are the requirement that biomedical applications need [235]. Thus, it is widely used in tissue engineering mostly because its ability; conductive to subject cells to electrical stimulation. The most cell cultures applications that apply CPs are:

- Cardiovascular applications

The electrical condition pathways in heart is the most important factor to consider when fabricate medical device or scaffold using with the cells. The cardiac cells are connecting with each other by electric impulses and transmit signal to appropriate speed and direction. So, CPs has been brought and demonstrated in cell cultures. PANI was selected to excite cells with various approaches; covalently attached oligopeptides and electrospinning PANI modified with gelatin shown the promising result in cardiac support [236]. PPy blended with heparin gave a good result for endothelial cell culture [237] while PPy blended with hyaluronic acid (HA) promoted vascularisation [238]. However, CPs still have the limitation on their mechanical properties so, blending the large molecules could possibly let them mimic the native myocardium [236].

- Neural applications

Neurons also need electrical signal to communicate among them as described in 4.2.1, and they must interact with the surface of scaffold to maintain signal quality and cells activation so, CPs were introduced and expressed in neuronal cultures. PPy films was shown the great result in increasing neurite lengths of PC12 in culture when compared with control (Schmidt et al., 1997). However, coating PPy on to culture substrates shown the improve of neurite outgrowth and help to protect neurons from degradation [239]. PEDOT has been introduced

to use in neural culture because it has higher conductivity and chemical stability when compared to other CPs, which many research studies have shown promising results for neurite lengths and outgrowth.

PEDOT:PSS scaffolds

Most conducting polymers (CPs) are not biocompatible, and so are generally not useful for tissue engineering for many stem cells support (Chapter 3). However, they can be integrated with other biopolymers to enhance their ability of cell attachment. The conductive property is very important to promote the nerve cell so, conducting polymers were developed in many ways to determine whether they could be hosts for the outgrowth cells. PEDOT:PSS films have been shown to promote the long-term survival of neuronal cells with poly(L-lysine) coating. It also has been shown to display strong neuronal responses when coated with multi-electrode arrays (MEAs) to stimulate the delivery. PEDOT:PSS has also been coated on Parylene^{TM} C film and used *in vivo* electrocorticography (ECoG) in rats. Moreover, electrochemical transistor (OECT) with PEDOT:PSS based materials were developed for use in recording brain activity *in vivo*. This finding leads to the use of PEDOT:PSS in this chapter for the potential benefits for neurons outgrowth and incorporation with alginate to reduce the oxidative stress in the same time. The example of using PEDOT:PSS is summarised in Table 4.6.

Table 4.6 A summary of using PEDOT:PSS for neurons regeneration.

Research	Result	Reference
The effects of the viability of neural stem cells by employing	The primary embryonic neurons survived.	[50]
PEDOT:PSS coating on the materials used	Neurons had long-term adhesion on the surface by coating poly(L-lysine) to improve it.	[240]
Stimulating the neurons delivery by coating PEDOT:PSS on the electrodes compare with the uncoated	PEDOT:PSS coating was displayed a strong neuronal responses on multi-electrode arrays (MEAs) which use to stimulate the delivery.	[241]
In vivo of adapting PEDOT:PSS on parylene-C film in elctrocorticography (ECoG) and further development	The sharp-wave of neurons signal were successfully recorded	[242]
electrochemical transistor (OECT) for recording the brain activity based on PEDOT:PSS	The strong signal-to-noise ratio (SNR) were record and compared with surface electrodes	[243]
The impact of PEDOT:PSS on neuronal synaptic activity and glial-cell activity	It has not been fully investigated but the electrodes from PEDOT:PSS was involved the design	[244]
In vitro of PEDOT:PSS interfaces support the neuronal synaptic network and reduce the neuroglia	PEDOT:PSS can be exploited for the neurons development when layered in culture and reduced glial in long-term culture	[245]

Moreover, 3D scaffolds of PEDOT:PSS mixing with 3-glycidoxypropyltrimethoxysilane (GOPS) by an ice-templating method showed the greater result of mouse fibroblasts (3T3-L1) outgrowth and can control the protein conformation and cell functions for longer and larger cell cultures [246]. (3-Glycidyloxypropyl)trimethoxysilane (GOPS) is an epoxy-silane coupling agent, whose epoxide group is capable of undergoing reaction with both

nucleophilic reagents, such as carboxylic acids and amines, and electrophiles. The nucleophilicity of the reagent will determine whether the reaction mechanism involves the lone pair of electrons on the nucleophilic oxygen atom or the less-substituted electrophilic carbon atom within the oxirane (epoxy) ring to form a covalent bond [247]. The non-bonded electron lone pair on both the oxygen atom in the oxirane ring and the nitrogen of e.g. an amine are also capable of associating through the formation of hydrogen bonds facilitating the opening of the epoxy through electron rearrangement [83] and formation of another covalent bond, this time between the oxygen-hydrogen atoms. This formation of neutral species, in turn, makes them suitable for use in biomedical applications and cell culture.

Consequently, GOPS has been used in biomedical applications as a surface modification in order to immobilise DNA, antibodies, glucose oxidase including cell culture of bone, dental also neurons. Herein, GOPS has been used successfully in hippocampal neurons culture on micropatterned with poly-d-lysine (PDL) lines and stimulation of neural circuits after 3 weeks [248]. So, GOPS are preferentially localised and generated the dendrite of cell in the cortex to corresponding dendrite in cell culture [249].

An individual alginate and PEDOT:PSS was investigated the biocompatibility and shown the great result and strong neuronal signals. In this study, the combining both materials together were examined for potential in better neurons attachment and support the synaptic networks in short and long term culture (*i.e.* 7 and 14 days).

4.5 Experimental: Materials and processing techniques

4.5.1 Scaffold preparation for neurons experiment

Films preparation

Alginate (2 wt%) and PEG (2.5 wt%) were mixed with PEDOT: PSS solution (25 mL). A PVA stock solution of 25 wt% concentration in deionised water, was added to the above

mixture, which was homogenised using magnetic stirring for 3h. The concentrated mixture of alginate and PEDOT:PSS was prepared following the fibres mixture solution method reported in Chapter 3. The films with constant mass were cast by transferring polymer mixtures (6 g) to plastic petri dishes with 9 mm diameter. The films were aged overnight at room temperature for drying ensuring that no air bubbles were trapped within the films. After that, the dried samples were cross-linked with $CaCl_2$ (50 mM) for 15 mins before residual $CaCl_2$ was removed, washing the films with deionised water and dried the cross-linked samples at room temperature for 36 hours. In order to investigate the effect of temperature on the properties of the composite films, the film samples were heat treated in an oven at 150 ºC for 10 mins. Several various additives; (PEG, EG, and GOPS (3-glycidyloxypropyl)trimethoxysilane) were added to compare the viability, cross-linked with and without $CaCl_2$ are summarised in Table 4.7. Finally, the films were punched into small circular pieces with a 6 mm tissue puncher and placed in the well-plates shown in Figure 4.3. As a control sample, neat alginate films were produced using similar procedures.

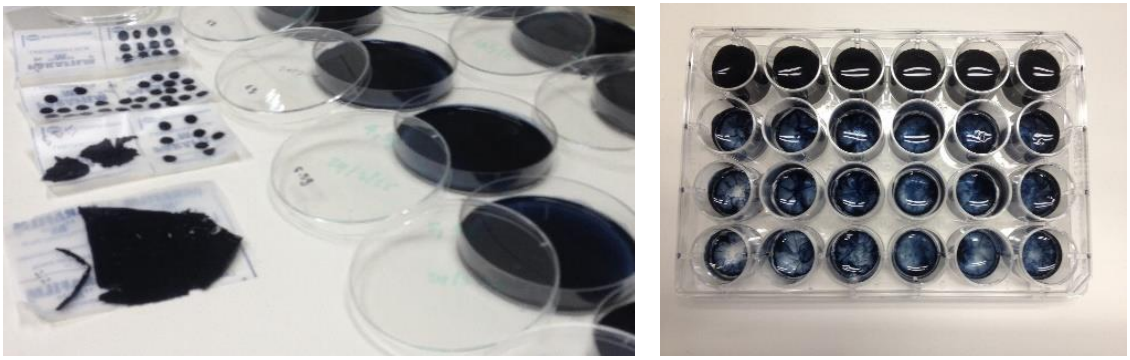

(a) (b)

Figure 4.3 Film preparation for neural outgrowth, the solutions were cast on the petri dish, dried at room temperature, cross-linked with $CaCl_2$ then dried at room temperature before punched into small pieces and put into a 24 well-plate. (a) The films prepared which in the petri dish contain alginate, PEDOT:PSS, and PVA while the films on the paper were already cross-linked with $CaCl_2$, dried and punch into small pieces. (b) The circular pieces of film with diameter 6 mm were transferred to 24-well plate for further neural growth experiments.

Table 4.7 A summary of the substrates prepared for the neurons outgrowth experiments

Conditions	Materials combination
1	Coverslip control
2	PEDOT:PSS + 1% GOPS + PEG + alginate
3	PEDOT:PSS + 1% GOPS + EG or PEG + alginate ($NaHCO_3$ casting)
4	PEDOT:PSS + 1% GOPS + EG + 25% PVA + alginate
5	PEDOT:PSS + EG + 25% PVA + alginate
6	PEDOT:PSS + alginate with $CaCl_2$
7	PEDOT:PSS + 1% GOPS + EG + 25% PVA + alginate

Seeding neurons preparation

Coverslips were placed in each well of the 24-well-plate then circular pieces of film with 6 mm diameter were placed into each well apart from the last column (Figure 4.3b). The column of last was used as a control to monitor the effect of substrate/support on the cell adhesion and growth. Every well was washed with 70 % ethanol for 3 h with shaking, then rinsed three to four times with culture water (5 mL) and left to dry in the control environment. Then, following surface coating with poly(L-lysine) (PLL, stock 10 mg/ml) beforehand, diluted 10 times with the PLL in cell culture water, before the plates leaving at 37 °C, 5 % CO_2 incubator overnight (Figure 4.4).

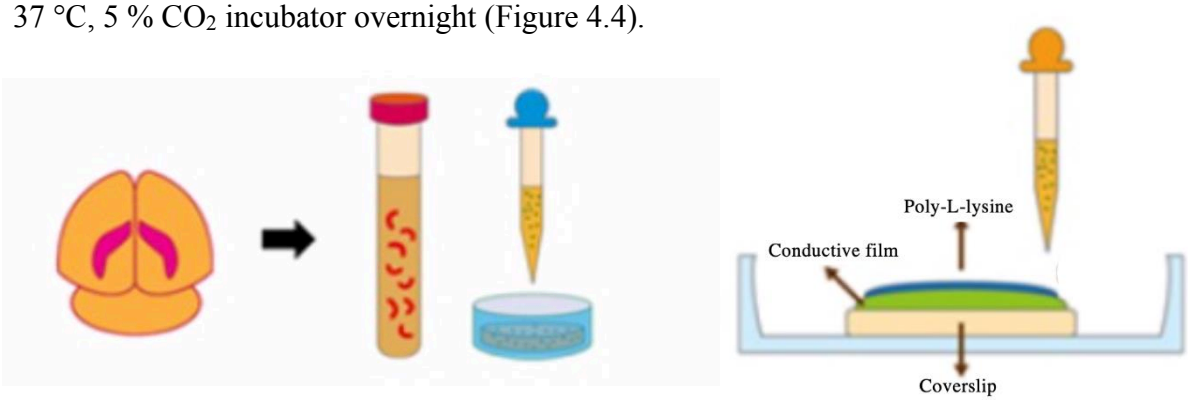

Figure 4.4 The dissection of cortex from the embryo of rat which added into media before placing on the coverslip that placed the conductive film on top and coated with poly(L-lysine) in the well plate.

For seeding cells, well-plates were washed again with culture water (3 x 5mL) and a quick rinse with the plating media and filled each well with fresh plating media (1.5 mL), approximately 100,000 neurons were placed into each well. After 2 h, the plating medium was replaced with feeding medium (3 mL) to avoid the growth of glial cells. The plates were kept in the incubator at 37 °C, 5% CO_2 for 7 and 14 days.

The above well plate was aged for 7 days, after which the plate was rinsed with PBS and observed by viability/cytotoxicity assay kit for animal live and dead cells (supplier Biotium). The assay was diluted in PBS by using the transparent solution (substrate calcein) 2 % wt and the red solution (Ethidium homodier III) 0.5 %wt then each well was filled with the prepared stain solution (200 µl). Each film was removed and placed on the glass slide for analysis using fluorescence microscopy (wide-field imaging, Leica DM IRBE inverted microscope), images were obtained of different areas of the film by Volocity software. Include excitation and emission wavelengths used to obtain the images.

Determination of effects of $CaCl_2$ on neuron growth

Alginate (2 wt%) alginate with de-ionised water and the resulting solution was cast on a petri dish, left for 12 h., then cross-linked with various aqueous solutions of $CaCl_2$ of different molarity: 2 mM, 5 mM, 25 mM, 50 mM and 100 mM. Neurons were seeded on films and incubated for 7 and 14 days.

4.5.2 Data Analysis

Data were transferred to imageJ software to count the number of dead and live cells. For each film composition, 10 samples were obtained for analysis and comparison of the results. The use of stem cells are derived from embryos tissue, which is governed by ethical and legal issues, and these need to be destroyed after the experiments have been concluded.

4.6 Results and discussion

The conductive fibres developed in Chapter 3 were carried forward to examine the possibilities to seeding neurons and monitor the number of living cells growth. However, after seeding the neurons and having left them in an incubator for 7 and 14 days only dead cells were observed (Figure 4.5 a).

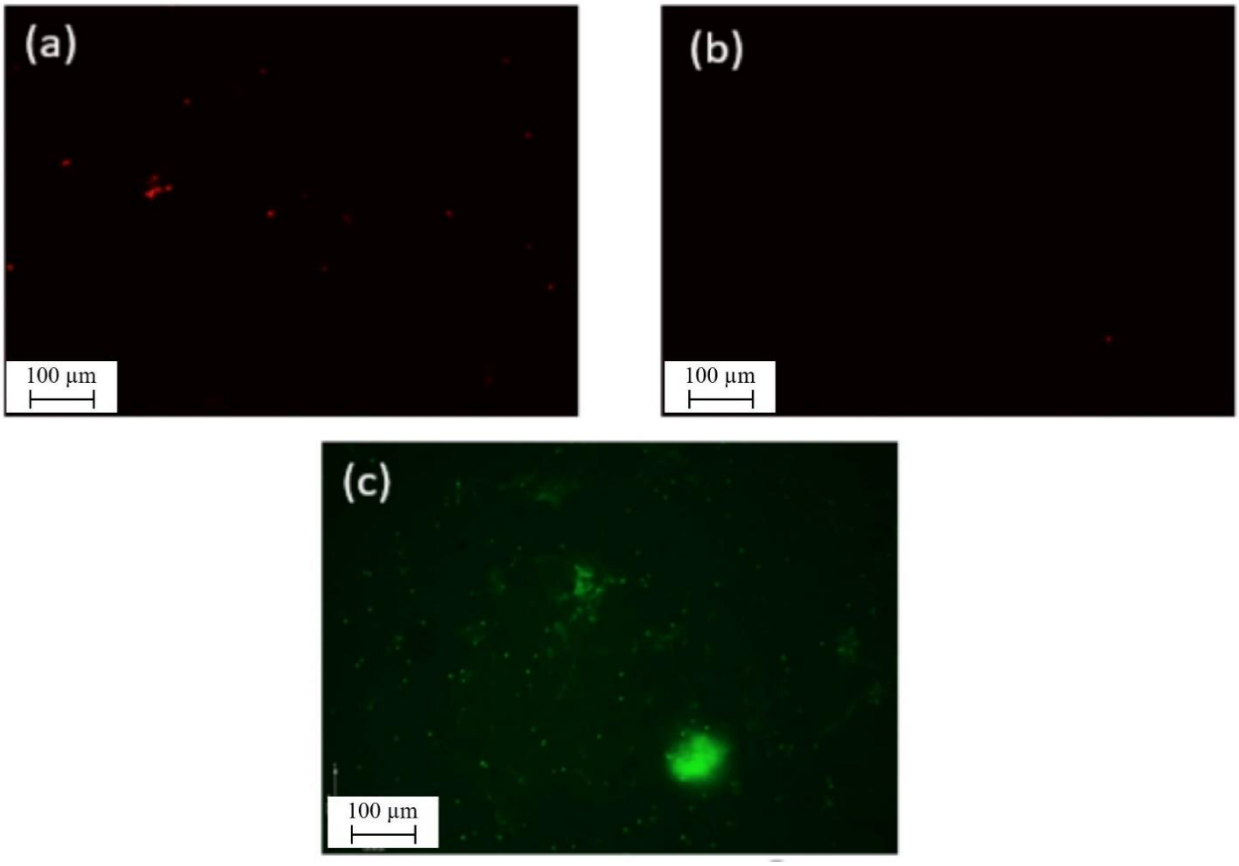

Figure 4.5 Fluorescence microscopy images showing growth of neural cells on substrates coated with poly(L-lysine) for 7 and 14 days (a) alginate conductive fibres cross-linked with 15 wt%, scale bar = 100 µm (b) conductive composite films (ALG-PEDOT:PSS-PEG) cross-linked with 15 wt% $CaCl_2$, scale bar = 100 µm and (c) glass cover slip without $CaCl_2$, scale bar = 100 µm.

Thus, the conductive films were prepared under the same conditions as the fibres to optimise the surface area affected the cells attachment. These films were observed after a period (7 and

14 days) in the incubator, the living cells were still barely visible beyond the fibres seen in Figure 4.5 b. Varying the concentration of $CaCl_2$ (2-100 mM) on neat alginate films confirmed the potential for growing neurons on the films, compared with a blank well covered with a glass cover slip, but without $CaCl_2$.

After the neurons had been seeded on films and incubated for 7 and 14 days. The highest population of neurons on glass cover slip was observed, followed by the film containing 50 mM of $CaCl_2$, as seen in Figure 4.6 (Appendix; Figure of 2 mM, 5 mM, 25 mM, and 100 mM). This experiment confirmed that the alginate supported neurons when the correct amount of $CaCl_2$ was incorporated. Both high G and high M samples were cross linked with 50 mM $CaCl_2$ to find the best profile for neurons and this confirmed that high M was more friendly to the cells (Figure 4.7).

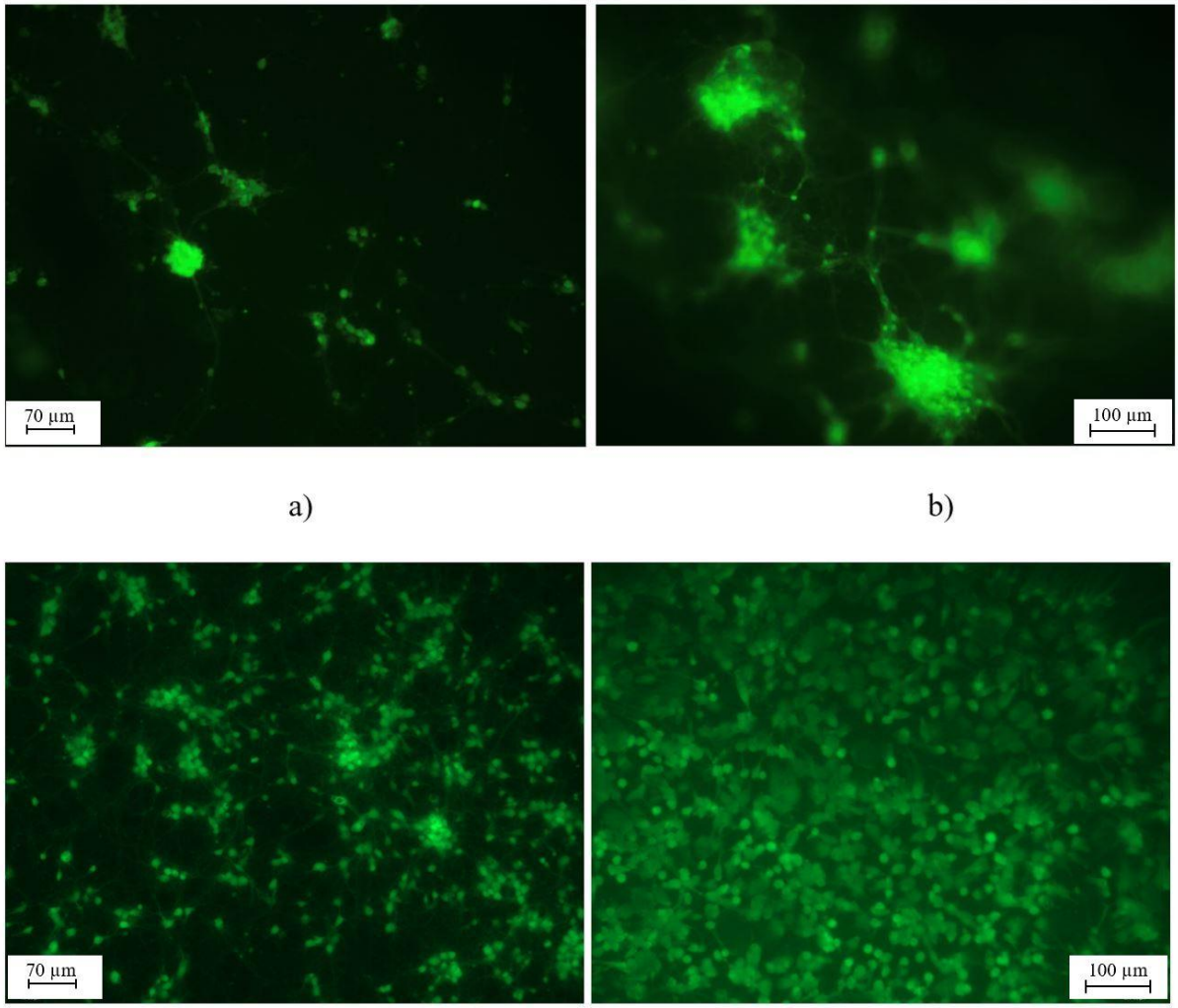

Figure 4.7 The results of a) alginate films with 50 mM $CaCl_2$ after 7 days, scale bar = 70 µm b) alginate films with 50 mM $CaCl_2$ after 14 days, scale bar = 100 µm compared to c) cover glass slip control well after 7 days, scale bar = 70 µm and d) cover glass slip control well after 14 days, scale bar = 100 µm.

A large number of live neurons are apparent in the control well but some neurite connections are still visible on the 50 mM $CaCl_2$ alginate film. After 7 days, the neurite connections on the alginate films with 50 mM $CaCl_2$ (Figure 4.5 a) were found to be healthier than alginate films with 15 wt% $CaCl_2$ (Figure 4.6 a) also the number and density of living cells were both

increased. This result confirmed that the concentration of $CaCl_2$ effected the conditions of cell growth which Wojda (2008) reported, *i.e.* calcium ion are essential for neurons to generate their signal and prevent the degradation but the higher calcium concentration in the growing conditions could be toxic to the cells instead.

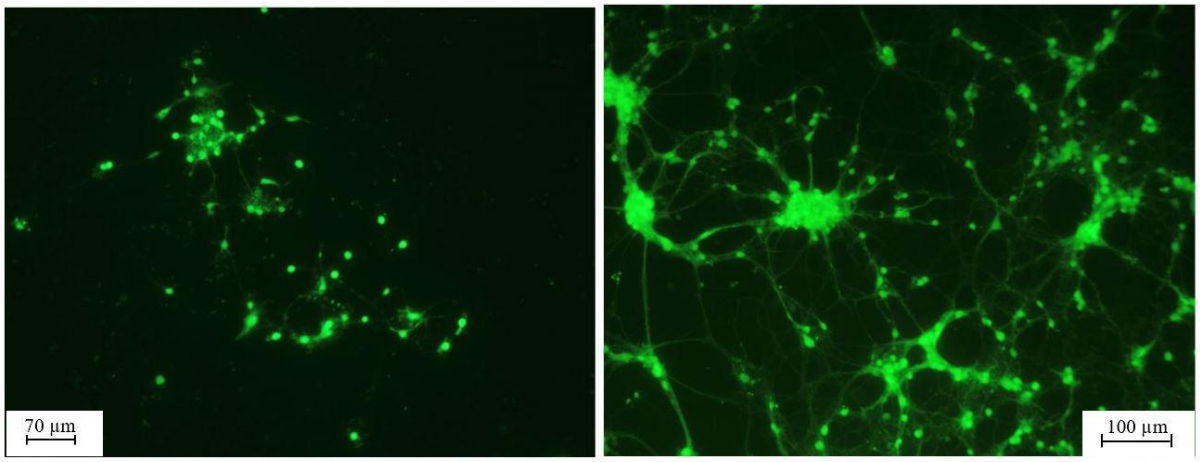

a) b)

Figure 4.8 The results of a) alginate films with high G crosslinked with 50 mM $CaCl_2$ after 7 days compared, scale bar = 70 µm with b) alginate films with high M crosslinked with 50 mM $CaCl_2$ after 7days, scale bar = 100 µm showed the result of better attachment of neurons on high M alginate than high G alginate.

The experiment was carried out to find the best method of coating poly(L-lysine) on the surface of the films to introduce positive charge and enhance cell adhesion and make them suitable for neurons in further experiments. The 2 wt% high M alginate crosslinked with 50 mM $CaCl_2$ was used in this experiment with a traditional step to remove residue of poly(L-lysine) by leaving in the incubator for 2 h and ensuring the seeding medium was introduced immediately, compared with the additional drying step prior to coating with poly(L-lysine) by allowing the films to dry before filling the well with the seeding medium. The greatest evidence of attachment was found in the additional drying steps when samples were left for 7 days in the incubator (Figure 4.8).

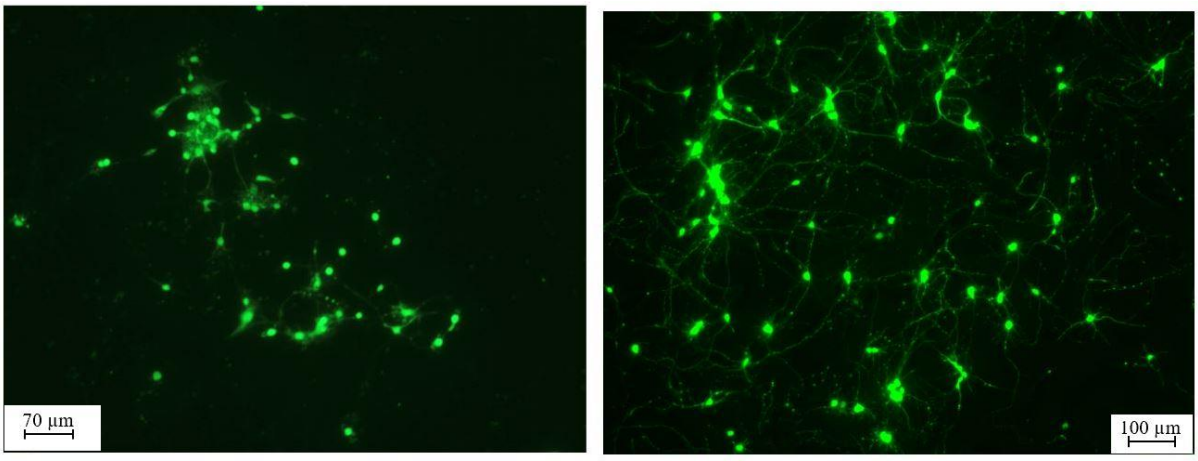

a) b)

Figure 4.9 The results of a) alginate films with 50mM $CaCl_2$ and traditional poly(L-lysine) method after 7 days showed survived neurons, scale bar = 70 µm while b) alginate films, 50 mM $CaCl_2$ with drying method poly(L-lysine) after 7 days, scale bar = 100 µm showed more dispersion and longer neurite of neurons.

According to the alginate properties (discussed in Chapter 1), a high M is more compatible with the cells as the density of cross-linking is lower which allows cells to generate and grow better than high G. However, there is no evidence where this result is applied to every cell culture. While poly-L-lysine enhances the interaction between cells and substrates surface by increasing the positive-charged on the membrane to interact with negative-charged from cells [250] and the result of coating poly(L-lysine) on alginate films (Figure 4.9) showed the better attachment of neurons.

The neuron cell count was initially determined following incubation on different materials (Figure 4.10 a) using the variation of the $CaCl_2$ crosslinking concentration to produce the highest cell counts at a concentration of 50 mM, although the growth on glass coverslips was observed to be far greater. With the incorporation of a drying step prior to the additional of poly(L-lysine), cell attachment was improved across all conditions (Figure 4.10 b). However, the glass coverslip again attached more cells than the alginate films. In conclusion, these experiments suggested that the best level of growth was observed with 2 wt% of high M

alginate when crosslinked with $CaCl_2$ 50 mM and combined with an additional drying step of poly(L-lysine) to promote the growth of neurons.

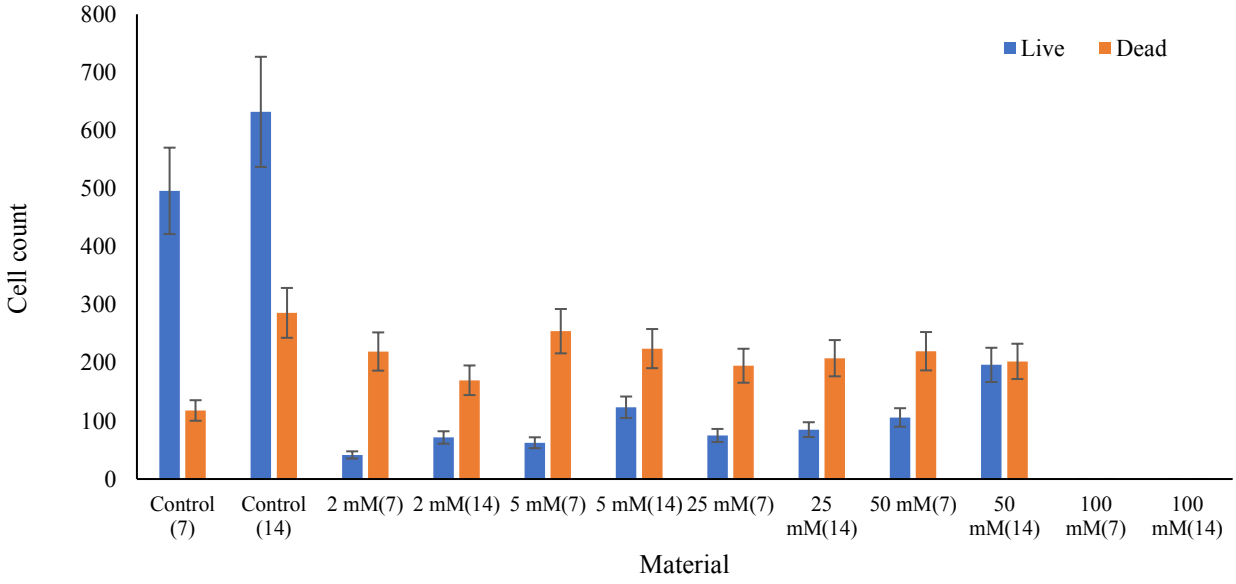

a)

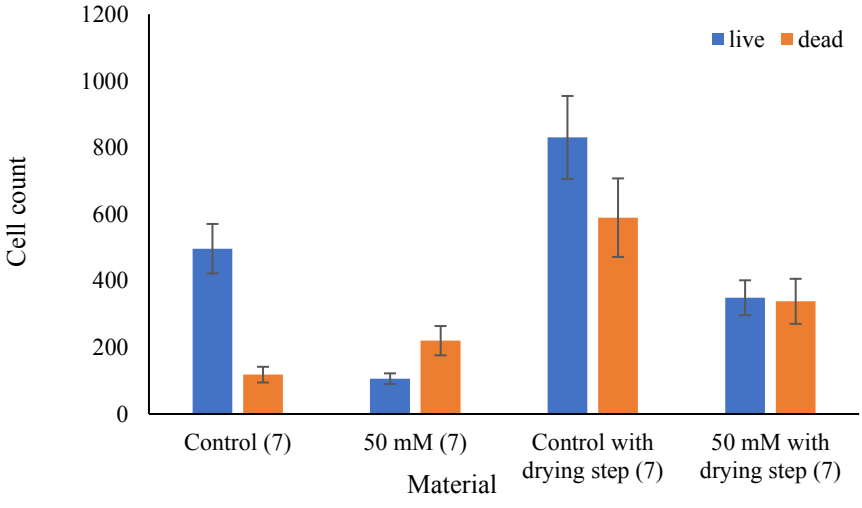

b)

Figure 4.10 neuron cell count following a) incubation on different materials which were control well on the coverslip and films with 2mM, 5mM, 25mM, 50mM and 100mM $CaCl_2$ crosslinked, b) an additional drying step prior to the additional of poly(L-lysine) on coverslip control well and 50mM $CaCl_2$ crosslinked films.

Chapter 4. Conductive composite films for neural implants

To continue with the introduction of the conductive polymer into alginate, films containing various additives (*e.g.* PEDOT:PSS, GOPS, (3-glycidyloxypropyl)trimethoxysilane, PEG, EG, and PVA) were prepared. The selection of PEDOT:PSS as an additive was to introduce conductivity into the alginate films to promote the growth of neurons (discussed in Section 4.4). The addition of PEG has previously been shown to enhance the electrical conductivity in the context of the fibres (see Chapter 3) and to improve the biocompatibility of the films. PEG individual was used to improve and influence the number neurons in hydrogel [251]. PEG was used to guided neurons outgrowth on the adhesive scaffolds [252]. Therefore, adding PEG into alginate and PEDOT films makes it possible to support and guide the neurons to promote with neurite lengths on scaffold. Even so, EG is considered as a toxic organic compound but as it can increase the conductivity as same as PEG (previously explained in Chapter 3) so, EG was carried out into this research because there is no evidence to confirm that EG directly affect to neurons yet. However, PVA has shown significant cell promotion when blended with alginate, not only PC12 cells [128] but also with bone tissue engineering [253]. Moreover, when PVA and alginate were blended they improved cell compatibility in terms of cell adhesion and faster cell growth [254]. Finally, GOPS was added into films in order to increase the cell number, which was explained through the example of PEDOT scaffolds in Section 4.4.

The cast films were crosslinked with and without 50 mM $CaCl_2$ and the films were compared following treatment with and without a heating step to enhance the conductivity. These data were collected after 7 and 14 days and then compared with the alginate films and glass coverslip control wells. Therefore, the experiments included the following conditions:

1. PEDOT:PSS + 1% GOPS + PEG + alginate
2. PEDOT:PSS + 1% GOPS + EG or PEG + alginate ($NaHCO_3$ casting)
3. PEDOT:PSS + 1% GOPS + EG + 25% PVA + alginate
4. PEDOT:PSS + EG + 25% PVA + alginate
5. PEDOT:PSS + alginate with $CaCl_2$

6. PEDOT:PSS + 1% GOPS + EG + 25% PVA + alginate

The populations of neurons were estimated from photomicrographs that have been examined by using infrared microscopy and attempts were made to exclude glia and endothelial cells. Five separate neural counts were performed in 10 different known areas of samples that had been microtomed/sectioned , then the population of neurons in a unit volume were calculated. However, it is acknowledged that some cells may have been missed if they were obscured by other cells, and others may be out of the focus in a photograph. Moreover, the difficulty in distinguishing glial cells from small neuron cells may lead to inaccuracies in determining the population.

The fluorescence images were used to determine the numbers of neurons demonstrating outgrowth on films and coverslips. The combination of alginate with conductive polymer films shows the variability of neuron attachment, however, most of them were still less attached when compared to the control coverslips. All preparation conditions yielded samples with homogeneous structures, but the alginate film showed the most significant number of neurons outgrowth, with the cell body surrounded by a neurite network (Appendix Figure 4.11). The neuronal viability of the coverslips as control samples showed the best level of attachment and the rest outgrowth of cells when compared to alginate and the composite films, but when considering the quality of the cells obtained from both films, they gave promising results based on the number of living cells (Figure 4.12).

The summary of the highest cell growth observed for the alginate with conductive polymers under different growth conditions are shown in Fig. 4.12. The degree to which the neurons become attached to the alginate containing the conductive polymer films is influenced by the different growth conditions, but most of the samples were still less attached when compared to the control cover slips. The alginate containing no $CaCl_2$ cross-liker and with no annealing displayed the highest attachment and also the EG performed better than PEG additive in samples following both 7 and 14 days.

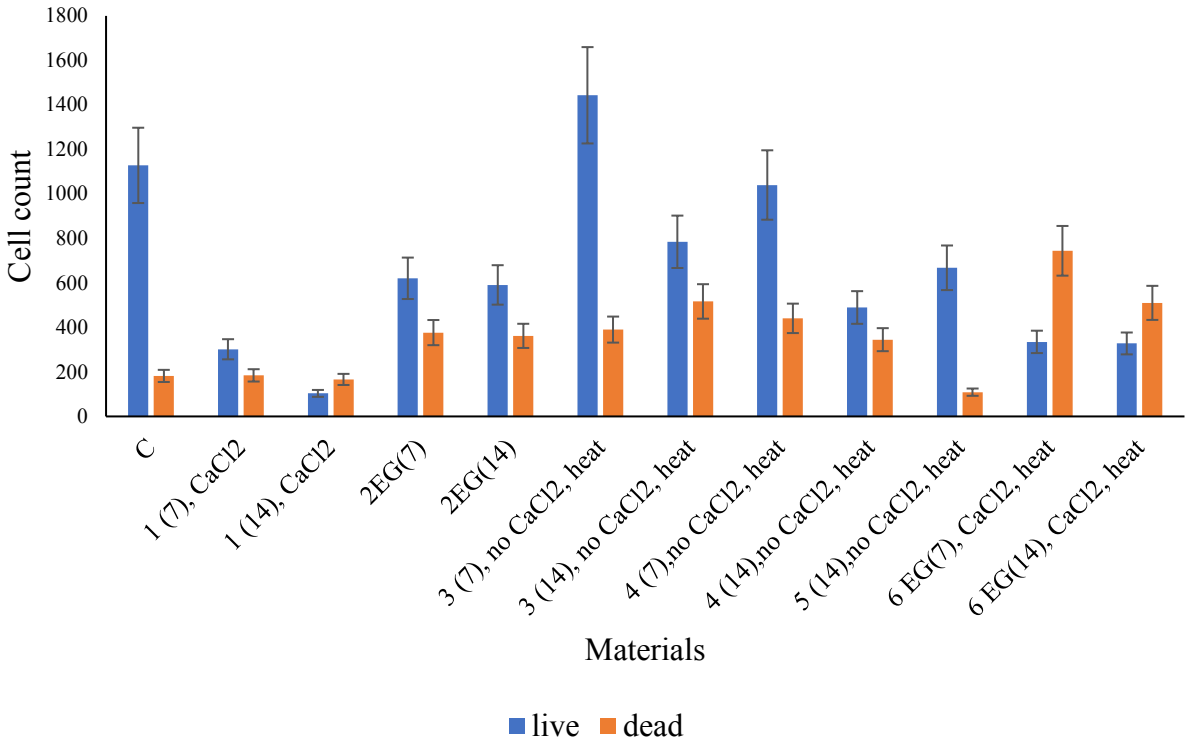

Figure 4.12 Summary of the highest cell growth from different conditions. Key: C = control coverslips, 1. PEDOT:PSS + 1% GOPS + PEG + alginate, 2. PEDOT:PSS + 1% GOPS + EG or PEG + alginate ($NaHCO_3$ casting), 3. PEDOT:PSS + 1% GOPS + EG + 25% PVA + alginate, 4. PEDOT:PSS + EG + 25% PVA + alginate, 5. PEDOT:PSS + alginate with $CaCl_2$, PEDOT:PSS + 1% GOPS + EG + 25% PVA + alginate.

From a determination of the population of neurons in each sample within a specified area, it was found that the less than 30% of the neuron cells that were initially seeded underwent further development. Within the control well, a population of around 18% of living cells was found, suggesting that the procedure used to seed cells did not cause the death of cells that was observed during the incubation time. However, the films prepared without $CaCl_2$ (condition 3) displayed a population of around 25% of developed neurons cells, which is slightly larger than the control well and greater than other conditions which shown around 2-13% of living cells.

Considering all of the conditions tested, including the control well, the cortex cells have been found to grow best on alginate and PEDOT:PSS conductive films, in the absence of $CaCl_2$ cross-linker, but containing GOPS, EG, and PVA additives. The presence of GOPS is believed to help to increase the number of developed cells, as explained in section 4.4. EG was added to enhance conductivity of PEDOT:PSS [125,126] and PVA yielded significant cell promotion [248]. Moreover, in common with finding reported by Wojda (2008), the $CaCl_2$ cross-linker has been found to be harmful to the cells rather than helping cell growth of. Surprisingly, it was also found that when the alginate was tested in the presence of additives salt ions were not needed to form cross-links, but the films obtained in this way were brittle and would not swell in media when compared to those cross linked with $CaCl_2$.

The key benefit of this research was to establish the cortex cell growth on conductive films which had been prepared from alginate, PEDOT:PSS and selected additives. This is novel finding, which had not previously been studied as shown in the reference sources cited in Table 4.5 for alginate films and Table 4.6 for PEDOT:PSS blends. Although, the limitation of counting cells visually could lead to some error,caused by cells obscuring one other, the use of particle tracking code was not possible as the cells contain dendrites.

4.7 Conclusions

The blends containing the alginate and PEDOT:PSS films were seeded with neurons and investigated in this chapter. A study of the production of uniform composite films offers a great opportunity for applications involving the outgrowth of neurons in scaffolds. This study was carried out fibres produced within Chapter 3 to demonstrate neuronal culture, but the result shows non-growing cell along the fibre so, films with same conditions were examined, but these also gave negative results. Therefore, a further study was undertaken to find the effects of different growth parameters: type of alginate, cross-linker concentrations, additive and heat treatment. Consequently, the following points can be highlighted from this research:

1. The findings suggest that alginate with high M alginate gave the better support for neurons cell culture than high G alginate.

2. Moreover, not only can alginate support the outgrowth of neurons, but the conductive films prepared also give promising results to promote cell growth. The highlight findings also suggest that the greater number of living cells were found on the prepared films (alginate + PEDOT:PSS + 1% GOPS + EG + 25% PVA) when compared to the coverslip but it suggests the potential to improve the density of cells should have been taken in the future.

3. Adding additives to scaffolds gave better cell attachment while a $CaCl_2$ cross-linker yielded fewer neurons than the absence of crosslinker, which confirms the result of Wojda (2008) that calcium can be toxic to cells.

4. Surprisingly, EG supported more neurons than PEG but enhanced the conductivity to a lower degree than the PEDOT:PSS/alginate fibres in Chapter 3. However, it is still not possible to conclude that EG promotes neurite network growth as the heating step might have lost EG from the scaffolds, through evaporation, which may leave only low or non-toxic compounds to enhance the neurons' outgrowth. A mixture of EG in water was found to begin evaporation at around 44 ˚C and when increasing temperature the majority of the EG evaporated [255].

5. When PVA was added into the films it helped to promote the cell growth because PVA is improving the cell adhesive on the surface of films for neurons to attach [256].

6. This study showed that addition of GOPS with PEDOT led to a greater density of neurons, which agreed with the literature findings involving the use of GOPS in hippocampal neurons culture on micropatterned with poly-d-lysine (PDL) lines [249]

7. Heat treatment not only increased the fibre conductivity (Chapter 3) but also the number of the neurons in the scaffold. This could be due to the effect of the increased conductivity, allowing cells to transmit their signal better or perhaps that the heat removes some toxic compounds from the membrane.

Finally, the mechanical properties and electronical conductivity are also important and would affect the function of the cell. This work should have been carried out but the scaffolds produced were brittle to allow this, although determining both properties would be beneficial to understand more about cell adhesion.

Chapter 5

Biopolymer-organoclay composite hydrogels for controlled drug delivery

5.1 Introduction

The preliminary positive results of biocompatibility associated with the model neuronal implants in Chapter 3, demonstrate the potential of using alginate in tissue engineering. This chapter expands the use of alginate by discussing the synthesis of alginate-organically modified clay (organoclay) hybrid hydrogels and demonstrates their properties and potential for application in controlled drug release which focusing on slow release of drug and could further benefit to target drug release. Alginate displays an excellent gel forming structure as discussed in the literature review; it also has a wide range uses in medical applications, including tissue engineering, wound dressing, and is well known for drug delivery and cell encapsulation, which will be discussed in this chapter. Consequently, this research aims to develop alginate hydrogel by using organoclay as a cross-linker to prolong drug release. The addition of an organoclay, a layered material, has also been shown to confer unique host-guest chemistry, chemical, electrical, and mechanical properties. They are very useful for

carrying drug molecules, enzymes or proteins, and release small molecules slowly with time, and this will be discussed in greater detail in this chapter as well. The resulting physical and chemical properties of the hydrogels prepared are compared with a baseline calcium alginate hydrogel. Both rheological and thermal properties are reported and the controlled release of a model pharmaceutical compound is examined to determine the ability of hydrogel to facilitate drug release.

5.2 Drug delivery

5.2.1 Introduction

The term 'drug delivery' describes the action of a system that introduces pharmaceutical to treat a therapeutic in a patient's body. Drugs can be delivered to body by different routes: buccal, oral, pulmonary, transdermal, ocular, nasal, sublingual, vaginal, or anal [257][258]. A summary of each route is shown in Table 5.1.

Table 5.1 Summarised routes to drug using selected delivery systems

Route	Drug delivery system	Formula
Buccal	Drugs are applied between the gum and cheek without passing them to the liver. It is limited to only small drug molecule with lipophilic properties.	Tablets, gels, lozenges, patches.
Nasal	Drugs are used to treat the inside nose to upper trachea in spray/aerosol form.	Liquid, powder.
Ocular	Drugs are absorbed through the eye.	Gels, droplet
Oral	Drugs can be swallowed and absorbed in the gastrointestinal tract.	Tablet, gels, liquid
Pulmonary	Drugs are delivered by inhalation through the mouth, to treat lung diseases.	Liquid, Powder.

Sublingual	Drugs are placed and absorbed under the tongue which is rapidly absorbed into the bloodstream.	Tablet, patches
Transdermal	Drugs are released by application to the skin and absorbed more deeply through the epidermis to the dermis.	Gels, patches
Vaginal or Anal	Drugs are delivered to treated infections of the vaginal or anal area. It can be used when other routes are contraindicated. Vaginal drug and hormones are delivered without passing to the liver and gastrointestinal tract.	Gels, tablets, pessaries, suppositories

The drug delivery system can be steady, controlled, or targeted depending on the aim of therapy. The targeted drug delivery is the system that enable drugs molecule to be released at the specific desired target and enhance the curing efficacy without off-target effects, while the steady and controlled systems are only absorbed into the bloodstream [259]. The targeted drug delivery system can be used in any route of delivery system. The mechanisms of targeted drug delivery can be subdivided into two further types as follows [260]:

- Active targeting describes the situation where a system transports the drug and delivers it to a specific location.
- Passive targeting describes the situation where drug accumulation occurs at the specific location form by tissue permeability alone.

There are very few drugs that can directly introduce to the body because of toxicity and the side effects so, to optimise the best performance of using drug, the appropriated carrier or vehicle is involved to transport drug to the target.

5.2.2 Drug delivery vehicles

Drugs need to be dispersed or dissolved into a suitable matrix substance to reduce their toxicity and side effects also protecting the drugs from degradation before being injected,

swallowed, applied or sprayed, which is called a "structured delivery vehicle". So, the structured delivery system is entrapped or encapsulated drug molecule within matrix substance and benefits stable release at the target [261]. The vehicle structures that have been found in the market are emulsions, gels, liposomes, polymers, dendrimers, solid-lipid nanoparticles, and composite nanoparticles. Selected examples of vehicle structure systems are summarised in Table 5.2.

Table 5.2 Selected examples of vehicle structure systems for drug delivery

Structure	Mechanism	Ref
Emulsion	Stabilised immiscible combination; oil and water with surfactants, emulsifiers and thickeners are used to carry drugs. It can classify by type of emulsions as followed: - Macroemulsions are lower emulsifier component with temperature sensitive and stabilised by kinetic energy. The mixture is cloudy or milky liquid. - Microemulsions are formed instantly with high emulsifier levels. The mixture is translucent to clear liquid.	[262]
Liposome	Spheroidal vehicle is encapsulated drug and offered stable release. It is suitable for wide range of drugs and can carry large drug loads inside them.	[263] [264]
Nanoparticles	Modifying nanoparticles to optimise the bioavailability, decrease clearance and increase stability are used to carry drug to the target desired specific tissue target.	[265]
Microspheres	The smaller version of sphere shape is prepared with *"free flowing powdered drug delivery systems"*. Drugs are dispersed in a polymer matrix which can comprise both natural or synthetic polymers.	[266]

Furthermore, there are more drug vehicles that have been successfully utilised and have advantages as drug delivery systems, such as niosomes, monoclonal antibodies, injectable, and hydrogels.

The basic functions that are required for an effective drug delivery system are biocompatibility, bioactivity, safety, degradation, and low also cost. Targeted drug delivery systems additionally require:

- *Rate of elimination of drug-carrier conjugate (KR)*

The best delivery systems are to release drug at the desired target and vehicles should not release the drug rapidly, nor be removed from the circulatory systems. So, the design of vehicles needs to consider the primary forces: electrodynamic, electrostatic, and hydrogen bonding, for their overall properties.

- *Rate of release of free drug at the non-target site (KDRC)*

As drug release occurs when the vehicles are taken up in the systems, the release of drug away from the target is non-beneficial and could possibly be toxic to the body. So, it is necessary to observe the amount of actual drug released at the target from which a calculation may be undertaken to determine the appropriate concentration of pharmaceutical into the vehicles.

- *Rate of delivery of drug-carrier conjugate to the target site (KT)*

If the release of drug to the target is too slow, then treatment at the target site may be delayed, causing further tissue injury or cell damage.

- *Rate of release of free drug at the target site (KTDR)*

The capacity of drug delivery systems to control the release rate is also considered to ensure the accumulation of drug at target site.

- *Rate of removal of free drug from the target site (KTDC)*

To maintain the therapeutic effect, drugs need to be designed specifically for while they are delivered to cytoplasm, drug release must happen within the cell.

- *Rate of elimination of the drug-carrier conjugate and free drug from the body (*KDS_{elim} *and* KD_{elim}*)*

Removal of the drug carrier and excessive quantities of drugs from the circulatory system occurs mainly in the liver with rapid rate to avoid toxicity to the body [267][268].
However, during the development of a drug delivery system, it is necessary to perform the delivery *in vitro* prior to delivery *in vivo* to measure the drug release rate, degradation time, toxicity, *etc.* and optimise the best effective drug in use.

5.3 Hydrogel

Hydrogels are 3-D networks comprising chemically or physically bonded polymer(s) which may be swollen with water without dissolution. They are simply made from hydrophilic polymers by cross-linking reaction of one or more monomers which are both natural or synthetic materials, depending on purposes and abilities of hydrogels needed. Hydrogels can be classified by different basic characteristics as follows [269]:

- Classified by their origin (natural or synthetic).
- Classified by polymeric composition (homopolymer, copolymer or multipolymer).
- Classified by their physical structure and chemical composition (amorphous, semi-crystalline or crystalline).
- Classified by cross-linking type (chemical; covalent cross-linking, oxidation, copolymerisation or physical; ionotropic gelation, hydrophobic interaction, complex coacervation, hydrogen boding).

- Classified by appearances (matrix, film or microsphere)
- Classified by electrical charge network (non-ionic, ionic, amphoteric electrolyte, or zwitterionic)

Moreover, they are controlled by environmental conditions *e.g.* temperature, pressure, pH, light, sound, ultrasound, electric, magnetic, chemical *etc.*, which influence swelling or de-swelling reversibly in water, shown in Figure 5.1.

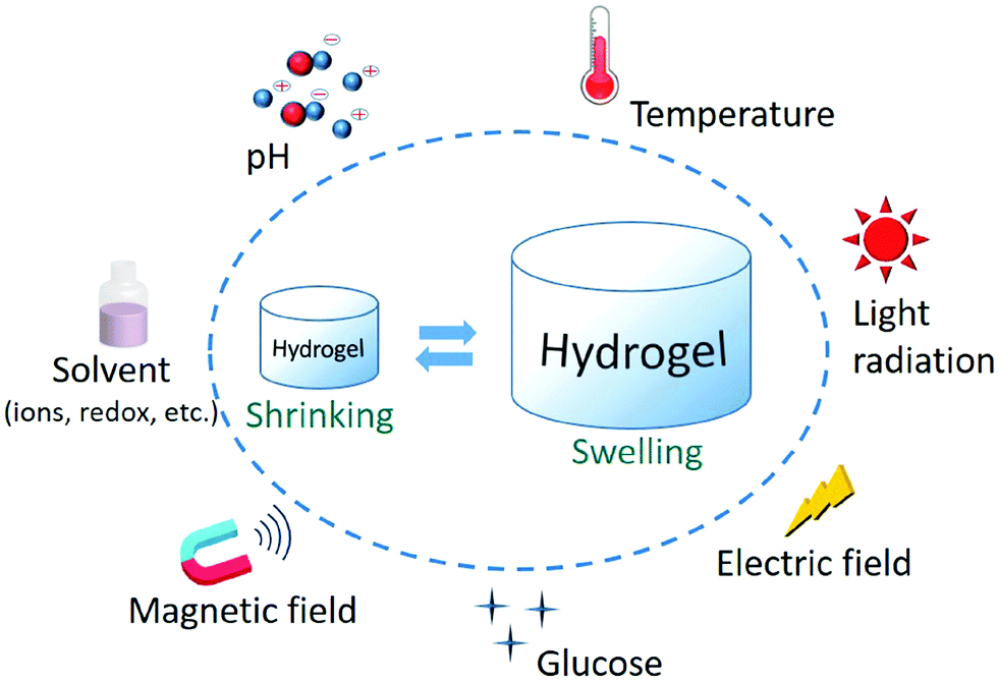

Figure 5.1 The stimuli-responsive environments that control and influence swelling and de-swelling in hydrogels [270].

The essential properties of hydrogels are swelling, liquid capturing, softness, elasticity, flexibility, and absorbency, *etc.* However, hydrogels generally have poor mechanical properties and are difficult to measure because they contain high water content and can evaporate during the test. Therefore, they still can be analysed by measuring the elasticity and viscoelasticity. Hydrogels can be integrated in any shape and size to fit the applications and have been found in wide range of applications such as biomedical applications, cosmetics,

agriculture, food, and drugs, *etc.* Selected examples of the biomedical application of hydrogels are summarised in Table 5.3.

Table 5.3 Selected examples of hydrogels in biomedical applications and their mechanisms

Applications	Mechanism	Ref
Drug delivery	Hydrogels can control release rate under conditions: pH, temperature, enzymes, or physical stimuli.	[271]
Dyes and heavy metal ions removal	Hydrogels can adsorb both dyes and heavy metal ions in water on their surface which the capacity and availability is influenced by the functional groups of hydrogels.	[272]
Scaffold for tissue engineering	As hydrogels structure are similar to the extracellular matrix of many tissues, they have been used as agents for filling vacant spaces, vehicle of bioactive molecules and cell support scaffolds.	[273]
Contact lenses	Oxygen permeability, water content, good optical facilities, hydrolysis and sterilisation stability, nontoxic, wettability, flexibility and biological tolerance are hydrogels properties which benefit for contact lenses production.	[274]
pH-sensors	Transformation of hydrogel by swelling and shrinking in different transducers; optical, mechanical and bending plate transducers are used in pH-sensitive hydrogels.	[275]
Biosensors	Hydrogels are used as sensor parts barrier, immobilisation matrices, and provide excellent environments to protect enzymes and biomolecules before active.	[276]
Injectable hydrogel for spinal cord regeneration	The gaps between spinal cord tissue and injury site can be filled and injected by encapsulation hydrogels of cell or drug.	[277]

Furthermore, superporous hydrogels can be prepared by controlling the degree of cross-linking in matrix and the association between hydrogel and aqueous environment result in faster swelling in pores when compare to mesh conventional hydrogels [275].

Hydrogels can be prepared from natural, synthetic, or semi-synthetic polymers. Natural hydrogels are generally derived from proteins or polysaccharides, such as collagen, gelatine, fibrin, hyaluronic acid, chitosan, starch, and alginate, *etc.* [202]. Synthetic hydrogels are commonly made from poly(vinyl alcohol), poly(vinyl pyrrolidinone), poly(ethylene oxide), poly(acrylic acid), and polystyrene, *etc.* [278]. Semi-synthetic polymers *e.g.* methylcellulose, carboxymethyl cellulose, hydroxyethyl cellulose, and hydroxypropyl methylcellulose *etc.* [279] are employed to produce semi-synthetic hydrogels. For drug delivery applications, the choice of hydrogel has implications for their ability to swell and de-swell to release drug components. The reversible swollen properties in response to different environmental stimuli allow the drug to diffuse into the circulatory system, and the highly porous structure can carry different varieties of drugs and protein (hydrogels can deliver drugs in the form of both hydrophobic and hydrophilic compounds). There have been many studies undertaken showing successful drug delivery by hydrogels, and selected examples are summarised in Table 5.4.

Table 5.4 Selected examples of drug delivery using hydrogel materials

Hydrogel	Drug delivery system	Ref
Polyurethane	Hydrophobic NSAID hydrogel were sustained in the circulation up to 40 h for oral administration.	[280]
Folic acid and pH sensitive cross-linked	Hydrophobic hydrogel could deliver at site-specific. Also, studied sustained release of curcumin *in vitro*.	[281]
Locust bean gum and xanthan	Slow release of drug from niosomes hydrogel was studied *in vitro.*	[282]

PEG and Bovine Serum Albumin	Hydrophobic hydrogel contains with >96 % water could release the soluble compounds from 2.4 mm-thick hydrogel disk and with higher molecular weight of PEG gave more porosity within hydrogels.	[283]
Cream, lotions and ointments	Hydrogel improves contact dermatitis symptoms with non-greasy touch, hydrates and soothing skin, extended drug absorption and is easily removed from the skin.	[284]

5.4 Alginate hydrogel

As a result of the gelling property of alginate described in Chapter 1, alginate hydrogels can be easily modified by chemical means or physical cross linking to improve their physiochemical properties or biological properties which can be in various forms: beads, microspheres, gel, microparticles, or hydrogels. The modifications are mostly presented in hydroxyl groups or carboxyl groups cross-linked with long alkyl chains or aromatic groups by covalent bonds [285]. Alginate properties which are relevant to drug delivery, include that they are biocompatible, non-immunogenic, and nontoxic. They also can support a wide range of drugs loading by entrapping drug molecule inside their structure in gels or beads form. In common with hydrocolloids, they benefit in the design of release controlled system [286]. Alginate can form into two types of gel: a gel dependent on pH and an ionotropic gel, *i.e.* alginate can form into gel when the pH is decreased, while cross-linking is needed for ionotropic gel to form [287]. Alginate has been used in both immediate-release systems and to prolong the release (*i.e.,* slow the rate) depending on the amount and formulation.

The “swelling-dissolution-erosion” is the process which gives alginate with calcium chloride unique properties to influence the ratio of drug release. The delayed release was found when higher calcium ions were involved within the gelling process. Calcium chloride cross-linkers

display denser and more prolonged drug release when compared to other cross-linking agents [288]. Alginate is considered as liposomes drug delivery system which deliver drug in phospholipid vehicle. Furthermore, alginate can incorporate with others compounds such as chitosan, cellulose, gelling agents, *etc.* to modify the desired drug release system. A summary of the different delivery systems from alginate are given in Table 5.5.

Table 5.5 A summary of selected drug delivery systems derived from alginate

System	Applications	Ref
Oral	Beads, pellets, microspheres, nanoparticles hydrogels, *etc.* were found in floating systems, mucoadhesive systems, raft forming systems, expandable or swellable systems.	[289]
Injectable	Alginate was used as a vehicle in nanoparticle-based drug delivery systems by encapsulating to reduce toxicity of nanoparticles, more efficacy and undesirable side effects.	[290]
Ocular	Sustained drug release was found in low molecular weight of alginate containing with brimonidine tartrate. It improved tolerability, pharmacodynamics activity and reduce intraocular pressure compared with traditional eye drops.	[291]
Nasal	Nasal spray with alginate gave better response and drug absorption within vascular.	[292]
Tackling obesity and weight management	Calcium alginate was combined in beverage or nutrition bar to reduce postprandial glycaemic response and energy intake.	[293]
Wound dressing	Alginate dressing ensures wounds environments remain moist and protect them from bacterial (previously explained in Chapter 1).	

Vaccine	Alginate was used as protector of oral vaccine from physiological vagaries which has been found in freeze-dried or microspheres form.	[294]
Tissue engineering	Alginate scaffolds was developed for tissue engineering (previously explained in Chapter 4).	
Miscellaneous	Alginate was reduced the symptoms of symptomatic gastroesophageal reflux disease which have been found in the present pharmacy market shown in Table 5.6.	[295]

Evidence for biocompatibility was found in many *in vivo* studies and consequently alginate has been considered by the Food and Drug Administration (FDA) and as a result alginate can be used as an ingredient for oral administration. Therefore, alginate has been explored for a wide range of drug delivery applications which included *in situ* gel formation, targeted drug delivery, controlled release, and other specific medical purposes. The list of alginate-based commercial pharmaceuticals is presented in Table 5.6.

Table 5.6 Selected alginate based market pharmaceuticals.

Pharmaceutical type	Product	Alginate and Drugs	Description
Oral administration	Gastrotuss® baby syrup	Magnesium alginate and simethicone	Prevents reflux, use for the symptoms of respiratory, choking, dysphagia, heartburn, belching and irritability in the stomach
	Algicid® suspension/tablets	Sodium alginate and potassium bicarbonate	
	Gaviscon Double Action Liquid/tablets®	Sodium alginate and sodium bicarbonate plus calcium carbonate	
Dermal application	Flaminal Forte® gel	Hydrated alginate and biologic enzyme	
	Purilon Gel®	Calcium alginate and Carboxymethylcellulose	Use for dry scab and necrotic area
	Saf-Gel®	Sodium/calcium alginate and Carbomer	Provides some moisture in wound
	Hyalogran® dressing	Sodium alginate and ester of hyaluronic acid	Absorbs fluid and removes necrotic tissue
	SeaSorb® dressing	Calcium alginate	Provides moist environment for wounds and turn fibres into gel
	Tromboguard® dressing	Sodium/calcium alginate and biological active plus silver cations	Bleeding controlled and antibacterial

	Fibracol Plus® dressing	Calcium alginate and collagen	Provides some moisture in wound, tissue and epithelialisation
	Algivon® dressing	Calcium alginate and Manuka honey	Use for sloughy and malodorous wound
	Guardix-SG®	Sodium alginate and poloxamer	Use for spine and thyroid post-operations by creating a barrier to separate injured tissues
Rectal administration	Natalsid® suppositories	Sodium alginate	Anti-inflammation after operation
Periodontal application	Progenix putty®, Progenix plus® injection	Sodium alginate and bone matrix in collagen	For regeneration of periodontal diseases
	Emdogain® gel	Propylene glycol alginate and enamel matrix derivative	
Arthroscopic application	ChondroArt 3D® injection	Alginate with agarose and autologous chondrocytes	For degeneration of cartilage

Alginate based pharmaceuticals are available for use by both children and adults *e.g.* to reduce reflux (*i.e.* heartburn and oesophagitis symptoms); in this form they contain bicarbonate and can be retained in the stomach for several hours to entrap the gastric fluid for long periods, also the acid in the oesophagus.

Moreover, obesity and type 2 diabetes can be treated by alginates which adapt to gastric emptying or constrain the glucose transportation and absorption within the intestines. They also help to reduce the enzymic activity between glucose from carbohydrate in the intestines.

The negative charges in the alginate structure disrupt bacterial growth around the wound area and also stop the leakage of intracellular substances. Therefore, there are many of alginate based wound dressings on the market because of the antibacterial and antifungal properties also provide moisture for the wound surface. Alginates have also been found to act against some viruses by protecting the cell with the strong anionic charge and the positive charge of the cell. Furthermore, for blood coagulation, calcium alginate has been reported to aid activation with haemostatic and thrombin, alginate has also been used as an antioxidant and an anti-inflammatory in cytokine. In addition, calcium alginate has been reported to reduce plasma cholesterol levels in rat models which is beneficial in the reduction of blood pressure.

5.5 Organoclay

The emergence of nanomaterials has had a significant impact on the development of alginates by offering materials with superior properties. Organoclays are considered as a hybrid material with chemically modified of clay minerals that allow the investigation of novel materials and new applications, mostly in nanocomposites. Clay minerals consist of silica-oxygen tetrahedral sheets with aluminium or magnesium octahedral sheets present in small crystalline domains. The aluminium or magnesium ions are positively charged which can attract anions to their surface and arrange in layer charge [296].

Studies have reported range of synthesis routes for organoclays *via* different experimental conditions and involving several kinds of organic compounds. The development of modification methods includes a variety of methods such as adsorption, ion exchange

between inorganic and organic cations, reaction with acids, dihydroxylation and calcination, plasma treatment, *etc.* Of these, the ion exchange method is the most popular preparation method for the isolation organoclays, wherein the organoclays are synthesised within solutions by cation exchange or solid state reactions. The routes for developing organoclay is summarised in Table 5.7.

Table 5.7 The summarise of developing organoclay [297]

Organoclay studies	Year
Replacing interlayer cations with methylene blue by using ammonium ions in clay cation exchange. Hydrochlorides or hydroiodides solutions was used to treat montmorillonite, beidellite or nontronite clay which adsorbed organic ions and risen the spacing among them.	1939
Developing montmorillonite clay spacing with glycerol by unambiguous method.	1945
Analysis of montmorillonite and organic liquids aliphatic di- and polyamines and glycols, polyglycols and polyglycol ethers was found that active amine were available on base and glycerol and glycol were occurred between layer space without displacing cations.	
The interactions of clay and organic compounds were prepared from smectites and quaternary ammonium salts. Also, swelling gel with organoclay dispersing in organic liquids was reported.	
Hydrophilic conversion to hydrophobic of swelling organoclay in organic liquid was obtained from bentonites reacted with various aliphatic ammonium salts.	1950

Organoclay are used as pollutants adsorbent in water and air, rheological control agent, paints, cosmetics, refractory vanish, and thixotropic fluids, *etc.*

The synthesis of organoclay is based on reactions between clay and organic compounds. The smectites and vermiculites interlayer space are displaced by polar molecules when disperse in

water with displacement reactions. Various chemical interactions: hydrogen bonds, ion-dipole interaction, co-ordination bonds, acid base reactions, charge transfer and van de Waals forces, is influenced the neutral molecules adsorption in smectites. Organoclay can be prepared by cation exchange or solid-state reaction [298].

- Cation exchange reaction: the cation exchange reaction by solution of quaternary alkylammonium cations or organic compounds is occurred within interlayer of clay.
- Solid-state reaction: the intercalation of organic molecules into dried clay can be introduced without using solvents by solid-state reaction.

For the current research, a synthetic aminopropyl-functionalised magnesium phyllosilicate clay (organoclay) was prepared using sol-gel chemistry-based synthesis route (see experimental section). The as prepared organoclay comprises central brucite sheet of octahedral MgO/OH units which is sandwiched between aminopropyl-functionalised silicate network to give highly disordered clay with approximate composition $Si_8Mg_6R_8O_{16}(OH)$. Previous studies have shown that dispersion of dried powders of organoclay in water results into protonation of aminopropyl side chains. This facilitates repulsion between the protonated stacked layers to give exfoliated dispersion of sheets [299]–[301].

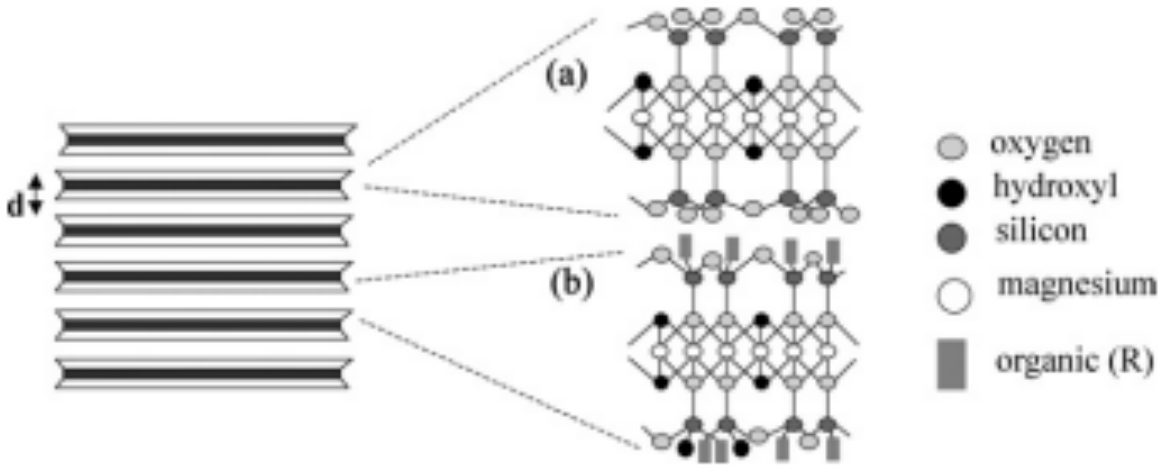

Figure 5.2 Organoclay structure [300]

The previous reports have shown that the exfoliated sheets are highly positively charged, which was attributed to the positively charged oaminopropyl functionalities associated with the delaminated layers of the organoclay.

Organoclay implementation and applications

Organoclays interact with functional biomolecules such as enzymes, DNA, or drug molecules, and nanocomposites make up at least 70 % (by volume) of industrial applications. They also have been used for a range of commercial applications such as adsorbents, control agents, cosmetics, medical care applications, oil well drilling fluids, and greases, *etc.*[298].

Layered materials are first separated by dispersing them in water and this results in the spacing between each layer (d, Figure 5.2) in the amino-functional group. These functional groups are free to interact with negatively charged biomolecules or organic functionalities through electrostatic interactions and produce functional bio-(organic)inorganic hybrid nanocomposites for biocatalysis, biosensing and controlled release applications [300], [302]–[304].

5.6 Experimental: Materials and processing technique

5.6.1 Materials

In common with previous experiments, sodium alginate with high gularonic acid (G) and medium viscosity has been used for the experiments throughout this chapter. Ibuprofen and all other reagents were purchased from Sigma-Aldrich and used without further purification.

5.6.2 Hydrogel preparation for drug delivery experiment

(a) Organoclay synthesis

Organoclays were synthesised by dissolving magnesium(II) chloride hexahydrate (0.84 g) in ethanol (20 g) then 3-aminopropyltriethoxysilane (1.3 mL) was introduced dropwise with

rapid stirring [299]. The addition rapidly produced a white precipitate that was kept stirring overnight. The slurry was isolated by centrifugation, washed with ethanol three times (3 x 50 mL) before drying at 40 °C. The dried organoclay thus prepared was pulverized before use in subsequent experiments.

(b) Exfoliation of organoclay

Exfoliation of the as-synthesized organoclay was achieved by dispersing 3 wt% of finely ground clay powder in distilled water followed by twice ultrasonicating the dispersion for 15 minutes. This produced a clear suspension of an delaminated sheets of the organoclay.

(c) Preparation of alginate-organoclay hybrid hydrogels

The alginate (4 %wt) solution was prepared and allowed to dry in containers at room temperature. Freshly exfoliated dispersions of organoclay sheets (3 wt%) was then added to the vial containing a dry layer of alginate. The mixture was allowed to age overnight. The hydration of the biopolymer layer in presence of organoclay sheets produced a self-supported hydrogel. The volume ratio (v/v) of alginate solution and organoclay solution was set at 1:1. The steps for preparation of the hydrogel are shown in Figure 5.3.

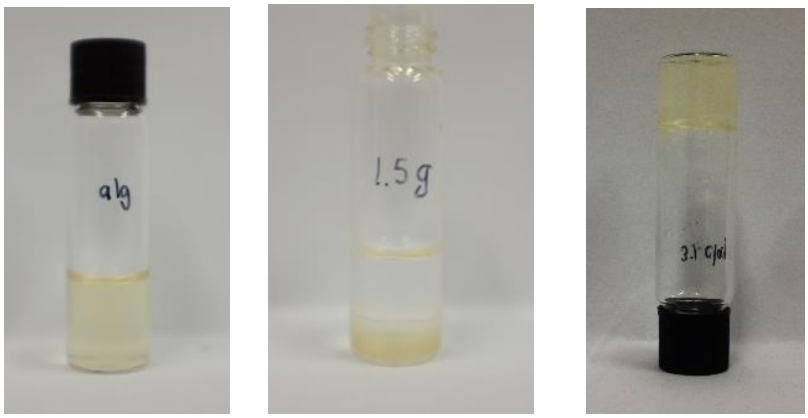

a) b) c)

Figure 5.3 Photographs showing stepwise formation of alginate-organoclay hybrid hydrogels a) a vial containing alginate solution was kept for drying b) upon evaporation of water from the alginate solution, suspension of an exfoliated organoclay was added to the vial containing dried alginate film, c) an overnight aging allowed slow diffusion of organoclay nanoparticles into the alginate matrix produced self-supported hybrid hydrogel.

For the drug delivery experiment, ibuprofen (10 mg mL^{-1}) was added to the previously prepared aqueous alginate solution, organoclay (3 wt% dispersed in water) was added and the hydrogel was obtained after leaving this at room temperature for 12h. Hydrogels used for further characterisation and analysis the drug release rate by UV-Vis spectroscopic technique.

(d) Synthesis of calcium cross-linked alginate (Ca-alginate) hydrogels

An aqueous calcium(II) chloride solution (50 mM) was added dropwise to the alginate solution (4 wt%) with constant stirring. The resulting mixture was allowed to stand overnight (12h) which produced self-standing hydrogels.

5.7 Characterisation and analysis techniques

5.7.1 Swelling ratio

The swelling property was determined by mass measurements. The hydrogel was completely dried at room temperature, cut into pieces, and soaked in water at different time intervals (15 mins, 30 mins, 1 h, and 2 h). The swelling ratio was then calculated using equation (4.1):

$$Q = \frac{We - Wd}{Wd} \qquad (4.1)$$

where Q is the swelling ratio, We is swollen gel mass, and Wd is dried gel mass. The experiment is shown in Fig 5.4 and an average of 10 samples were used in the experiment.

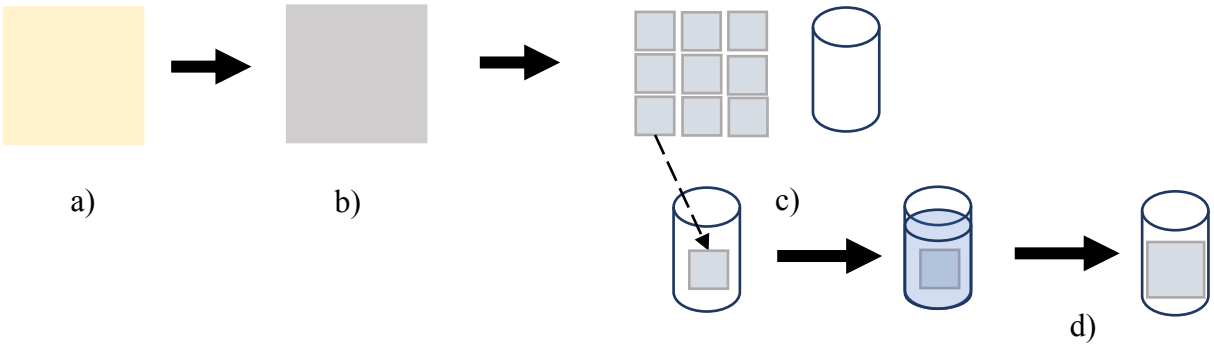

Figure 5.4 The experiment of determining the swelling ratio of the gels a) as prepared alginate-organoclay hydrogel monolith, b) the hybrid hydrogel dried at room temperature, c) the complete dried hydrogel monolith is cut into pieces, weighting each piece and vial before being filled up with water, and d) water is removed after time intervals and the swollen hydrogel is weighed.

5.7.2 Fourier Transform Infrared Spectroscopy

Fourier Transform Infrared (FTIR) spectroscopy with the Spectrum 100 Optical spectrometer (PerkinElmer, UK) was used to take the emission and transmittance spectra of hydrogel prepared in the range of resolution 0.5 cm^{-1} over the spectral range 4000 to 500 cm^{-1} to examine structural and compositional aspects within the hydrogel. After crosslinking with calcium chloride, the organo composite hydrogel, was investigated as both wet and dried conditions to investigate the effects of drying. The results present in 5.8.2 were taken by using a dried hydrogel.

5.7.3 Rheology

The viscosity measurements were carried out using a Haake Mars II Rheometer; typical sample size was 5 mL. The plates were set at 20 °C with a 1 mm separation, and the shear rate was modified between 0.1 to 100 (1/s) in logarithmic steps. As with the FTIR spectroscopy, the hydrogel with the calcium crosslinker was used to compare this with the

organoclay-alginate composite hydrogel containing 3, 5, and 8 wt% organoclay suspended in water.

5.7.4 Differential Scanning Calorimetry

Thermal analysis was conducted on alginate and comparisons made between alginate both with and without calcium ions and hydrogel prepared by TA Q200 differential scanning calorimeter (DSC). Freeze dried samples (17.32 ± 0.66 mg) were placed into specific sealed aluminium pans and heated at a rate of 10 °C/min from 20 to 300 °C in a flowing N_2 atmosphere (50 cm^3/min.).

5.7.5 Scanning Electron Microscopy

To observe the hydrogel prepared structure, the hydrogel was freeze dried and sputter coated with gold before observation using a JEOL IT 300 scanning electron microscope (SEM) at an acceleration voltage of 10 kV.

5.7.6 Ultraviolet-Visible Spectroscopy for drug delivery study

Hydrogels with ibuprofen loaded were placed into 1 L dI water flask bottle with the sealed cap as seen in Figure 5.5. The solution was taken at regular time intervals. The release rate of ibuprofen in water was monitored by the measuring the changes of absorption intensity peaks at 264 nm, using UV-Vis spectroscopy. An average of 10 samples were collected and calculated.

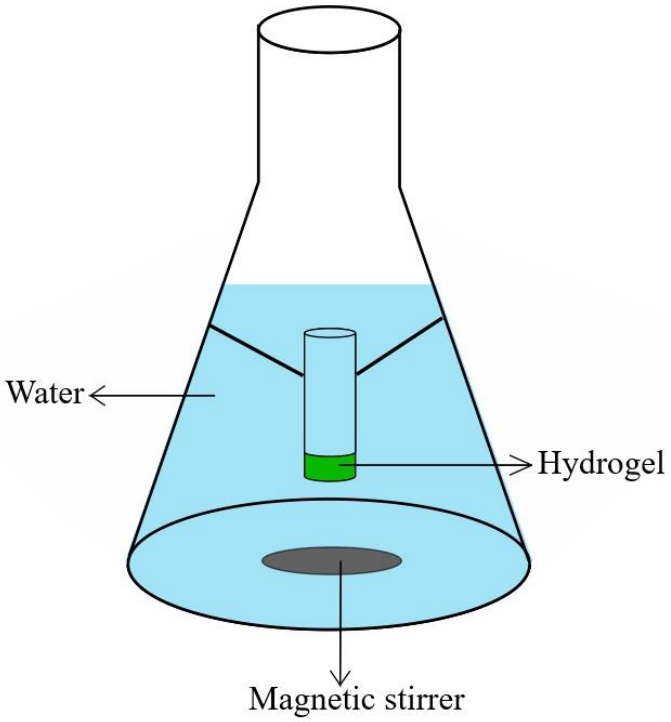

Figure 5.5 Schematic representation of measurement of drug release experiment. Hydrogel loaded with drug were place in to 1 L dI water and stirred with magnetic stirrer with low speed to circulate water in the flask. The solution was sampled at regular intervals for UV-Vis spectroscopy and returned to flask after each examination to maintain the volume of the water.

5.8 Results and Discussion

5.8.1 Swelling ratio

The swelling behaviour of a hydrogel was monitored at room temperature at different time intervals (0, 15, 30, 60, and 120 mins respectively) and significant increases were observed, shown in Figure 5.6. The hydrogel absorbed water quickly during the first hour then the rate slowed as more water was incorporated into the structure. From time to time, hydrogels were

swollen in water up to maximum of 23-24 times their initial weight. Moreover, the fully swollen hydrogel was dried at room temperature and the swelling properties investigated again, this study found that the hydrogel reabsorbed water without dissolving. However, the amount of water absorbed was lower but faster than the freshly dried hydrogel. The results clearly demonstrated the ability of hydrogel to absorb water, become dried, and to reform as a hydrogel but one in which the swelling ratio has changed.

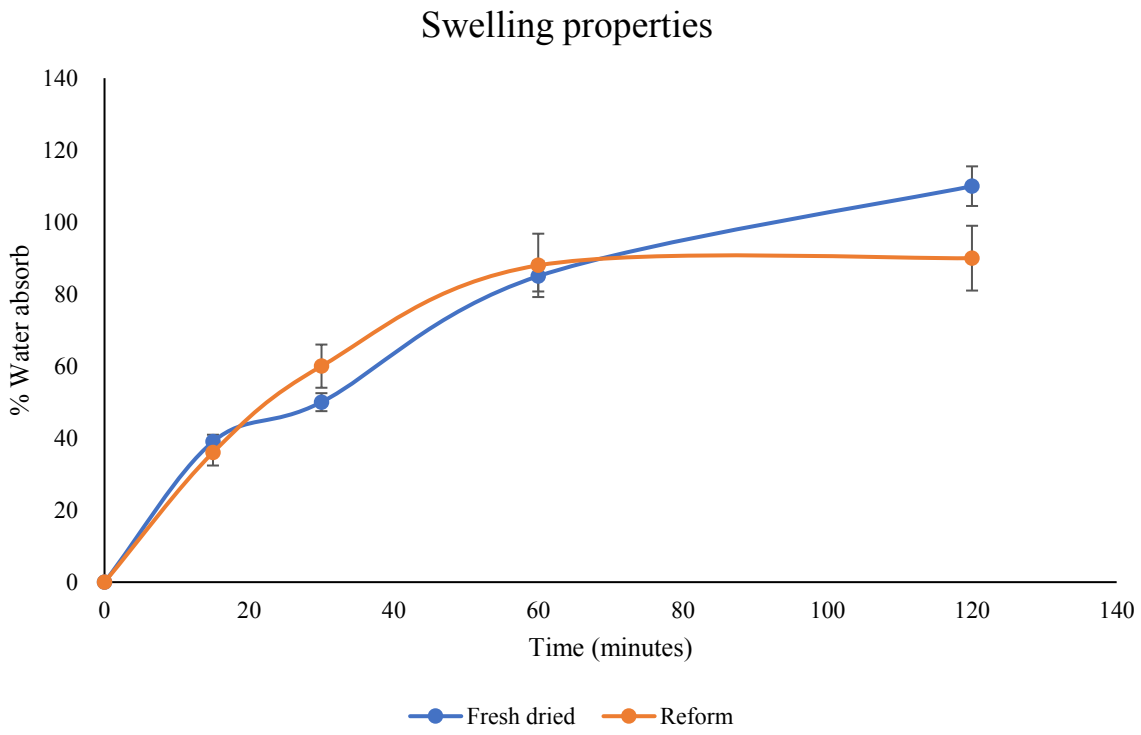

Figure 5.6 Swelling ratio trends of freshly dried hydrogel and reformed hydrogel

5.8.2 Fourier Transform Infrared Spectroscopy result

Structural and compositional aspects of the organo composite hydrogel interactions between the organoclay and alginate were confirmed by the measurement of emission and transmittance spectra. This study compared alginate with calcium chloride cross-linked, organoclay, and organo composite hydrogel. FTIR spectra of the hydrogel in Figure 5.7 show peaks corresponding to Mg-O/Mg-O-Si (560 cm^{-1}), Si-O-Si (1041 and 977 cm^{-1}), Si-C (1135 cm^{-1}), and N-H (1555 cm^{-1}); these peaks also occur in the organoclay structure as well, which

confirms that the structure of the hydrogel contained organoclay. The important region of both hydrogels contains O-H stretching bands (3320 cm^{-1}) but the organo composite hydrogel also includes the N-H stretching band (3010 cm^{-1}) which arises from the organoclay. Both hydrogels were similar in terms of the aliphatic (C-H) content which arises from the alginate. Most importantly, the C-N amine stretching (1050 cm^{-1}) peak was only found in the hybrid hydrogel which possibly shows the reaction between the alginate (carboxylic functional group) and the organoclay (amine functional group) had been occurred. The possible chemical structure is shown in Figure 5.8. However, there was no further evidence to support the new chemical bonding between alginate and organoclay hydrogel. The identification of stretching is summarised in Table 5.8.

Table 5.8 FTIR spectra identification of Alg-$CaCl_2$, Clay and hybrid hydrogel

Samples	Identification
Alg-$CaCl_2$	3320 cm^{-1} (hydroxyl O-H stretching)
Clay	3010 cm^{-1} (amine N-H stretching), 1135 cm^{-1} (Si-C), 1041 and 977 cm^{-1} (Si-O-Si stretching), 560 cm^{-1} (Mg-O bending)
Alg-Clay	3320 cm^{-1} (hydroxyl O-H stretching), 3010 cm^{-1} (amine N-H stretching), 1555 cm^{-1} (N-H bending), 1135 cm^{-1} (Si-C), 1041 and 977 cm^{-1} (Si-O-Si stretching), 560 cm^{-1} (Mg-O bending)

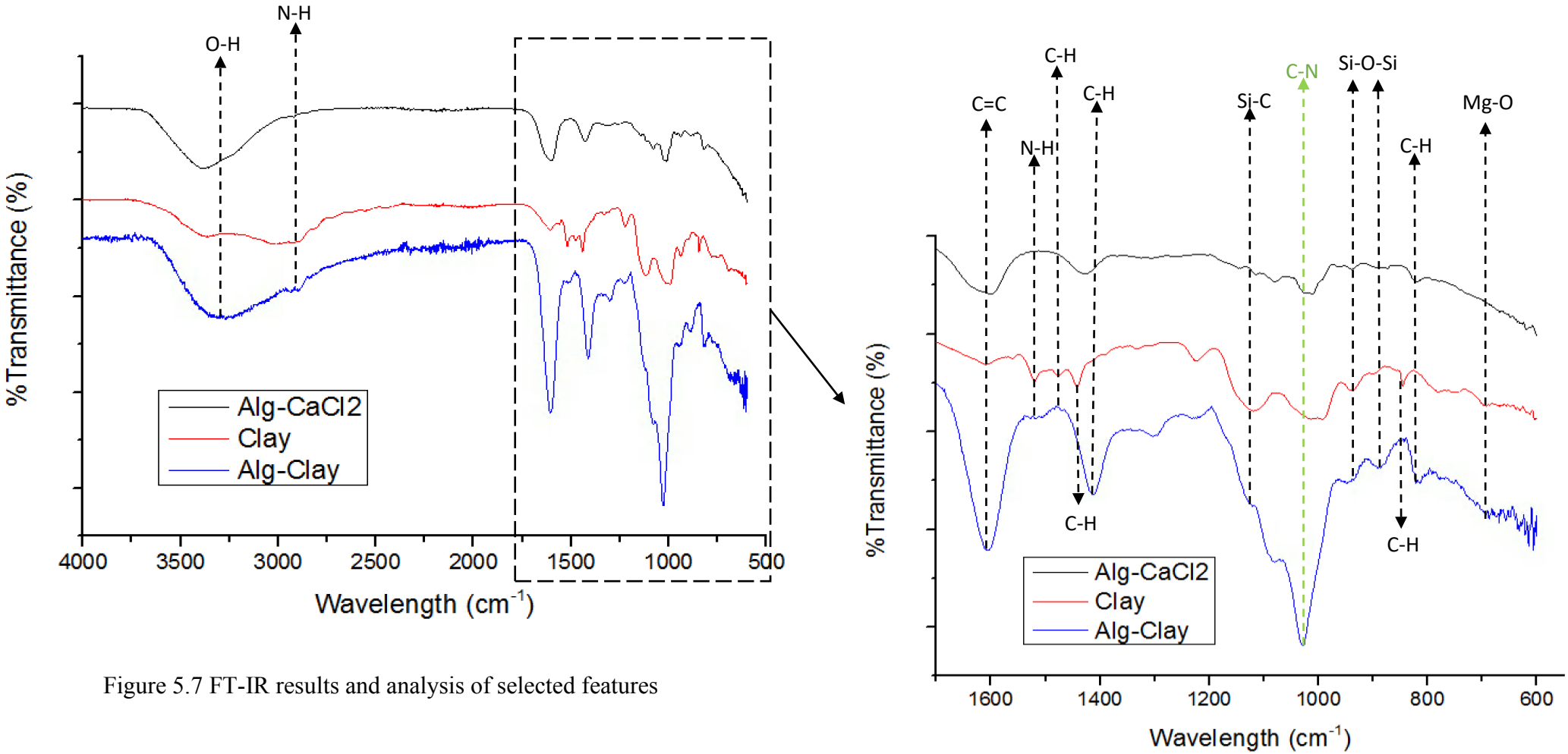

Figure 5.7 FT-IR results and analysis of selected features

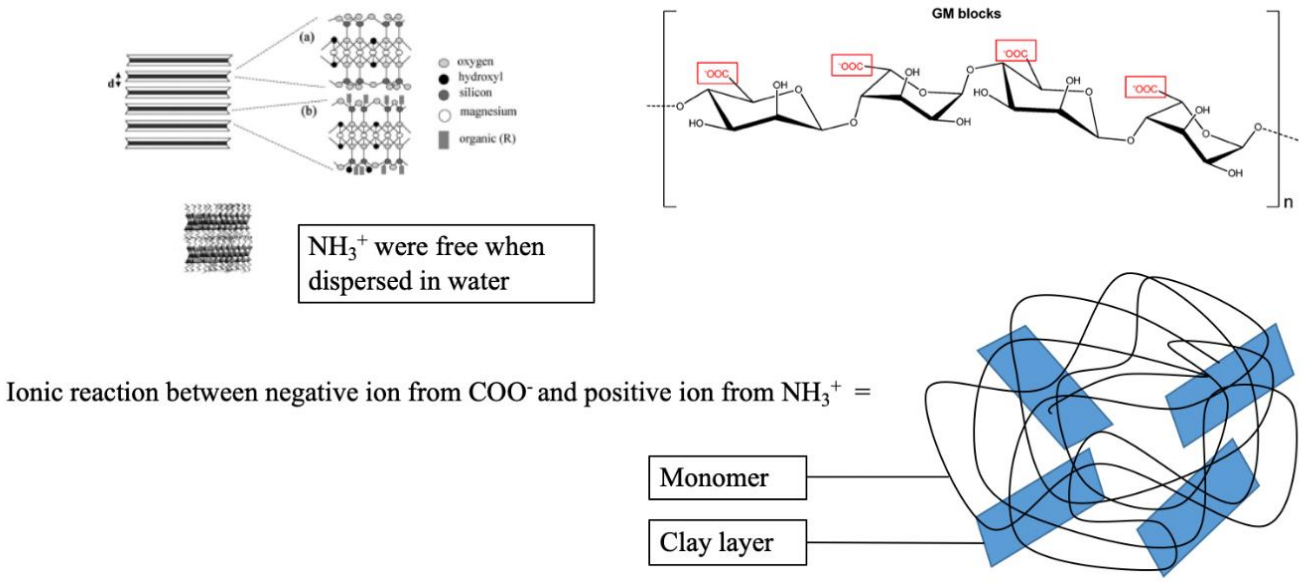

Figure 5.8 Schematic representation demonstrating chemical interactions between alginate and organoclay. The electrostatic interactions between positively charged aminopropyl-functionalities associated with the organoclay and negatively charged carboxylic functionalities of the polysaccharide facilitate cross-linking of the biopolymer chains to produce 3D interlinked network of alginate-organoclay hybrid hydrogel.

5.8.3 Rheology

The viscoelastic properties of the hydrogel were carried out in the rheometer and assessed by amplitude of frequency sweeps and oscillatory sweeps. Frequency amplitude sweeps of alginate solution, alginate with $CaCl_2$ cross-linked hydrogel, alginate with organoclay hydrogel were undertaken. Figure 5.10 presents the shear viscosity and elastic component (storage) G' and viscosity component (loss) G'' hydrogel, these parameters represent the solid and liquid stages of the materials. The shear rate dependence of the shear viscosity of the hydrogels is shown in Figure 5.9. The gelation of alginate with $CaCl_2$ cross-linked presented the increasing shear viscosity while shear rate approached zero because the fluid cannot flow at the rest which was shown the strongest gel and followed by hybrid hydrogel and alginate solution.

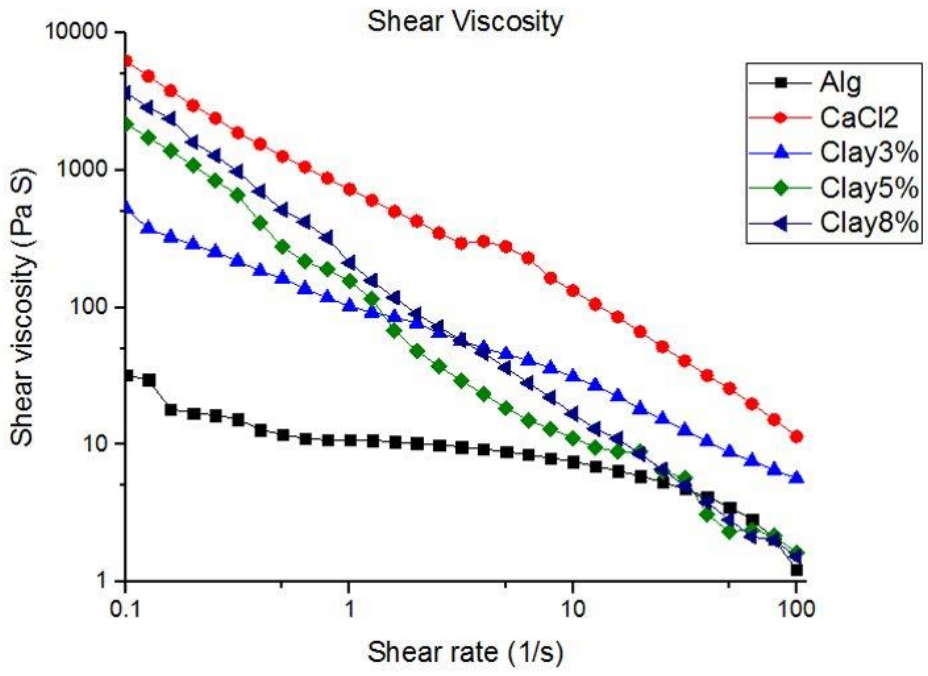

Figure 5.9 Shear rate dependence of shear viscosity examined for five samples: alginate solution (black), alginate with $CaCl_2$ cross-linked (red), alginate and 3 wt% organoclay hydrogel (blue), alginate and 5 wt% organoclay hydrogel (green) and alginate and 8 wt% organoclay hydrogel (navy).

Furthermore, the test was carried out with 5 conditions hydrogels containing 3 wt% alginate and 3, 5, and 8 wt% organoclay dispersed in water. The frequency sweep test of all the hydrogel samples including alginate crosslinked with $CaCl_2$ shown the higher G' than G'' which confirmed that they display more elastic rather than viscous behaviour. Addition, the composite gel prepared with higher composition of organoclay tend to give denser gel as the shear modulus of 8 wt% of organoclay was higher than both 3 and 5 wt%. The shear thinning of hydrogel shows the interaction between particles and the free space in the hydrogel [66]. Moreover, the lower shear thinning shows the fluid behaviour of hydrogel which benefits to injectable trough the needle [279]. Therefore, the lower shear modulus of hydrogel can load more drug particle for the delivery which was 3 wt% of organoclay in this research. Although the hydrogels containing 5 and 8 wt% organoclay display the greater density they are easy to break when increasing shear viscosity solution. This occurs because they are less flexible and contain larger amounts of clay particles with less free space as shown in Figure 5.9 so that the shear rate approaches zero in a similar fashion to the alginate solution.

The frequency sweep test was used to determine the dependence of the shear modulus on the angular frequency between 0.1 to 10 Hz. The high frequency represents the short time behaviour of materials while low frequency presents the long-term behaviour. Firstly, for both hydrogels it was found that G' was higher than G'', which confirms that the elastic, rather than the viscous, character when the load is applied. Secondly, linear plots are seen in both the G' and G'' graphs of the hydrogel containing calcium chloride and also the recorded shear modulus was higher than the composite hydrogel, thus confirming that it was denser than the hybrid hydrogel (Figure 5.10 a), b)). Thirdly, the composite hydrogels prepared were shown gel-alike behaviour which confirmed the electrostatic interactions between the carboxylic functional groups of alginate and cationic aminopropyl functional groups of the organoclay sheets. In contrast, in the case of Ca-alginate hydrogels, the strong interactions between Ca^{2+} ions and alginate chains (to form the egg box model) were attributed to the increased G' and G'' values.

a)

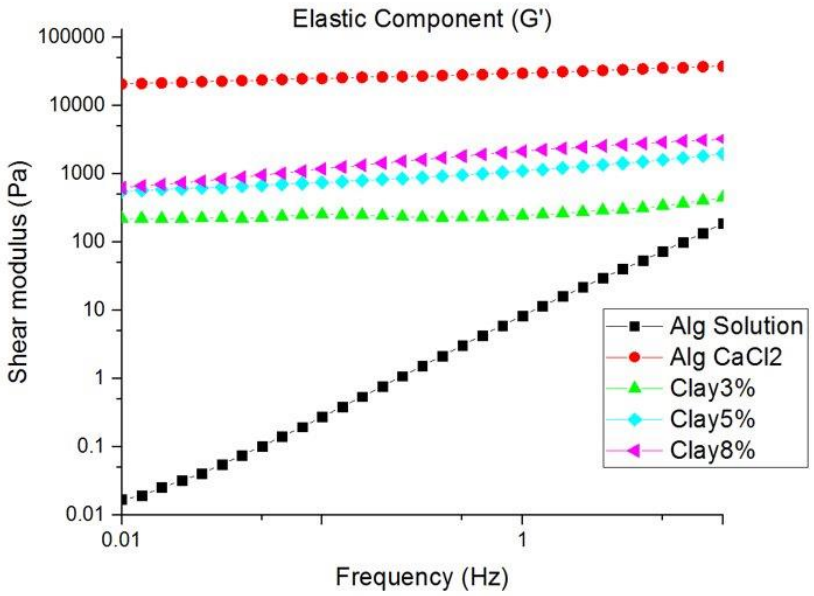

b)

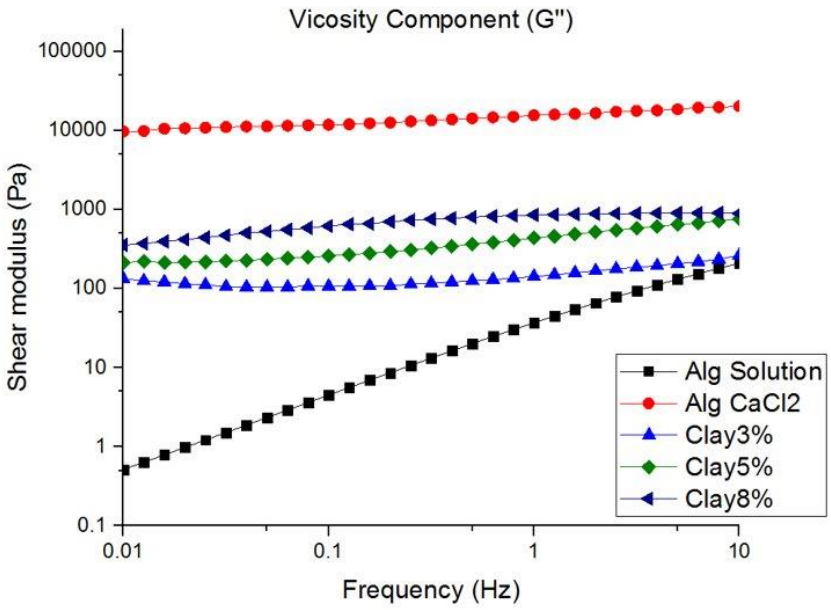

Figure 5.10 The viscoelastic properties a) G' and b) G'' of the hydrogels and the alginate solution show that the alginate + $CaCl_2$ displays the highest density followed by alginate with 8 wt% organoclay, 5 wt% organoclay, then 3wt% organoclay, and the alginate solution respectively.

Therefore, the sweep test confirmed that for all the hydrogel samples the elastic component is higher than the viscous component, while the alginate solution only shows viscosity properties. Moreover, the rheology test shows that the hydrogel has potential as containing the lower concentration (3 wt%) of organoclay yields sufficient the free space for the drug molecule to become attached within, which will be used further in this research.

5.8.4 Differential Scanning Calorimetry

The interaction between the alginate and the organoclay were examined using differential scanning calorimetry (DSC) and compared with the alginate containing $CaCl_2$. The blend of alginate with $CaCl_2$ displayed two endothermic peaks at 114 ˚C and 129 ˚C, while the composite hydrogel showed multiple (broader) endothermic peaks at 87, 91, 115, and 129 ˚C (Figure 5.11).

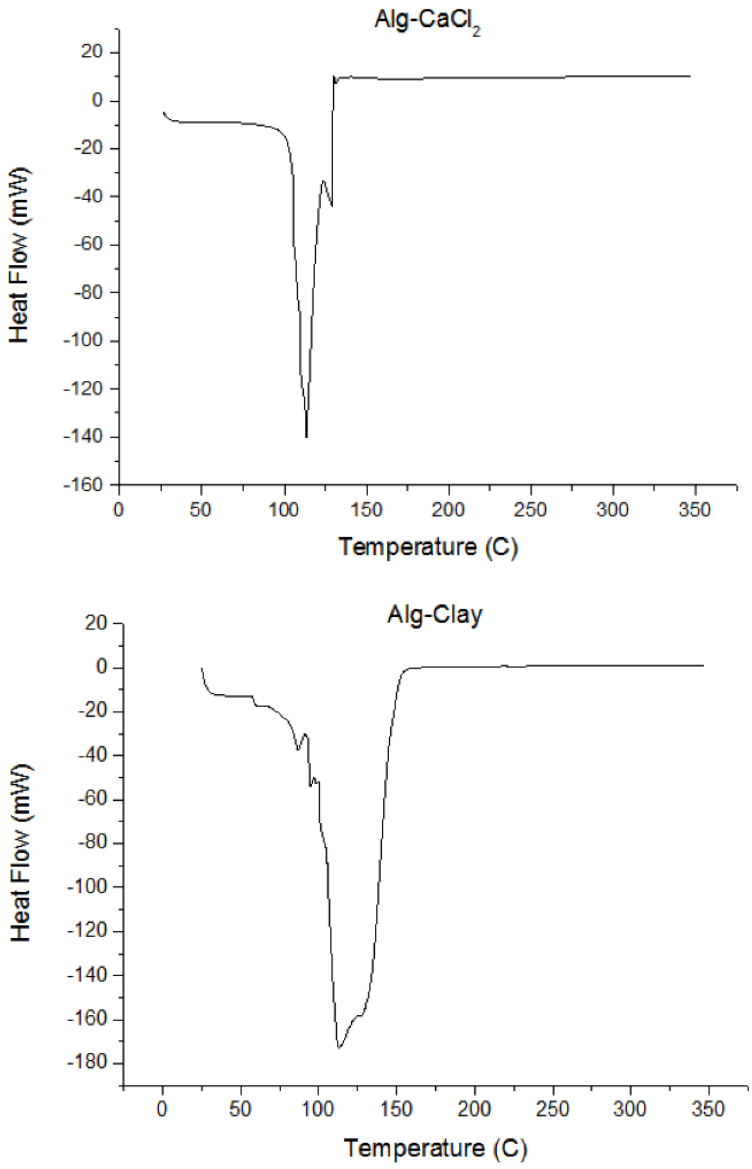

Figure 5.11 DSC result of a) the alginate with calcium chloride b) the organo composite hydrogel.

The results indicate that the Calcium-crosslinked alginate melts over a narrower range, indicating greater purity or the presence of fewer species. In contrast, the organoclay-alginate hydrogel melts over a much broader range and displays multiple thermal events. This is

consistent with the nanocomposite hydrogels form weaker cross-linked networks compared to the calcium-alginate hydrogels.

5.8.5 Scanning Electron Microscopy

SEM images were acquired of the organoclay particles (Figure 5.12) to determine whether the hydrogel structure could be discerned. The samples shown are Ca-alginate hydrogel and composite hydrogel used within this study. The dense, porous structure of the Ca- alginate hydrogel can be seen in the images (Figure 5.13) while the larger porous structure was found in alginate organoclay hydrogel (Figure 5.14)

Firstly, the overall images of dried organoclay particles were observed by SEM with 50 µm and 10 µm scale and were found to form into different size ranges. The average size as seen in Figure 5.12 is around 50 µm.

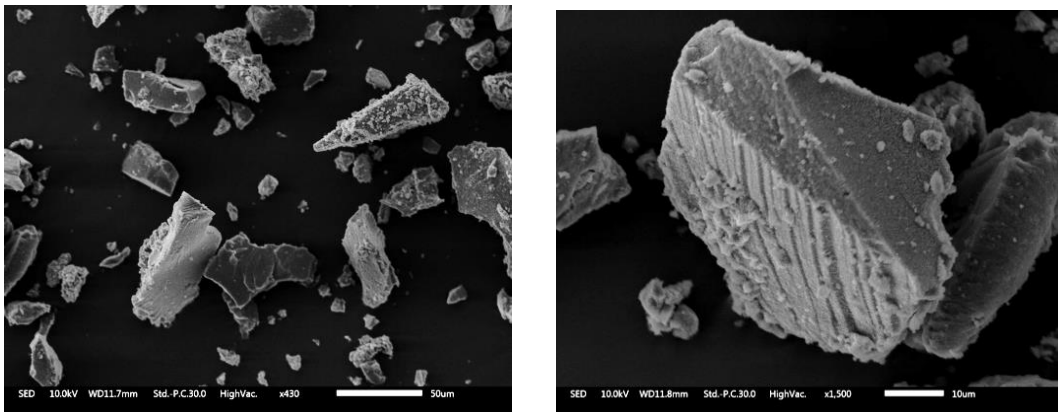

Figure 5.12: SEM images of organoclay particles (scales are 50µm and 10µm)

Secondly, the SEM images of freeze-dried Ca-alginate was observed at the same area with different scales: 100 µm, 50 µm, 20 µm, and 10 µm (Figure 5.13). The cellular pores which are sponge like are clearly seen in the 10 µm image. These pores influence the water intake, allowing the hydrogel to swell. The uniform porous structure was very dense which difficult to measure the pore size.

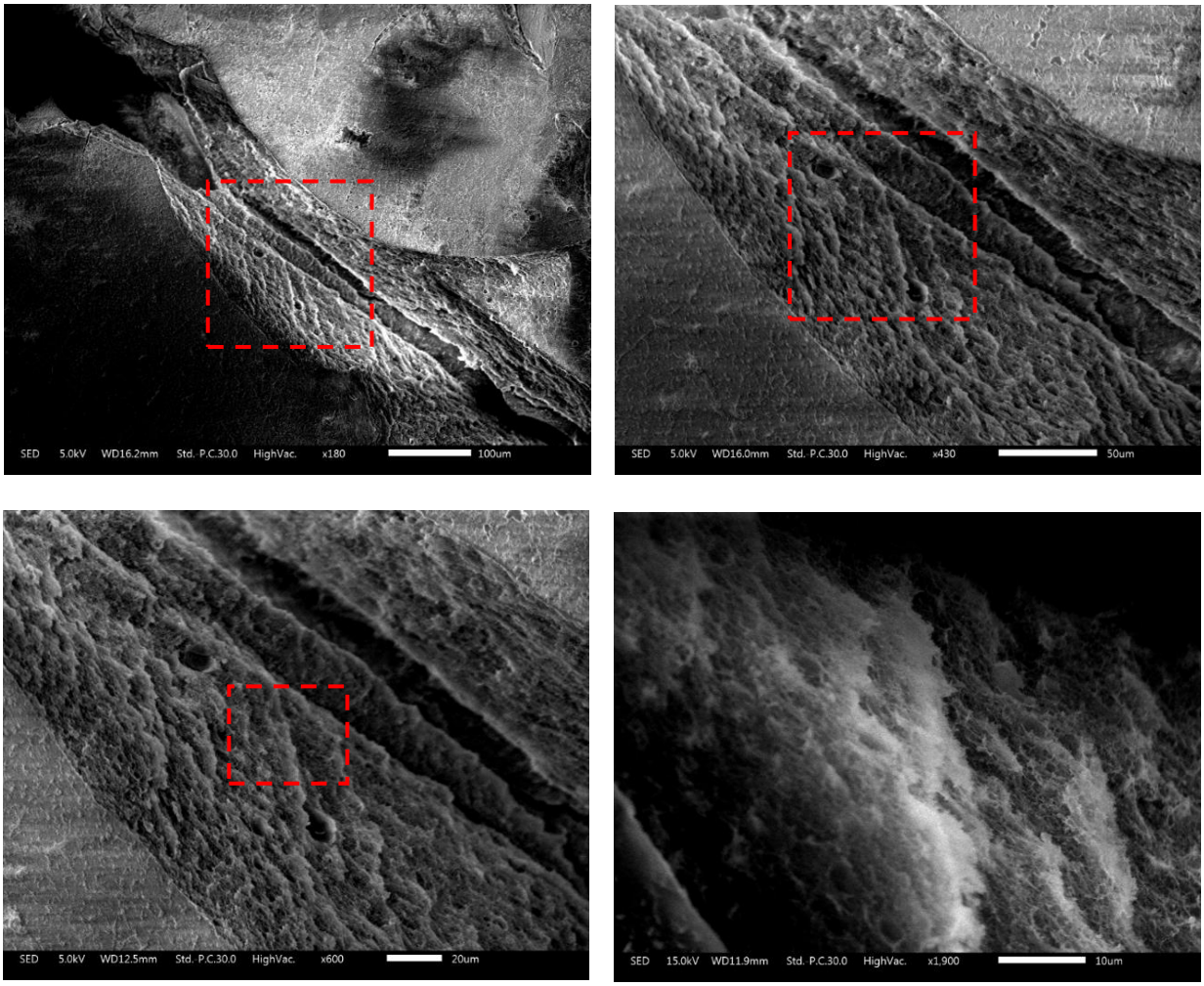

Figure 5.13: SEM images of calcium alginate hydrogel (scales are 100 µm, 50 µm, 20 µm, and 10 µm) while the red square shows the area of the image under greater magnification.

Thirdly, the SEM images of freeze-dried alginate organoclay hybrid was also observed in the same region with different scales: 100 µm, 50 µm, 20 µm, and 10 µm (Figure 5.14). The pore size was larger when compared to Ca-alginate but these pores were typically in different sizes. The average pore size is range between 10-50 µm as seen in Figure 5.14. Moreover, the porous structure of hybrid hydrogel found can be confirmed that alginate and organoclay are cross-linked and formed into a hydrogel which could confer further functional benefits.

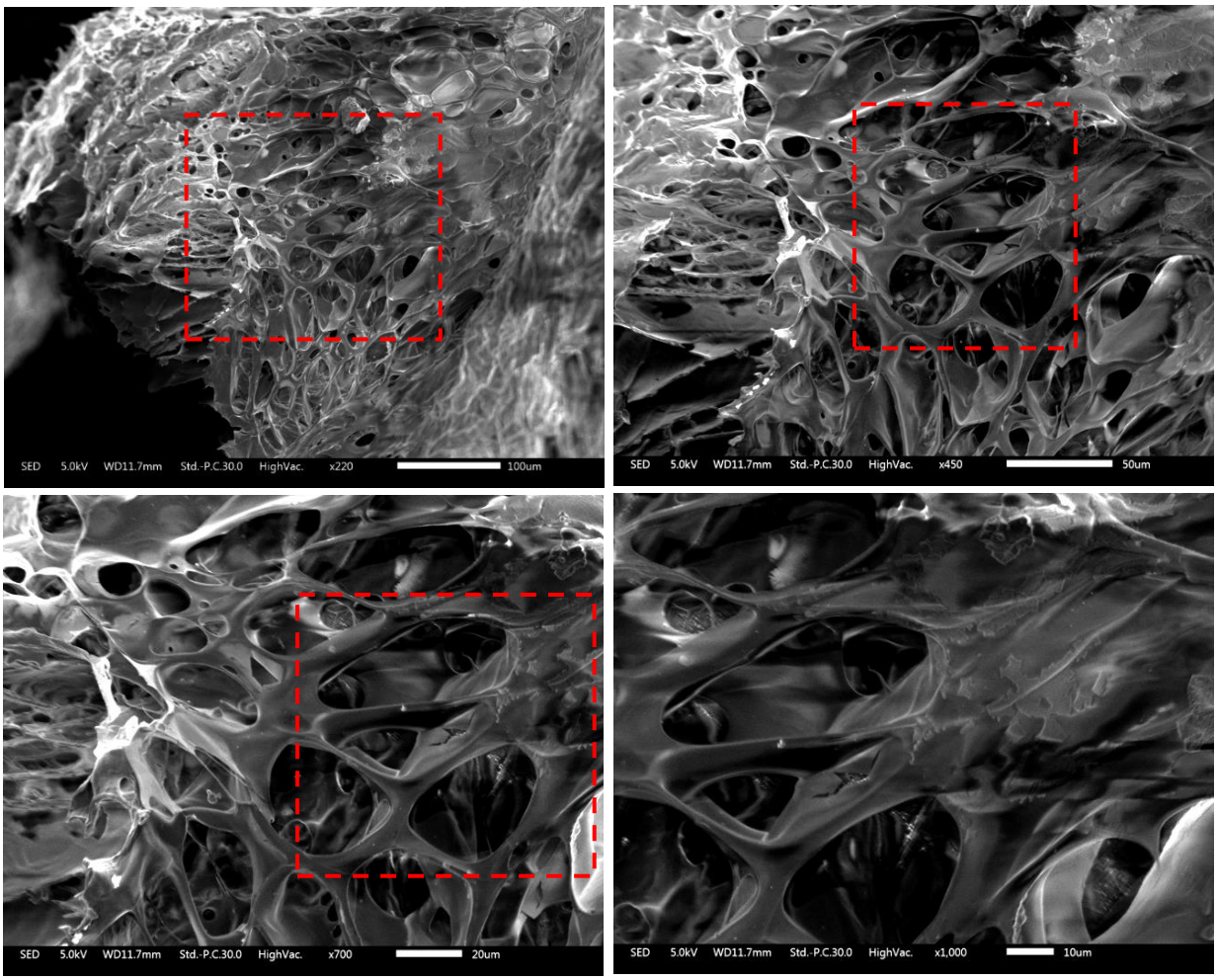

Figure 5.14: SEM images of organo composite hydrogel (scales are 100 µm, 50 µm, 20 µm, and 10 µm) while the red square shows the area of the image under different magnification.

Additionally, the freeze-dried hydrogels containing organoclay concentrations of 8 and 5 wt% were examined and compared to the composition containing 3 wt%. The rheological data confirmed that the hydrogels containing the higher concentration of organoclay are more dense and have less free space than those containing lower concentrations as shown in Figure 5.15. However, the pore density of hybrid hydrogel was lower than Ca-alginate as seen in Figure 5.13.

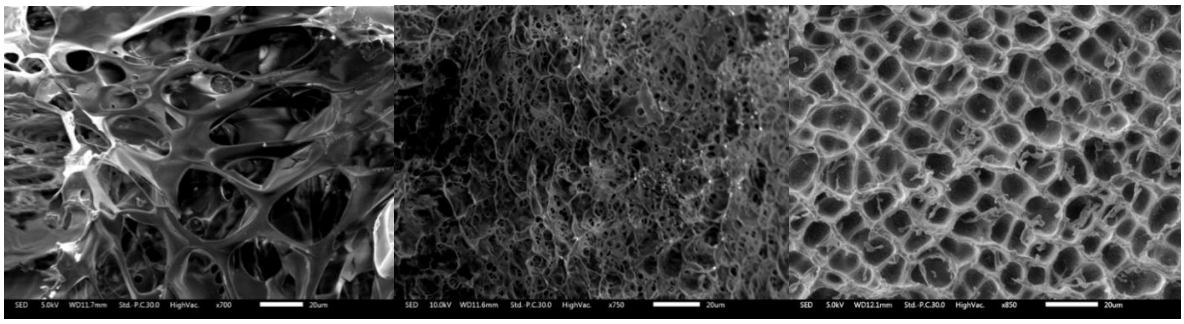

a) b) c)

Figure 5.15: SEM images of hybrid hydrogel with a) 3 wt% organoclay b) 5 wt% organoclay and c) 8 wt% organoclay with the same magnifying (scale bar = 20μm), showing the porous structure and the density of hydrogels. The pores size of c) 8 wt% show smaller, more uniform, and higher density with less free space when compared to a) 3 wt% and b) 5 wt% or organoclay contents.

5.8.6 Ibuprofen release result

It has been suggested the protonated aminopropyl groups in the clay layer interact with the carboxylate groups of ibuprofen (Figure 5.16) and extend the release rate of the drug. A composite hydrogel prepared was loaded with ibuprofen salt (the calibration curve of ibuprofen shown in Figure 2.2) and the release rate was studied in water at room temperature and compared with Ca-alginate hydrogel over a similar period of time.

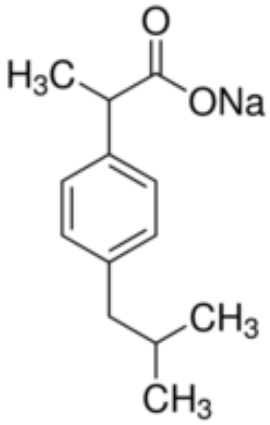

Figure 5.16 The chemical structure of sodium ibuprofen which shows the carboxylate groups that will interact with the clay layers

The release rate of the hybrid hydrogel (with an ibuprofen salt concentration of 10 mg mL^{-1}) was studied and found that first significant release of almost 40 % of the ibuprofen salt occurred within 4h and slightly decreased after that (Figure 5.17). After 30h of experiment, approximately 68 % of the drug had been released. To compare this with Ca-alginate hydrogel, the drug was first released up to 55 % within 4h and 80 % after 30h. This result confirmed that hydrogel with organoclay facilitated slow release of ibuprofen for a longer period of time compared to Ca-alginate hydrogel. The slow release of the drug molecules could be assigned to the strong electrostatic interactions between the negatively charged ibuprofen and exfoliated sheets dispersed in the alginate gel matrix.

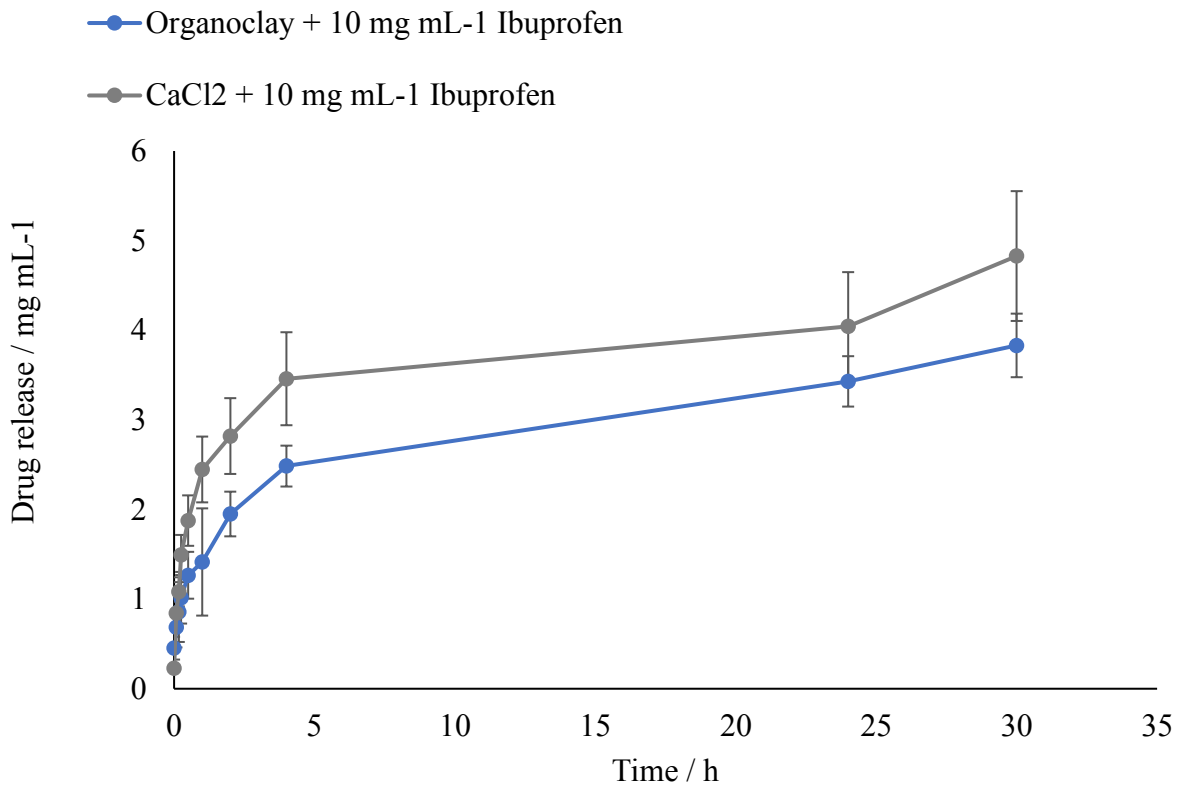

Figure 5.17 Drug elution profile of alginate hydrogels crosslinked with either $CaCl_2$ or organoclay. Although both systems displayed similar trend in the release profiles, the organoclay-hydrogel systems showed comparatively slow release of the drug molecules.

The drug release experiment was carried out in water to provide a basic understanding of the materials behaviour and to demonstrate their potential. The benefit of this study was to be able to compare the hybrid hydrogel behaviour and its potential for sustained drug release from an alginate that has not been cross-linked to improve its gelling ability. Comparable similar work required modifying the backbone of alginate and using EGDMA as a cross-linker [305]. However, the work presented here lacks an *in vivo* study which would be important as drug release would be expected to behave differently *in vivo*. A more realistic *in*

vitro study could have involved release into PBS and at 37 °C as this would more mimic the conditions seen in the human body.

5.9 Conclusion

The experiments undertaken within this chapter clearly demonstrate the solubility properties and the ability of hybrid hydrogel prepared from alginate and organoclay. From which the following conclusion can be made.

1. The hybrid hydrogels showed excellent swelling ability in water and can reform after drying.
2. The electrostatic interactions between alginate and organoclay sheets directed the formation of hydrogel.
3. Significantly the results show the dual functionality of the organoclay matrix such that the aminopropyl-functionalities cross-link the alginate chains and provide anchoring sites to immobilise/encapsulate the drug molecules within the hydrogel matrix.
4. The density of the composite hydrogel was lower than calcium hydrogel which is confirmed by the rheology result and DSC.
5. The SEM images shown the similarity of hydrogel structure. Although, the improvement could still be made, possibly by element mapping to understand to relation between them.
6. A slow release rate of ibuprofen was observed in water at room temperature.

From the experience and knowledge gained from this study it may be possible to make improvements in changing factors for future work as follows:

1. Effect of temperature and pH on the drug release profiles from the hybrid hydrogels?

2. If the concentration of calcium chloride change would it is still hold drug for longer time as result or not including temperature and pH as well.
3. Explore controlled drug release applications of the hybrid hydrogels by encapsulating other anti-inflammatory drug molecules, such as aspirin, mefenamic acid, naproxen etc.

Thus, this research is open the application of alginate with combination of organoclay and this could benefit for bio materials uses.

Chapter 6

Conclusions and future work

6.1 Conclusions

The research work presented in this thesis demonstrates the potential of using alginate for engineering and medical applications by developing its properties and characterising these through various analytical methods. The key findings from the experimental chapters (3-5) are summarised below:

Chapter 3: The novel composite blends were spun into a continuous fibre format and the electrical conductivity of the fibres could be increased significantly through the application of different treatments. The mechanical properties and conductivity of the resulting fibres were examined and compared to neat alginate fibres. Alginate based PEDOT:PSS fibres, doped with PEG and annealed, formed fibres with similar surface roughness and fibre diameter to neat alginate fibres. The addition of PEG conferred significant conductivity (a 2-fold increase) but this made the fibres more brittle due to increased hydrogen bonding arising from the presence of PEG. The heat treatment of PEG-doped fibres also increased the electrical conductivity significantly (a 20-fold increase) and could improve the ultimate stress (an increase around 40 MPa) and Young's modulus (an increase around 1 GPa) compared to untreated fibres.

These fibres might be considered for use in biomedical applications which require electrical conductivity (such as scaffolds for cells or as smart textiles, *etc.*) or as carriers in drug delivery. However, the focus for this research was on scaffolds for cells, especially neuronal cells. In fact, the fine fibres which were obtained from electrospinning (with average diameter 170 μm) have been found to be more efficient for the regeneration of neurons than existing substrates, as they provide contact guidance for cells and also direct the extension of axons [306]. Furthermore, the electrical conductivity of fibres obtained from this research (around 23 S cm^{-1}) has been found to be suitable for the regeneration of neurons, as can be generated with a minimum requirement of 0.6 S cm^{-1} on electrically conductive glass [307].

The data presented from the experimental study imply that the combination of alginate with a commercially available conductive polymer (PEDOT:PSS) and a PEG dopant could offer benefits to industrial textiles, engineering applications, or biomedical applications. Therefore, the fibres obtained in this study were progressed further to examine their biocompatibility with neuronal outgrowth in Chapter 4.

Chapter 4: The conductive fibres obtained from Chapter 3 were initially observed with neuronal outgrowth but the result was negative when compared to coverslip control. However, it has been found that very fine alginate nanofibres produced through electrospinning offered directionality to neurite outgrowth, and the most efficient form of neuron regeneration has been found when using the electroconductive materials [308][309]. Consequently, in this work, conductive films, formed from alginate and PEDOT:PSS, were developed to examine the biocompatibility of the materials. Various conditions, additives and treatments were applied to optimise the properties and the resulting films were compared for the best biocompatibility.

The key discoveries from this experimental study were that the uniform composite films were compatible with neurons as evidenced by the generation of neuronal outgrowth on the films prepared. The degree of swelling observed in the medium was no more than 10% by volume and caused no change in shape, although the prepared films were very fragile, especially in those alginate films containing a low content of Ca^{2+}, making it difficult to examine their mechanical and electrical properties. The known toxicity of Ca^{2+} to culture led to the

observation that conductive films containing a calcium chloride cross-linker show lower cell density when compared to the films without Ca^{2+}. The incorporation of several additives (EG, PEG, GOPS, and PVA), combined with heat treatment improved the compatibility of the films with neurons.

Although the conductive films can support neurons when compared to the control, further investigation on the conductive films are required for the realisation their use in biomedical applications. This empirical study has shown a potential pathway towards using alginate and PEDOT:PSS as a biomaterial for the outgrowth of around 25% of the neurons or nerve cells implants, which slightly better than PPy/collagen but still lower than the number of neurons when compared to neat alginate nanofibres [107][230]. However, when making this comparison it must be remembered that the literature materials were cultured on PC12 plates, and the result might be different if the prepared films had been seeded with PC12.

Currently, the regeneration and restoration of function in damaged nerves have limited capacity in clinical therapies, and studies have been largely performed on conductive metal materials and glass coverslips. The present research suggests that conductive films could constitute a proper environment to provide and facilitate the newly formed cells in order to increase the cell number and biocompatibility with the human body.

Chapter 5: A further study on the medical application of alginate was investigated, wherein the hybrid hydrogel from alginate and organoclay was prepared for a simulated drug delivery application and compared with traditional Ca-alginate hydrogel.

The analysis of a blend containing alginate and organoclay (3 wt%) confirmed that they underwent cross-linking in the absence of a dedicated cross-linking agent. The freeze-dried hybrid hydrogel displayed a porous structure with a relatively uniform distribution of pore sizes, which were in turn larger than the pores found in the Ca-alginate hydrogel. The swelling ability of the hydrogel was shown by the extent of the initial intake water and re-swelling following drying and rehydration, without change in the shape or size of the pores. The burst release of a drug molecule, ibuprofen from within the composite hydrogel was observed to occur within the first 5 minutes. This was also observed with the Ca-alginate

hydrogel, but the release rate of the alginate/organoclay nanocomposite was slower and thus the delivery time longer than Ca-alginate.

This experimental study presents a new combination of alginate and organoclay without using the cross-linker which shows the potential for the delivery of ibuprofen and could benefits in the development of future medical applications. While various hydrogel drug delivery systems have been studied to exemplify different aspects: slow release, target release, or fast release, this research focused on a slow-release system. The covalent cross-linked hydrogels are considered to be stable and elastic while those which are ionic in nature are less stable and exhibit reduced mechanical properties. Alginate has been extensively investigated for drug delivery and widely used in wound dressing commercially which mostly involving with cross-linker to perform their stability. For example, in a literature study an ionotropic gelation technique of alginate hydrogel containing an ibuprofen had released 60% of the pharmaceutical within a 2h period and more than 90% after 48h [310], suggesting that alginate alone released the drug comparatively quickly. Significantly, this work demonstrates a new approach for the fabrication of nanocomposite hydrogels, which results in a slower ibuprofen release (around 68% over a 30h period under similar conditions) when compared to alginate hydrogel alone. The rehydration of biopolymer films using an aqueous dispersion of exfoliated organoclay produced a self-supported hydrogel. Importantly, the work demonstrates that the organoclay not only facilitates the cross-linking of alginate chain network to yield a self-supported hydrogel but also provides a binding site for the guest molecules such as ibuprofen. This opens excellent opportunities to further exploit the host-guest properties of the hydrogels. For example, a range of functional molecules such anti-inflammatory drugs, proteins, enzymes, magnetically-, electrically- and optically active nanoparticles can be encapsulated within the alginate-organoclay hydrogels to produce functional hybrid materials with potential applications in controlled drug release, biocatalysis, biosensing, soft actuators, and environmental remediation.

Taken together, the research presented in this thesis is novel and has provided new insights into the design and construction of alginate based composite materials at different length scales. This work has added to the relatively of knowledge that exists on alginate, and its

application development, and demonstrates the ability to modify its properties by spinning into fibres, neural outgrowth culture, and combining it with an organoclay. The novel findings have the potential to strongly influence on alginate properties. Key modifications by adding conductive polymer and organoclay to alginate have potential advantages in medical applications which might be of value to industry and wider society. The hydrogel prepared in this research offers the benefit of avoiding drug burst when the pharmaceutical is first consumed, thus extending the drug's effective duration. Finally, the findings also point to the use alginate without cross-linker to enhance hydrogel stability by interacting with organoclay which can hold the drug molecule strongly within them and help to maintain the drug release over time.

6.2 Suggestions for future work

Owing to the variety of topics covered within this thesis, there are many potential areas that could be improved further. However, based on experience and knowledge gained through this research some of the author's ideas for the improvement of the study within each experimental chapter are presented.

Extension to Chapter 3: The principal finding of this chapter was that the conductivity of the fibres could be increased with the addition of a PEG dopant and an annealing process. However, the mechanical properties of fibres prepared were lower when compared to the relevant research that using the same spinning process which have increased the tensile strength up to 120 MPa and elongation at break up to 130% and shown the flexibility of woven fibres that can fabricate into patches and can be used on human skin and monitoring the movement [ref] (Figure 6.1). Therefore, the improvement of the fibres properties should be studied to achieve the better result of high conductivity with good mechanical properties to use as a fabric or scaffold. Although, the fibres obtained from this research performed a very high conductivity, but the mechanical properties were lower than 100 MPa which was brittle and non-flexible, with the mechanical suggested the fibres would be more benefits in textile industrial.

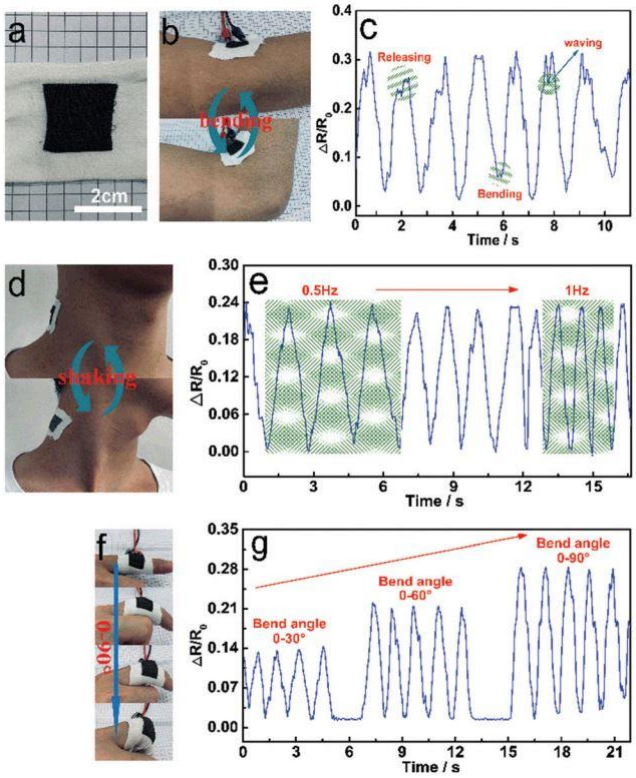

Figure 6.1: *Motion-sensing fabric based on the PEDOT:PSS/SA composite fibres for monitoring human body movement. (a) Photograph of the sensing fabric and resistance response of the sensing fabric attached to the elbow (b and c), neck (d and e) and finger (f and g).* [72]

Furthermore, this process was by no means optimal. Based on this finding, a more detailed parametric study might be envisaged where the density can be examined by hydrostatic balance or analytical according to the standard ASTM D792 [311]. While the alignment of fibres should be studied further by CurveAlign platform and MATLAB software [312] to understand the structure of fibres and reason for the effects of the annealing process on the fibres. Moreover, alginate has been spun into fibres using the electrospinning technique [88] (Figure 6.2) to obtain nanofibres which could be rendered conductive to optimise a wide range of applications. The mechanical and electrical conductivity properties need to be observed as well as the wet spinning conductive fibres.

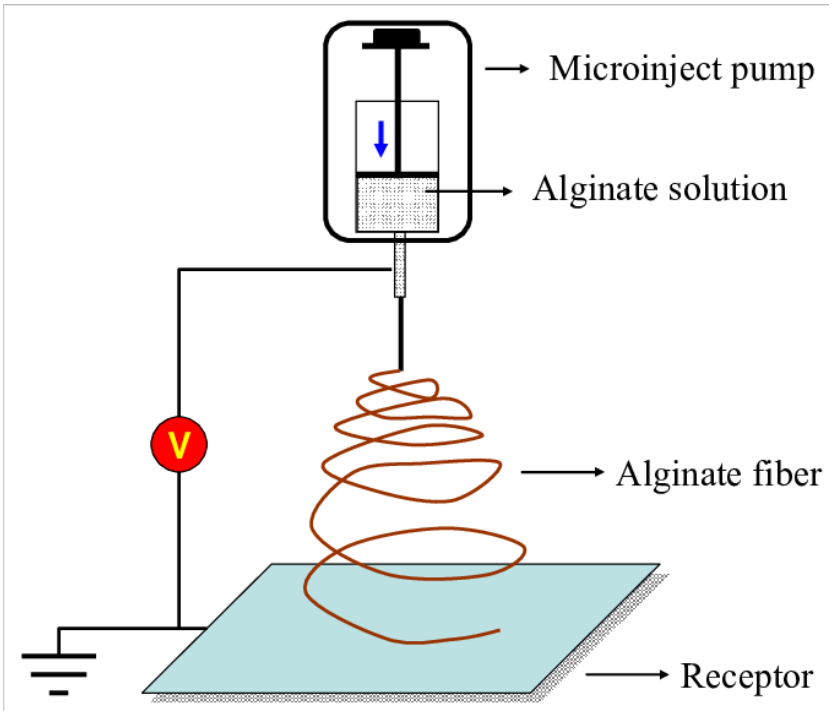

Figure 6.2 The electrospinning process of alginate [89]

Extension to Chapter 4: The composite films prepared were brittle and consequently their mechanical properties could not be examined within the current project. As this aspect of the materials is of interest further research would focus on determining mechanical properties for the films. This would take two forms: (a) examining whether the brittleness can be reduced by the incorporation of a toughening agent such as gelatin, PVA, or PEO which contains a strong polar solvent, *etc.* and (b) employing a more dedicated tensile testing and electrical conductivity apparatus with a suitably calibrated, bend test technique (Figure 6.3) or using the ball on three balls test combine with numerical simulations [313] to enable tensile properties to be determined. The conductivity testing can be investigated by means of electrochemical impedance spectroscopy (EIS) [314]. It might also be of interest to extend the conductive film study to another biological cell *e.g.* neural stem cells, nerve cells, or heart cells.

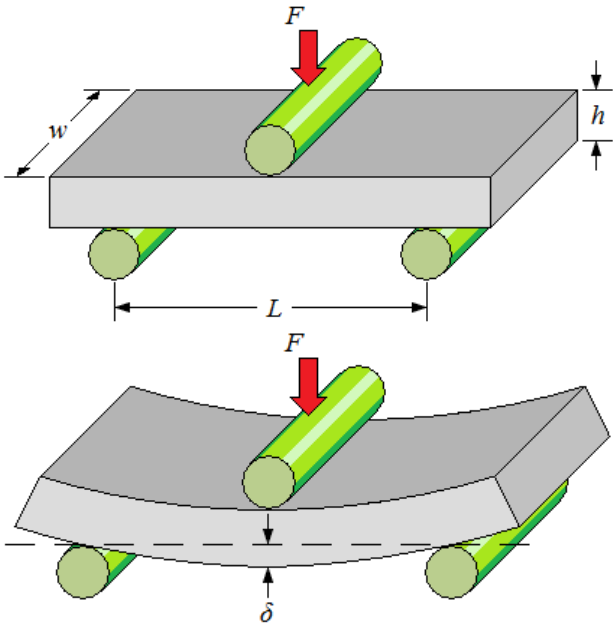

Figure 6.3 The bend test technique is observed by applying load at three points which will cause the materials bend, a tensile force is given on the lower surface opposite the midpoint. The material's strength is described by the flexural strength [314].

Extension to Chapter 5: Hybrid hydrogel structures were found to be porous materials, but within the existing experimental study, no attempt was made to control pore size or distribution. However, if conditions could be identified to control the pore size then it might be possible to control the drug release rate. A future study might include the incorporation of a 'blowing agent' to generate an inert gas through the gelling polymer to modify the pores generated [315]. The BET experimental technique could be used to determine pore size and distribution as a function of preparation method [316]. When the concentration of ibuprofen in the hydrogel was increased from 10 mg mL^{-1} to 20 mg mL^{-1} in order to study the release in water, a different of trend was observed. It showed that release rate from Ca-alginate was slower than the hybrid hydrogel (Figure 6.4), which was contrary to the result obtained for the 10 mg mL^{-1} loading. However, these experiments were undertaken over a limited timescale and observations were concluded after 6 hours because the high concentration of ibuprofen overwhelmed the spectrometer. At high drug loadings the available sites for this interaction to take place may have been largely occupied causing the 'excess' unassociated

drug to be more readily available to be released initially. At this loading a rapid initial burst release was obtained, and it is likely that sustained release would also be observed at later time points which would be benefit to study in the future.

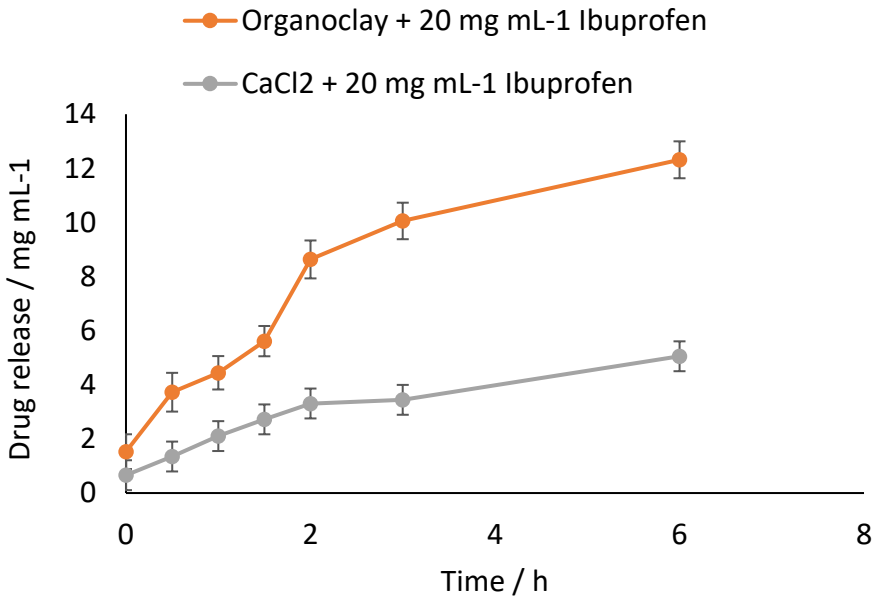

Figure 6.4: Drug elution profile of alginate hydrogels crosslinked with either $CaCl_2$ or organoclay with 20 mg mL^{-1} ibuprofen. Both hydrogels were shown to release rapidly during the first hour while organoclay hydrogel released more drug than Ca-alginate hydrogel over 6h.

However, the choice of organic clay with positive cations layers could also be useful to focus on as it could give the different properties and applications. According to the ability of alginate, cells and other drug with propionic acid which list on Table 6.1 are suggested for the future experiment as well.

Table 6.1 The example of drugs that can be applied with the hybrid hydrogel

Drug	Chemical structure
Flurbiprofen	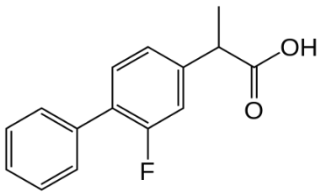
Ketoprofen	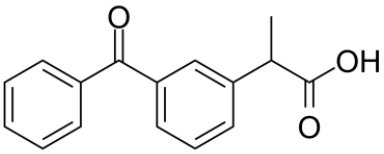
Tiaprofenic Acid	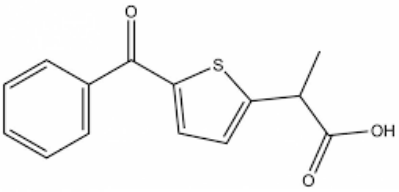
Naproxen	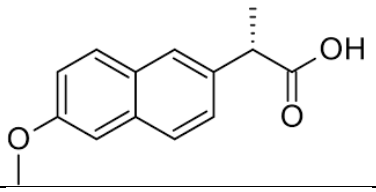
Fenoprofen	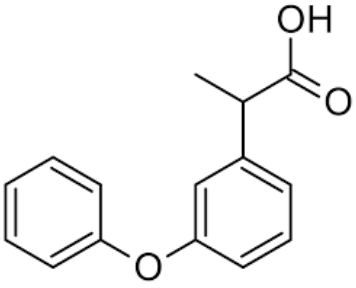

Finally, with all the improvements that might be studied in the future, these should bring greater understanding and develop the applications of alginate in terms of conductive fibres, neural outgrowth, and drug delivery.

References

[1] F. W. Harris, “INTRODUCTION TO POLYMER SCIENCE.,” in *American Chemical Society, Polymer Preprints, Division of Polymer Chemistry*, 1984, vol. 25, no. 2, doi: 10.1021/ed058p837.

[2] C. E. Carraher and Jr., “Introduction to Polymer Chemistry,” *J. Chem. Educ.*, vol. 58, no. 11, p. 528, 2006, doi: 10.1007/978-0-387-68619-6.

[3] P. Christian, “Polymer chemistry,” in *Electrospinning for Tissue Regeneration*, 2011.

[4] D. F. Williams, “On the nature of biomaterials,” *Biomaterials*, 2009, doi: 10.1016/j.biomaterials.2009.07.027.

[5] S. Kumbar, C. Laurencin, and M. Deng, *Natural and Synthetic Biomedical Polymers*. 2014.

[6] A. H. Clark and S. B. Ross-Murphy, “Biopolymer Network Assembly. Measurement and Theory,” in *Modern Biopolymer Science*, 2009, pp. 1–27.

[7] S. H. Othman, “Bio-nanocomposite Materials for Food Packaging Applications: Types of Biopolymer and Nano-sized Filler,” *Agric. Agric. Sci. Procedia*, vol. 2, pp. 296–303, 2014, doi: 10.1016/j.aaspro.2014.11.042.

[8] J. Y. Wong, J. D. Bronzino, and D. R. Peterson, *Biomaterials Principles and practices*, vol. 1, no. 2. 2012.

[9] A. Aravamudhan, D. M. Ramos, A. A. Nada, and S. G. Kumbar, “Natural Polymers,” in *Natural and Synthetic Biomedical Polymers*, 2014.

[10] O. G. Jones and D. J. McClements, “Functional biopolymer particles: Design, fabrication, and applications,” *Comprehensive Reviews in Food Science and Food Safety*, vol. 9, no. 4. pp. 374–397, 2010, doi: 10.1111/j.1541-4337.2010.00118.x.

[11] P. K. Dutta, J. Duta, and V. S. Tripathi, “Chitin and Chitosan: Chemistry, properties and applications,” *J. Sci. Ind. Res. (India).*, 2004.

[12] P. Zhao *et al.*, "A study of chitosan hydrogel with embedded mesoporous silica nanoparticles loaded by ibuprofen as a dual stimuli-responsive drug release system for surface coating of titanium implants," *Colloids Surfaces B Biointerfaces*, vol. 123, pp. 657–663, 2014, doi: 10.1016/j.colsurfb.2014.10.013.

[13] E. Quinlan, A. López-Noriega, E. Thompson, H. M. Kelly, S. A. Cryan, and F. J. O'Brien, "Development of collagen-hydroxyapatite scaffolds incorporating PLGA and alginate microparticles for the controlled delivery of rhBMP-2 for bone tissue engineering," *J. Control. Release*, 2015, doi: 10.1016/j.jconrel.2014.11.021.

[14] L. S. Nair and C. T. Laurencin, "Biodegradable polymers as biomaterials," *Progress in Polymer Science (Oxford)*, vol. 32, no. 8–9. pp. 762–798, 2007, doi: 10.1016/j.progpolymsci.2007.05.017.

[15] K. I. Draget, O. Smidsrød, and G. Skjåk-Bræk, "Alginates from Algae," in *Biopolymers Online*, 2005.

[16] I. D. Hay, Z. U. Rehman, A. Ghafoor, and B. H. A. Rehm, "Bacterial biosynthesis of alginates," *Journal of Chemical Technology and Biotechnology*. 2010, doi: 10.1002/jctb.2372.

[17] L. E. Rioux, S. L. Turgeon, and M. Beaulieu, "Characterization of polysaccharides extracted from brown seaweeds," *Carbohydr. Polym.*, 2007, doi: 10.1016/j.carbpol.2007.01.009.

[18] D. E. Clark and H. C. Green, "Alginic acid and process of making same.," *Pat. US2036922 A.*, 1936, doi: 10.1215/03616878-25-5-953.

[19] T. Y. Wong, L. A. Preston, and N. L. Schiller, "Alginate Lyase: Review of Major Sources and Enzyme Characteristics, Structure-Function Analysis, Biological Roles, and Applications," *Annu. Rev. Microbiol.*, 2000, doi: 10.1146/annurev.micro.54.1.289.

[20] H. Hecht and S. Srebnik, "Structural Characterization of Sodium Alginate and Calcium Alginate," *Biomacromolecules*, 2016, doi: 10.1021/acs.biomac.6b00378.

[21] M. Rinaudo, "Biomaterials based on a natural polysaccharide: alginate," *TIP*, 2014, doi: 10.1016/s1405-888x(14)70322-5.

[22] G. T. Grant, E. R. Morris, D. A. Rees, P. J. C. Smith, and D. Thom, "Biological interactions between polysaccharides and divalent cations: The egg-box model," *FEBS Lett.*, 1973, doi: 10.1016/0014-5793(73)80770-7.

[23] M. Rinaudo, "Main properties and current applications of some polysaccharides as biomaterials," *Polymer International*. 2008, doi: 10.1002/pi.2378.

[24] M. A. LeRoux, F. Guilak, and L. A. Setton, “Compressive and shear properties of alginate gel: Effects of sodium ions and alginate concentration,” *J. Biomed. Mater. Res.*, 1999, doi: 10.1002/(SICI)1097-4636(199910)47:1<46::AID-JBM6>3.0.CO;2-N.

[25] H. J. Kong, M. K. Smith, and D. J. Mooney, “Designing alginate hydrogels to maintain viability of immobilized cells,” *Biomaterials*, 2003, doi: 10.1016/S0142-9612(03)00295-3.

[26] H. Ertesvåg, “Alginate-modifying enzymes: Biological roles and biotechnological uses,” *Frontiers in Microbiology*. 2015, doi: 10.3389/fmicb.2015.00523.

[27] M. Otterlei, K. Østgaard, G. Skjåk-Bræk, O. Smidsr∅d, P. Soon-Shiong, and T. Espevik, “Induction of Cytokine Production from Human Monocytes Stimulated with Alginate,” *J. Immunother.*, 1991, doi: 10.1097/00002371-199108000-00007.

[28] G. Klöck *et al.*, “Biocompatibility of mannuronic acid-rich alginates,” *Biomaterials*, vol. 18, no. 10, pp. 707–713, 1997, doi: 10.1016/S0142-9612(96)00204-9.

[29] H. Zimmermann, S. G. Shirley, and U. Zimmermann, “Alginate-based encapsulation of cells: Past, present, and future,” *Current Diabetes Reports*. 2007, doi: 10.1007/s11892-007-0051-1.

[30] G. Orive, S. Ponce, R. M. Hernández, A. R. Gascón, M. Igartua, and J. L. Pedraz, “Biocompatibility of microcapsules for cell immobilization elaborated with different type of alginates,” *Biomaterials*, 2002, doi: 10.1016/S0142-9612(02)00118-7.

[31] S. N. Pawar and K. J. Edgar, “Alginate derivatization: A review of chemistry, properties and applications,” *Biomaterials*, vol. 33, no. 11. pp. 3279–3305, 2012, doi: 10.1016/j.biomaterials.2012.01.007.

[32] S. Pelletier, P. Hubert, E. Payan, P. Marchal, L. Choplin, and E. Dellacherie, “Amphiphilic derivatives of sodium alginate and hyaluronate for cartilage repair: Rheological properties,” *J. Biomed. Mater. Res.*, 2001, doi: 10.1002/1097-4636(200101)54:1<102::AID-JBM12>3.0.CO;2-1.

[33] P. Severino, C. F. da Silva, L. N. Andrade, D. de Lima Oliveira, J. Campos, and E. B. Souto, “Alginate Nanoparticles for Drug Delivery and Targeting,” *Curr. Pharm. Des.*, 2019, doi: 10.2174/1381612825666190425163424.

[34] R. Detsch, B. Sarker, T. Zehnder, G. Frank, and A. R. Boccaccini, “Advanced alginate-based hydrogels,” *Materials Today*, vol. 18, no. 10. pp. 590–591, 2015, doi: 10.1016/j.mattod.2015.10.013.

[35] B. Yao, C. Ni, C. Xiong, C. Zhu, and B. Huang, “Hydrophobic modification of sodium

alginate and its application in drug controlled release," *Bioprocess Biosyst. Eng.*, 2010, doi: 10.1007/s00449-009-0349-2.

[36] P. P. Lehenkari and M. A. Horton, "Single integrin molecule adhesion forces in intact cells measured by atomic force microscopy," *Biochem. Biophys. Res. Commun.*, 1999, doi: 10.1006/bbrc.1999.0827.

[37] L. Y. Koo, D. J. Irvine, A. M. Mayes, D. A. Lauffenburger, and L. G. Griffith, "Co-regulation of cell adhesion by nanoscale RGD organization and mechanical stimulus," *J. Cell Sci.*, 2002.

[38] S. E. Sakiyama-Elbert and J. A. Hubbell, "Functional biomaterials: Design of novel biomaterials," *Annu. Rev. Mater. Sci.*, 2001, doi: 10.1146/annurev.matsci.31.1.183.

[39] a N. a Blandino, M. Macias, and D. Canter, "Formation of Calcium Alginate Gel Capsules : Influence of Sodium Alginate and CaC12 Concentration on Gelation Kinetics," *J. Biosci.*, vol. 88, no. 6, pp. 686–689, 1999, doi: http://dx.doi.org/10.1016/S1389-1723(00)87103-0.

[40] B. B. Crow and K. D. Nelson, "Release of bovine serum albumin from a hydrogel-cored biodegradable polymer fiber," *Biopolymers*, 2006, doi: 10.1002/bip.20442.

[41] C. K. Kuo and P. X. Ma, "Ionically crosslinked alginate hydrogels as scaffolds for tissue engineering: part 1. Structure, gelation rate and mechanical properties.," *Biomaterials*, vol. 22, no. 6, pp. 511–21, 2001, doi: 10.1016/S0142-9612(00)00201-5.

[42] A. D. Augst, H. J. Kong, and D. J. Mooney, "Alginate hydrogels as biomaterials," *Macromol. Biosci.*, vol. 6, no. 8, pp. 623–633, 2006, doi: 10.1002/mabi.200600069.

[43] Y. Suzuki *et al.*, "Evaluation of a novel alginate gel dressing: Cytotoxicity to fibroblasts in vitro and foreign-body reaction in pig skin in vivo," *J. Biomed. Mater. Res.*, 1998, doi: 10.1002/(SICI)1097-4636(199802)39:2<317::AID-JBM20>3.0.CO;2-8.

[44] X. Zhao, N. Huebsch, D. J. Mooney, and Z. Suo, "Stress-relaxation behavior in gels with ionic and covalent crosslinks," 2010, doi: 10.1063/1.3343265.

[45] P. Eiselt, J. Yeh, R. K. Latvala, L. D. Shea, and D. J. Mooney, "Porous carriers for biomedical applications based on alginate hydrogels," *BEiselt, P. al. 'Porous carriers Biomed. Appl. based alginate hydrogels', Biomater. 21(19), pp. 1921–1927. doi 10.1016/S0142-9612(00)00033-8.iomaterials*, vol. 21, no. 19, pp. 1921–1927, 2000, doi: 10.1016/S0142-9612(00)00033-8.

[46] K. Y. Lee, K. H. Bouhadir, and D. J. Mooney, "Controlled degradation of hydrogels

using multi-functional cross-linking molecules," *Biomaterials*, 2004, doi: 10.1016/j.biomaterials.2003.09.030.

[47] K. Y. Lee, M. C. Peters, K. W. Anderson, and D. J. Mooney, "Controlled growth factor release from synthetic extracellular matrices," *Nature*, 2000, doi: 10.1038/35050141.

[48] H. Tanaka and Y. Sato, "PHOTOSENSITIVITY OF POLYVINYLESTERS OF SUBSTITUTED CINNAMYLIDENEACETIC ACIDS.," *J Polym Sci Part A-1 Polym Chem*, 1972, doi: 10.1002/pol.1972.170101114.

[49] J. W. Lu, Y. L. Zhu, Z. X. Guo, P. Hu, and J. Yu, "Electrospinning of sodium alginate with poly(ethylene oxide)," *Polymer (Guildf).*, 2006, doi: 10.1016/j.polymer.2006.09.027.

[50] S. M. Richardson-Burns, J. L. Hendricks, B. Foster, L. K. Povlich, D. H. Kim, and D. C. Martin, "Polymerization of the conducting polymer poly(3,4-ethylenedioxythiophene) (PEDOT) around living neural cells," *Biomaterials*, vol. 28, no. 8, pp. 1539–1552, 2007, doi: 10.1016/j.biomaterials.2006.11.026.

[51] S. Zhao, M. Cao, H. Li, L. Li, and W. Xu, "Synthesis and characterization of thermo-sensitive semi-IPN hydrogels based on poly(ethylene glycol)-co-poly(ε-caprolactone) macromer, N-isopropylacrylamide, and sodium alginate," *Carbohydr. Res.*, 2010, doi: 10.1016/j.carres.2009.11.014.

[52] K. W. Lee *et al.*, "Sustained release of vascular endothelial growth factor from calcium-induced alginate hydrogels reinforced by heparin and chitosan," 2004, doi: 10.1016/j.transproceed.2004.08.078.

[53] J. L. Drury, T. Boontheeku, and D. J. Mooney, "Cellular cross-linking of peptide modified hydrogels," *J. Biomech. Eng.*, 2005, doi: 10.1115/1.1865194.

[54] J. A. Rowley, Z. Sun, D. Goldman, and D. J. Mooney, "Biomaterials to spatially regulate cell fate," *Adv. Mater.*, 2002, doi: 10.1002/1521-4095(20020618)14:12<886::AID-ADMA886>3.0.CO;2-I.

[55] J. W. Lee, Y. J. Park, S. J. Lee, S. K. Lee, and K. Y. Lee, "The effect of spacer arm length of an adhesion ligand coupled to an alginate gel on the control of fibroblast phenotype," *Biomaterials*, 2010, doi: 10.1016/j.biomaterials.2010.03.063.

[56] S. Degala, W. R. Zipfel, and L. J. Bonassar, "Chondrocyte calcium signaling in response to fluid flow is regulated by matrix adhesion in 3-D alginate scaffolds," *Arch. Biochem. Biophys.*, 2011, doi: 10.1016/j.abb.2010.08.003.

[57] M. B. Evangelista *et al.*, “Upregulation of bone cell differentiation through immobilization within a synthetic extracellular matrix,” *Biomaterials*, 2007, doi: 10.1016/j.biomaterials.2007.04.028.

[58] N. Sachan, S. Pushkar, A. Jha, and A. Bhattcharya, “Sodium alginate: the wonder polymer for controlled drug delivery,” *J. Pharm. Res.*, 2009.

[59] M. Kalyanaraman *et al.*, “Controlled microfluidic production of alginate beads for in situ encapsulation of microbes,” 2009, doi: 10.1109/BSEC.2009.5090482.

[60] B. Amsden and N. Turner, “Diffusion characteristics of calcium alginate gels,” *Biotechnol. Bioeng.*, vol. 65, no. 5, pp. 605–610, 1999, doi: 10.1002/(SICI)1097-0290(19991205)65:5<605::AID-BIT14>3.0.CO;2-C.

[61] J. S. Boateng, K. H. Matthews, H. N. E. Stevens, and G. M. Eccleston, “Wound healing dressings and drug delivery systems: A review,” *Journal of Pharmaceutical Sciences*. 2008, doi: 10.1002/jps.21210.

[62] B. Balakrishnan, M. Mohanty, A. C. Fernandez, P. V. Mohanan, and A. Jayakrishnan, “Evaluation of the effect of incorporation of dibutyryl cyclic adenosine monophosphate in an in situ-forming hydrogel wound dressing based on oxidized alginate and gelatin,” *Biomaterials*, 2006, doi: 10.1016/j.biomaterials.2005.08.021.

[63] C. Wiegand, T. Heinze, and U. C. Hipler, “Comparative in vitro study on cytotoxicity, antimicrobial activity, and binding capacity for pathophysiological factors in chronic wounds of alginate and silver-containing alginate,” *Wound Repair Regen.*, 2009, doi: 10.1111/j.1524-475X.2009.00503.x.

[64] A. B. G. Lansdown, U. Mirastschijski, N. Stubbs, E. Scanlon, and M. S. Ågren, “Zinc in wound healing: Theoretical, experimental, and clinical aspects,” *Wound Repair and Regeneration*. 2007, doi: 10.1111/j.1524-475X.2006.00179.x.

[65] S. J. Horn, “Bioenergy from brown seaweeds,” *Sci. Technol.*, 2000.

[66] K. H. Bouhadir, E. Alsberg, and D. J. Mooney, “Hydrogels for combination delivery of antineoplastic agents,” *Biomaterials*, 2001, doi: 10.1016/S0142-9612(01)00003-5.

[67] K. Y. Lee, K. H. Bouhadir, and D. J. Mooney, “Degradation behavior of covalently cross-linked poly(aldehyde guluronate) hydrogels,” *Macromolecules*, 2000, doi: 10.1021/ma991286z.

[68] H. J. Kong, E. Alsberg, D. Kaigler, K. Y. Lee, and D. J. Mooney, “Controlling degradation of hydrogels via the size of cross-linked junctions,” *Adv. Mater.*, 2004, doi: 10.1002/adma.200400014.

[69] H. J. Kong, D. Kaigler, K. Kim, and D. J. Mooney, “Controlling rigidity and degradation of alginate hydrogels via molecular weight distribution,” *Biomacromolecules*, 2004, doi: 10.1021/bm049879r.

[70] D. J. McHugh, *Seaweeds uses as Human Foods*. 2003.

[71] D. J. Mchugh, “Production, properties and uses of alginates,” in *Production and Utilization of Products from Commercial Seaweeds*, 1987.

[72] M. Wang, Q. Gao, J. Gao, C. Zhu, and K. Chen, “Core-shell PEDOT:PSS/SA composite fibers fabricated: Via a single-nozzle technique enable wearable sensor applications,” *J. Mater. Chem. C*, 2020, doi: 10.1039/c9tc05527d.

[73] F. S. Rocha, A. J. Gomes, C. N. Lunardi, S. Kaliaguine, and G. S. Patience, “Experimental methods in chemical engineering: Ultraviolet visible spectroscopy—UV-Vis,” *Can. J. Chem. Eng.*, 2018, doi: 10.1002/cjce.23344.

[74] S. H. Lee, S. M. Park, and L. P. Lee, “Optical methods in studies of olfactory system,” in *Bioelectronic Nose: Integration of Biotechnology and Nanotechnology*, 2014.

[75] P. Gabbott, *Principles and Applications of Thermal Analysis*. 2008.

[76] M. Djabourov, J. Leblond, and P. Papon, “Rheology of the sol-gel transition,” *J. Phys.*, 1988, doi: 10.1051/jphys:01988004902033300ï.

[77] J. W. Dobrucki and U. Kubitscheck, “Fluorescence Microscopy,” in *Fluorescence Microscopy: From Principles to Biological Applications: Second Edition*, 2017.

[78] A. Mohammed and A. Abdullah, “Scanning Electron Microscopy (Sem): a Review,” *Proc. 2018 Int. Conf. Hydraul. Pneum. - HERVEX*, 2018.

[79] J. C. Li, Y. Wang, and D. C. Ba, “Characterization of Semiconductor Surface Conductivity by Using Microscopic Four-Point Probe Technique,” 2012, doi: 10.1016/j.phpro.2012.03.568.

[80] F. Wang and J. Shao, “Modified Weibull distribution for analyzing the tensile strength of bamboo fibers,” *Polymers (Basel).*, 2014, doi: 10.3390/polym6123005.

[81] G. Wallace and L. Kane-Maguire, “Conductive polymers,” *Encyclopedia of Biomaterials and Biomedical Engineering*, vol. 1. pp. 374–383, 2004, [Online]. Available: http://www2.dekker.com/sdek/abstract~db=enc~content=a713554087.

[82] R. Balint, N. J. Cassidy, and S. H. Cartmell, “Conductive polymers: Towards a smart biomaterial for tissue engineering,” *Acta Biomater.*, vol. 10, no. 6, pp. 2341–2353, 2014, doi: 10.1016/j.actbio.2014.02.015.

[83] A. Mirabedini, J. Foroughi, and G. G. Wallace, “Developments in conducting polymer

fibres: from established spinning methods toward advanced applications," *RSC Adv.*, 2016, doi: 10.1039/C6RA05626A.

[84] Y. Qin, "Alginate fibres: An overview of the production processes and applications in wound management," *Polymer International*. 2008, doi: 10.1002/pi.2296.

[85] T. Mikołajczyk, M. Boguń, A. Kurzak, and G. Szparaga, "Zinc alginate fibres with a tricalcium phosphate (TCP) nanoadditive," *Fibres Text. East. Eur.*, 2009.

[86] Y. Qin, "Silver-containing alginate fibres and dressings," *Int. Wound J.*, 2005, doi: 10.1111/j.1742-4801.2005.00101.x.

[87] M. Miraftab, Q. Qiao, J. F. Kennedy, C. J. Knill, and M. R. Groocock, "Advanced wound-care materials: Ultra high absorbing fibres made from alginates containing branan ferulate and carboxymethyl cellulose," *J. Text. Inst. Part 1 Fibre Sci. Text. Technol.*, 2004, doi: 10.1533/joti.2003.0063.

[88] T. C. Mokhena, M. J. Mochane, A. Mtibe, M. J. John, E. R. Sadiku, and J. S. Sefadi, "Electrospun alginate nanofibers toward various applications: A review," *Materials (Basel).*, 2020, doi: 10.3390/ma13040934.

[89] J. Sun and H. Tan, "Alginate-based biomaterials for regenerative medicine applications," *Materials*. 2013, doi: 10.3390/ma6041285.

[90] D. Fang, Y. Liu, S. Jiang, J. Nie, and G. Ma, "Effect of intermolecular interaction on electrospinning of sodium alginate," *Carbohydr. Polym.*, 2011, doi: 10.1016/j.carbpol.2011.01.054.

[91] C. D. Saquing *et al.*, "Alginate-polyethylene oxide blend nanofibers and the role of the carrier polymer in electrospinning," *Ind. Eng. Chem. Res.*, 2013, doi: 10.1021/ie302385b.

[92] H. Nie, A. He, J. Zheng, S. Xu, J. Li, and C. C. Han, "Effects of chain conformation and entanglement on the electrospinning of pure alginate," *Biomacromolecules*, 2008, doi: 10.1021/bm701349j.

[93] V. V. N. Phanikumar, V. R. Rikka, B. Das, R. Gopalan, B. V. Appa Rao, and R. Prakash, "Investigation on polyvinyl alcohol and sodium alginate as aqueous binders for lithium-titanium oxide anode in lithium-ion batteries," *Ionics (Kiel).*, 2019, doi: 10.1007/s11581-018-2751-8.

[94] B. Vigani *et al.*, "Electrospun alginate fibers: Mixing of two different poly(ethylene oxide) grades to improve fiber functional properties," *Nanomaterials*, 2018, doi: 10.3390/nano8120971.

[95] C. A. Bonino *et al.*, “Electrospinning alginate-based nanofibers: From blends to crosslinked low molecular weight alginate-only systems,” *Carbohydr. Polym.*, 2011, doi: 10.1016/j.carbpol.2011.02.002.

[96] Y. J. Lee and W. S. Lyoo, “Preparation and characterization of high-molecular-weight atactic poly(vinyl alcohol)/sodium alginate/silver nanocomposite by electrospinning,” *J. Polym. Sci. Part B Polym. Phys.*, 2009, doi: 10.1002/polb.21784.

[97] C. A. Bonino, K. Efimenko, S. I. Jeong, M. D. Krebs, E. Alsberg, and S. A. Khan, “Three-dimensional electrospun alginate nanofiber mats via tailored charge repulsions,” *Small*, 2012, doi: 10.1002/smll.201101791.

[98] T. C. Mokhena, N. V. Jacobs, and A. S. Luyt, “Electrospun alginate nanofibres as potential bio-sorption agent of heavy metals in water treatment,” *Express Polym. Lett.*, 2017, doi: 10.3144/expresspolymlett.2017.63.

[99] M. Castellano, M. Alloisio, R. Darawish, A. Dodero, and S. Vicini, “Electrospun composite mats of alginate with embedded silver nanoparticles: Synthesis and characterization,” *J. Therm. Anal. Calorim.*, 2019, doi: 10.1007/s10973-018-7979-z.

[100] S. V. G. Nista, J. Bettini, and L. H. I. Mei, “Coaxial nanofibers of chitosan-alginate-PEO polycomplex obtained by electrospinning,” *Carbohydr. Polym.*, 2015, doi: 10.1016/j.carbpol.2015.03.063.

[101] K. Y. Lee, L. Jeong, Y. O. Kang, S. J. Lee, and W. H. Park, “Electrospinning of polysaccharides for regenerative medicine,” *Advanced Drug Delivery Reviews*. 2009, doi: 10.1016/j.addr.2009.07.006.

[102] Z. Ye, W. Xu, R. Shen, and Y. Yan, “Emulsion electrospun PLA/calcium alginate nanofibers for periodontal tissue engineering,” *J. Biomater. Appl.*, 2020, doi: 10.1177/0885328219873561.

[103] J. Ferguson, C. Dougleris, and G. R. McKay, “Rheological and coagulation features in the wet spinning process,” *J. Nonnewton. Fluid Mech.*, vol. 6, no. 3–4, pp. 333–338, 1980, doi: 10.1016/0377-0257(80)80010-3.

[104] D. Puppi and F. Chiellini, “Wet-spinning of biomedical polymers: from single-fibre production to additive manufacturing of three-dimensional scaffolds,” *Polymer International*, vol. 66, no. 12. pp. 1690–1696, 2017, doi: 10.1002/pi.5332.

[105] J. J. Qin, J. Gu, and T. S. Chung, “Effect of wet and dry-jet wet spinning on the shear-induced orientation during the formation of ultrafiltration hollow fiber membranes,” *J. Memb. Sci.*, vol. 182, no. 1–2, pp. 57–75, 2001, doi: 10.1016/S0376-7388(00)00552-4.

[106] B. Guo, L. Glavas, and A.-C. Albertsson, “Biodegradable and electrically conducting polymers for biomedical applications,” *Prog. Polym. Sci.*, vol. 38, no. 9, pp. 1263–1286, 2013, doi: 10.1016/j.progpolymsci.2013.06.003.

[107] T. H. Qazi, R. Rai, and A. R. Boccaccini, “Tissue engineering of electrically responsive tissues using polyaniline based polymers: A review,” *Biomaterials*, vol. 35, no. 33. 2014, doi: 10.1016/j.biomaterials.2014.07.020.

[108] C. I. Awuzie, “Conducting Polymers,” 2017, doi: 10.1016/j.matpr.2017.06.036.

[109] S. Ghosh, T. Maiyalagan, and R. N. Basu, “Nanostructured conducting polymers for energy applications: Towards a sustainable platform,” *Nanoscale*. 2016, doi: 10.1039/c5nr08803h.

[110] D. Kumar and R. C. Sharma, “Advances in conductive polymers,” *European Polymer Journal*. 1998, doi: 10.1016/S0014-3057(97)00204-8.

[111] G. G. Wallace, P. R. Teasdale, G. M. Spinks, and L. A. P. Kane-Maguire, *Conductive Electroactive Polymers*. 2008.

[112] N. Hall, “Twenty-five years of conducting polymers,” *Chemical Communications*. 2003, doi: 10.1039/b210718j.

[113] A. E. Daugaard, S. Hvilsted, T. S. Hansen, and N. B. Larsen, “Conductive polymer functionalization by click chemistry,” *Macromolecules*, 2008, doi: 10.1021/ma702731k.

[114] T. H. Le, Y. Kim, and H. Yoon, “Electrical and electrochemical properties of conducting polymers,” *Polymers*. 2017, doi: 10.3390/polym9040150.

[115] T. V. Vernitskaya and O. N. Efimov, “Polypyrrole: A conducting polymer (synthesis, properties, and applications),” *Uspekhi Khimii*. 1997, doi: 10.1070/RC1997v066n05ABEH000261.

[116] L. X. Wang, X. G. Li, and Y. L. Yang, “Preparation, properties and applications of polypyrroles,” *React. Funct. Polym.*, 2001, doi: 10.1016/S1381-5148(00)00079-1.

[117] R. Ansari, “Polypyrrole Conducting Electroactive Polymers: Synthesis and Stability Studies,” *E-Journal Chem.*, 2006, doi: 10.1155/2006/860413.

[118] S. Bhadra, D. Khastgir, N. K. Singha, and J. H. Lee, “Progress in preparation, processing and applications of polyaniline,” *Progress in Polymer Science (Oxford)*. 2009, doi: 10.1016/j.progpolymsci.2009.04.003.

[119] G. Ciric-Marjanovic, “Recent advances in polyaniline research: Polymerization mechanisms, structural aspects, properties and applications,” *Synthetic Metals*. 2013,

doi: 10.1016/j.synthmet.2013.06.004.

[120] R. Liu and Z. Liu, “Polythiophene: Synthesis in aqueous medium and controllable morphology,” *Chinese Sci. Bull.*, 2009, doi: 10.1007/s11434-009-0217-0.

[121] F. Louwet *et al.*, “PEDOT/PSS: Synthesis, characterization, properties and applications,” in *Synthetic Metals*, 2003, vol. 135–136, pp. 115–117, doi: 10.1016/S0379-6779(02)00518-0.

[122] M. Lefebvre, Z. Qi, D. Rana, and P. G. Pickup, “Chemical synthesis, characterization, and electrochemical studies of poly(3,4-ethylenedioxythiophene)/ Poly(styrene-4-sulfonate) composites,” *Chem. Mater.*, 1999, doi: 10.1021/cm9804618.

[123] R. Jalili, J. M. Razal, P. C. Innis, and G. G. Wallace, “One-step wet-spinning process of poly(3,4-ethylenedioxythiophene): poly(styrenesulfonate) fibers and the origin of higher electrical conductivity,” *Adv. Funct. Mater.*, vol. 21, no. 17, pp. 3363–3370, 2011, doi: 10.1002/adfm.201100785.

[124] H. Okuzaki, Y. Harashina, and H. Yan, “Highly conductive PEDOT/PSS microfibers fabricated by wet-spinning and dip-treatment in ethylene glycol,” *Eur. Polym. J.*, vol. 45, no. 1, pp. 256–261, 2009, doi: 10.1016/j.eurpolymj.2008.10.027.

[125] Y. Ding, M. A. Invernale, and G. A. Sotzing, “Conductivity trends of pedot-pss impregnated fabric and the effect of conductivity on electrochromic textile,” *ACS Appl. Mater. Interfaces*, vol. 2, no. 6, pp. 1588–1593, 2010, doi: 10.1021/am100036n.

[126] J. Ouyang, Q. Xu, C. W. Chu, Y. Yang, G. Li, and J. Shinar, “On the mechanism of conductivity enhancement in poly(3,4- ethylenedioxythiophene):poly(styrene sulfonate) film through solvent treatment,” *Polymer (Guildf).*, vol. 45, no. 25, pp. 8443–8450, 2004, doi: 10.1016/j.polymer.2004.10.001.

[127] S. K. M. Jönsson *et al.*, “The effects of solvents on the morphology and sheet resistance in poly(3,4-ethylenedioxythiophene)-polystyrenesulfonic acid (PEDOT-PSS) films,” *Synth. Met.*, vol. 139, no. 1, pp. 1–10, 2003, doi: 10.1016/S0379-6779(02)01259-6.

[128] N. Golafshan, M. Kharaziha, and M. Fathi, “Tough and conductive hybrid graphene-PVA: Alginate fibrous scaffolds for engineering neural construct,” *Carbon N. Y.*, 2017, doi: 10.1016/j.carbon.2016.10.042.

[129] E. J. Lee, F. K. Kasper, and A. G. Mikos, “Biomaterials for tissue engineering,” in *Annals of Biomedical Engineering*, 2014, vol. 42, no. 2, pp. 323–337, doi: 10.1007/s10439-013-0859-6.

[130] A. Pandey, R. K. Sharma, and K. Balani, “Introduction to Biomaterials,” *Biosurfaces: A Materials Science and Engineering Perspective*, pp. 1–64, 2015.

[131] J. Park and J. Bronzino, *Biomaterials: principles and applications*. 2002.

[132] S. Bhat and A. Kumar, “Biomaterials and bioengineering tomorrow’s healthcare,” *Biomatter*. 2013, doi: 10.4161/biom.24717.

[133] B. D. Ratner, A. S. Hoffman, F. J. Schoen, and J. E. Lemons, *Biomaterials science: an introduction to materials in medicine*. 2004.

[134] A. Kashi and S. Saha, “Ethics in biomaterials research,” *Journal of Long-Term Effects of Medical Implants*. 2009, doi: 10.1615/JLongTermEffMedImplants.v19.i1.30.

[135] Y. Ikada, “Challenges in tissue engineering,” *J. R. Soc. Interface*, vol. 3, no. 10, pp. 589–601, 2006, doi: 10.1098/rsif.2006.0124.

[136] C. A. Van Blitterswijk, L. Moroni, J. Rouwkema, R. Siddappa, and J. Sohier, “Tissue Engineering - An Introduction,” *Tissue Engineering*, 2008.

[137] F. Akter, “Principles of Tissue Engineering,” in *Tissue Engineering Made Easy*, 2016, pp. 3–16.

[138] R. Langer and J. P. Vacanti, “Tissue engineering.,” *Science*, vol. 260, no. 5110, pp. 920–6, 1993, doi: 10.1126/science.8493529.

[139] D. J. Richards, Y. Tan, J. Jia, H. Yao, and Y. Mei, “3D printing for tissue engineering,” *Israel Journal of Chemistry*. 2013, doi: 10.1002/ijch.201300086.

[140] F. J. O’Brien, “Biomaterials & scaffolds for tissue engineering,” *Mater. Today*, vol. 14, no. 3, pp. 88–95, 2011, doi: 10.1016/S1369-7021(11)70058-X.

[141] L. D. K. Buttery and A. E. Bishop, “Introduction to tissue engineering,” in *Biomaterials, Artificial Organs and Tissue Engineering*, 2005, pp. 193–200.

[142] P. Macchiarini and E. Kondratieva, “Features of ethical expertise in planning and conducting clinical research in regenerative medicine,” *Cell. Transplant. Tissue Eng.*, 2011.

[143] W. E. Thasler, T. S. Weiss, K. Schillhorn, P. T. Stoll, B. Irrgang, and K. W. Jauch, “Charitable state-controlled foundation human tissue and cell research: Ethic and legal aspects in the supply of surgically removed human tissue for research in the academic and commercial sector in Germany,” *Cell Tissue Bank.*, 2003, doi: 10.1023/A:1026392429112.

[144] J. Slack, “Molecular biology of the cell,” in *Principles of Tissue Engineering*, 2007.

[145] I. Kelava and M. A. Lancaster, “Stem Cell Models of Human Brain Development,”

Cell Stem Cell. 2016, doi: 10.1016/j.stem.2016.05.022.

[146] M. C. Puri and A. Nagy, "Concise review: Embryonic stem cells versus induced pluripotent stem cells: The game is on," *Stem Cells*. 2012, doi: 10.1002/stem.788.

[147] C. Sala, M. Ribes, T. Muiños, L. Sancho, and P. Chicón, "Current Applications of Tissue Engineering in Biomedicine," *J. Biochips Tissue Chips*, vol. 2013, pp. 1–14, 2013, doi: 10.4172/2153-0777.S2-004.

[148] J. Darnell, H. Lodish, A. Berk, L. Zipursky, P. Matsudaira, and D. Baltimore, "Overview of Neuron Structure and Function," *Molecular Cell Biology*. 1999, doi: 10.1002/iub.155.

[149] N. T. Carnevale and M. L. Hines, *The NEURON book*. 2006.

[150] M. L. Hines and N. T. Carnevale, "Neuron: A Tool for Neuroscientists," *Neurosci.*, vol. 7, no. 2, pp. 123–135, 2001, doi: 10.1177/107385840100700207.

[151] D. Câmara, *Bio-Inspired Networking*. 2015.

[152] S. Persheyev, Y. Fan, A. Irving, and M. J. Rose, "BV-2 microglial cells sense micro-nanotextured silicon surface topology," *J. Biomed. Mater. Res. - Part A*, 2011, doi: 10.1002/jbm.a.33159.

[153] E. S. Ereifej *et al.*, "Nanopatterning effects on astrocyte reactivity," *J. Biomed. Mater. Res. - Part A*, 2013, doi: 10.1002/jbm.a.34480.

[154] M. Li, H. H. Zhou, T. Li, C. Y. Li, Z. Y. Xia, and Y. Y. Duan, "Polyurethane/poly(Vinyl alcohol) hydrogel coating improves the cytocompatibility of neural electrodes," *Neural Regen. Res.*, 2015, doi: 10.4103/1673-5374.172325.

[155] C. Boehler, T. Stieglitz, and M. Asplund, "Nanostructured platinum grass enables superior impedance reduction for neural microelectrodes," *Biomaterials*, 2015, doi: 10.1016/j.biomaterials.2015.07.036.

[156] P. Rejmontová *et al.*, "Adhesion, proliferation and migration of NIH/3T3 cells on modified polyaniline surfaces," *Int. J. Mol. Sci.*, 2016, doi: 10.3390/ijms17091439.

[157] D. Mantione *et al.*, "Poly(3,4-ethylenedioxythiophene):GlycosAminoGlycan Aqueous Dispersions: Toward Electrically Conductive Bioactive Materials for Neural Interfaces," *Macromol. Biosci.*, 2016, doi: 10.1002/mabi.201600059.

[158] C. Hadler *et al.*, "Photochemical coating of Kapton® with hydrophilic polymers for the improvement of neural implants," *Mater. Sci. Eng. C*, 2017, doi: 10.1016/j.msec.2017.02.020.

[159] S. De Astis *et al.*, "Nanostructured TiO2surfaces promote polarized activation of

microglia, but not astrocytes, toward a proinflammatory profile," *Nanoscale*, 2013, doi: 10.1039/c3nr03534d.

[160] L. R. Pires, D. N. Rocha, L. Ambrosio, and A. P. Pêgo, "The role of the surface on microglia function: Implications for central nervous system tissue engineering," *J. R. Soc. Interface*, 2015, doi: 10.1098/rsif.2014.1224.

[161] V. Onesto *et al.*, "Nano-topography Enhances Communication in Neural Cells Networks," *Sci. Rep.*, 2017, doi: 10.1038/s41598-017-09741-w.

[162] D. A. Koutsouras *et al.*, "PEDOT:PSS microelectrode arrays for hippocampal cell culture electrophysiological recordings," *MRS Commun.*, 2017, doi: 10.1557/mrc.2017.34.

[163] A. Bachhuka, J. D. Hayball, L. E. Smith, and K. Vasilev, "The Interplay between Surface Nanotopography and Chemistry Modulates Collagen i and III Deposition by Human Dermal Fibroblasts," *ACS Appl. Mater. Interfaces*, 2017, doi: 10.1021/acsami.6b15932.

[164] J. A. Bradley, H. H. Luithardt, M. R. Metea, and C. J. Strock, "In vitro screening for seizure liability using microelectrode array technology," *Toxicol. Sci.*, 2018, doi: 10.1093/toxsci/kfy029.

[165] C. D. Johnson, A. R. D'Amato, D. L. Puhl, D. M. Wich, A. Vesperman, and R. J. Gilbert, "Electrospun fiber surface nanotopography influences astrocyte-mediated neurite outgrowth," *Biomed. Mater.*, 2018, doi: 10.1088/1748-605X/aac4de.

[166] A. K. H. Achyuta, V. S. Polikov, A. J. White, H. G. Pryce Lewis, and S. K. Murthy, "Biocompatibility assessment of insulating silicone polymer coatings using an in vitro glial scar assay," *Macromol. Biosci.*, 2010, doi: 10.1002/mabi.200900451.

[167] S. D. Boomkamp, M. O. Riehle, J. Wood, M. F. Olson, and S. C. Barnett, "The development of a rat in vitro model of spinal cord injury demonstrating the additive effects of rho and ROCK inhibitors on neurite outgrowth and myelination," *Glia*, 2012, doi: 10.1002/glia.22278.

[168] S. Sommakia, J. L. Rickus, and K. J. Otto, "Glial cells, but not neurons, exhibit a controllable response to a localized inflammatory microenvironment in vitro," *Front. Neuroeng.*, 2014, doi: 10.3389/fneng.2014.00041.

[169] J. M. Zuidema, G. P. Desmond, C. J. Rivet, K. R. Kearns, D. M. Thompson, and R. J. Gilbert, "Nebulized solvent ablation of aligned PLLA fibers for the study of neurite response to anisotropic-to-isotropic fiber/film transition (AFFT) boundaries in

astrocyte-neuron co-cultures," *Biomaterials*, 2015, doi: 10.1016/j.biomaterials.2014.12.046.

[170] C. A. R. Chapman, H. Chen, M. Stamou, P. J. Lein, and E. Seker, "Mechanisms of Reduced Astrocyte Surface Coverage in Cortical Neuron-Glia Co-cultures on Nanoporous Gold Surfaces," *Cell. Mol. Bioeng.*, 2016, doi: 10.1007/s12195-016-0449-4.

[171] A. F. Jeffery, M. A. Churchward, V. K. Mushahwar, K. G. Todd, and A. L. Elias, "Hyaluronic acid-based 3D culture model for in vitro testing of electrode biocompatibility," *Biomacromolecules*, 2014, doi: 10.1021/bm500318d.

[172] I. Smith *et al.*, "Neuronal-glial populations form functional networks in a biocompatible 3D scaffold," *Neurosci. Lett.*, 2015, doi: 10.1016/j.neulet.2015.10.044.

[173] D. N. Rocha, J. P. Ferraz-Nogueira, C. C. Barrias, J. B. Relvas, and A. P. Pêgo, "Extracellular environment contribution to astrogliosis—lessons learned from a tissue engineered 3D model of the glial scar," *Front. Cell. Neurosci.*, 2015, doi: 10.3389/fncel.2015.00377.

[174] K. C. Spencer, J. C. Sy, R. Falcón-Banchs, and M. J. Cima, "A three dimensional in vitro glial scar model to investigate the local strain effects from micromotion around neural implants," *Lab Chip*, 2017, doi: 10.1039/c6lc01411a.

[175] K. M. Koss, M. A. Churchward, A. F. Jeffery, V. K. Mushahwar, A. L. Elias, and K. G. Todd, "Improved 3D hydrogel cultures of primary glial cells for in vitro modelling of neuroinflammation," *J. Vis. Exp.*, 2017, doi: 10.3791/56615.

[176] C. O'Rourke, C. Lee-Reeves, R. A. L. Drake, G. W. W. Cameron, A. J. Loughlin, and J. B. Phillips, "Adapting tissue-engineered in vitro CNS models for high-throughput study of neurodegeneration," *J. Tissue Eng.*, 2017, doi: 10.1177/2041731417697920.

[177] B. W. Kristensen, J. Noraberg, P. Thiébaud, M. Koudelka-Hep, and J. Zimmer, "Biocompatibility of silicon-based arrays of electrodes coupled to organotypic hippocampal brain slice cultures," *Brain Res.*, 2001, doi: 10.1016/S0006-8993(00)03304-7.

[178] E. S. Ereifej, M. M. C. Cheng, G. Mao, and P. J. VandeVord, "Examining the inflammatory response to nanopatterned polydimethylsiloxane using organotypic brain slice methods," *J. Neurosci. Methods*, 2013, doi: 10.1016/j.jneumeth.2013.04.023.

[179] S. Usmani *et al.*, "3D meshes of carbon nanotubes guide functional reconnection of segregated spinal explants," *Sci. Adv.*, 2016, doi: 10.1126/sciadv.1600087.

[180] E. Leclerc, J. L. Duval, C. Egles, S. Ihida, H. Toshiyoshi, and A. Tixier-Mita, "In vitro cyto-biocompatibility study of thin-film transistors substrates using an organotypic culture method," *J. Mater. Sci. Mater. Med.*, 2017, doi: 10.1007/s10856-016-5815-1.

[181] E. Gabriel and J. Gopalakrishnan, "Generation of ipsc-derived human brain organoids to model early neurodevelopmental disorders," *J. Vis. Exp.*, 2017, doi: 10.3791/55372.

[182] B. Nasr *et al.*, "Self-organized nanostructure modified microelectrode for sensitive electrochemical glutamate detection in stem cells-derived brain organoids," *Biosensors*, 2018, doi: 10.3390/bios8010014.

[183] G. Nzou *et al.*, "Human cortex spheroid with a functional blood brain barrier for high-throughput neurotoxicity screening and disease modeling," *Sci. Rep.*, 2018, doi: 10.1038/s41598-018-25603-5.

[184] N. R. Wevers *et al.*, "High-throughput compound evaluation on 3D networks of neurons and glia in a microfluidic platform," *Sci. Rep.*, 2016, doi: 10.1038/srep38856.

[185] Y. Li *et al.*, "RNAi-mediated ephrin-B2 silencing attenuates astroglial-fibrotic scar formation and improves spinal cord axon growth," *CNS Neurosci. Ther.*, 2017, doi: 10.1111/cns.12723.

[186] F. Yin, Y. Zhu, Y. Wang, and J. Qin, "Engineering Brain Organoids to Probe Impaired Neurogenesis Induced by Cadmium," *ACS Biomater. Sci. Eng.*, 2018, doi: 10.1021/acsbiomaterials.8b00160.

[187] A. Saryyeva, M. Nakamura, J. K. Krauss, and K. Schwabe, "C-Fos expression after deep brain stimulation of the pedunculopontine tegmental nucleus in the rat 6-hydroxydopamine Parkinson model," *J. Chem. Neuroanat.*, 2011, doi: 10.1016/j.jchemneu.2011.08.003.

[188] K. Badstuebner, U. Gimsa, I. Weber, A. Tuchscherer, and J. Gimsa, "Deep Brain Stimulation of Hemiparkinsonian Rats with Unipolar and Bipolar Electrodes for up to 6 Weeks: Behavioral Testing of Freely Moving Animals," *Parkinsons. Dis.*, 2017, doi: 10.1155/2017/5693589.

[189] J. F. Maya-Vetencourt *et al.*, "A fully organic retinal prosthesis restores vision in a rat model of degenerative blindness," *Nat. Mater.*, 2017, doi: 10.1038/nmat4874.

[190] E. S. Ferreira *et al.*, "Long-Term Effects of Anterior Thalamic Nucleus Deep Brain Stimulation on Spatial Learning in the Pilocarpine Model of Temporal Lobe Epilepsy," *Neuromodulation*, 2018, doi: 10.1111/ner.12688.

[191] J. M. Karp, P. D. Dalton, and M. S. Shoichet, "Scaffolds for Tissue Engineering," *MRS*

Bull., vol. 28, no. 04, pp. 301–306, 2003, doi: 10.1557/mrs2003.85.

[192] C. Frantz, K. M. Stewart, and V. M. Weaver, "The extracellular matrix at a glance," *Journal of Cell Science*. 2010, doi: 10.1242/jcs.023820.

[193] G. Chen, T. Ushida, and T. Tateishi, "Scaffold design for tissue engineering," *Macromolecular Bioscience*, vol. 2, no. 2. pp. 67–77, 2002, doi: 10.1002/1616-5195(20020201)2:2<67::AID-MABI67>3.0.CO;2-F.

[194] S. Stratton, N. B. Shelke, K. Hoshino, S. Rudraiah, and S. G. Kumbar, "Bioactive polymeric scaffolds for tissue engineering," *Bioactive Materials*. 2016, doi: 10.1016/j.bioactmat.2016.11.001.

[195] B. D. Ulery, L. S. Nair, and C. T. Laurencin, "Biomedical applications of biodegradable polymers," *Journal of Polymer Science, Part B: Polymer Physics*. 2011, doi: 10.1002/polb.22259.

[196] A. Eltom, G. Zhong, and A. Muhammad, "Scaffold Techniques and Designs in Tissue Engineering Functions and Purposes: A Review," *Advances in Materials Science and Engineering*. 2019, doi: 10.1155/2019/3429527.

[197] S. J. Hollister, "Porous scaffold design for tissue engineering," *Nature Materials*. 2005, doi: 10.1038/nmat1421.

[198] S. Yang, K. F. Leong, Z. Du, and C. K. Chua, "The design of scaffolds for use in tissue engineering. Part I. Traditional factors," *Tissue Engineering*. 2001, doi: 10.1089/107632701753337645.

[199] L. Liverani, V. Guarino, V. La Carrubba, and A. R. Boccaccini, "Porous biomaterials and scaffolds for tissue engineering," in *Encyclopedia of Biomedical Engineering*, 2018.

[200] E. Sachlos, J. T. Czernuszka, S. Gogolewski, and M. Dalby, "Making tissue engineering scaffolds work. Review on the application ofsolid freeform fabrication technology to the production of tissue engineeringscaffolds," *European Cells and Materials*. 2003, doi: 10.22203/ecm.v005a03.

[201] E. S. Place, J. H. George, C. K. Williams, and M. M. Stevens, "Synthetic polymer scaffolds for tissue engineering," *Chem. Soc. Rev.*, 2009, doi: 10.1039/b811392k.

[202] M. R. Singh, S. Patel, and D. Singh, "Natural polymer-based hydrogels as scaffolds for tissue engineering," in *Nanobiomaterials in Soft Tissue Engineering: Applications of Nanobiomaterials*, 2016.

[203] K. Y. Lee and D. J. Mooney, "Alginate: Properties and biomedical applications,"

Progress in Polymer Science (Oxford). 2012, doi: 10.1016/j.progpolymsci.2011.06.003.

[204] H. Onoe *et al.*, "Metre-long cell-laden microfibres exhibit tissue morphologies and functions," *Nat. Mater.*, 2013, doi: 10.1038/nmat3606.

[205] T. J. Hinton *et al.*, "Three-dimensional printing of complex biological structures by freeform reversible embedding of suspended hydrogels," *Sci. Adv.*, 2015, doi: 10.1126/sciadv.1500758.

[206] A. W. Justin, R. A. Brooks, and A. E. Markaki, "Multi-casting approach for vascular networks in cellularized hydrogels," *J. R. Soc. Interface*, 2016, doi: 10.1098/rsif.2016.0768.

[207] S. Sämfors, K. Karlsson, J. Sundberg, K. Markstedt, and P. Gatenholm, "Biofabrication of bacterial nanocellulose scaffolds with complex vascular structure," *Biofabrication*, 2019, doi: 10.1088/1758-5090/ab2b4f.

[208] K. Akeda *et al.*, "Three-dimensional alginate spheroid culture system of murine osteosarcoma," *Oncol. Rep.*, 2009, doi: 10.3892/or_00000527.

[209] G. A. Salg *et al.*, "The emerging field of pancreatic tissue engineering: A systematic review and evidence map of scaffold materials and scaffolding techniques for insulin-secreting cells," *Journal of Tissue Engineering*. 2019, doi: 10.1177/2041731419884708.

[210] B. Bugarski, Q. Li, M. F. A. Goosen, D. Poncelet, R. J. Neufeld, and G. Vunjak, "Electrostatic droplet generation: Mechanism of polymer droplet formation," *AIChE J.*, 1994, doi: 10.1002/aic.690400613.

[211] M. Shachar, O. Tsur-Gang, T. Dvir, J. Leor, and S. Cohen, "The effect of immobilized RGD peptide in alginate scaffolds on cardiac tissue engineering," *Acta Biomater.*, 2011, doi: 10.1016/j.actbio.2010.07.034.

[212] S. C. N. Chang *et al.*, "Injection molding of chondrocyte/alginate constructs in the shape of facial implants," *J. Biomed. Mater. Res.*, 2001, doi: 10.1002/1097-4636(20010615)55:4<503::AID-JBM1043>3.0.CO;2-S.

[213] A. M. Gharravi, M. Orazizadeh, K. Ansari-Asl, S. Banoni, S. Izadi, and M. Hashemitabar, "Design and fabrication of anatomical bioreactor systems containing alginate scaffolds for cartilage tissue engineering," *Avicenna J. Med. Biotechnol.*, 2012.

[214] K. L. Spiller, S. A. Maher, and A. M. Lowman, "Hydrogels for the repair of articular

cartilage defects," *Tissue Eng. - Part B Rev.*, 2011, doi: 10.1089/ten.teb.2011.0077.

[215] E. Alsberg, K. W. Anderson, A. Albeiruti, R. T. Franceschi, and D. J. Mooney, "Cell-interactive alginate hydrogels for bone tissue engineering," *J. Dent. Res.*, 2001, doi: 10.1177/00220345010800111501.

[216] E. Alsberg, K. W. Anderson, A. Albeiruti, J. A. Rowley, and D. J. Mooney, "Engineering growing tissues," *Proc. Natl. Acad. Sci. U. S. A.*, 2002, doi: 10.1073/pnas.192291499.

[217] K. Y. Lee, E. Alsberg, and D. J. Mooney, "Degradable and injectable poly(aldehyde guluronate) hydrogels for bone tissue engineering," *J. Biomed. Mater. Res.*, 2001, doi: 10.1002/1097-4636(200108)56:2<228::AID-JBM1089>3.0.CO;2-9.

[218] H. R. Lin and Y. J. Yen, "Porous alginate/hydroxyapatite composite scaffolds for bone tissue engineering: Preparation, characterization, and in vitro studies," *J. Biomed. Mater. Res. - Part B Appl. Biomater.*, 2004, doi: 10.1002/jbm.b.30065.

[219] K. Suzuki *et al.*, "Reconstruction of rat peripheral nerve gap without sutures using freeze- dried alginate gel," *J. Biomed. Mater. Res.*, 2000, doi: 10.1002/(SICI)1097-4636(20000315)49:4<528::AID-JBM11>3.0.CO;2-1.

[220] P. Prang *et al.*, "The promotion of oriented axonal regrowth in the injured spinal cord by alginate-based anisotropic capillary hydrogels," *Biomaterials*, 2006, doi: 10.1016/j.biomaterials.2006.01.053.

[221] T. Hashimoto, Y. Suzuki, K. Suzuki, T. Nakashima, M. Tanihara, and C. Ide, "Peripheral nerve regeneration using non-tubular alginate gel crosslinked with covalent bonds," 2005, doi: 10.1007/s10856-005-0524-1.

[222] Y. Khotimchenko and M. Khotimchenko, "Healing and Preventive Effects of Calcium Alginate on Carbon Tetrachloride Induced Liver Injury in Rats," *Mar. Drugs*, 2004, doi: 10.3390/md203108.

[223] M. Dvir-Ginzberg, I. Gamlieli-Bonshtein, R. Agbaria, and S. Cohen, "Liver tissue engineering within alginate scaffolds: Effects of cell-seeding density on hepatocyte viability, morphology, and function," *Tissue Eng.*, 2003, doi: 10.1089/107632703768247430.

[224] S. Zmora, R. Glicklis, and S. Cohen, "Tailoring the pore architecture in 3-D alginate scaffolds by controlling the freezing regime during fabrication," *Biomaterials*, 2002, doi: 10.1016/S0142-9612(02)00146-1.

[225] R. Glicklis, L. Shapiro, R. Agbaria, J. C. Merchuk, and S. Cohen, "Hepatocyte

behavior within three-dimensional porous alginate scaffolds," *Biotechnol. Bioeng.*, 2000, doi: 10.1002/(SICI)1097-0290(20000205)67:3<344::AID-BIT11>3.0.CO;2-2.

[226] M. Xu, P. K. Kreeger, L. D. Shea, and T. K. Woodruff, "Tissue-engineered follicles produce live, fertile offspring," *Tissue Eng.*, 2006, doi: 10.1089/ten.2006.12.2739.

[227] P. K. Kreeger, J. W. Deck, T. K. Woodruff, and L. D. Shea, "The in vitro regulation of ovarian follicle development using alginate-extracellular matrix gels," *Biomaterials*, 2006, doi: 10.1016/j.biomaterials.2005.06.016.

[228] M. Heise, R. Koepsel, A. J. Russell, and E. A. McGee, "Calcium alginate microencapsulation of ovarian follicles impacts FSH delivery and follicle morphology," *Reprod. Biol. Endocrinol.*, 2005, doi: 10.1186/1477-7827-3-47.

[229] T. Andersen, B. L. Strand, K. Formo, E. Alsberg, and B. E. Christensen, "Chapter 9. Alginates as biomaterials in tissue engineering," *Carbohydr. Chem*, vol. 37, pp. 227–258, 2012, doi: 10.1039/9781849732765-00227.

[230] E. K. Purcell, D. Ph, A. Singh, B. Tech, and D. R. Kipke, "Alginate composition effects on a neural stem cell-seeded scaffold.," *Tissue Eng. Part C. Methods*, vol. 15, no. 4, pp. 541–50, 2009, doi: 10.1089/ten.tec.2008.0302.

[231] B. Eftekharzadeh, F. Khodagholi, A. Abdi, and N. Maghsoudi, "Alginate protects NT2 neurons against H2O2-induced neurotoxicity," *Carbohydr. Polym.*, 2010, doi: 10.1016/j.carbpol.2009.10.040.

[232] J. P. Frampton, M. R. Hynd, M. L. Shuler, and W. Shain, "Fabrication and optimization of alginate hydrogel constructs for use in 3D neural cell culture," *Biomed. Mater.*, vol. 6, no. 1, 2011, doi: 10.1088/1748-6041/6/1/015002.

[233] M. Matyash, F. Despang, R. Mandal, D. Fiore, M. Gelinsky, and C. Ikonomidou, "Novel Soft Alginate Hydrogel Strongly Supports Neurite Growth and Protects Neurons Against Oxidative Stress," *Tissue Eng. Part A*, vol. 18, no. 1–2, pp. 55–66, 2012, doi: 10.1089/ten.tea.2011.0097.

[234] X. Li *et al.*, "Culture of neural stem cells in calcium alginate beads," *Biotechnol. Prog.*, 2006, doi: 10.1021/bp060185z.

[235] M. Gajendiran *et al.*, "Conductive biomaterials for tissue engineering applications," *J. Ind. Eng. Chem.*, vol. 51, pp. 12–26, 2017, doi: 10.1016/j.jiec.2017.02.031.

[236] M. Li, Y. Guo, Y. Wei, A. G. MacDiarmid, and P. I. Lelkes, "Electrospinning polyaniline-contained gelatin nanofibers for tissue engineering applications," *Biomaterials*, 2006, doi: 10.1016/j.biomaterials.2005.11.037.

[237] B. Garner, A. Georgevich, A. J. Hodgson, L. Liu, and G. G. Wallace, “Polypyrrole-heparin composites as stimulus-responsive substrates for endothelial cell growth,” *J. Biomed. Mater. Res.*, 1999, doi: 10.1002/(SICI)1097-4636(199902)44:2<121::AID-JBM1>3.0.CO;2-A.

[238] R. Ravichandran, S. Sundarrajan, J. R. Venugopal, S. Mukherjee, and S. Ramakrishna, “Applications of conducting polymers and their issues in biomedical engineering,” *Journal of the Royal Society Interface*. 2010, doi: 10.1098/rsif.2010.0120.focus.

[239] B. C. Thompson *et al.*, “Conducting polymers, dual neurotrophins and pulsed electrical stimulation - Dramatic effects on neurite outgrowth,” *J. Control. Release*, 2010, doi: 10.1016/j.jconrel.2009.09.016.

[240] J. E. Collazos-Castro, J. L. Polo, G. R. Hernández-Labrado, V. Padial-Cañete, and C. García-Rama, “Bioelectrochemical control of neural cell development on conducting polymers,” *Biomaterials*, vol. 31, no. 35, pp. 9244–9255, 2010, doi: 10.1016/j.biomaterials.2010.08.057.

[241] Y. Furukawa, A. Shimada, K. Kato, H. Iwata, and K. Torimitsu, “Monitoring neural stem cell differentiation using PEDOT-PSS based MEA,” *Biochim. Biophys. Acta - Gen. Subj.*, vol. 1830, no. 9, pp. 4329–4333, 2013, doi: 10.1016/j.bbagen.2013.01.022.

[242] G. Cellot *et al.*, “PEDOT:PSS interfaces support the development of neuronal synaptic networks with reduced neuroglia response in vitro,” *Front. Neurosci.*, vol. 9, no. JAN, 2016, doi: 10.3389/fnins.2015.00521.

[243] L. H. Jimison *et al.*, “PEDOT:TOS with PEG: a biofunctional surface with improved electronic characteristics,” *J. Mater. Chem.*, vol. 22, no. 37, p. 19498, 2012, doi: 10.1039/c2jm32188b.

[244] F. Pires, Q. Ferreira, C. A. V. Rodrigues, J. Morgado, and F. C. Ferreira, “Neural stem cell differentiation by electrical stimulation using a cross-linked PEDOT substrate: Expanding the use of biocompatible conjugated conductive polymers for neural tissue engineering,” *Biochim. Biophys. Acta - Gen. Subj.*, vol. 1850, no. 6, pp. 1158–1168, 2015, doi: 10.1016/j.bbagen.2015.01.020.

[245] N. Alegret *et al.*, “Three-Dimensional Conductive Scaffolds as Neural Prostheses Based on Carbon Nanotubes and Polypyrrole,” *ACS Appl. Mater. Interfaces*, 2018, doi: 10.1021/acsami.8b16462.

[246] A. M. D. Wan *et al.*, “3D conducting polymer platforms for electrical control of protein conformation and cellular functions,” *J. Mater. Chem. B*, 2015, doi:

10.1039/c5tb00390c.

[247] C. Tarducci, E. J. Kinmond, J. P. S. Badyal, S. A. Brewer, and C. Willis, “Epoxide-Functionalized Solid Surfaces,” *Chem. Mater.*, vol. 12, no. 7, pp. 1884–1889, Jul. 2000, doi: 10.1021/cm0000954.

[248] Y. Nam, D. W. Branch, and B. C. Wheeler, “Epoxy-silane linking of biomolecules is simple and effective for patterning neuronal cultures,” *Biosens. Bioelectron.*, vol. 22, no. 5, pp. 589–597, Dec. 2006, doi: 10.1016/j.bios.2006.01.027.

[249] J. I. Valenzuela and F. Perez, “Diversifying the secretory routes in neurons,” *Front. Neurosci.*, vol. 9, Oct. 2015, doi: 10.3389/fnins.2015.00358.

[250] J. Wang, L. Tian, N. Chen, S. Ramakrishna, and X. Mo, “The cellular response of nerve cells on poly-L-lysine coated PLGA-MWCNTs aligned nanofibers under electrical stimulation,” *Mater. Sci. Eng. C*, 2018, doi: 10.1016/j.msec.2018.06.025.

[251] R. Mooney *et al.*, “Control of neural cell composition in poly(ethylene glycol) hydrogel culture with soluble factors,” *Tissue Eng. - Part A*, 2011, doi: 10.1089/ten.tea.2010.0654.

[252] L. M. Y. Yu, N. D. Leipzig, and M. S. Shoichet, “Promoting neuron adhesion and growth,” *Materials Today*. 2008, doi: 10.1016/S1369-7021(08)70088-9.

[253] S. T. Bendtsen, S. P. Quinnell, and M. Wei, “Development of a novel alginate-polyvinyl alcohol-hydroxyapatite hydrogel for 3D bioprinting bone tissue engineered scaffolds,” *J. Biomed. Mater. Res. - Part A*, 2017, doi: 10.1002/jbm.a.36036.

[254] S. H. Cho, S. H. Oh, and J. H. Lee, “Fabrication and characterization of porous alginate/polyvinyl alcohol hybrid scaffolds for 3D cell culture,” *J. Biomater. Sci. Polym. Ed.*, 2005, doi: 10.1163/1568562054414658.

[255] M. Rusdi, Y. Moroi, H. Nakahara, and O. Shibata, “Evaporation from water-ethylene glycol liquid mixture,” *Langmuir*, 2005, doi: 10.1021/la040134g.

[256] W. Shen and Y. Lo Hsieh, “Biocompatible sodium alginate fibers by aqueous processing and physical crosslinking,” *Carbohydr. Polym.*, vol. 102, no. 1, pp. 893–900, 2014, doi: 10.1016/j.carbpol.2013.10.066.

[257] J. Cashman, “Routes of administration,” in *Clinical Pain Management Second Edition: Acute Pain, 2nd Edition*, 2008.

[258] T. Kerz, G. Paret, and H. Herff, “Routes of drug administration,” in *Cardiac Arrest: The Science and Practice of Resuscitation Medicine*, 2007.

[259] K. K. Jain, “Drug delivery systems - An overview,” *Methods Mol. Biol.*, 2008, doi:

10.1007/978-1-59745-210-6_1.

[260] M. F. Attia, N. Anton, J. Wallyn, Z. Omran, and T. F. Vandamme, “An overview of active and passive targeting strategies to improve the nanocarriers efficiency to tumour sites,” *Journal of Pharmacy and Pharmacology*. 2019, doi: 10.1111/jphp.13098.

[261] S. Maiti and K. K. Sen, “Introductory Chapter: Drug Delivery Concepts,” in *Advanced Technology for Delivering Therapeutics*, 2017.

[262] J. Wadhwa, A. Nair, and R. Kumria, “Emulsion forming drug delivery system for lipophilic drugs,” *Acta Poloniae Pharmaceutica - Drug Research*. 2012.

[263] A. Akbarzadeh *et al.*, “Liposome: Classification, preparation, and applications,” *Nanoscale Res. Lett.*, 2013, doi: 10.1186/1556-276X-8-102.

[264] L. Sercombe, T. Veerati, F. Moheimani, S. Y. Wu, A. K. Sood, and S. Hua, “Advances and challenges of liposome assisted drug delivery,” *Frontiers in Pharmacology*. 2015, doi: 10.3389/fphar.2015.00286.

[265] S. A. A. Rizvi and A. M. Saleh, “Applications of nanoparticle systems in drug delivery technology,” *Saudi Pharmaceutical Journal*. 2018, doi: 10.1016/j.jsps.2017.10.012.

[266] K. K. Kim and D. W. Pack, “Microspheres for Drug Delivery,” in *BioMEMS and Biomedical Nanotechnology*, 2006.

[267] I. K. Kwon, S. C. Lee, B. Han, and K. Park, “Analysis on the current status of targeted drug delivery to tumors,” *J. Control. Release*, 2012, doi: 10.1016/j.jconrel.2012.07.010.

[268] J. K. Mills and D. Needham, “Targeted drug delivery,” *Expert Opinion on Therapeutic Patents*. 1999, doi: 10.1517/13543776.9.11.1499.

[269] E. M. Ahmed, “Hydrogel: Preparation, characterization, and applications: A review,” *Journal of Advanced Research*, vol. 6, no. 2. 2015, doi: 10.1016/j.jare.2013.07.006.

[270] L. H. Fu, C. Qi, M. G. Ma, and P. Wan, “Multifunctional cellulose-based hydrogels for biomedical applications,” *Journal of Materials Chemistry B*. 2019, doi: 10.1039/c8tb02331j.

[271] T. R. Hoare and D. S. Kohane, “Hydrogels in drug delivery: Progress and challenges,” *Polymer*. 2008, doi: 10.1016/j.polymer.2008.01.027.

[272] W. S. Wan Ngah, L. C. Teong, and M. A. K. M. Hanafiah, “Adsorption of dyes and heavy metal ions by chitosan composites: A review,” *Carbohydrate Polymers*. 2011, doi: 10.1016/j.carbpol.2010.11.004.

[273] I. M. El-Sherbiny and M. H. Yacoub, “Hydrogel scaffolds for tissue engineering:

Progress and challenges," *Glob. Cardiol. Sci. Pract.*, 2013, doi: 10.5339/gcsp.2013.38.

[274] P. C. Nicolson and J. Vogt, "Soft contact lens polymers: An evolution," *Biomaterials*, 2001, doi: 10.1016/S0142-9612(01)00165-X.

[275] Y. Qiu and K. Park, "Environment-sensitive hydrogels for drug delivery," *Advanced Drug Delivery Reviews*. 2012, doi: 10.1016/j.addr.2012.09.024.

[276] J. Tavakoli and Y. Tang, "Hydrogel based sensors for biomedical applications: An updated review," *Polymers*. 2017, doi: 10.3390/polym9080364.

[277] D. Macaya and M. Spector, "Injectable hydrogel materials for spinal cord regeneration: A review," *Biomedical Materials*. 2012, doi: 10.1088/1748-6041/7/1/012001.

[278] M. Hamidi, A. Azadi, and P. Rafiei, "Hydrogel nanoparticles in drug delivery," *Advanced Drug Delivery Reviews*, vol. 60, no. 15. pp. 1638–1649, 2008, doi: 10.1016/j.addr.2008.08.002.

[279] S. J. Buwalda, K. W. M. Boere, P. J. Dijkstra, J. Feijen, T. Vermonden, and W. E. Hennink, "Hydrogels in a historical perspective: From simple networks to smart materials," *Journal of Controlled Release*. 2014, doi: 10.1016/j.jconrel.2014.03.052.

[280] L. Polo Fonseca, R. Bergamo Trinca, and M. Isabel Felisberti, "Thermo-responsive polyurethane hydrogels based on poly(ethylene glycol) and poly(caprolactone): Physico-chemical and mechanical properties," *J. Appl. Polym. Sci.*, 2016, doi: 10.1002/app.43573.

[281] J. J. Pillai, A. K. T. Thulasidasan, R. J. Anto, D. N. Chithralekha, A. Narayanan, and G. S. V. Kumar, "Folic acid conjugated cross-linked acrylic polymer (FA-CLAP) hydrogel for site specific delivery of hydrophobic drugs to cancer cells," *J. Nanobiotechnology*, 2014, doi: 10.1186/1477-3155-12-25.

[282] C. Sandolo, T. Coviello, P. Matricardi, and F. Alhaique, "Characterization of polysaccharide hydrogels for modified drug delivery," 2007, doi: 10.1007/s00249-007-0158-y.

[283] J. Ong, J. Zhao, A. W. Justin, and A. E. Markaki, "Albumin-based hydrogels for regenerative engineering and cell transplantation," *Biotechnology and Bioengineering*. 2019, doi: 10.1002/bit.27167.

[284] I. Schnitzler, C. Hausen, and C. Klein, "Hydrogel for natural cosmetic purposes," 2012.

[285] H. Zhu, Q. Zhang, and S. Zhu, "Alginate Hydrogel: A Shapeable and Versatile

Platform for in Situ Preparation of Metal-Organic Framework-Polymer Composites," *ACS Appl. Mater. Interfaces*, vol. 8, no. 27, pp. 17395–17401, 2016, doi: 10.1021/acsami.6b04505.

[286] S. K. Tam, J. Dusseault, S. Bilodeau, G. Langlois, J. P. Hallé, and L. Yahia, "Factors influencing alginate gel biocompatibility," *J. Biomed. Mater. Res. - Part A*, 2011, doi: 10.1002/jbm.a.33047.

[287] C. H. Goh, P. W. S. Heng, and L. W. Chan, "Alginates as a useful natural polymer for microencapsulation and therapeutic applications," *Carbohydrate Polymers*, vol. 88, no. 1. pp. 1–12, 2012, doi: 10.1016/j.carbpol.2011.11.012.

[288] K. Y. Lee, J. A. Rowley, P. Eiselt, E. M. Moy, K. H. Bouhadir, and D. J. Mooney, "Controlling mechanical and swelling properties of alginate hydrogels independently by cross-linker type and cross-linking density," *Macromolecules*, vol. 33, no. 11, pp. 4291–4294, 2000, doi: 10.1021/ma9921347.

[289] W. P. Voo, C. W. Ooi, A. Islam, B. T. Tey, and E. S. Chan, "Calcium alginate hydrogel beads with high stiffness and extended dissolution behaviour," *Eur. Polym. J.*, 2016, doi: 10.1016/j.eurpolymj.2015.12.029.

[290] J. Lee and K. Y. Lee, "Injectable microsphere/hydrogel combination systems for localized protein delivery," *Macromol. Biosci.*, 2009, doi: 10.1002/mabi.200800317.

[291] W. Liu, M. Griffith, and F. Li, "Alginate microsphere-collagen composite hydrogel for ocular drug delivery and implantation," *J. Mater. Sci. Mater. Med.*, 2008, doi: 10.1007/s10856-008-3486-2.

[292] C. Bitter, K. Suter-Zimmermann, and C. Surber, "Nasal drug delivery in humans," *Curr. Probl. Dermatol.*, 2011, doi: 10.1159/000321044.

[293] S. Wichchukit, M. H. Oztop, M. J. McCarthy, and K. L. McCarthy, "Whey protein/alginate beads as carriers of a bioactive component," *Food Hydrocoll.*, 2013, doi: 10.1016/j.foodhyd.2013.02.013.

[294] J. L. Romalde, A. Luzardo-Alvárez, C. Ravelo, A. E. Toranzo, and J. Blanco-Méndez, "Oral immunization using alginate microparticles as a useful strategy for booster vaccination against fish lactoccocosis," *Aquaculture*, 2004, doi: 10.1016/j.aquaculture.2004.02.028.

[295] W. O. Rohof, R. J. Bennink, A. J. P. M. Smout, E. Thomas, and G. E. Boeckxstaens, "An alginate-antacid formulation localizes to the acid pocket to reduce acid reflux in patients with gastroesophageal reflux disease," *Clin. Gastroenterol. Hepatol.*, 2013,

doi: 10.1016/j.cgh.2013.04.046.

[296] L. B. de Paiva, A. R. Morales, and F. R. Valenzuela Díaz, “Organoclays: Properties, preparation and applications,” *Applied Clay Science*, vol. 42, no. 1–2. pp. 8–24, 2008, doi: 10.1016/j.clay.2008.02.006.

[297] J. L. Vickery, S. Thachepan, A. J. Patil, and S. Mann, “Immobilisation and encapsulation of functional protein-inorganic constructs.,” *Mol. Biosyst.*, vol. 5, no. 7, pp. 744–749, 2009, doi: 10.1039/b903652k.

[298] S. S. Bhattacharya and M. Aadhar, “Studies on Preparation and analysis of Organoclay Nano Particles,” *Res. J. Eng. Sci.*, vol. 3, no. 3, pp. 10–16, 2014.

[299] A. J. Patil, E. Muthusamy, and S. Mann, “Synthesis and self-assembly of organoclay-wrapped biomolecules,” *Angew. Chemie - Int. Ed.*, vol. 43, no. 37, pp. 4928–4933, 2004, doi: 10.1002/anie.200453868.

[300] A. J. Patil and S. Mann, “Self-assembly of bio–inorganic nanohybrids using organoclay building blocks,” *J. Mater. Chem.*, vol. 18, no. 39, p. 4605, 2008, doi: 10.1039/b805653f.

[301] A. J. Patil and S. Mann, “Bio-inorganic Nanohybrids Based on Organoclay Self-assembly,” in *Bio-inorganic Hybrid Nanomaterials: Strategies, Syntheses, Characterization and Applications*, 2008, pp. 239–270.

[302] A. J. Patil, M. Li, and S. Mann, “Integrative self-assembly of functional hybrid nanoconstructs by inorganic wrapping of single biomolecules, biomolecule arrays and organic supramolecular assemblies,” *Nanoscale*, vol. 5, no. 16, p. 7161, 2013, doi: 10.1039/c3nr02796a.

[303] J. E. Martin, A. J. Patil, M. F. Butler, and S. Mann, “Guest-molecule-directed assembly of mesostructured nanocomposite polymer/organoclay hydrogels,” *Adv. Funct. Mater.*, vol. 21, no. 4, pp. 674–681, 2011, doi: 10.1002/adfm.201002138.

[304] S. C. Holmström, A. J. Patil, M. Butler, and S. Mann, “Influence of polymer co-intercalation on guest release from aminopropyl-functionalized magnesium phyllosilicate mesolamellar nanocomposites,” *J. Mater. Chem.*, vol. 17, no. 37, p. 3894, 2007, doi: 10.1039/b705158a.

[305] R. Surya, M. D. Mullassery, N. B. Fernandez, and D. Thomas, “Synthesis and characterization of a clay-alginate nanocomposite for the controlled release of 5-Flurouracil,” *J. Sci. Adv. Mater. Devices*, 2019, doi: 10.1016/j.jsamd.2019.08.001.

[306] S. H. Lim, “Biomaterials strategies for neural regeneration: The impact of surface

topography and biofunctional cues," 2010.

[307] T. M. O'Shea, A. L. Wollenberg, A. M. Bernstein, D. B. Sarte, T. J. Deming, and M. V. Sofroniew, "Smart Materials for Central Nervous System Cell Delivery and Tissue Engineering," in *RSC Smart Materials*, 2017.

[308] J. He, X.-M. Wang, M. Spector, and F.-Z. Cui, "Scaffolds for central nervous system tissue engineering," *Front. Mater. Sci.*, vol. 6, no. 1, pp. 1–25, 2012, doi: 10.1007/s11706-012-0157-5.

[309] A. Jakobsson, M. Ottosson, M. C. Zalis, D. O'Carroll, U. E. Johansson, and F. Johansson, "Three-dimensional functional human neuronal networks in uncompressed low-density electrospun fiber scaffolds," *Nanomedicine Nanotechnology, Biol. Med.*, 2017, doi: 10.1016/j.nano.2016.12.023.

[310] B. Arica *et al.*, "In vitro and in vivo studies of ibuprofen-loaded biodegradable alginate beads," *J. Microencapsul.*, vol. 22, no. 2, pp. 153–165, Mar. 2005, doi: 10.1080/02652040400026319.

[311] ASTM International, "D792 − 13: Standard Test Methods for Density and Specific Gravity (Relative Density) of Plastics by Displacement," in *ASTM Book of Standards*, 2013.

[312] Y. Liu, A. Keikhosravi, G. S. Mehta, C. R. Drifka, and K. W. Eliceiri, "Methods for quantifying fibrillar collagen alignment," in *Methods in Molecular Biology*, 2017.

[313] H. Zielke, M. Abendroth, and M. Kuna, "Determining fracture mechanical properties for brittle materials using the ball on three balls test combined with numerical simulations," *Theor. Appl. Fract. Mech.*, 2016, doi: 10.1016/j.tafmec.2016.09.001.

[314] A. González-Cortés, "Electrochemical Impedance Spectroscopy," in *Agricultural and Food Electroanalysis*, 2015.

[315] H. B. Chen, Y. Z. Wang, M. Sánchez-Soto, and D. A. Schiraldi, "Low flammability, foam-like materials based on ammonium alginate and sodium montmorillonite clay," *Polymer (Guildf).*, 2012, doi: 10.1016/j.polymer.2012.10.029.

[316] K. Sing, "The use of nitrogen adsorption for the characterisation of porous materials," 2001, doi: 10.1016/S0927-7757(01)00612-4.

Appendix

The fluorescence images were used to determine the numbers of neurons demonstrating outgrowth on films and coverslips. The combination of alginate with conductive polymer films show the variability of neuron attachment, however, most of them were still less attached when compared to the control coverslips which Figure 4.6 shown the neurons populations on films with different concentration of $CaCl_2$

7days

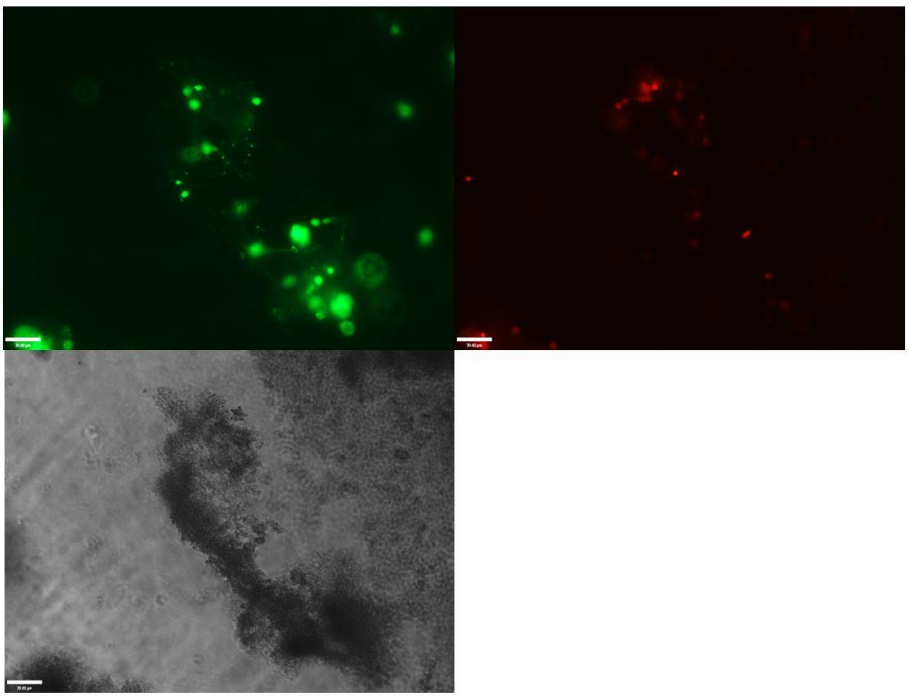

2 mM $CaCl_2$

14days

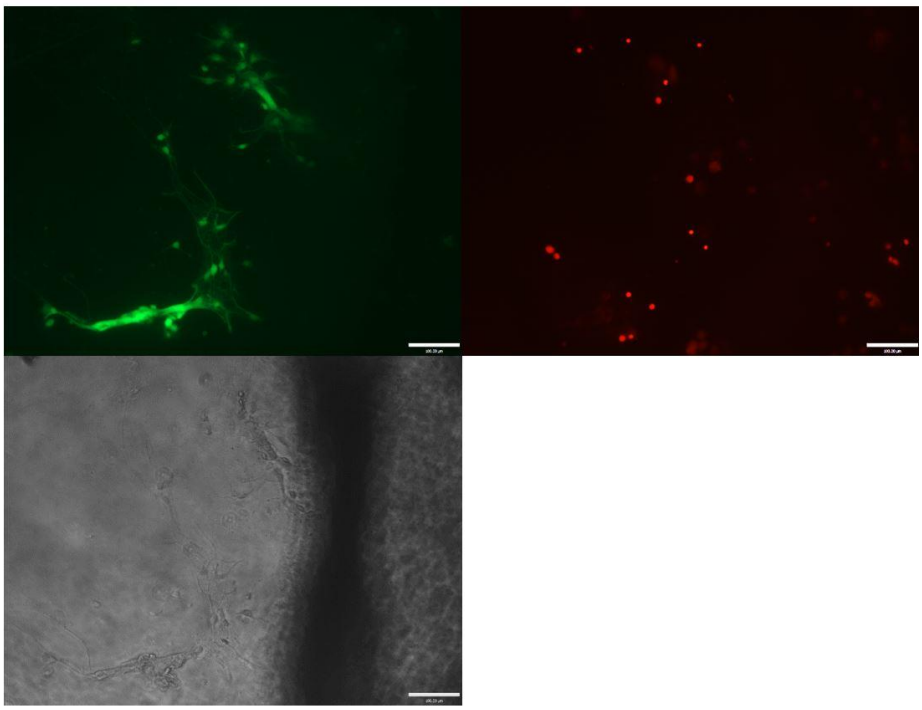

7days

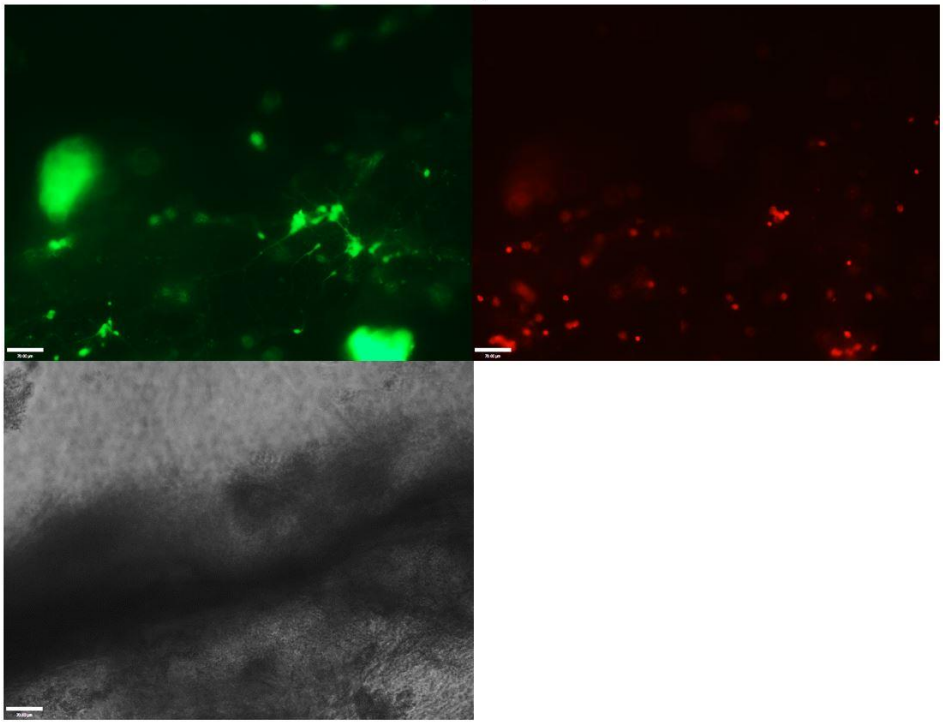

5 mM $CaCl_2$

14days

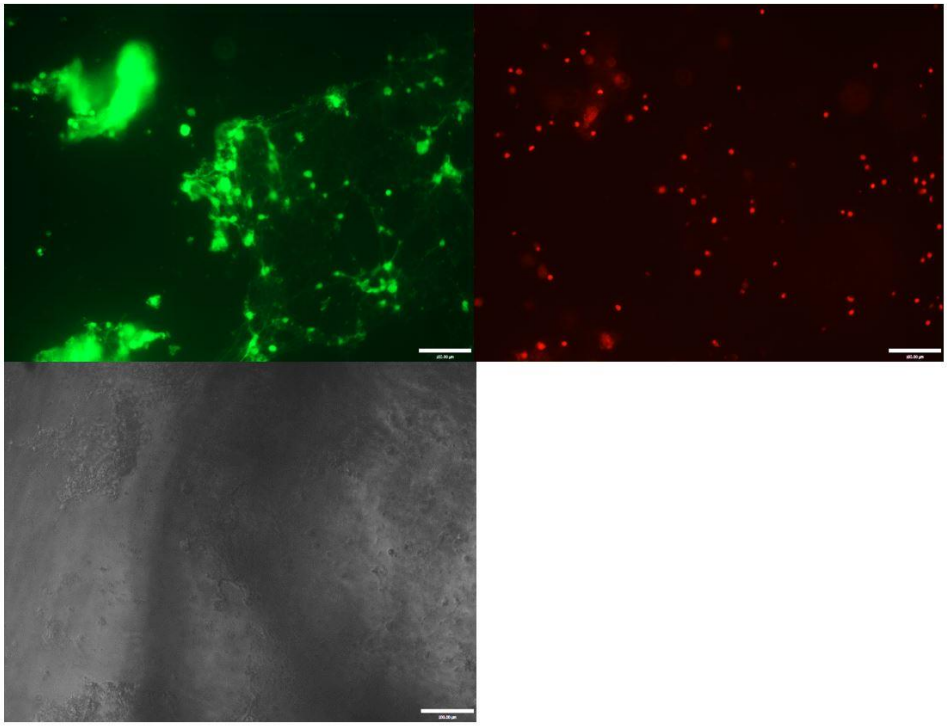

7days

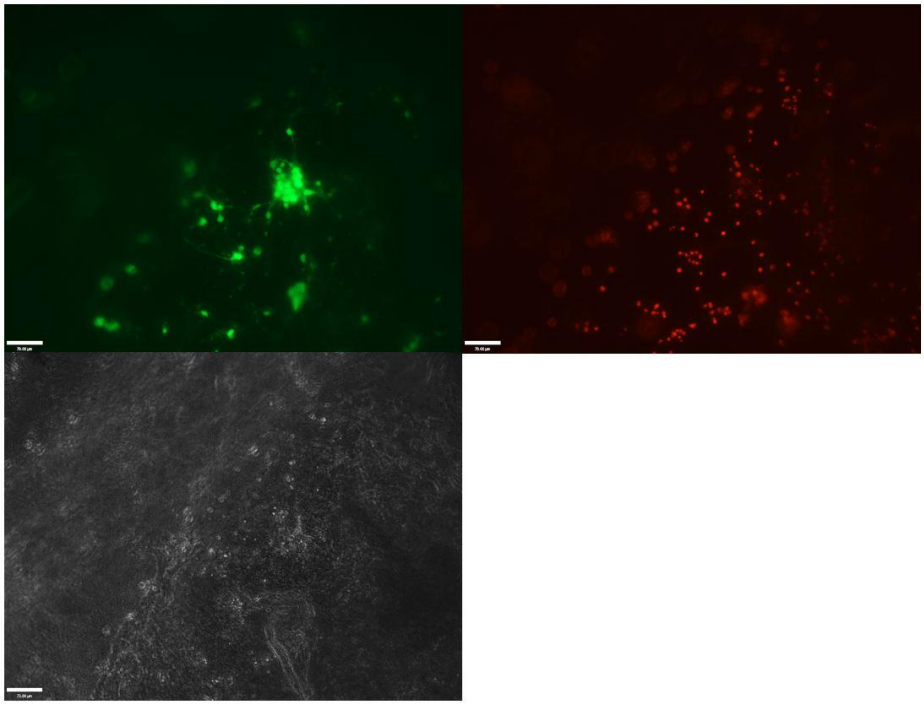

25 mM $CaCl_2$

14days

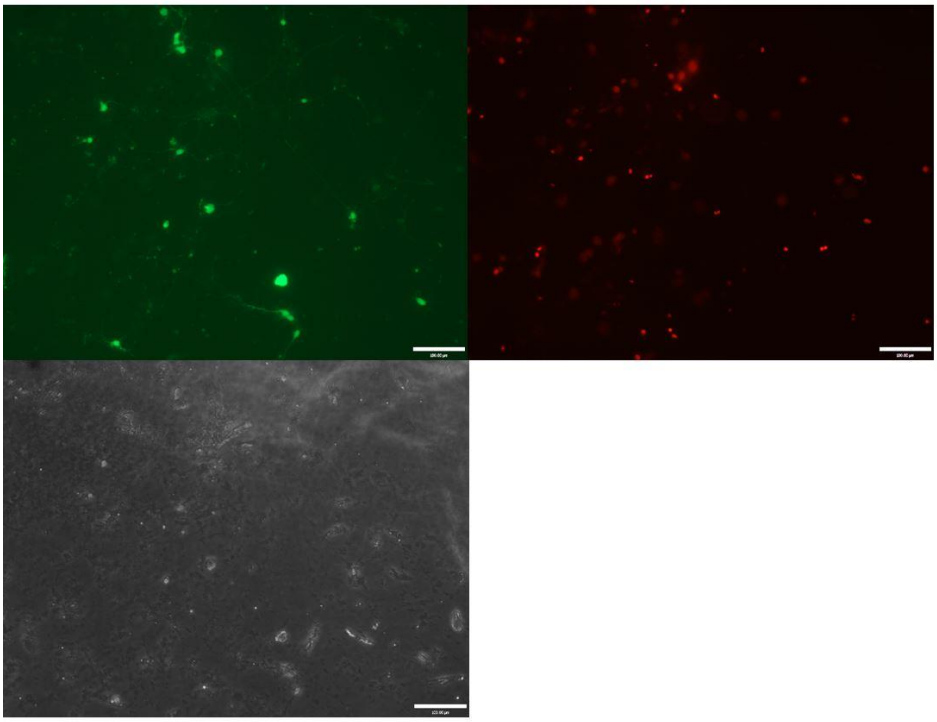

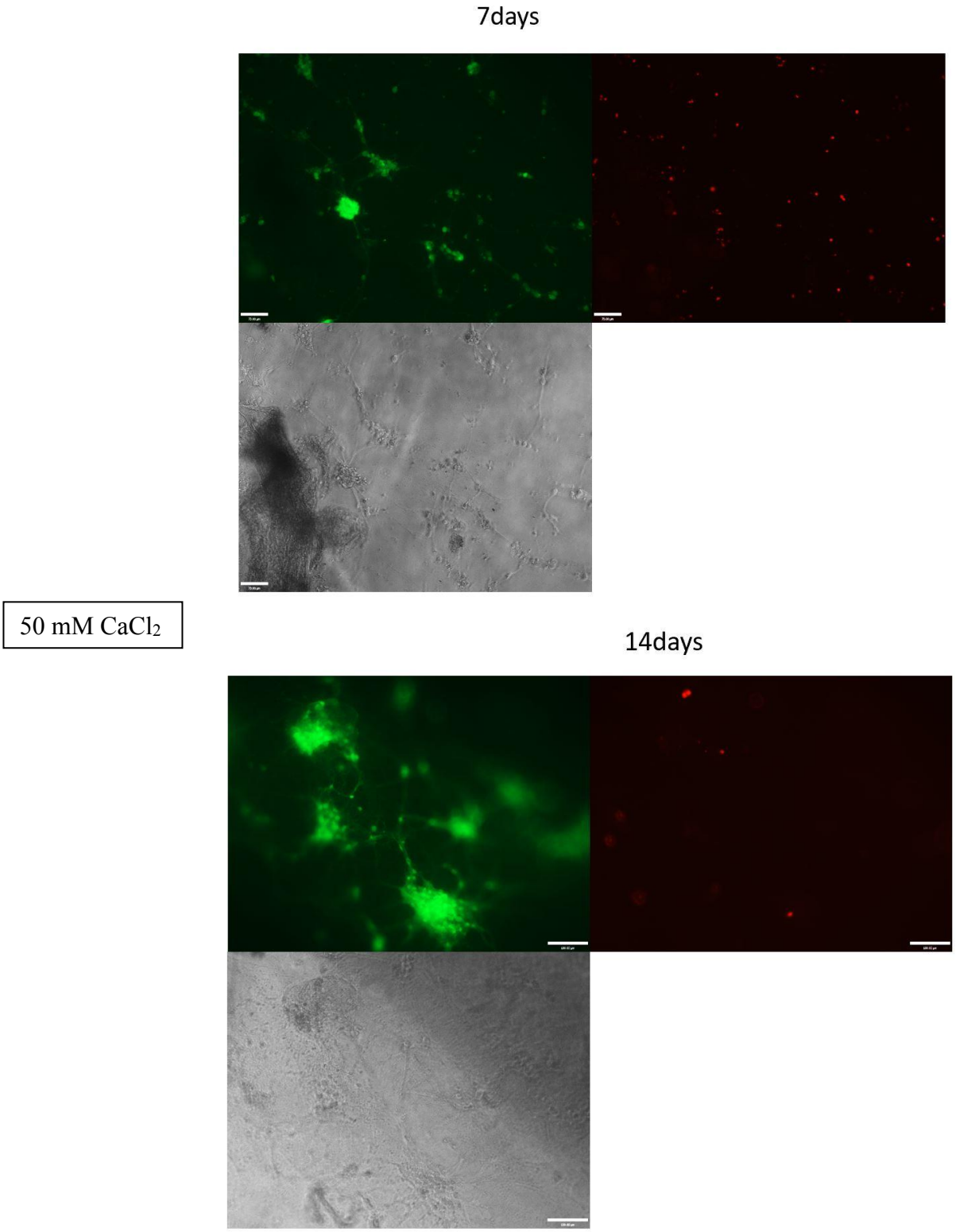

Figure 4.6 The neurons populations growth on conductive films with different concentration of $CaCl_2$ (2mM, 5mM, 25mM and 50mM).

All preparation conditions yielded samples with homogeneous structures, but the alginate film showed the most significant number of neurons outgrowth, with the cell body surrounded by a neurite network Figure 4.10)

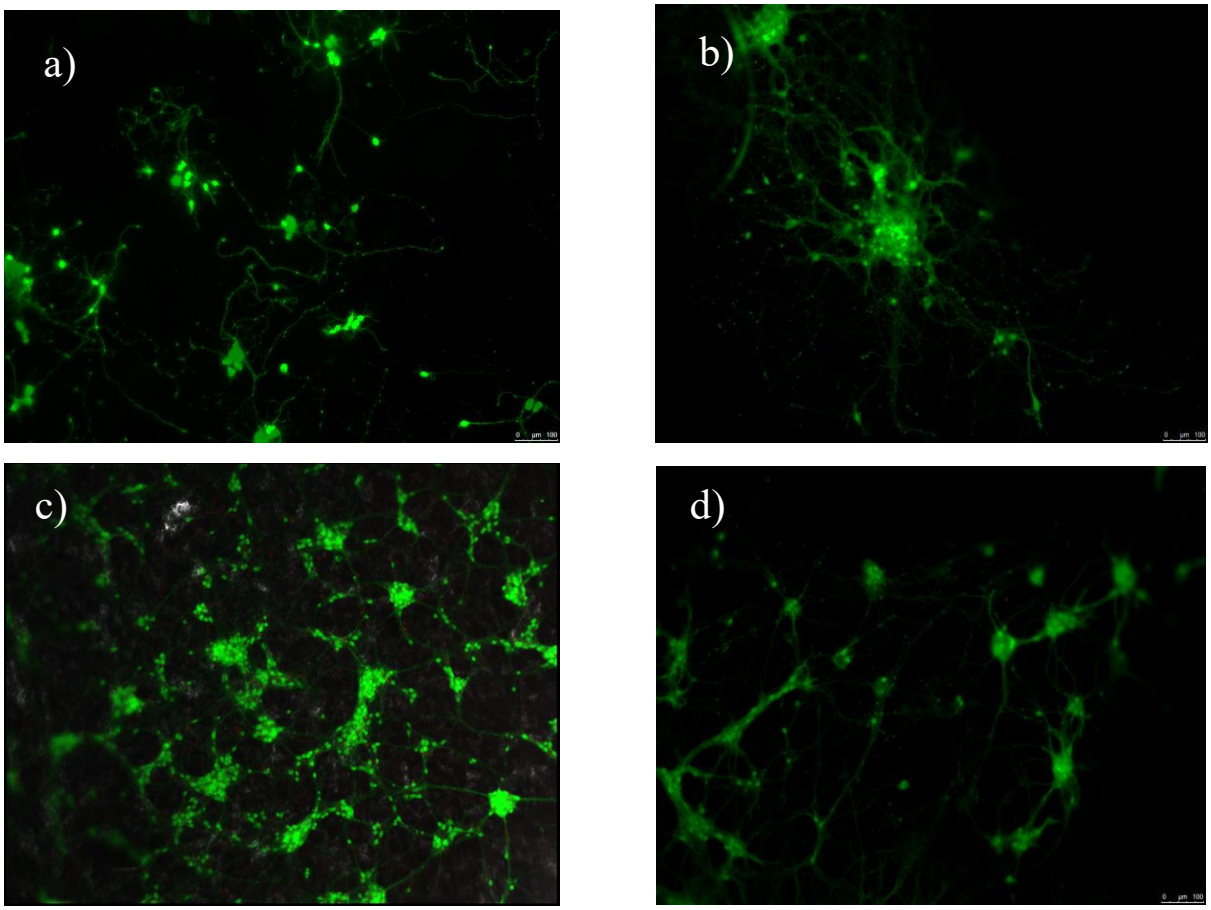

1. PEDOT:PSS + 1% GOPS + PEG + alginate

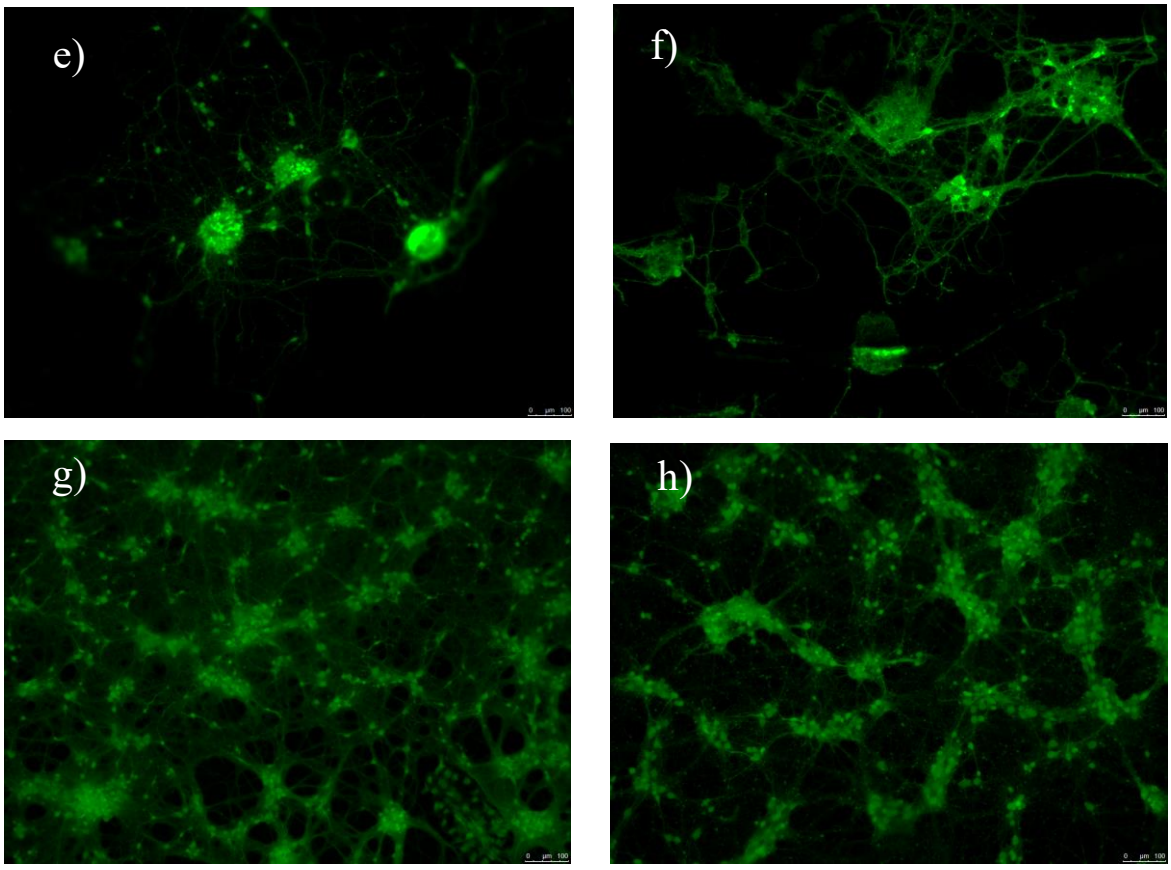

2. PEDOT:PSS + 1% GOPS + EG or PEG + alginate ($NaHCO_3$ casting)

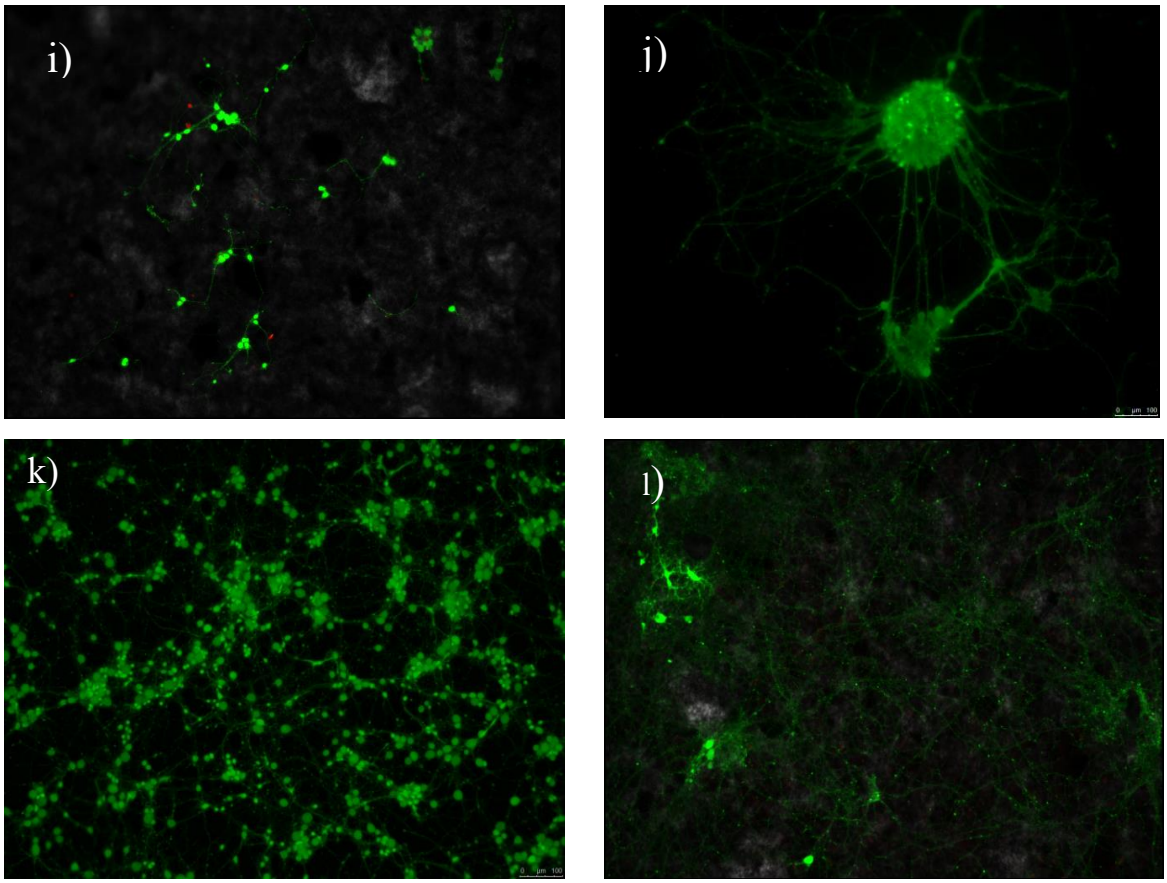

3. PEDOT:PSS + 1% GOPS + EG + 25% PVA + alginate

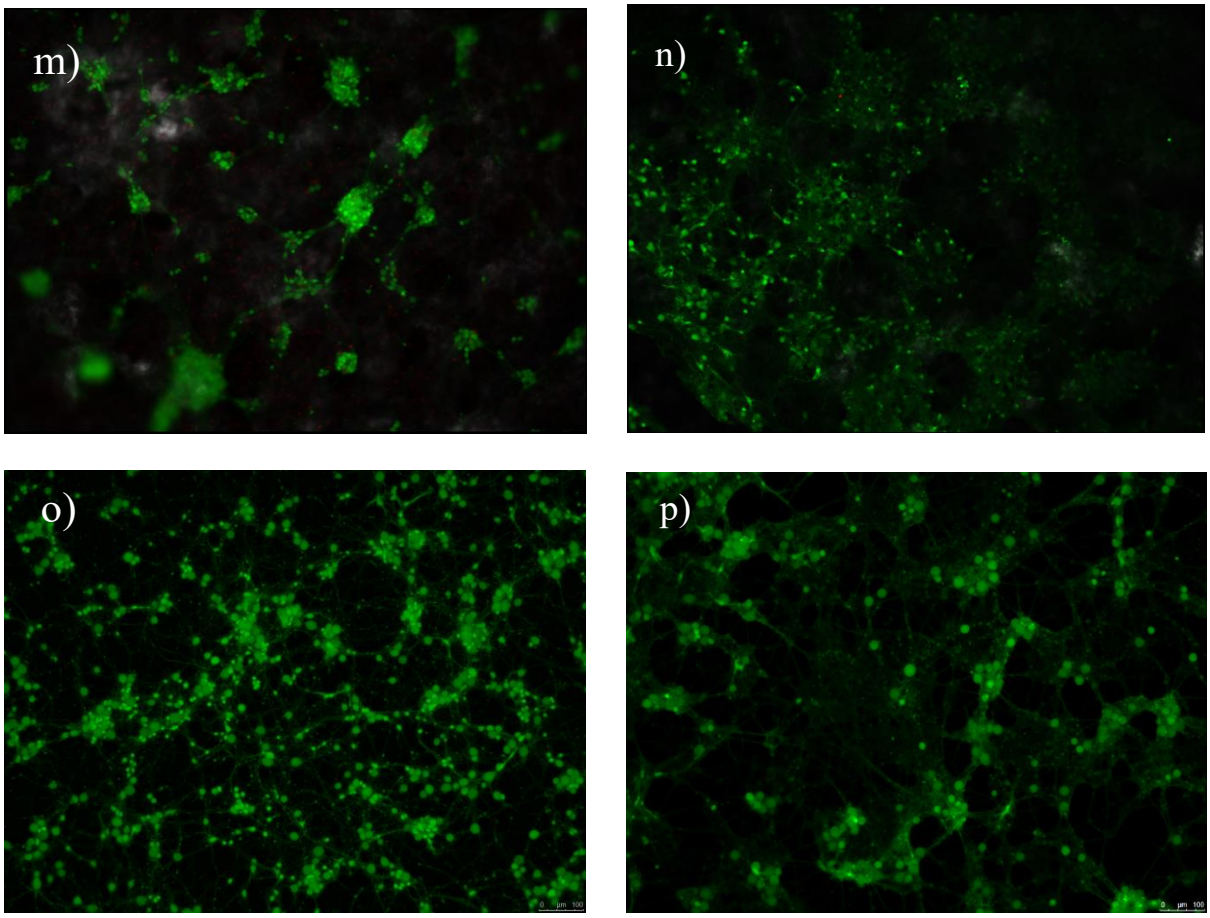

4. PEDOT:PSS + EG + 25% PVA + alginate

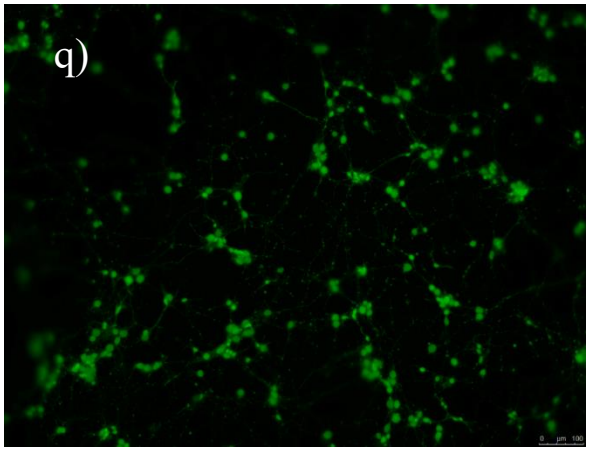

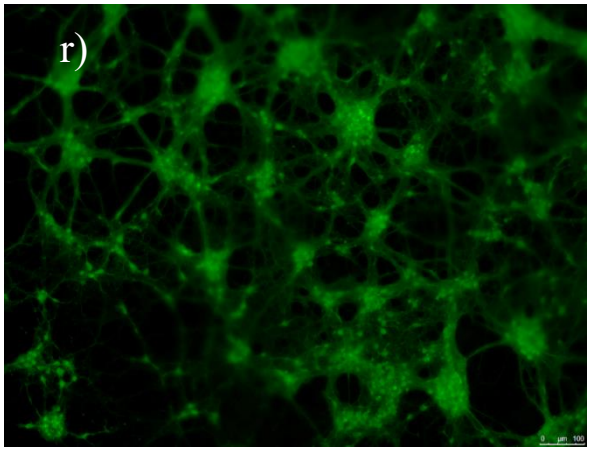

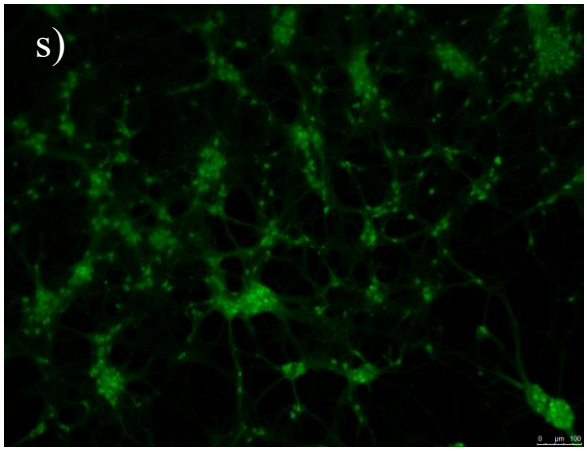

5. PEDOT:PSS + alginate with $CaCl_2$

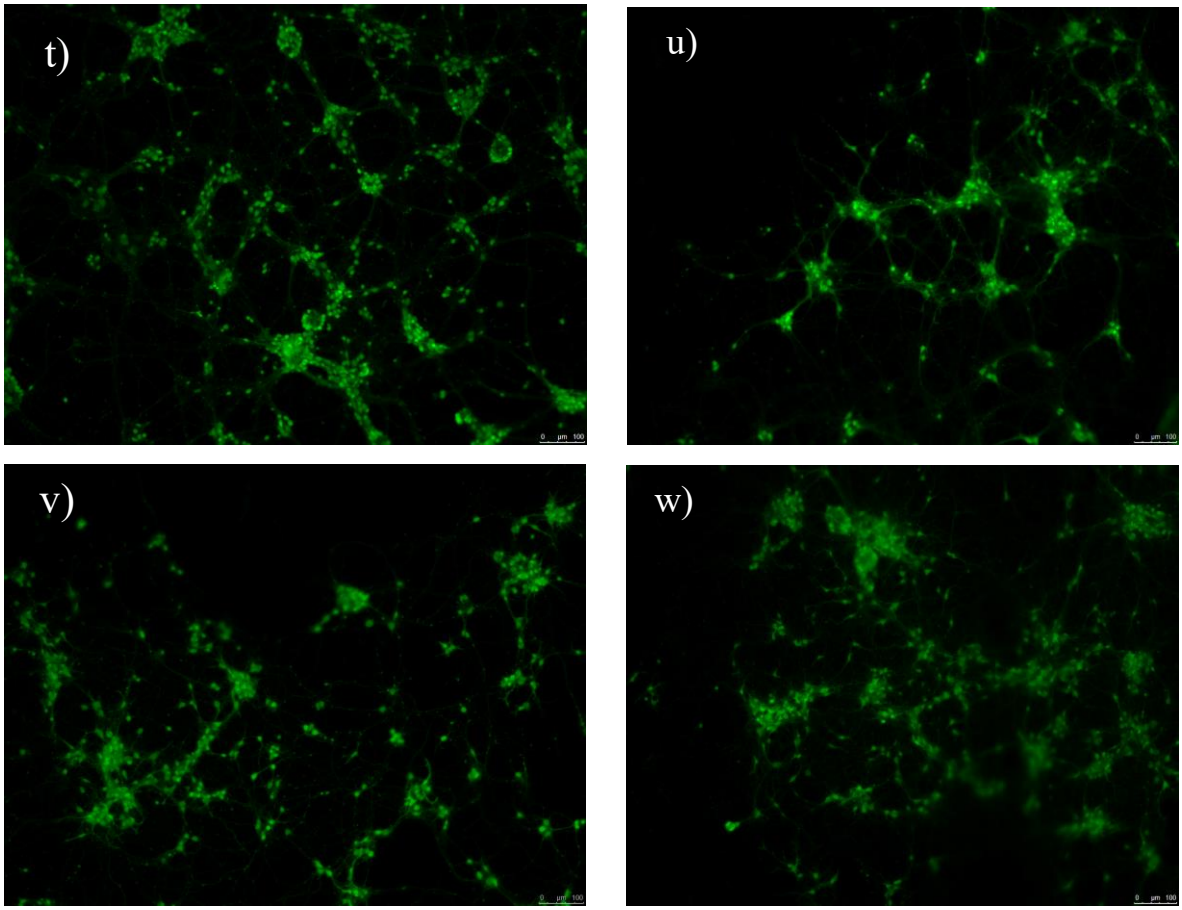

6. PEDOT:PSS + 1% GOPS + EG + 25% PVA + alginate

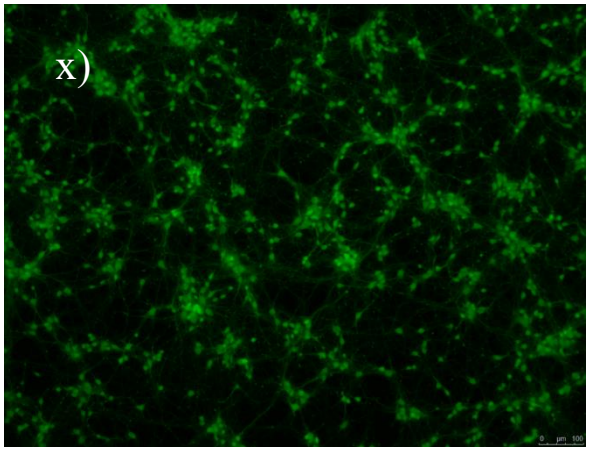

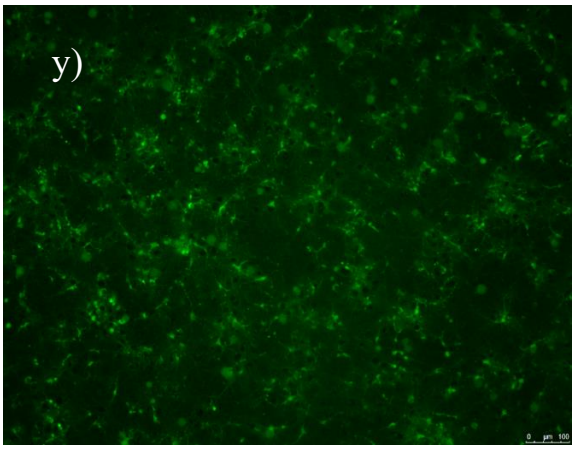

7. Control

Figure 4.10 The summary of living neurons cells on scaffolds in different conditions where the left column represents cultures after 7 days, and the right column represents cultures after 14 days.